

**POLITECNICO DI TORINO**

**Corso di Laurea Magistrale  
in Ingegneria biomedica**

**Tesi di Laurea Magistrale**

**Comparison of different inertial sensors setups and  
algorithms to estimate gait spatio-temporal parameters**



Relatori  
Laura Gastaldi  
Valentina Agostini

Candidata  
Elisa Digo  
Matr. 233234

Anno Accademico 2017-2018



*A zia Giudy*



## Abstract

The aim of this master thesis was the comparison of different inertial sensors setups and algorithms to estimate gait spatio-temporal parameters. The study was conducted at Politecnico di Torino in collaboration with the Neurorehabilitation Department of the Molinette Hospital. The experimental tests concerning the comparison and validation of algorithms concentrated on the analysis of gait in healthy elderly people, but also some pathological subjects affected by Parkinson's disease were tested.

Gait spatio-temporal parameters play a fundamental key role in different fields. They are useful to provide information about alterations in human movement patterns, to predict disability and risk of falling in elderly subjects and to verify the effectiveness of a rehabilitation program. Inertial sensors system directly measures acceleration and angular velocity during motion. Even if affected by drift problems during the signals integration, inertial sensor units (IMUs) allow to overcome some limitations typical of other instruments such as the optical motion capture systems. In detail, they are portable and non-invasive, they do not require a specific laboratory environment to perform the analysis and they can capture unlimited large number of steps without capture volume restrictions. All these characteristics make them recommended for the gait analysis and for the estimation of spatio-temporal parameters.

The focus of this thesis was the assessment of spatio-temporal parameters using Xsens Inertial Sensors. A stereophotogrammetric system, based on two Optitrack V120:Trio bars, was used as the gold standard for the validation of the parameters estimated by inertial measurement units. Nine healthy elderly subjects ( $67.4 \pm 5.1$  years) were tested. They were over 64 years old and have no neurological or musculoskeletal disorders. Three Xsens inertial sensors and six passive reflective markers were positioned on the subjects at the same time. The IMUs were placed on the trunk and on the two heels, whereas the markers were fixed on the toe, on the heel and on the malleolus of each foot.

The subjects were asked to walk back and forth at a self-selected normal speed along a 6.5 meters path. The test was repeated for two different conditions, the single-task and the dual-task. The first one consisted only in walking following a line, whereas the second one consisted in talking and answering questions about habits and interests while walking. The spatial synchronization between the two Optitrack bars was developed by a global coordinate system aligned with the motion trajectory.

The temporal synchronization of the two Optitrack bars and the inertial sensors was obtained with an external event, asking the subjects to impact the right heel on the ground before starting to walk. In this way the starting point of acquisitions was selected as the instant corresponding to the maximum peak of the vertical right heel acceleration and to the frame corresponding to the minimum vertical trajectory of the right heel marker.

The data analysis consisted in the identification of gait events both in markers trajectories and in inertial sensors signals. Secondly, the estimation of gait spatio-temporal parameters was performed.

Heel-strike (HS) and toe-off (TO) were first identified considering the horizontal trajectories of markers. HS was identified as the frame before the heel marker change of direction, whereas TO was defined as the first frame of the toe marker change of direction. Subsequently, marker coordinates were also controlled in the vertical trajectories, verifying that the time instants of HS and TO coincided with the minimum frames. The subsequent step was the detection of gait events inside IMUs signals by applying two different algorithms. For the IMU-trunk setup, the acceleration along the z-axis allowed the identification of HSs and TOs in correspondence of the maximum and minimum peaks respectively. The discrimination between right and left sides was achieved through the alternation of sign of the trunk angular velocity around the vertical axis. For the IMU-heel setup, the sagittal angular velocity was considered. TO instants were identified as the maximum peaks, whereas HS were selected by searching the maxima between two TOs. After gait events identification, the following spatio-temporal parameters were estimated: stride time, stride frequency, step time, step frequency, stance time, stance duration, swing time, swing duration, single support time, single support duration, double support time, double support duration, foot symmetry and limp index.

The errors committed in evaluating gait spatio-temporal parameters using the two IMUs setups and associated algorithms were estimated as differences between the ones obtained with Optitrack and IMUs values. They were presented both with tables and Bland-Altman graphs. Afterwards, bar diagrams for the comparison of parameters values between the trials with single-task and those with dual-task were realized. Finally, the paired t-test between the two different conditions was performed in order to evaluate through the p-values the statistical significance of results.

The collected data from healthy subjects showed a good correspondence with previous literature data. Also the symmetry between right and left sides was underlined. The errors committed from the algorithm with the trunk acceleration were much lower than those of the algorithm with heels angular velocity.

This was due to the better identification of gait events guaranteed by the trunk algorithm with respect to the heels one. Furthermore, the inertial sensor on the trunk was firmer during the gait and offered the advantage to extract all the data from a single device.

For all these reasons, it was possible to assess that the trunk algorithm was more effective for the estimation of spatio-temporal parameters.

The trials with dual-task showed a decrease of gait speed for all the subjects. The p-values reported statistical significance for the following parameters: Optitrack step frequency ( $p=0,05$ ), Optitrack swing duration ( $p=0,03$ ), Optitrack double support time ( $p=0,03$ ), Optitrack double support duration ( $p=0,03$ ), Xsens with heels-IMUs stance time ( $p=0,05$ ) and Xsens with heels-IMUs double support time ( $p=0,05$ ). The lack of statistical significance ( $p\text{-value}>0,05$ ) for all the other spatio-temporal parameters was probably caused by the limited number of subjects.

A second test was performed on five patients with Parkinson's disease ( $58.8 \pm 3.8$  years). Four of them received the Deep Brain Stimulation (DBS) treatment, whereas the fifth was subjected to botulinum toxin infiltrations. They were asked to walk back and forth along a gangway of 7 meters wearing the same three inertial sensors previously used, one on the trunk and two on the heels. Two of them with the DBS implant were asked to repeat the test with different stimulation frequencies. The two algorithms used to identify gait events were the same tested on healthy subjects.

For pathologic patients, the spatio-temporal parameters estimated were presented in tables. Then, for two of them, bar diagrams for the comparison of parameters values among the different stimulation frequencies were realized.

The data of the patients with Parkinson's disease were comparable to those of healthy subjects. The comparison between the spatio-temporal parameters values at different stimulation frequencies showed an increase of the gait speed as the frequency decreased.

The thesis' structure is divided as follows:

- Chapter 1 focuses on the concept of walking, describing the sequence of events necessary to walk and the phases of gait. It also lists all the spatio-temporal parameters, their meanings and their important role in different fields. Then, it presents the description of all the instrumentations used to estimate these parameters, with their advantages and disadvantages. The final subchapter is dedicated to the literature algorithms proposed to estimate spatio-temporal parameters by using inertial sensors.
- Chapter 2 describes the two motion capture systems adopted for the test, Optitrack V120:Trio and Xsens inertial sensors. The first subchapter is dedicated to the system used as the gold standard and contains a general description of optical motion capture systems, the presentation of Optitrack V120:Trio cameras and the explanation of Motive software. The second subchapter is focused on Xsens and it contains a general analysis of inertial sensors, the presentation of Xsens MTx's and the description of MT Manager software.
- Chapter 3 is dedicated to describe all the preliminary tests made with healthy subjects before the principal one, with the attempt to define a complete and effective experimental setup. The four subchapters are respectively dedicated to the tests only with Optitrack, the tests only with Xsens, the tests with both instruments not synchronized and the tests with both instruments synchronized with each other.
- Chapter 4 explains in detail the materials and methods of the test with healthy subjects, describing the setting and the algorithms adopted. Then, it presents the results and the discussions.
- Chapter 5 starts with the description of the test made with patients with Parkinson's disease, continues with the presentation of the data collected for each of them and ends with the discussions.

## Summary

1. Gait analysis .....	1
1.1 Walking and gait cycle .....	1
1.2 Spatio-temporal parameters .....	6
1.3 Instrumentation .....	10
1.4 Algorithms for the spatio-temporal parameters estimation with IMUs .....	15
2. Motion capture systems .....	35
2.1 Stereophotogrammetric system: Optitrack.....	35
2.1.1 Optical Motion Capture System .....	35
2.1.2 V120:Trio .....	37
2.1.3 Motive software .....	40
2.2 Inertial Measurement Units: Xsens .....	45
2.2.1 Inertial sensors .....	45
2.2.2 Xsens Xbus Kit.....	49
2.2.3 MT Manager software.....	55
3. Preliminary tests.....	59
3.1 Preliminary tests with Optitrack.....	59
3.2 Preliminary tests with Xsens .....	71
3.3 Preliminary tests with Optitrack and Xsens not synchronized .....	83
3.4 Preliminary tests with Optitrack and Xsens synchronized .....	97
4. Test on healthy elderly subjects .....	131
4.1 Materials and methods.....	131
4.1.1 Participants .....	131
4.1.2 Instruments.....	131
4.1.3 Protocol .....	133
4.1.4 Signal processing and data analysis.....	134
4.2 Results.....	142
4.2.1 Normal speed with single-task .....	142
4.1.2 Normal speed with dual-task.....	164
4.2.3 Normal speed with single-task and with dual-task .....	186
4.3 Discussions .....	196

5. Test on pathologic subjects .....	201
5.1 Parkinson's disease .....	201
5.2 Materials and methods .....	205
5.3 Data analysis.....	207
5.3.1 Patient 1 (Parkinson's disease, DBS).....	209
5.3.2 Patient 2 (Parkinson's disease Pisa syndrome, botulinum toxin).....	213
5.3.3 Patient 3 (Parkinson's disease, DBS).....	215
5.3.4 Patient 4 (Parkinson's disease, DBS).....	217
5.3.5 Patient 5 (Parkinson's disease, DBS).....	221
5.4 Discussions .....	223
References.....	225
Ringraziamenti .....	229

## 1. Gait analysis

### 1.1 Walking and gait cycle

Activities in daily life require men and women to move in their environment. The typical mode of human locomotion consists in walking from one place to the other (Zijlstra, 2004).

Even if walking is the body's natural way of moving, the lower limbs' versatility allows also to face up to doorways, changing surfaces, stairs and obstacles (Perry, 1992).

The pattern of movement recognised as human walking is the result of the interaction between three systems: the central nervous one, the peripheral nervous one and the musculoskeletal effector one.

The sequence of events necessary for walking is (Figure 1.1.1):

1. Registration and activation of the gait command in the central nervous system.
2. Transmission of the gait signals to the peripheral nervous system.
3. Contraction of muscles.
4. Generation of forces and moments in correspondence of synovial joints.
5. Regulation of the joint forces and moments by the rigid skeletal segments based on their anthropometry.
6. Displacement of the segments (functional gait).
7. Generation of ground reaction forces.

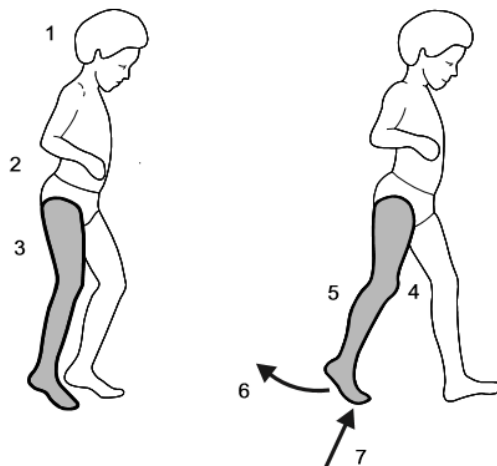


Figure 1.1.1\_The sequence of events necessary for walking from n°1 to n°7. (C. L Vaughan, 1999)

The act of walking combines the simultaneous repetition of sequences of limb motion and the maintenance of stance stability. Since each sequence involves a series of interactions that involve the total body mass and two multi-segmented lower limbs, it is recommended to view gait from several different aspects.

There are three basic approaches (Perry, 1992):

- the first one subdivides the gait cycle according to the reciprocal floor contacts by the two feet;
- the second one uses the time and distance qualities of the stride;
- the third one identifies the events within the gait cycle and names these intervals as the functional phases of gait.

As the first approach explains, until the person's destination is reached, there is the repetition of a series of events. One limb plays the role of mobile support, while the other one advances itself to a new support site. Then, the limbs reverse their roles. A single sequence of these functions for one limb is called a gait cycle (GC). It is defined as the time interval between two successive occurrences of one of the repetitive events of walking. Generally, the start of the gait cycle coincides with the moment of heel strike. In this way, if it the GC starts with the initial contact of the right foot, then it will end only when the same foot touches the ground again (S. Lee, 2005).

Each gait cycle is divided into two periods, stance and swing. The first one is defined as the period of time in which the foot is in contact with the ground. The second one, instead, is defined as the period of time in which the foot is in the air for limb advancement. According to the sequence of floor contact by the two feet, stance is subdivided into three intervals (Figure 1.1.2):

1. *Initial double stance* or *First double support*. It is the interval time just after the initial contact. The two feet share body weight equally because they are both on the floor.
2. *Single stance* or *Single limb support*. It is the interval time during which the body's entire weight is resting on one extremity. It begins when the opposite foot is lifted for swing.
3. *Terminal double stance* or *Second double support*. It is the interval time that begins with floor contact by the other foot and continues until the original stance limb is lifted for swing. The two feet share body weight equally again.

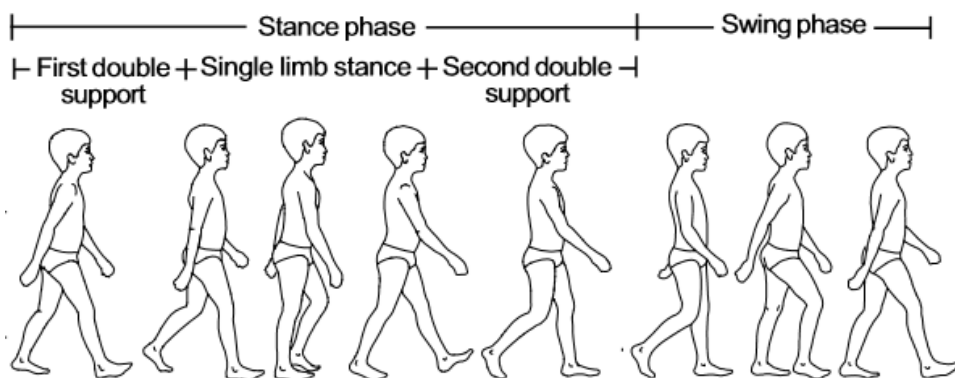


Figure 1.1.2\_The normal gait cycle of an 8-year-old boy. (C. L Vaughan, 1999)

The normal distribution of the floor contact periods is indicated in Table 1.1.1. When gait velocity increases, both stance and swing times get shorter. In addition, walking faster proportionally lengthens single limb support and shortens the two double support intervals. The reverse is true as the walking speed is slower (Perry, 1992).

FLOOR CONTACT PERIODS	
<b>Stance</b>	60%
<b>Initial Double Stance</b>	10%
<b>Single Limb Support</b>	40%
<b>Terminal Double Stance</b>	10%
<b>Swing</b>	40%

Table 1.1.1\_The floor contact periods.

The second method identifies the gait cycle with the term *stride* and uses the time and distance qualities to describe it. The stride is defined on the basis of the actions of one limb. In fact, its duration is the interval between two consecutive floor contacts of the same foot. The stride is the sum of two steps, a right one and a left one (Figure 1.1.3). As a result, the duration of the step is the interval between an initial contact of one foot and the following initial contact of the other one.

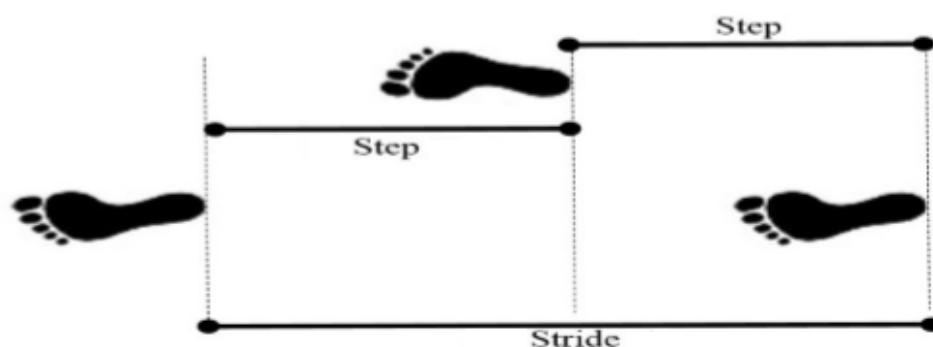


Figure 1.1.3\_Stride and step definitions from feet contact. (C. P. Meena, 2015)

The third approach identifies a series of motion patterns performed by hip, knee and ankle during the gait cycle. Each stride implies both an alignment between the body and the supporting limb during stance and an advancement of the other limb during swing. These functional patterns are defined *the phases of gait*.

As Perry affirmed in 1992, each stride contains eight functional patterns (Figure 1.1.4):

1. *Initial contact* (0%). It is the moment when the foot just touches the floor.
2. *Loading response* (0-10%). It begins with initial floor contact and continues until the other foot is lifted for swing. It is also called initial double stance period.
3. *Mid stance* (10-30%). It begins as the other foot is lifted and continues until body weight is aligned over the forefoot.
4. *Terminal stance* (30-50%). It begins with heel rise and continues until the other foot strikes the ground.
5. *Pre swing* (50-60%). It begins with initial contact of the opposite limb and ends with ipsilateral toe-off.
6. *Initial Swing* (60-70%). This phase begins with lift of the foot from the floor and ends when the swinging foot is opposite the stance foot. It is approximately one-third of the swing period.
7. *Mid swing* (70-85%). This second phase of the swing period begins as the swinging limb is opposite the stance limb and ends when the tibia is vertical.
8. *Terminal swing* (85-100%). This final phase of swing begins with a vertical tibia and ends when the foot strikes the floor.

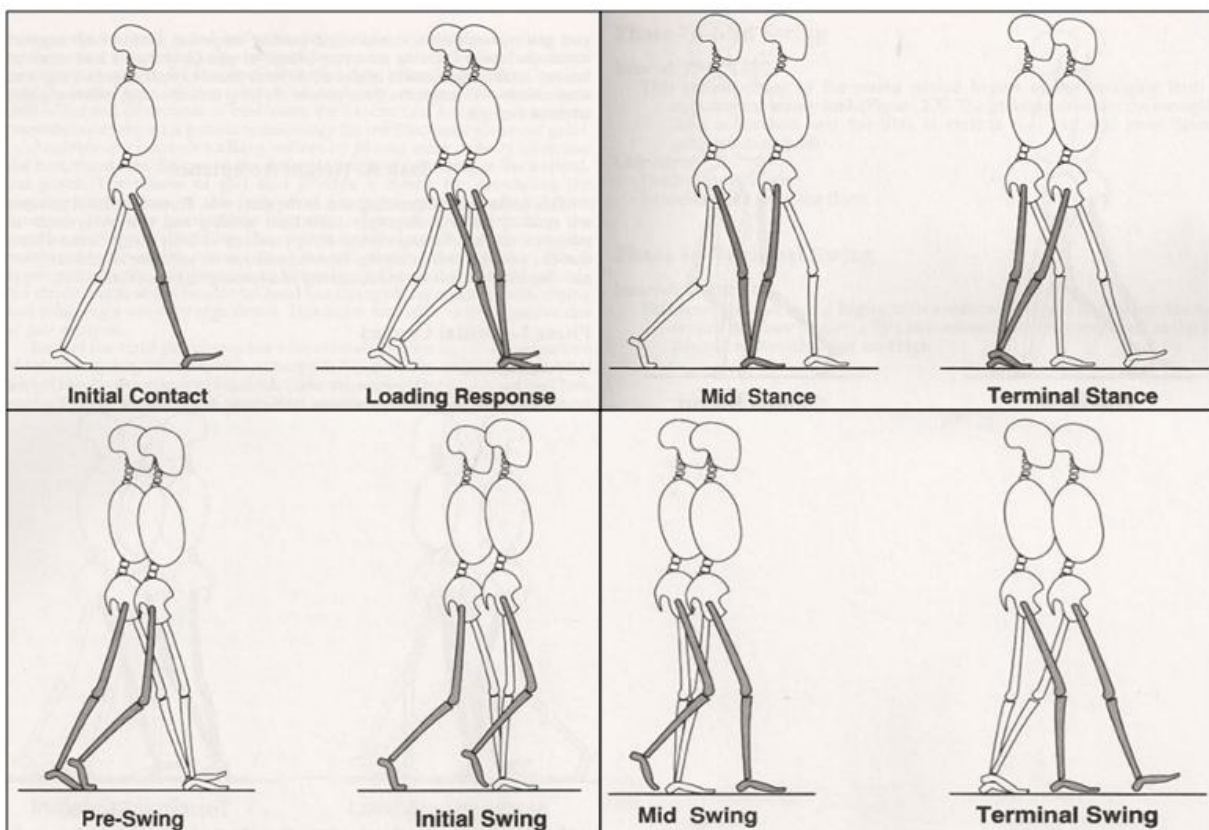


Figure 1.1.4\_The eight phases of gait. (Perry, 1992)

The combination of sequential movements allows the limb to accomplish three basic tasks: weight acceptance, single limb support and limb advancement.

1. The first task of *weight acceptance* consists in transferring the body weight on the limb that has just completed the swing phase. It includes two phases: the initial contact and the loading response.
2. The second task of *single limb support* gives to one limb the total responsibility for supporting body weight. The phases involved in this task are two: mid stance and terminal stance. Moreover, pre swing can be considered a stance phase of single limb support.
3. The third task of *limb advancement* provides an advancement of the limb with three postures: ascent, progress and preparation for the next stance interval. Four gait phases are involved in this task: pre-swing (end of stance), initial swing, mid swing and terminal swing.

On the basis of all the three approaches, Perry created a scheme with the division of the gait cycle according to periods, tasks and phases (Figure 1.1.5).

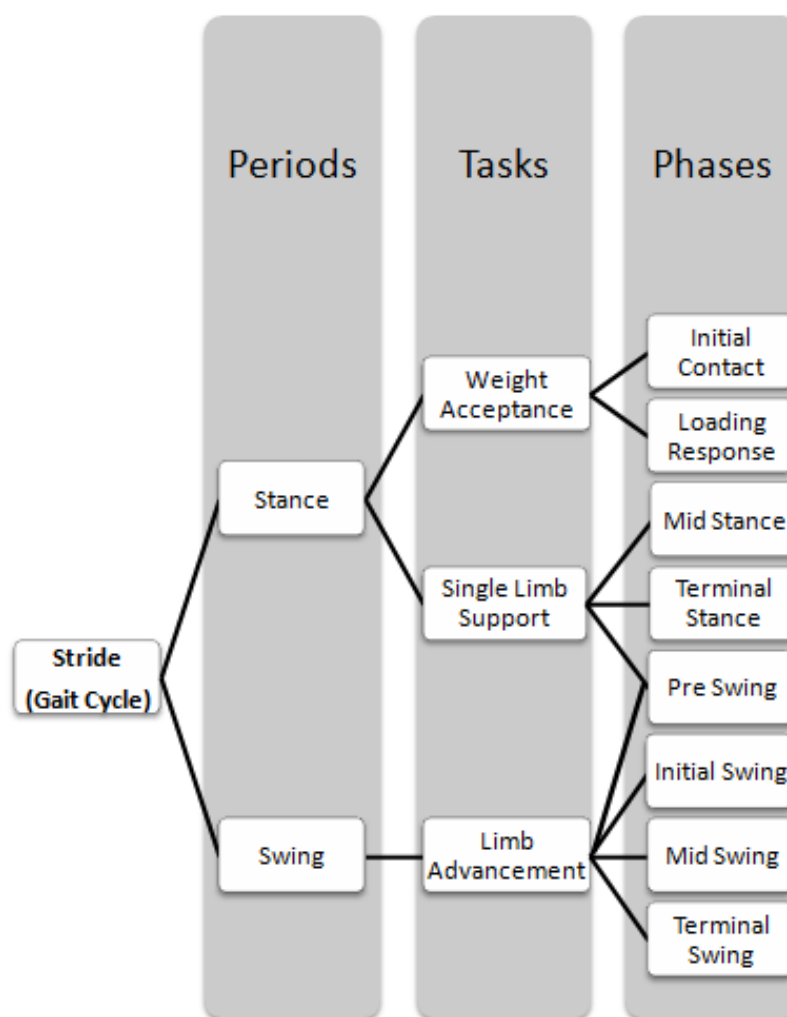


Figure 1.1.5\_The scheme with the division of GC according to periods, tasks and phases.

## 1.2 Spatio-temporal parameters

Walking is one of the most common human physical activities. For this reason, the analysis and the study of body movement during gait represents a real need. During the past two decades, gait analysis developed from an academic discipline to a useful tool. Artists from the classical Greece and Rome wanted to understand the shape and the alignment of the limbs during different movements. During the Renaissance, Leonardo da Vinci, Galileo, Newton, and Borelli were involved in human dissection and in biomechanics studies. In the 1880s Marey in Paris and Muybridge in California made the earliest kinematics studies on human walking. The Figure 1.2.1 shows one of the plates realized by Muybridge in 1887:

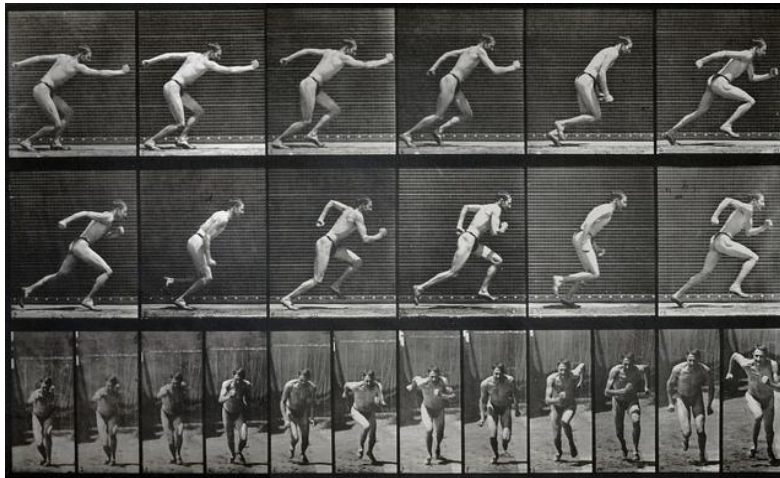


Figure 1.2.1\_Plate 59 from Animal Locomotion Series of Eadweard Muybridge (1887).

During the 1940s and the 1950s a group working in California undertook the first major study of the gait kinematics. It was necessary to wait until the late 1970s to see the development of measurement systems based on television cameras directly linked to computers (Whittle, 1996). Today, gait analysis takes advantage of many technologies and has a central role in very different fields, such as sport and clinic. Clinicians are able to use the instrumentation for the gait analysis in their routine clinical practice to evaluate the patients' health status, their treatments and their rehabilitation programs for musculo-skeletal and neurological disorders. Gait analysis allows to reveal the mechanisms of human movement by identifying factors related to the lower limbs (C. P. Meena, 2015). Among the numerous measurement of gait analysis, spatial-temporal parameters are often used in the clinical field. They represent a quantitative description of the main events of gait and therefore reflect the ability of the patient to fulfil the three tasks identified by Perry. A prolonged double stance phase, an asymmetric gait, the reduction of walking speed and an increased stride width are examples of important information useful for the diagnosis of pathological gait and for the evaluation of the results obtained after treatments (F. Bagané, 2012).

Furthermore, spatio-temporal gait parameters variability can be used to predict risk of falling and future disability in the elderly subjects. Finally, they can provide information about movement pattern's changes, they can help to decide rehabilitation progress and they can contribute to evaluate the effectiveness of a rehabilitation program (Caulfield, 2012). All the existing methods for the estimation of gait spatio-temporal parameters have to follow some guidelines (Beauchet, 2006):

- Measurements should be performed in a reproducible and well-lit environment;
- Clothing should be comfortable and non-restrictive;
- Different gait speed should be measured, preferably in randomized order (i.e. slow, normal, fast);
- The analysis should start when the subjects are already walking, in order to observe the true state gait;
- Standardized and clear walking instructions should be given to the subjects;
- The highest possible number of gait cycles should be analysed, in order to evaluate stride-to-stride variability.

The estimation of spatio-temporal parameters is based on the previous detection of gait events (GEs). As it is shown in the Figure 1.2.2, all the gait events are defined on the basis of feet contact with the ground during stance phase (B. Mariani, 2013):

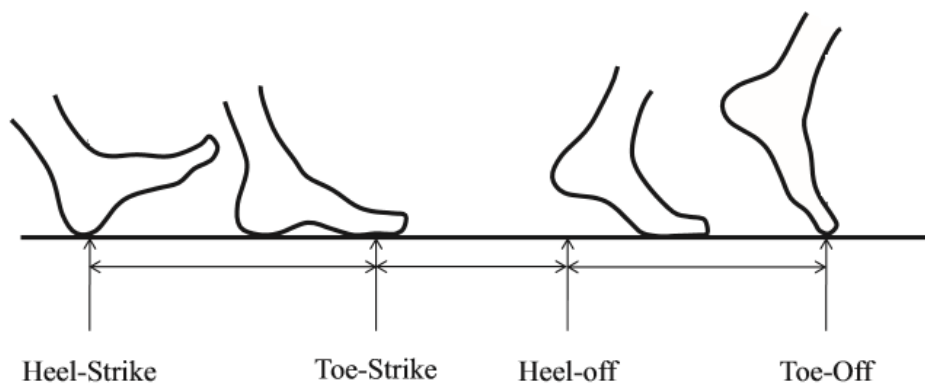


Figure 1.2.2\_Gait events during stance. (B. Mariani, 2013)

- Heel-Strike (HS). It is the impact of the heel on the ground and it represents the beginning of both the stance and the load phases.
- Toe-Strike (TS). It is the impact of the toe on the ground and it represents the end of the load phase and the beginning of the foot-flat one.
- Heel-Off (HO). It is the detachment of the heel from the ground and it starts the push phase.
- Toe-Off (TO). It is the detachment of the toe from the ground and it concludes both the push and the stance phases.

Starting from gait events, it is possible to define a lot of useful spatio-temporal parameters:

- Temporal parameters (Figure 1.2.3):
  - *Stride time* (s), the time between two consecutive HS of the same foot;
  - *Stride frequency* (Hz), the rate of completing the stride;
  - *Step time* (s), the time between two consecutive HS of different feet;
  - *Step frequency* (Hz), the rate of completing the step;
  - *Foot symmetry* (%GC), the step time as percentage of gait cycle;
  - *Stance time* (s), the time between HS and TO of the same foot;
  - *Stance duration* (%GC), the stance time as percentage of the gait cycle;
  - *Load time* (s), the time between HS and TS of the same foot;
  - *Load duration* (%GC), the load time as percentage of the gait cycle;
  - *Foot-flat time* (s), the time between TS and HO of the same foot;
  - *Foot-flat duration* (%), the foot-flat time as percentage of the gait cycle;
  - *Push time* (s), the time between HO and TO of the same foot;
  - *Push duration* (%GC), the push time as percentage of the gait cycle;
  - *Swing time* (s), the time between TO and HS of the same foot;
  - *Swing duration* (%GC), the swing time as percentage of the gait cycle;
  - *Double support time* (s), the time between HS of one foot and TO of the other;
  - *Double support duration* (%GC), the double support time as percentage of the gait cycle;
  - *Single support time* (s), the time of support on one foot corresponding to the swing time of the other.
  - *Single support duration* (%GC), the single support time as percentage of the gait cycle;
  - *Limp index*, the ratio of the stance times of the two feet;

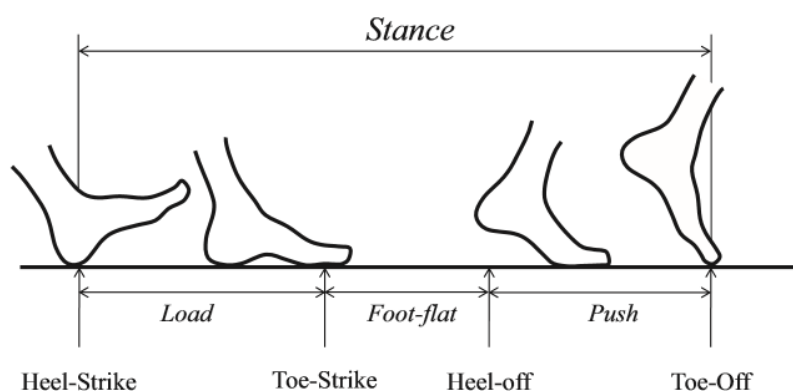


Figure 1.2.3\_Temporal parameters of inner stance phase. (B. Mariani, 2013)

- Spatial parameters (Figure 1.2.4):
  - *Stride length* (m), the distance of two consecutive HS of the same foot;
  - *Stride length/height* (%), the stride length normalized by subject height;
  - *Step length* (m), the distance of two consecutive HS of different feet;
  - *Step length/height* (%), the step length normalized by subject height;
  - *Step width* (m), the lateral distance of feet;

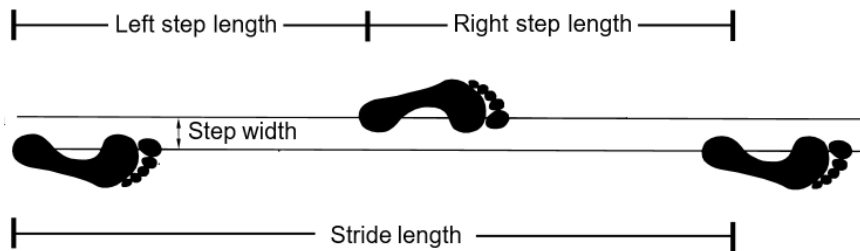


Figure 1.2.4\_Spatial parameters (C. L Vaughan, 1999).

- Spatio-temporal parameters:
  - *Walking speed* (m/s), the average instantaneous speed within the gait cycle;
  - *Walking speed/height* (Hz), the walking speed normalized by subject height;
  - *Cadence* (strides/min), the number of strides in a minute.

The Figure 1.2.5 summarizes the phase of gait useful to detect the spatio-temporal parameters:

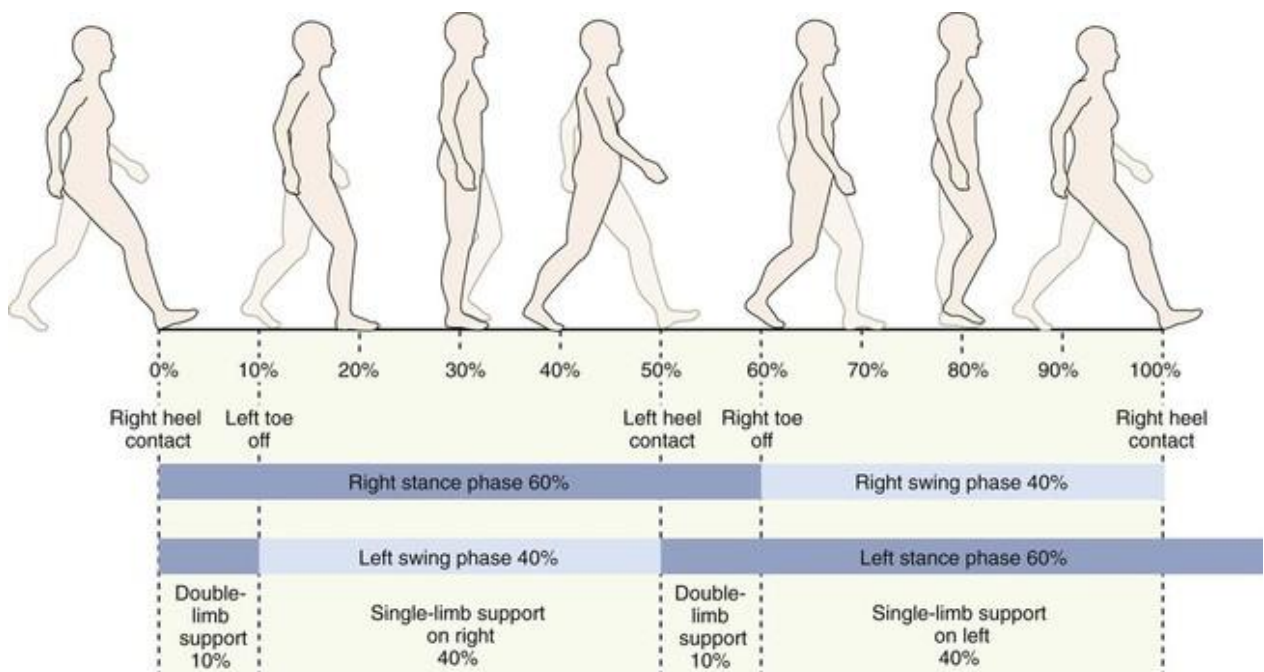


Figure 1.2.5\_Phases of gait (Neumann, 2010).

### 1.3 Instrumentation

Various technologies have been proposed to estimate step-by-step gait temporal and spatial parameters from foot contacts:

1. *Force platforms.* Force platforms or force plates measure reaction forces and establish the point of application and the direction of the resultant reaction force. They typically have rectangular shape and dimensions of about 40 cm by 60 cm. The forces measured include (Figure 1.3.1):

- the vertical ground reaction force
- the force in the anterior–posterior direction
- the force in the medial–lateral direction

For the simplicity of their use, force platforms are widely adopted for gait analysis (McGinnis, 2013).

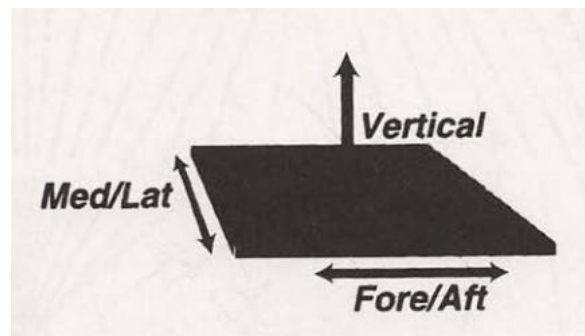


Figure 1.3.1\_ Force plate and direction of forces recorded (Perry, 1992).

2. *Instrumented mats.* While a force platform simply measures a resultant reaction force, the pressure sensors distributed on the instrumented mats quantify the pressure exerted on a specific area. As force platforms, also pressure mats are widely used in gait analysis for their simplicity (McGinnis, 2013). The Figure 1.3.2 in the following page shows an example of instrumented mat called GAITRite Walkway.

Both force platforms and instrumented mats have the same advantages: the simplicity of use and the possibility of estimating spatial gait parameters in addition to temporal ones. However, they suffer from the same limitations:

- they require extensive laboratory space;
- they force subjects to walk in a specific environment;
- they are relatively costly.

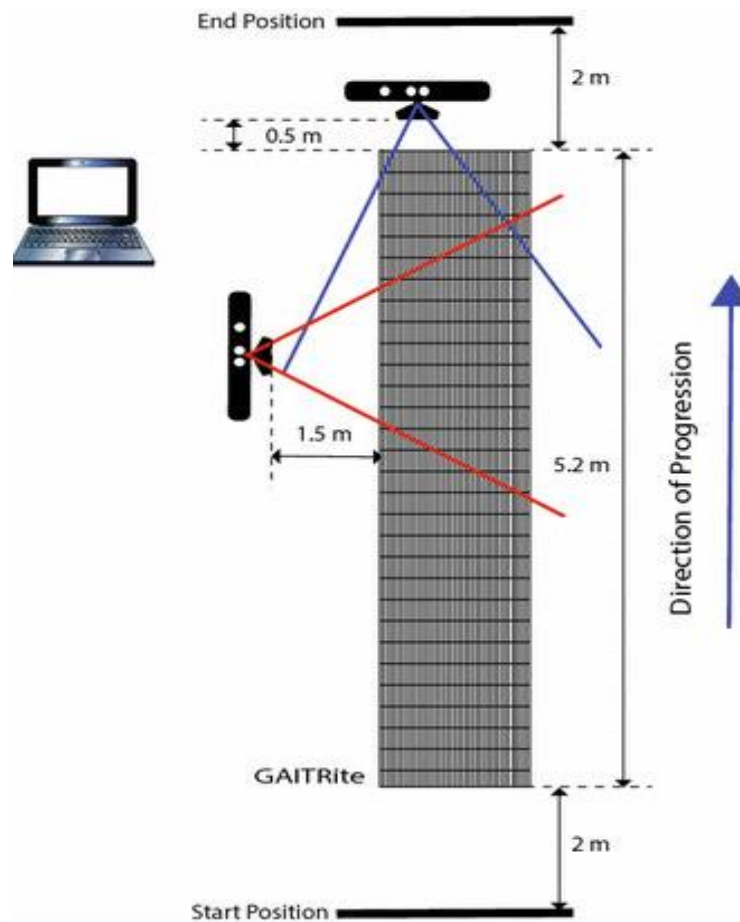


Figure 1.3.2\_Example of an instrumented mat, the GAITRite Walkway. In the scheme there are the dimensions and the distances of the setting (S. Motiian, 2015).

3. *Footswitches*. They consist of force sensing resistors and they are placed under the feet. They are portable and inexpensive, but they may require longer subject preparation and they can provide temporal parameters only. The Figure 1.3.3 show an example of footswitches configuration:



Figure 1.3.3\_Example of footswitches attached under the heel and the big toe (K. Aminian, 2002).

4. *Optical motion capture systems.* The optical motion capture systems are used to capture the three-dimensional movements of the body in a digital form. A software allows to reconstruct the 3D trajectory of markers placed on the body from 2D images offered by cameras. The potential of optical motion capture systems go beyond the estimation of the gait spatio-temporal parameters, since they are thought for 3D kinematics measurements. These systems have three limitations: they are more expensive than the above mentioned alternatives, they require a specific laboratory and they can record a small number of consecutive steps (D. Trojaniello, 2014). The Figure 1.3.4 shows the setting of an optical motion capture system:

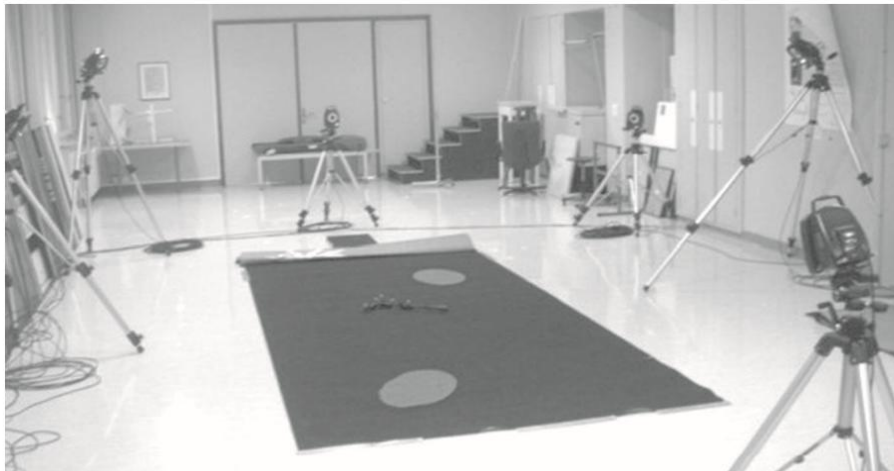


**Figure 1.3.4\_Volume of an optical motion capture system (B. Mariani, 2010).**

5. *Inertial measurement units.* In order to overcome all these limitations, scientists have introduced ambulatory gait systems, which are valid, easy-to-use and non-obtrusive. The use of accelerometers and gyroscopes for the analysis of human movement was suggested already in the 1970s. However, it is only from the beginning of 2000s that researchers estimation of spatio-temporal parameters is based on the measure of acceleration and angular velocity of trunk, thighs, shanks or feet (Hof, 2003). The rapid development of the Micro Electro Mechanical Systems (MEMS) technology of the last years allows the use of inertial sensors for quantitative gait analysis. Inertial sensors have many advantages: they are ultra-small size, portable and low cost. Furthermore, they do not require a specific laboratory, but they can be used everywhere. However, they are not so practical for the estimation of spatial parameters, because the integration of acceleration signals is subjected to drift. In addition, where the magnetometers are present, they are influenced by the surroundings and so they limit the settings for the analysis.

The future challenge in gait analysis using IMU (Inertial Measurement Units) or MIMU (Magnetic and Inertial Measurement Units) includes three aspects (Z. Wang, 2015):

- The accuracy of gait phases detection during walking, in order to identify gait events and to recognise a pathologic gait.
- The orientation information of lower body segments, which is very important for data analysis.
- The elimination of the accumulative drift error during the integration of acceleration signal by using to the cyclical nature of human walking.

For all these reasons, IMU or MIMU represent a promising technology for the identification of GEs and consequently for the estimation of gait spatio-temporal parameters. The following Figure 1.3.5 shows a subject wearing inertial sensors on feet, on shanks, on thighs, on chest, on wrists and on arms:



Figure 1.3.5\_A typical configuration of inertial sensors (Xsens).

The following Table 1.3.1 shows the most important advantages and disadvantages of the instrumentation adopted for the estimation of gait spatio-temporal parameters:

<b>Instruments</b>	<b>Advantages</b>	<b>Disadvantages</b>
<b>Force platforms</b>	<ul style="list-style-type: none"> <li>- Simple use</li> <li>- Both spatial and temporal parameters</li> </ul>	<ul style="list-style-type: none"> <li>- Extensive laboratory space</li> <li>- Specific environment</li> <li>- High cost</li> </ul>
<b>Instrumented mats</b>	<ul style="list-style-type: none"> <li>- Simple use</li> <li>- Both spatial and temporal parameters</li> </ul>	<ul style="list-style-type: none"> <li>- Extensive laboratory space</li> <li>- Specific environment</li> <li>- High cost</li> </ul>
<b>Footswitches</b>	<ul style="list-style-type: none"> <li>- Portable</li> <li>- Inexpensive</li> </ul>	<ul style="list-style-type: none"> <li>- Longer subject preparation</li> <li>- Temporal parameters only</li> </ul>
<b>Optical motion capture systems</b>	<ul style="list-style-type: none"> <li>- Spatio-temporal parameters</li> <li>- Kinematics measurements</li> </ul>	<ul style="list-style-type: none"> <li>- High cost</li> <li>- Specific laboratory</li> <li>- Small number of steps</li> </ul>
<b>Inertial Measurement Units</b>	<ul style="list-style-type: none"> <li>- Ultra-small size</li> <li>- Portable</li> <li>- Low-cost</li> <li>- Not a specific laboratory</li> </ul>	<ul style="list-style-type: none"> <li>- Drift errors when integrating the acceleration signals</li> <li>- Disturbances for magnetometers</li> </ul>

**Table 1.3.1\_The most important advantages and disadvantages of the instrumentation for the gait spatio-temporal parameters estimation.**

## 1.4 Algorithms for the spatio-temporal parameters estimation with IMUs

One of the first studies to analyze the relationship between measured accelerations and spatio-temporal gait parameters was that of Wiebren Zijlstra e At L. Hof of 2003-2004. They underlined the importance of accelerometers at the level of lower trunk in gait analysis, placing a tri-axial accelerometer at the level of the S2 vertebra. They observed that, during the transition from single to double support, the forward fall of the body changed into an upward movement. For this reason, Zijlstra and Hof affirmed that foot contact coincided with a change of sign of the forward acceleration of the lower trunk. On the basis of these expectations, they proposed the zero-crossing method and the peaks detection method, shown in Figure 1.4.1. According to the first method, the instant of foot contact is the switch from positive to negative; according to the second method, the instant of foot contact is the peak preceding the change of sign.

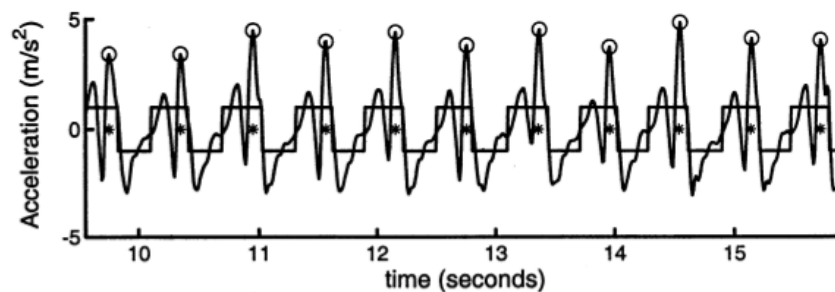


Figure 1.4.1\_Two methods of foot contact detection. Foot contacts detected from acceleration data are indicated by downward slopes of the block signal (zero-crossing method) and by the open circles around peak acceleration values (peak detection method) (Hof, 2003).

Once the heel strikes were individuated, their purpose was to obtain the spatio-temporal parameters of the subject validating through a stopwatch. It was very simple to find the step time, being the interval between two consecutive foot contacts; conversely, it was more complicated to individuate the step length and the walking speed. For this purpose the authors proposed the inverted pendulum model, according to which the vertical movement of the COM during walking was modelled as an approximately horizontal trajectory during double support and as a tracing of a compass during single support (Hof, 1997). According to this model, changes in height of COM depended on step length (Figure 1.4.2). Thus, when changes in height were known, step length could be estimated from geometrical characteristics (Hof, 2003):

$$\text{step length} = 2\sqrt{2lh - h^2}$$

In this equation  $l$  is leg length and  $h$  is the change in height of the COM, calculated by a double integration of the vertical acceleration. After obtaining many step lengths, mean step length was divided by mean step time in order to estimate walking speed.

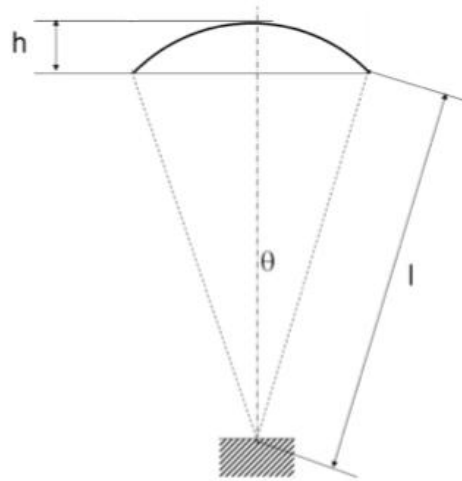


Figure 1.4.2\_ The scheme of the inverted pendulum model (R. C. González, 2007).

In 2004 the same authors noticed that the equation used for the assessment of step length was not so precise and then they decided to introduce, in a first approach, a standard multiplication factor equal to 1.25. In a second approach they obtained individual correction factors. As mean walking speed was known from the marker of the reference system, the individual multiplication factor was calculated as the ratio between mean walking speed and predicted speed (Zijlstra, 2004).

In 2007 R. González and his collaborators considered the work of Zijlstra as the starting point for calculating step time and proposed a modified pendulum model for mean step length estimation. They placed a tri-axial accelerometer at the level of the vertebra L3 and they use two cameras at the beginning and at the end of the walk as gold standard. They affirmed that the step length was the sum of the displacement during single stance phase ( $L_{ss}$ ) and the displacement during double stance phase ( $L_{ds}$ ) (R. C. González, 2007):

$$SL = L_{ss} + L_{ds}$$

They underlined that single stance phase began with the final contact of the contralateral foot and ended with the initial contact of the same foot. As also Zijlstra previously affirmed, the movement of body during the swing phase could be modelled by an inverted pendulum. Instead, the displacement of the hip during double stance could be modelled as the displacement of the centre of pressure in the foot and was proportional to foot length.

$$L_{ss} = 2\sqrt{2lh - h^2}$$

$$L_{ds} = Kp$$

In the first equation  $l$  and  $h$  have the same meaning given by Zijlstra: leg length and height of COM respectively; in the second equation  $K$  is proportionality constant and  $p$  is the foot length.

In 2009 A. Hartmann and her colleagues decided to compute spatio-temporal parameters placing a tri-axial accelerometer at the level of the vertebra S2 and using an electronic walkway with pressure sensors (GAITRite Walkway) as reference system. They demonstrated that the use of an accelerometer allowed measurement in real life conditions and represented a strongly valid means for the assessment of spatio-temporal gait parameters (A. Hartmann, 2009).

During the years the researchers noticed that the acceleration signal was often biased by the gravitational acceleration. Furthermore, they understood that the actual nature of walking also consisted of lower limb rotation around joint articulations. For both these two reasons, the use of miniature angular rate sensors called gyroscopes was proven to be an alternative technique for gait analysis. K. Aminian in 2002 and S. Lee in 2005 computed the values of temporal gait parameters from the angular velocity of shanks and thighs. Aminian and his colleagues decided to place three piezoelectric miniature gyroscopes on the subjects: one on the right shank, one on the left shank and one on the right thigh (K. Aminian, 2002). They used foot pressure sensors as reference system for validation. As Figure 1.4.3 shows, they searched for local minima before and after peaks in order to find toe-off and heel-strikes respectively.

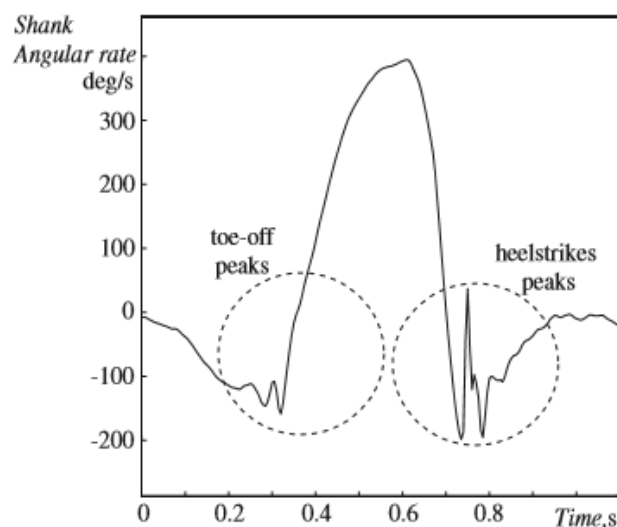


Figure 1.4.3\_Shank angular velocity showing the presence of peaks during the toe-off and heel-strike (K. Aminian, 2002).

In 2005 Lee and his colleagues used four wearing sensors, two on the shanks and two on the thighs. They adopted a motion capture system as the reference for validation (S. Lee, 2005). They identified heel-strikes as the positive spikes of the shanks angular velocity and the toe-off as the negative peaks of the thighs angular velocity. Both Aminian in 2002 and Lee in 2005 found stride time, stance time and double support time as time intervals between gait events. In order to assess spatial parameters, they both used a modified pendulum model. Particularly, Lee proposed a double pendulum model for the entire gait cycle and a new pendulum model for the first half of swing.

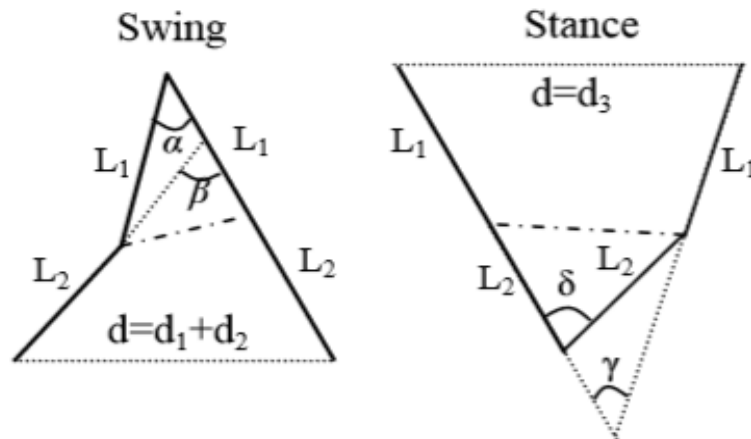


Figure 1.4.4\_Double pendulum model used to estimate stride length in normal gait (S. Lee, 2005).

In Figure 1.4.4  $L_1$  and  $L_2$  are the lengths of thigh and shank respectively. The stride length is broken into three different segments: the value of  $d_1+d_2$  is estimated during swing phase, whereas the value of  $d_3$  is estimated during the stance phase. Considering for example the left foot, there are four important angles used to assess the stride length:  $\alpha$  represents the left thigh rotation,  $\beta$  is the left shank rotation,  $\gamma$  stands for the right thigh rotation and  $\delta$  is the right shank rotation.

The effectiveness of both accelerometers and gyroscopes was investigated by different authors by mean of inertial sensors. As Zijlstra did with a triaxial accelerometer, many other authors decided to place an IMU on the lower trunk, in order to reduce the number of sensors, the quantity of data and the difficulty of analysis.

In 2011 Esser and his colleagues placed an inertial sensor at the level of L4 vertebra and estimated the step time as the interval corresponding to a complete movement of COM, obtained by a double integration of vertical acceleration during one gait cycle. They also estimated step length adopting the reverse pendulum model with a correction factor  $\gamma$  (P. Esser, 2011). In 2012 Bugané and other colleagues evaluated the peaks of the anterior-posterior acceleration measured by an inertial sensor covering the L4-L5 intervertebral space. They chose to validate their work with a motion capture system and two dynamometric platforms and they searched for a lot spatio-temporal parameters (F. Bugané, 2012). In the same year also McCamley worked with an IMU positioned at the lumbar level and searched for gait events as minima and maxima after applying a Gaussian CWT (Continuous Wavelet Transform) to the vertical acceleration.

The following Figure 1.4.5 shows the algorithm they adopted.

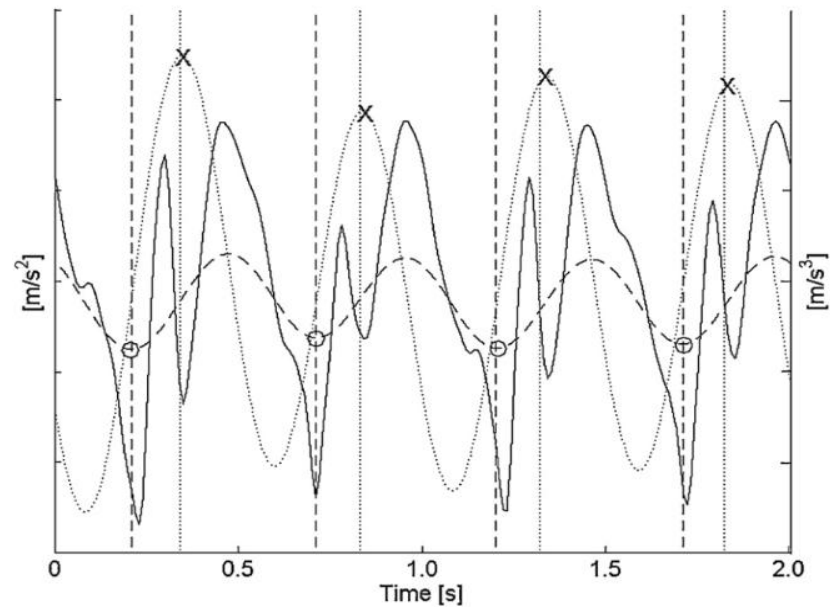


**Figure 1.4.5\_ Method for determining gait events. Vertical acceleration (solid line) is integrated and then differentiated using CWT (dashed line). Minima from this signal correspond to the ICs (O). Further differentiation (dotted line) provides maxima which correspond to the FCs (X). Vertical dashed and dotted lines identify the ICs and the FCs measured from the mat, respectively (J. McCamley, 2012).**

In the same year Köse, Cereatti and Della Croce tried to estimate step length using a single inertial measurement unit attached to the pelvis (Figure 1.4.6) with a stereophotogrammetric system as reference.



**Figure 1.4.6\_ The IMU attached to the belt and positioned to the right side of the subject pelvis (A. Köse, 2012).**

They decomposed the signal in detailed levels and reconstructed it after having applied thresholds. Inside the interval of interest they identified the maxima of vertical acceleration as heel-strikes, as the Figure 1.4.7 shows. Then they identified the minima of anterior-posterior acceleration as toe-off (Figure 1.4.8). Finally, they double integrated the anterior-posterior acceleration and obtained the step length between two consecutive heel-strikes (A. Köse, 2012).

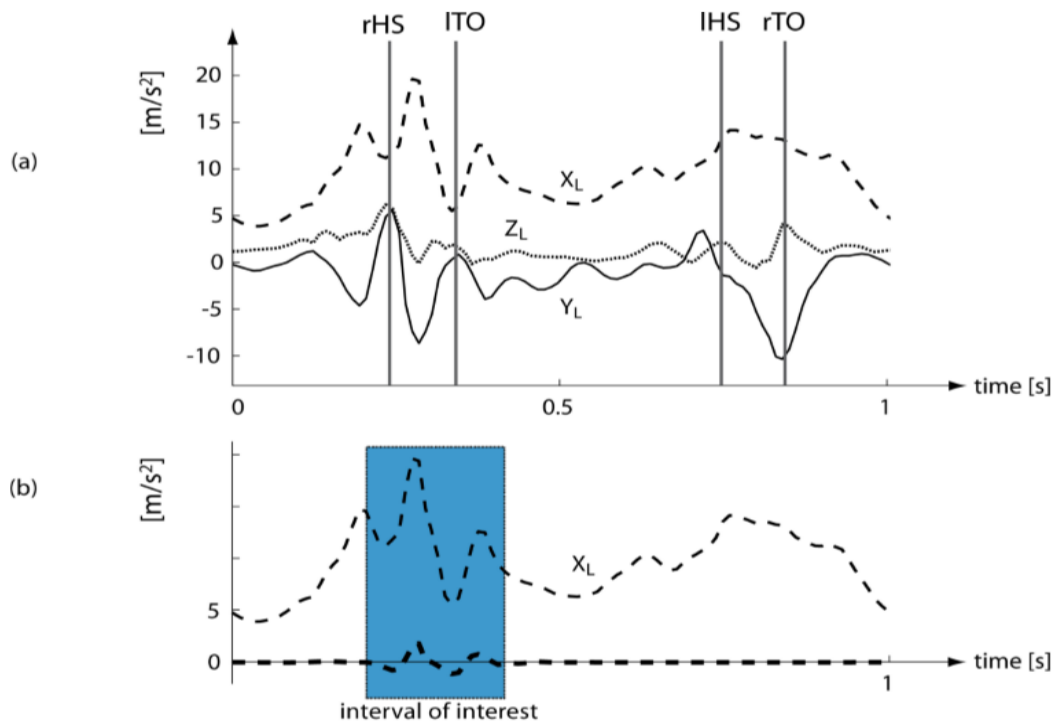


Figure 1.4.7\_ (a) Raw accelerometer signals with gait event timings superimposed (vertical lines). (b) Raw signal on  $X_L$  and corresponding reconstructed signal (thick dashed line) used for the definition of the interval of interest (A. Köse, 2012).

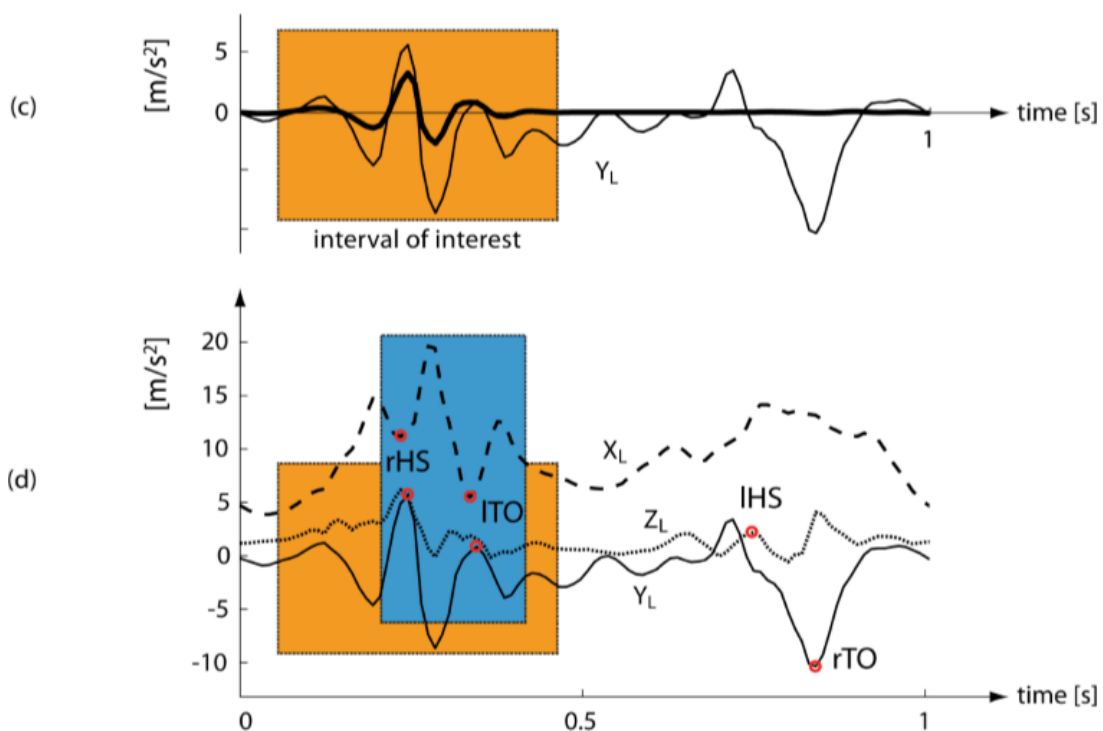


Figure 1.4.8\_ (c) Raw signal on  $Y_L$  and corresponding reconstructed signal (thick line) used for the definition of the interval of interest. (d) Circles show the reference points used to estimate gait events from the raw signals (A. Köse, 2012).

In 2013 Trojaniello, Cereatti and Della Croce made a comparison between accuracy, sensitivity and robustness of five different methods for the estimation of gait temporal parameters by a single sensor mounted on the lower trunk. The Table 1.4.1 describes the five tested methods:

	Sensor type	Sampling rate [Hz]	Sensor position	Subjects #	Shoes	Estimated GEs	Gold standard	Missed/extra GEs	Estimated parameters
Z-method [14]	3-axis acc	100	S2	15	Yes	IC	FPs	No	GEs; mean step length
G-method [11]	IMU	100	L3	6	Yes	IC; FC	FPs	No	Real time GEs
S-method [15]	3-axis acc	50	Waist	1	n.a.	IC	n.a.	n.a.	Step length
M-method [12]	IMU	100	L5	18	n.a.	IC; FC	Instrumented mat	No	GEs
K-method [16]	IMU	100	Right side waist	9	n.a.	IC; FC	SP system	n.a.	Step length

**Table 1.4.1\_Description of the tested gait event detection methods (D. Trojaniello, 2014).**

They tested healthy and barefoot subjects, validating their work with two force platforms and a motion capture system. They compared five methods: Z, G, S, M and K.

The Z-method was the one proposed by Zijlstra and Hof in 2003-2004 and described above. The G-method was introduced by Gonzales in 2010 and was based on the analysis of the filtered acceleration. When the area preceding the zero-crossing of the antero-posterior acceleration overcame a threshold, it was possible to introduce a search window and to identify the initial contact as the peak closest to zero-crossing. The final contact was the first local minimum of vertical acceleration from the instant corresponding to the initial contact (R. C. Gonzalez, 2010).

The Figure 1.4.9 shows the algorithm proposed by Gonzales in order to identify gait events:

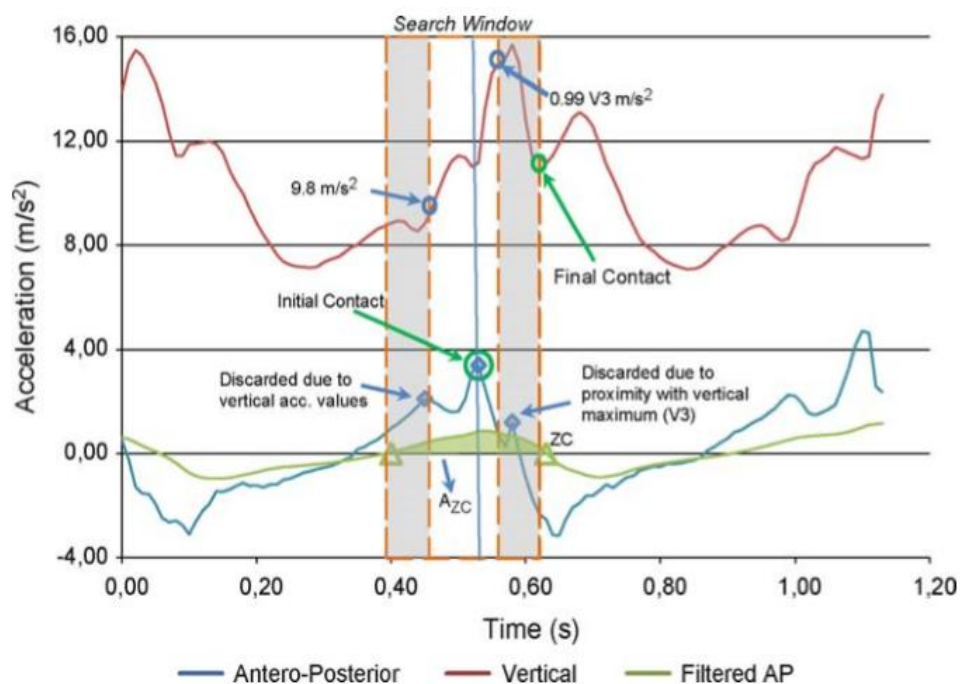


**Figure 1.4.9\_G-method. The algorithm proposed in order to detect gait events (R. C. Gonzalez, 2010).**

The S-method was proposed by Shin and Park in 2011. It consisted of the zero-crossing method applied to the norm of the tri-axial acceleration (Figure 1.4.10).

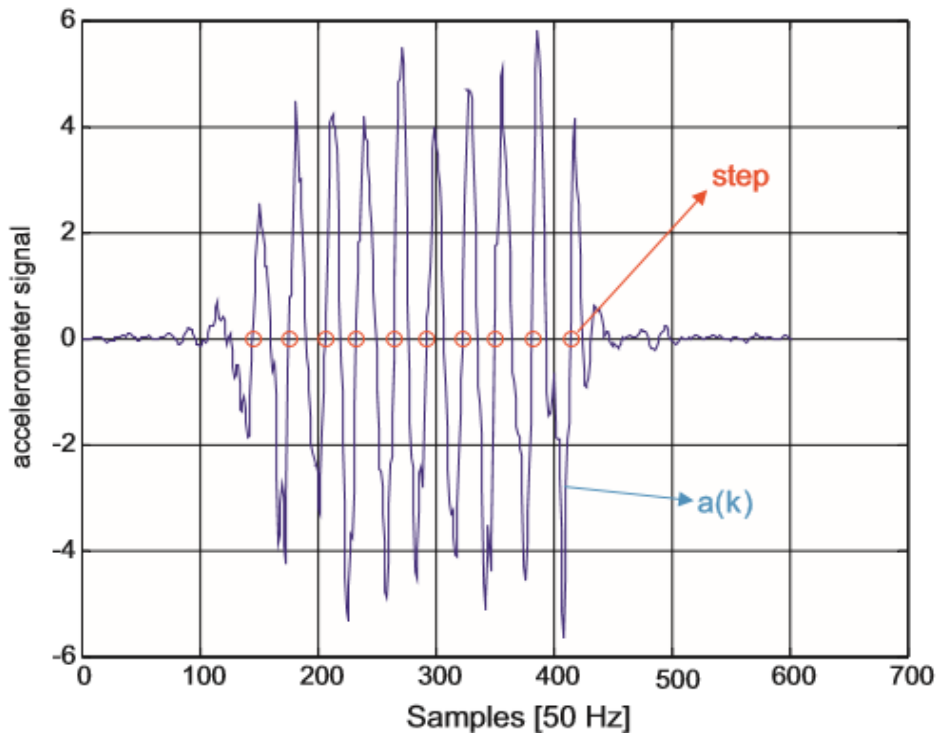


Figure 1.4.10\_S-method. The algorithm proposed in order to detect initial contact (S. H. Shin, 2011).

The last two algorithms, the M-method and the K-method, were those proposed respectively by McCamley and Köse in 2012 and already described above.

Trojaniello and her colleagues affirmed that all five methods were able to identify the initial contact in a correct way and for this reason the accuracy of stride and step time was acceptable.

The final contact was identified only for the methods G, M and K: in all of them there was imprecision in the assessment of stance, swing and double support time. Furthermore, the methods Z, S and M were accurate regardless of the exact position of the trunk sensor (D. Trojaniello, 2014).

Authors underlined that, even if placing a sensor near the CoM was very helpful, system based on MEMS gyroscopes and accelerometers suffered from measurement errors and integration drifts. These problems could be reduced by placing sensors on feet and assuming null velocity during foot-flat period of stance.

In 2010 B. Mariani and his collaborators placed two inertial wireless sensors on the back of the feet and used a motion capture system as reference. They placed three markers on each inertial sensor. In this way, they knew the initial conditions of position and orientation and so they obtained 3D vectors of orientation, velocity and trajectory by integrating the acceleration. From these vectors they were able to compute spatio-temporal parameters (B. Mariani, 2010).

Three years later, Mariani made another study placing an inertial sensor over the basis of first and second metatarsals. His purpose was to test the efficacy of inner-stance phase estimations as a potential outcome for clinical gait analysis. The Figure 1.4.11 shows the subphases of the stance phase:

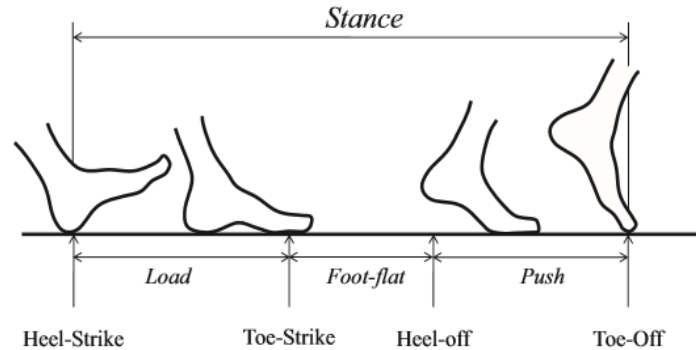


**Figure 1.4.11\_Temporal events during stance and corresponding inner-stance phases (B. Mariani, 2013).**

Mariani and his colleagues chose forty-two subjects and used pressure measuring pads as reference system for validation (Figure 1.4.12). Twelve subjects were healthy, whereas the other thirty had ankle orthopaedic disorders.



**Figure 1.4.12\_The configuration of measurement systems: an inertial measurement unit fixed on forefoot and a pressure-insole beneath the foot (B. Mariani, 2013).**

The authors analyzed four signals: the angular velocity, the derivative of the norm of the angular velocity, the norm of acceleration and the modulus of the derivative of the norm of acceleration (Figure 1.4.13). In this way they could be independent from IMU positioning. They searched for gait events as peaks or values compared to thresholds and finally they estimated temporal parameters such as stance time, load time, foot-flat time and push time by calculating time differences between these events (B. Mariani, 2013). In the conclusions they affirmed that the algorithm accuracy and precision were acceptable. According to their opinion, the readiness of the method adopted allowed to imply it for clinical use. Furthermore, they said that the search for heel-strike and toe-off gave better results if it was made in the acceleration signal. On the contrary, the search for heel-off and toe-strike was more accurate if it is made within the angular velocity signal.

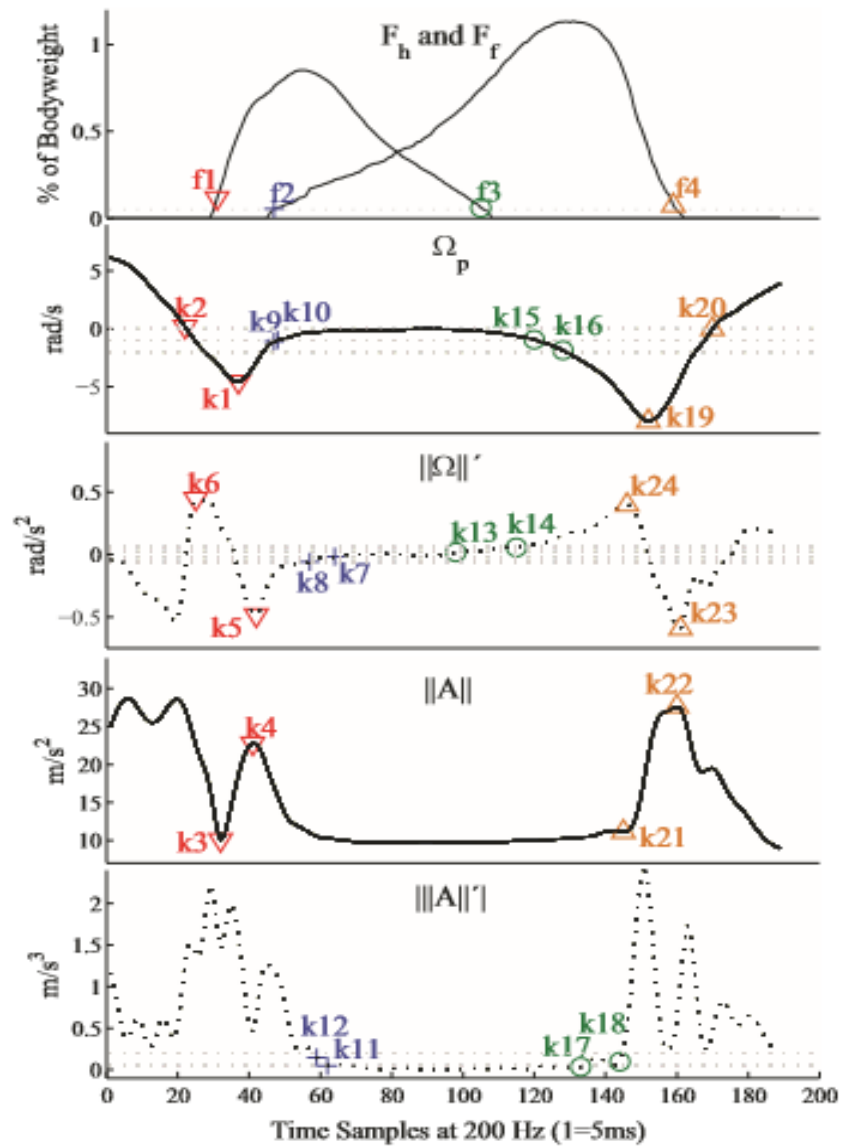


Figure 1.4.13\_ Kinematic and force signals with the detected features at Heel-strike ( $\nabla$ ), Toe-Strike (+), Heel-Off (o), and Toe-Off ( $\blacktriangle$ ), showed for one typical gait cycle of a healthy subject (B. Mariani, 2013).

In the same year Yang and Zhang used two inertial sensors placed laterally on the shanks in order to estimate spatio-temporal parameters for post-stroke hemiparetic gait. They found gait events on the basis of the angular velocity (S. Yang, 2013).

In 2014 Trojaniello, Cereatti et Al proposed and validated a method based on two MIMUs attached above subjects' ankles, using the GAITRite walkway as reference (Figure 1.4.14). They tested 40 elderly subjects: 10 healthy and 30 with different neurological diseases.



**Figure 1.4.14\_A subject wearing two MIMUs attached above the ankles and walking on the instrumented mat (D. Trojaniello, 2014).**

The authors decided to analyse the medio-lateral angular velocity and the antero-posterior acceleration. In order to reduce the search interval of initial and final contact, they eliminated the part of signal without events (Trusted swing interval) and the part of signal corresponding to the stance of the opposite leg (Trusted stance interval). They searched for gait events in the remaining interval and they identified the initial contact as the minimum of angular velocity and the final contact as the maximum of acceleration. Finally, they calculated stride time, step time, swing time and stance time as intervals between gait events (D. Trojaniello, 2014).

In their conclusions the authors underlined the efficacy of their algorithm in the reduction of the search interval of gait events. Furthermore, they affirmed that the method proposed was robust, because there were no missed or extra gait events. The performances were independent from the walking speed and precision was similar between healthy and pathologic subjects.

The Figure 1.4.15 shows the algorithm proposed by Trojaniello and her colleagues, with a particular attention to the reduction of the search interval for gait events. The signals are referred to affected side of a hemiparetic subject.

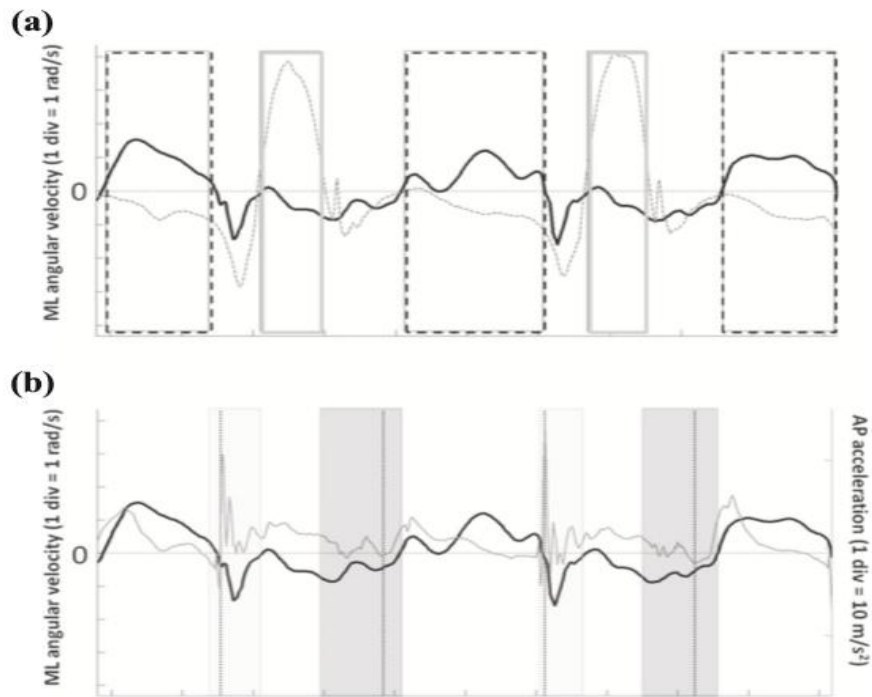


Figure 1.4.15\_ (a) Angular velocities in the sagittal plane (black one for the affected side). Rectangular frames represent trusted swing (dotted line) and trusted stance (solid line) intervals. (b) Medio-lateral angular velocity (black line) and AP acceleration (gray line). Coloured boxes represent time intervals for the IC (light gray) and FC (intense gray) search; vertical lines represent the GEs instants (D. Trojaniello, 2014).

In 2015 both Z. Whang and A. Rampp decided to place two IMUs laterally right below each ankle joint and to analyze the angular velocity in the sagittal plane. Whang tested 10 healthy subjects with their shoes and searched for toe-off and heel-strikes as minima before and after peaks respectively. Toe-strikes and heel-off, instead, were identified as values which overcame a threshold given by the average of angular velocity during stance (Figure 1.4.16).

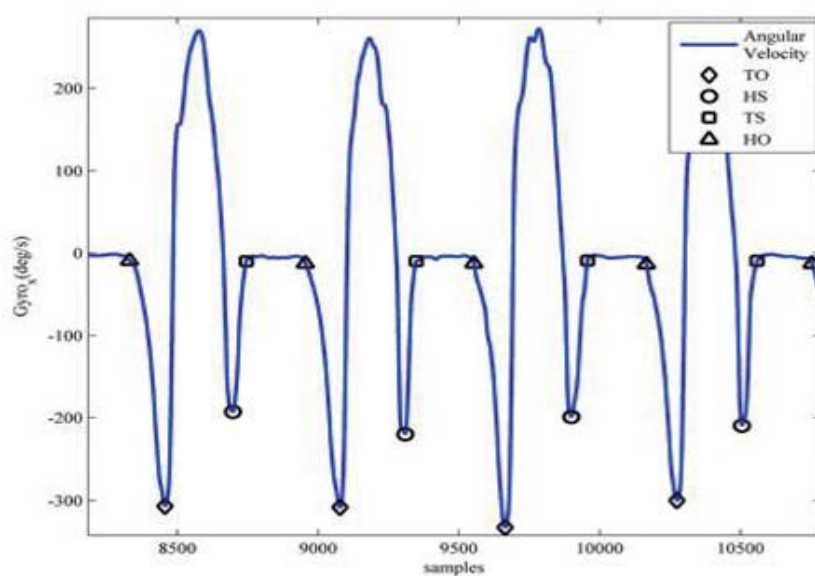


Figure 1.4.16\_The ankle angular velocity in the sagittal plane with GE marked with four symbols (Z. Wang, 2015).

Rampp and his colleagues tested 116 geriatric subjects with shoes, using the GAITrite Walkway as the reference system for validation. As the Figure 1.4.17 shows, they placed the IMU laterally on the shoes:

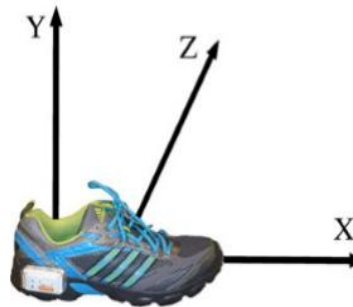


Figure 1.4.17\_Placement of the sensor and direction of axis (A. Rampp, 2015).

The authors analyzed the angular velocity around the sensor z-axis and applied the template matching in order to segment it. Then, they searched for heel-strikes and toe-off as minima and zero-crossing respectively. They also found mid stance as the middle of the window with the lowest energy. In order to verify that these gait events were correct, they checked these points in the acceleration along the sensor x-axis. Temporal parameters were obtained as time intervals between gait events (Figure 1.4.18).

Step length was estimated by double integrating the acceleration along the sensor x-axis. In order to eliminate drift, the velocity corresponding to the foot-flat was considered null and so the signal was integrated between two consecutive instants of mid stance.

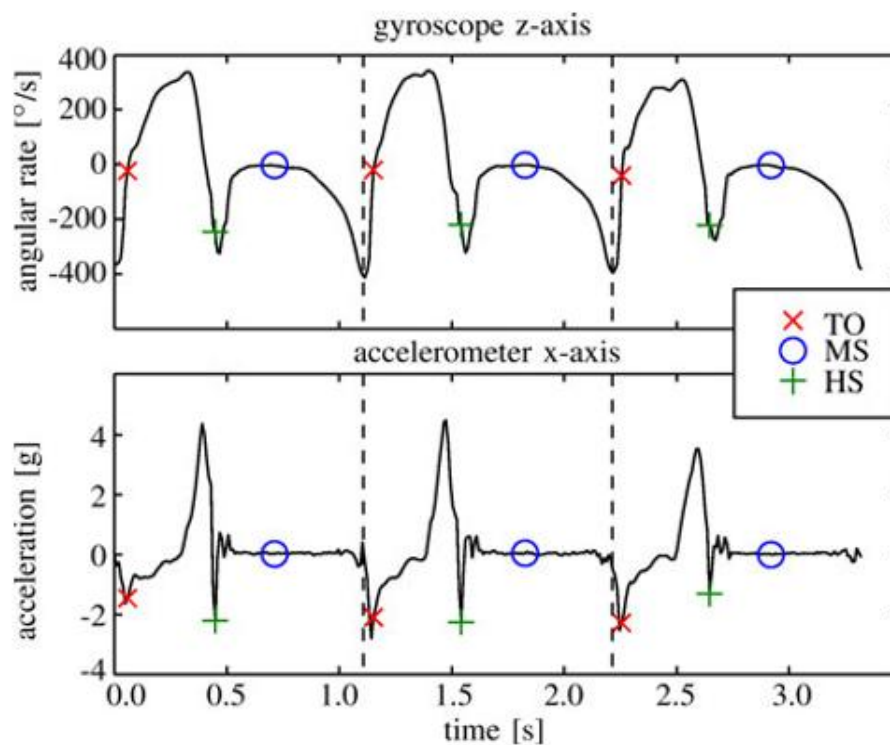
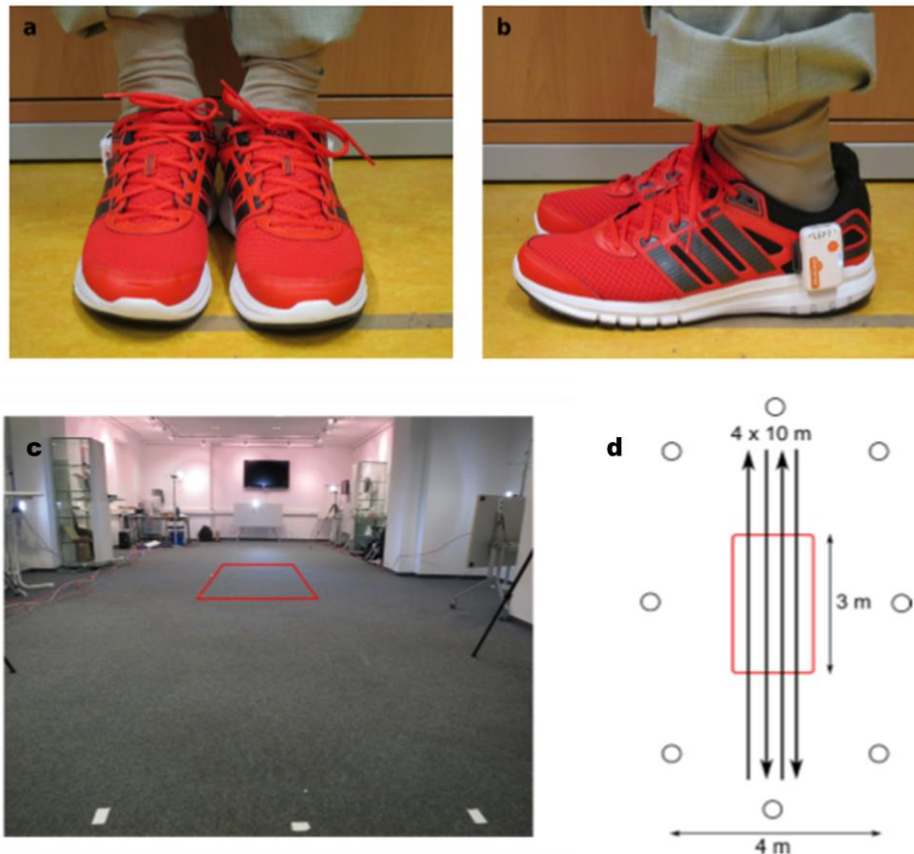


Figure 1.4.18\_Three segmented strides with TO, HS and MS events of a typical gait signal (A. Rampp, 2015).

In 2017 the same algorithm proposed by Rampf was tested by Kluge and his colleagues on 14 subjects: 10 healthy and 4 with Parkinson's disease. Two inertial sensors were placed laterally on the feet and a system of optical motion capture was used as reference for validation. The authors searched for toe-off as the zero-crossings of the angular velocity in the sagittal plane and for heel-strikes as the negative peaks of the anterior-posterior acceleration (F. Kluge, 2017). The placement of the sensors and the setting adopted for the test are shown in Figure 1.4.19:



**Figure 1.4.19\_** (a) Attachment of the sensors to the shoes: frontal view; (b) Attachment of the sensors to the shoes: lateral view; (c) Measurement setup; (d) Placement of cameras around the 10 m walkway. The test is repeated 4 times, as shown in the scheme (F. Kluge, 2017).

In the same year Lanovaz decided to validate a commercial inertial sensor system for spatio-temporal gait measurement in children (J. L. Lanovaz, 2017), whereas Misu compared the accuracy of two different methods for the assessment of temporal parameters (S. Misu, 2017). The last one and his colleagues placed two inertial sensors on the heels and tested 20 barefoot subjects: 10 young and 10 elderly. The reference system for validation consisted of two pairs of force-sensitive resistors attached under the feet.

The Figure 1.4.20 shows the placement of the inertial sensors on the heels.



Figure 1.4.20\_ Location of sensor attached on subject (S. Misu, 2017).

In the first method, called A-V method, they proposed to search for heel-strikes as peaks of vertically directed acceleration and for toe-off as peaks of the angular velocity in the sagittal plane. In the second method, the V-V one, they identified both the toe-off and the heel-strikes in the sagittal angular velocity. The TO were defined as the peaks and the HS as the maxima among the peaks. The Figure 1.4.21 and the Figure 1.4.22 shows the A-V method and the V-V method, respectively.

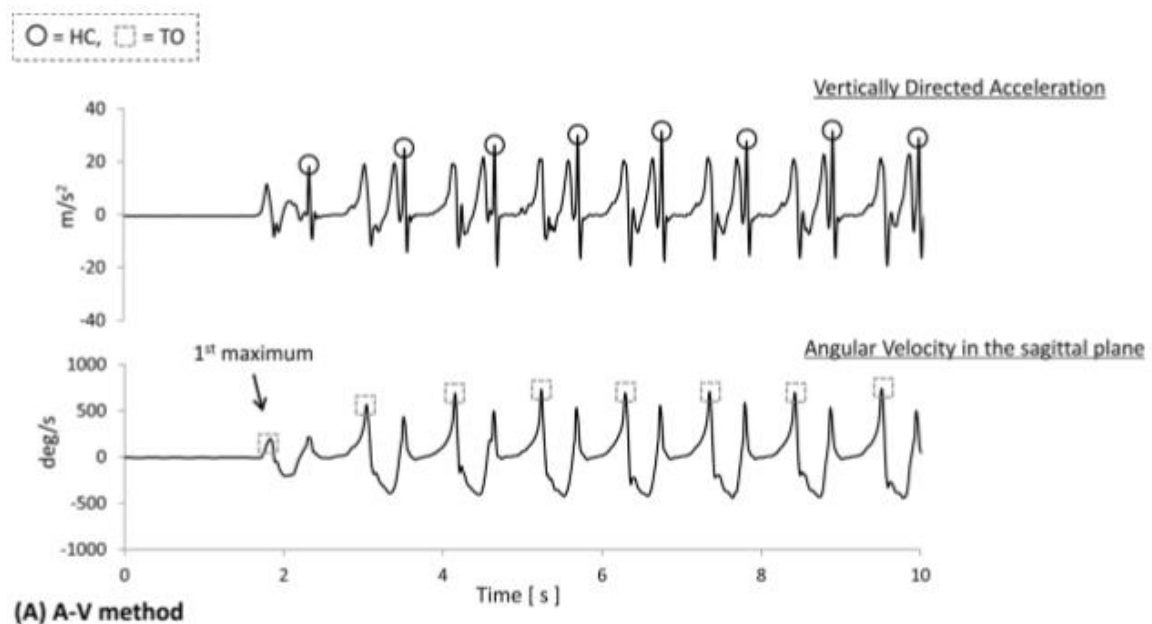


Figure 1.4.21\_ Diagram of the determination of gait events in the A-V method. Solid circles indicate the instants of HC and dashed squares indicate the instants of TO (S. Misu, 2017).

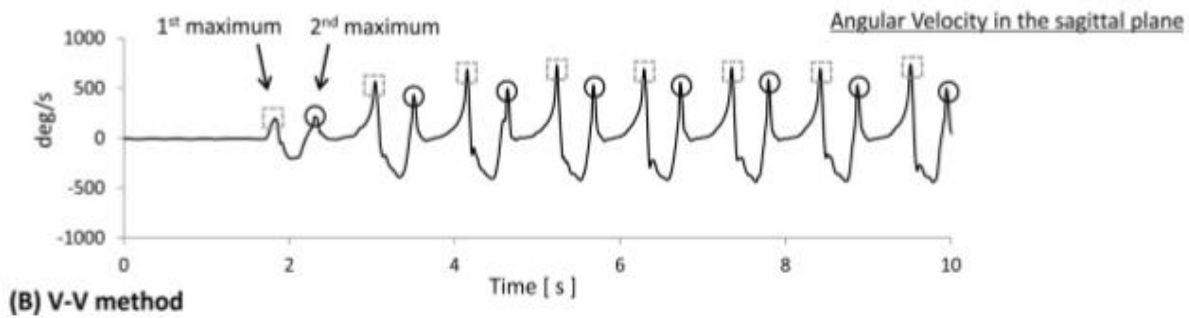


Figure 1.4.22\_ Diagram of the determination of gait events in the V-V method. Solid circles indicate the instants of HC and dashed squares indicate the instants of TO (S. Misu, 2017).

In conclusion, in literature there are so many studies and works which involved the use of inertial sensors for the estimation of spatio-temporal parameters. The desire was always to find a simple and effective algorithm in order to achieve this purpose as precisely as possible. The positioning of IMUs was varied: on trunk, on pelvis, on heels, on feet, on shanks. In general, the farther from the contact point the IMU is placed, the more complicated the identification of gait events is (D. Trojaniello, 2014). For this reason, the positioning of the inertial sensors on feet or heels allows to obtain more precise results. Furthermore, it facilitates the estimation of spatial parameters such as stride length or step length, because it allows to consider the foot-flat velocity null and to double integrate between two consecutive mid-stance instants. However, on the other hand, the feet and the heels are the two anatomical points subjected to greater movement during gait. As a result, sometimes it is preferred to place IMUs on shanks, on trunk or on pelvis, which are more rigid segments and allow a firmer attachment. In particular, the sensor on trunk or on pelvis allows to obtain all the information from a single IMU, also facilitating the clinical applications.

In addition to the search for the correct point to position the sensors, another central element is the health of the subjects. Many works only analyzed the gait of healthy populations, but many others tried to apply their algorithms also to pathologic subjects.

Today, the search for spatio-temporal parameters has numerous applications. The future aim is to develop increasingly precise algorithms solving problems such as drift and sensor positioning. Furthermore, the diffusion of sensors in clinical field is dictated by the need to analyze and better understand some specific neurological or musculoskeletal pathologies.

The following Table 1.4.2 summarizes all the articles used as references for this thesis. Every line is referred to a specific article. In the first column there are the paper titles, in the second one the spatio-temporal parameters estimated, in the third one the instrumentation adopted and in the fourth one the algorithm developed.

Articles	Spatio-temporal parameters	Instrumentation	Algorithm
"Spatio-temporal parameters of gait measured by an ambulatory system using miniature gyroscopes" Aminian, Najafi et Al (2002)	Stride time Stance time DS time Stride length Stride velocity	Three piezoelectric miniature gyroscopes (Murata): two on the shanks and one on the right thigh. Reference: foot pressure sensors (FSRs) under the right foot (two under the jaw and two under the heel).	<u>Temporal parameters:</u> - wavelet decomposition of angular velocity of shank - identification of local maxima (MS) - search for local minima after peaks (HS and TO) - calculation of differences between HS and TO. <u>Spatial parameters:</u> - application of double pendulum model for swing - application of double inverse pendulum model for stance
"Assessment of spatio-temporal gait parameters from trunk acceleration during human walking" Zijlstra e Hof (2003)	Stride time Step time Step length Walking speed	Tri-axial accelerometer (Kistler) at the level of S2 vertebra. Reference: two force transducers placed on a treadmill and a stopwatch.	<u>Temporal parameters:</u> - application of two methods (zero-crossing and peak detection) to antero-posterior acceleration in order to identify HS - calculation of stride and step times by differences <u>Spatial parameters:</u> application of reverse pendulum model to vertical acceleration
"Assessment of spatio-temporal parameters during unconstrained walking" Zijlstra (2004)	Stride time Step time Step length Walking speed	Tri-axial accelerometer (Kistler) at the level of S2 vertebra. Reference: stopwatch.	<u>Temporal parameters:</u> - application of the peak detection method to the antero-posterior acceleration in order to identify HS - calculation of step and stride times by differences. <u>Spatial parameters:</u> application of reverse pendulum model with correction factor to vertical acceleration.
"Detection of spatio-temporal gait parameters by using wearable motion sensors" Lee, Mase et Al (2005)	Stride time Stance time DS time Stride length	Four wearing sensors (NEC) at thighs and shanks. Reference: motion capture system (Vicon) with six markers (four on the sensors and two on the feet).	<u>Temporal parameters:</u> - peak detection in rotation angles (positive spikes at the tibia to identify HS, negative at the thigh to identify TO) - calculation of the various times by differences <u>Spatial parameters:</u> - double pendulum model for the entire gait cycle - double pendulum model for the first half of swing.
"Modified pendulum model for mean step length estimation" Gonzales, Alvarez et Al (2007)	Step time Step length	Tri-axial accelerometer (Xsens MTx) at the level of L3 vertebra. Reference: two cameras at the beginning and at the end of the walk and signs on the floor at every cm.	<u>Step time:</u> - search for maxima of main acceleration harmonica (HS = maxima of antero-posterior acceleration, TO = local minima of vertical acceleration) - calculation of step time by difference <u>Step length:</u> - application of reverse pendulum model for single stance phase - application of direct proportion pattern over the length of the foot for double stance phase
"Concurrent validity of a trunk tri-axial accelerometer system for gait analysis in older adults" Hartmann, Luzi et Al (2009)	Walking speed Cadence Step time Step length	Tri-axial accelerometer (DynaPort) at level of S2 vertebra. Reference: electronic walkway with pressure sensors (GAITRite system).	Algorithm not described.

<p>"3D gait assessment in young and elderly subjects using foot-worn inertial sensors" Mariani, Hoskovec et Al (2010)</p>	<p>Stride length Walking speed Foot clearance Turning angle</p>	<p>Two inertial wireless sensors (S-Sens) on the back of the foot. Reference: motion capture system (Vicon) with three markers on each inertial sensor.</p>	<p><u>S-T parameters:</u> - timing of cycles - knowledge of initial conditions of position and orientation - integration of acceleration without gravity and drift - determination of 3D vectors of orientation, velocity and trajectory - calculation of the parameters from these vectors</p>
<p>"Assessment of spatio-temporal gait parameters using inertial measurement units in neurological populations" Esser, Dawes et Al (2011)</p>	<p>Step length Step time Walking speed</p>	<p>Inertial sensor (Xsens MTx) at the level of L4 vertebra. Reference: stopwatch.</p>	<p><u>Step length:</u> - application of reverse pendulum model with correction factor to vertical acceleration <u>Step time:</u> - double integration of vertical acceleration in order to calculate the complete movement of CoM - calculation of step time as the time interval corresponding to the movement of CoM <u>Walking speed:</u> - ratio between mean step length medium and mean step time</p>
<p>"Bilateral step length estimation using a single inertial measurement unit attached to the pelvis" Köse, Cereatti e Della Croce (2012)</p>	<p>Step length</p>	<p>Inertial sensor (FreeSense Sensorize) on the right side of the body at the pelvis level. Reference: stereophotogrammetric system.</p>	<p><u>Step length:</u> - decomposition of signal in detail levels - signal reconstruction after threshold application - observation of the interval of interest - identification of HS and TO from maxima and minima of vertical and antero-posterior accelerations - integration of antero-posterior acceleration - calculation of step length by difference</p>
<p>"Estimation of spatio-temporal gait parameters in level walking based on a single accelerometer: validation on normal subjects by standard gait analysis" Bugané, Benedetti et Al (2012)</p>	<p>Stride length Step length Stride time Step time Stance time Swing time SS e DS duration Foot symmetry Walking speed Cadence</p>	<p>Inertial sensor (F4A) in correspondence of the space between L4 and L5 vertebrae. Reference: motion capture system (Vicon) and two dynamometric platforms (Kistler Instruments).</p>	<p><u>Temporal parameters:</u> - identification of the second peak of antero-posterior acceleration as HS - calculation of times by differences <u>Spatial parameters:</u> - double Integration of antero-posterior acceleration</p>
<p>"An enhanced estimate of initial contact and final contact instants of time using lower trunk inertial sensor data" John McCamley, Marco Donati et Al (2012)</p>	<p>Stride time Step time</p>	<p>Inertial sensor (Freesense Sensorize) at the lumbar level. Reference: instrumented mat of 4 meters.</p>	<p><u>Temporal parameters:</u> - application of a Gaussian CWT to vertical acceleration - identification of HS as minimum and TO as maximum - calculation of times by differences</p>
<p>"Quantitative estimation of foot-flat and stance phase of gait using foot-worn inertial sensors" Mariani, Rouhani et Al (2013)</p>	<p>Stance duration Load duration Foot-flat duration Push duration</p>	<p>Inertial sensors over the basis of first and second metatarsals. Reference: pressure measuring pads (Pedar-X).</p>	<p><u>Temporal parameters:</u> - analysis of the angular velocity, the derivative of its norm, the norm of acceleration and the modulus of its derivative - identification of HS and TO as peaks - identification of TS and HO on the basis of thresholds - calculation of times by differences</p>

<p>"Accuracy, sensitivity and robustness of five different methods for the estimation of gait temporal parameters using a single IMU mounted on the lower trunk" Trojaniello, Cereatti and Della Croce (2013)</p>	<p>Stride time Step time Stance time Swing time DS time</p>	<p>Inertial (Opal) sensor at the waist level. Reference: two force platforms (AMTI) and a stereophotogrammetric system (Vicon).</p>	<p><u>Temporal parameters:</u> - identification of gait events through 5 algorithms 1) Z-method. Application of the peak-detection method to antero-posterior acceleration in order to identify HS. 2) G-method. Identification of HS and TO peaks through zero-crossing method and some heuristic rules. 3) S-method. Identification of HS using the zero-crossing method applied to the curve obtained with a sliding window. 4) M-method. Identification of HS and TO respectively as minima and maxima after applying a Gaussian wavelet transformation. 5) K-method. Signal reconstruction after decomposition in levels and threshold application: identification of HS and TO on the basis of maxima and minima of vertical and antero-posterior acceleration. - calculation of parameters by differences</p>
<p>"Estimation of spatio-temporal parameters for post-stroke hemiparetic gait using inertial sensors" Yang, Zhang et Al (2013)</p>	<p>Walking speed Swing duration Stance duration TS ratio</p>	<p>Two inertial sensors (Inertia Link) placed laterally on the tibia. Reference: stopwatch.</p>	<p><u>Walking speed:</u> - segmentation and single integration of acceleration <u>Swing duration, stance duration and temporal symmetry ratio:</u> - HS and TO peaks identification on the basis of angular velocity - calculation of parameters between gait events</p>
<p>"Estimation of step-by-step spatio-temporal parameters of normal and impaired gait using shank-mounted magneto-inertial sensors: application to elderly, hemiparetic, parkinsonian and choreic gait" Trojaniello, Cereatti et Al (2014)</p>	<p>Stride time Step time Swing time Stance time Stride length</p>	<p>Two magneto-inertial sensors (Opal, APDM) just above the malleolus. Reference: GAITRite Electronic Walkway.</p>	<p><u>Temporal parameters:</u> - definition of time intervals in which HS and TO can be found excluding trusted swing and trusted stance intervals - identification of HS as the minimum value of the mid-lateral angular velocity and of TO as the minimum value of antero-posterior acceleration - calculation of times by differences <u>Stride length:</u> - double integration of antero-posterior acceleration</p>
<p>"Estimate spatial-temporal parameters of human gait using inertial sensors" Wang and Ji (2015)</p>	<p>Stance duration Swing duration Walking velocity Stride length</p>	<p>Two inertial sensors laterally on feet and facing outwards. Reference: stopwatch.</p>	<p><u>Temporal parameters:</u> - angular velocity segmentation in observation windows - identification of TO and HS respectively as minima before and after peaks and of TS and HO as values exceeding a threshold - calculation of temporal parameters by differences <u>Walking velocity:</u> - single integration of antero-posterior acceleration <u>Stride length:</u> - double integration of antero-posterior acceleration</p>

<p>"Inertial sensor-based stride parameter calculation from gait sequences in geriatric patients" Rampp, Barth et Al (2015)</p>	<p>Stride time Swing time Stance time Stride length</p>	<p>Inertial Platform (Shimmer 2R) laterally on the foot. Reference: electronic walkway containing pressure sensors (GAITRite system).</p>	<p><u>Temporal parameters:</u> - segmentation of angular velocity and antero-posterior acceleration through template matching - identification of TO and HS respectively at zero-crossing and minimum angular velocity peak - calculation of temporal parameters by differences <u>Stride length:</u> - double integration of antero-posterior acceleration</p>
<p>"Development and validity of methods for the estimation of temporal gait parameters from heel-attached inertial sensors in younger and older adults" Misu, Asai et Al (2017)</p>	<p>Stride time Step time Swing time Stance time</p>	<p>Two inertial sensors (MVP-RF8) on the right and left heel surfaces. Reference: force resistors (FSRs).</p>	<p><u>Temporal parameters:</u> - application of two methods: 1) A-V method. Identification of HS and TO respectively as vertical acceleration peaks and sagittal angular velocity peaks. 2) V-V method. Identification of TO and HS respectively as peaks and maxima among peaks of sagittal angular velocity. - for both methods calculation of times by differences.</p>
<p>"Towards Mobile Gait Analysis: Concurrent Validity and Test-Retest Reliability of an Inertial Measurement System for the Assessment of Spatio-Temporal Gait Parameters" Kluge, Gaßner et Al (2017)</p>	<p>Stride time Stance time Swing time Stride length Velocity</p>	<p>Two inertial sensors (Shimmer3) laterally on the ankles. Reference: motion capture system.</p>	<p><u>Temporal parameters:</u> - segmentation of angular velocity and antero-posterior acceleration through template matching - identification of TO and HS respectively as zero-crossing of the angular velocity and maximum decelerations in the direction of advancement - calculation of times as differences <u>Velocity:</u> - single integration of the antero-posterior acceleration <u>Stride length:</u> - double integration of the antero-posterior acceleration</p>
<p>"Validation of a commercial inertial sensor system for spatiotemporal gait measurements in children" Lanovaz, Oates et Al (2017)</p>	<p>Stride time Stance time Stride length Stride velocity</p>	<p>System of six inertial sensors (MobilityLab) on the back at L4-L5 and on the front of the legs near the malleolus. Reference: motion capture 3D system (Vicon) with markers on lateral femoral condyles, malleols, heels, and toes.</p>	<p><u>Temporal parameters:</u> - wavelet decomposition of angular velocity of shank - identification of local maxima (MS) - search for local minima after peaks (HS and TO) - calculation of differences between HS and TO <u>Spatial parameters:</u> - application of double pendulum model for swing - application of double inverse pendulum model for stance</p>

**Table 1.4.2\_A summarize of the articles used as references. It contains: the paper titles, the spatio-temporal parameters estimated, the instrumentation adopted and the algorithms developed.**

## 2. Motion capture systems

### 2.1 Stereophotogrammetric system: Optitrack

#### 2.1.1 Optical Motion Capture System

Since in a qualitative biomechanical analysis most of the qualities of a performance can be discerned using the vision, optical motion capture systems have a central role in this field. Components of a typical motion capture system usually include:

- one or more video cameras working in the infrared;
- passive or active markers visible from the cameras;
- a specialized software for the data organization and the digital representation of the movement.

The cameras produce sequential two-dimensional images of movement at specific time intervals depending on the speed and, consequently, on the frame rate. For example, the time between two consecutive frames recorded by a camera operating at 120 frames per second is  $1/120$  s or 0.0833 s. In a single recorded image the position of the body and its parts can be obtained relative to a fixed reference or to each other, whereas in subsequent images it is possible to determine the changes in position. All these analyses are feasible thanks to the presence of a set of markers visible in the infrared on the body of interest. When optical motion capture systems are involved in the analysis of human movement, the markers are placed on subjects (Figure 2.1.1). Once the human body is modelled as a system of rigid links connected through the joints, markers are attached to each body segment to define their 3D location and orientation (McGinnis, 2013).

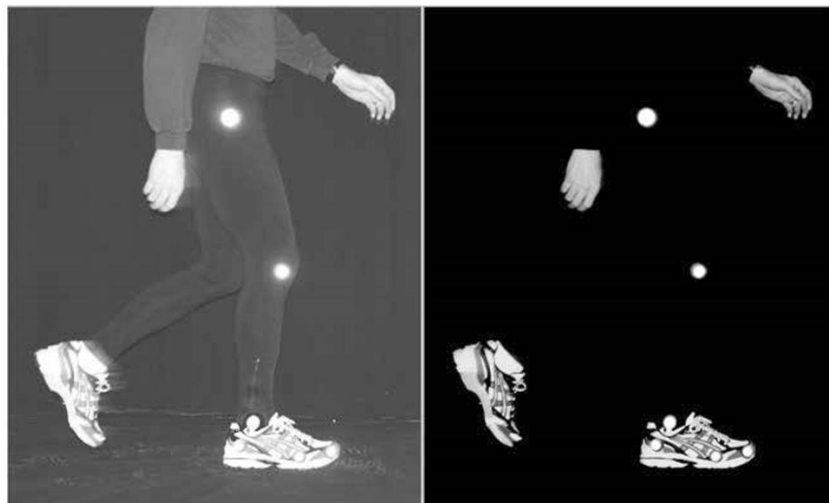


Figure 2.1.1\_The photo on the left shows the markers on the subject under normal lighting conditions. The photo on the right shows the same subject with lighting and camera exposure set to highlight only the markers (McGinnis, 2013).

Markers used by optical motion capture systems can be of two types, passive or active. Passive markers are spherical plastic supports covered with reflective film, whereas active markers are LED generating light signal in the infrared. The Table 2.1.1 summarizes the most important characteristics of passive and active markers:

Passive markers	Active Markers
Additional lighting device with specific wavelengths (780-820 nm)	No need of an additional lighting device and operation even in the dark
No need to power the devices	Need to power the devices
Need of pre-processing in order to identify and classify markers	No need of pre-processing in order to identify and classify markers
Possibility of markers occlusion	Possibility of markers occlusion
No need for cable synchronization	Need for cable synchronization

Table 2.1.1\_Summary of the most important characteristics of passive and active markers.

One camera may be enough to adequately record a two-dimensional or planar motion. However, if the need is to obtain three-dimensional coordinates of the body, it is advisable to record the movement by two or more cameras. The operation of the software that computes 3D coordinates from the 2D data of each camera is based on the concept of human stereoscopic vision. It represents the ability to perceive the three-dimensional nature of the objects thanks to the combined use of both eyes. The brain receives two different images of the same object from eyes and combines them into a single new three-dimensional view. In the same way stereophotogrammetry gives the x, y, z coordinates of a certain point in the fixed reference system of the setting. The following Figure 2.1.2 shows the comparison between the stereoscopic vision of the human brain and the stereophotogrammetry mechanism of an optical motion capture system.

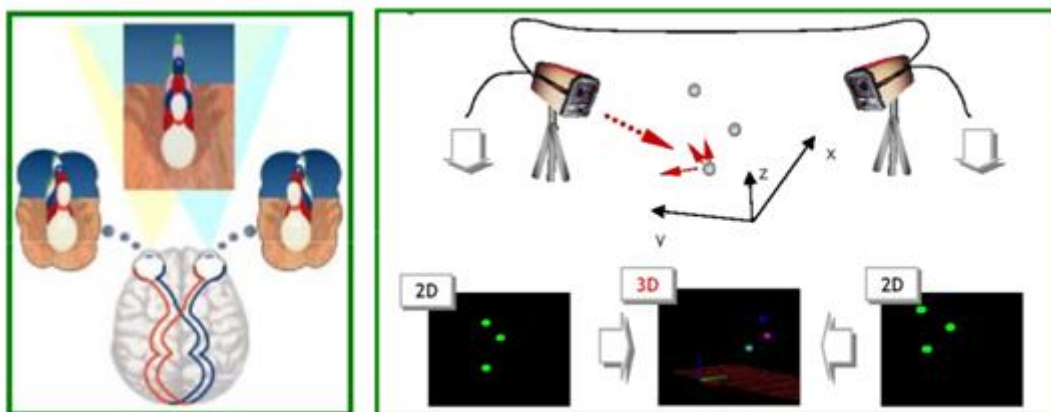


Figure 2.1.2\_ Stereoscopic vision of the brain vs stereophotogrammetry of a motion capture system software.

### 2.1.2 V120:Trio

In 2011 Optitrack has introduced a new optical motion capture system called V120:Trio. The most important quality of this tracking system is to offer the power of multiple-camera in a unique and compact solution. As the Figure 2.1.3 shows, each tracking bar V120:Trio has three cameras that detect reflected infrared light. The central one also allows to realize videos in the visible spectrum. The bars are self-contained, pre-calibrated and ready to track immediately after starting the software. These aspects make the system simple to use, but also very accurate and flexible. Furthermore, these tracking bars are easy to carry, enabling simple transport and rapid deployment of the entire Optitrack system. The V120:Trio is able to capture fast movements and to track markers down to sub-millimeter motions with high accuracy.

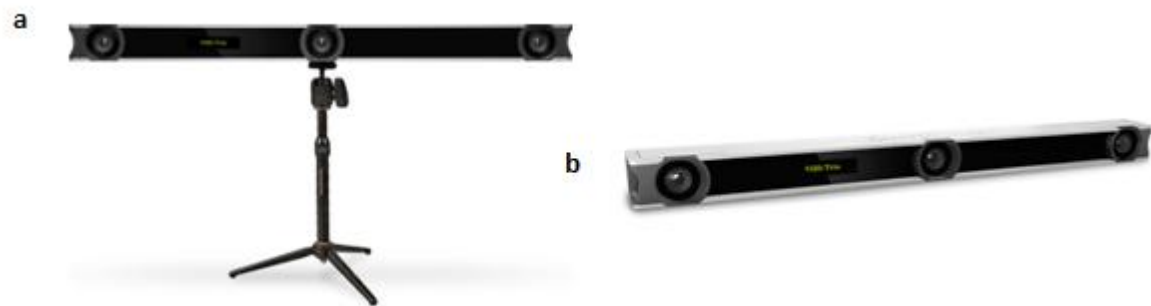


Figure 2.1.3\_a) Photo of V120:Trio on its tripod. c) Photo of V120:Trio.

As the following Figure 2.1.4 shows, the components of an Optitrack V120:Trio kit are:

- 1 bar V120:Trio
- 1 Quick Start Guide
- 1 license of Motive: Tracker
- 1 12V universal power supply
- 1 USB uplink cable of 5 meters
- 4 M3 small short marker bases
- 4 M4 medium short marker bases
- 4 M4 medium long marker bases
- 4 M3 7.9mm markers
- 4 M4 9.5mm markers
- 8 M4 12.7mm markers
- 10  $\varnothing 3/8$  rubber adhesive dots
- 10  $\varnothing 1/2$  rubber adhesive dots
- 1 Hand rigid body



Figure 2.1.4\_Photo of a box of an Optitrack V120:Trio.

Power, data and external synchronization are all transmitted between the I/O-X sync box and the tracking bar via a single cable, as the Figure 2.1.5 shows.

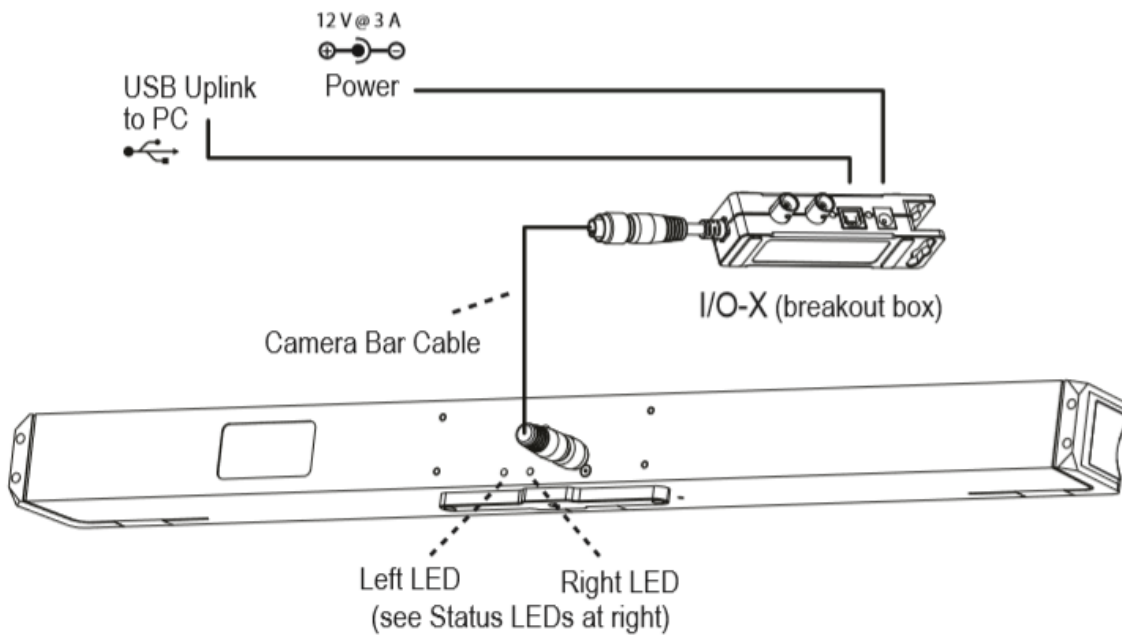


Figure 2.1.5\_Hardware plug in scheme.

The technical specifications of V120:Trio can be resumed in Table 2.1.2:

TECHNICAL SPECIFICATIONS	
Width	584.2 mm
Height	40.6 mm
Depth	50.8 mm
Weight	1.3 kg
Mounting	1/4"-20 tripod thread
Display	128 × 22 OLED
Resolution	640 × 480
Frame Rate	30, 60, 120 FPS
Accuracy	Sub-millimeter
Latency	8.333 ms
Lenses	Standard M12
Left and Right Cameras	800 nm IR pass filter
Middle Camera	800 nm IR pass filter w/ Filter Switcher
Led rings	26 (× 3) n° of LEDs 850 nm IR of wavelength Strobe or Continuous Illumination
Brightness	Adjustable
Input/Output	USB 2.0
Sync	internal or external (via IO-X)
Power	12V @ 3A

Table 2.1.2\_Technical specifications of V120:Trio.

The dimensions of an Optitrack V120:Trio are shown in the Figure 2.1.6:



Figure 2.1.6\_Camera body with dimensions.

### 2.1.3 Motive software

Motive is a software platform designed to control optical motion capture systems as V120:Trio for various tracking applications. Motive carries out two important tasks:

- it allows the user to calibrate and configure the system;
- it provides interfaces for both capturing and processing of 3D data.

Motive icon is shown in the Figure 2.1.7:

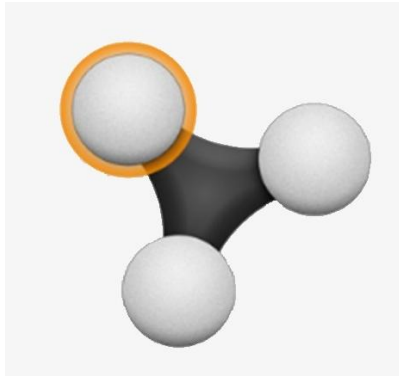


Figure 2.1.7\_The icon of Motive Software.

In Motive, the recorded data are stored in a file format called Take (TAK). It is a single motion capture recording that contains all the information necessary to recreate the entire capture: camera calibration, camera 2D data, data edits, solved joint angle data, reconstructed and labeled 3D data, tracking models and any additional device data. Multiple Take files can be grouped within a session folder, as the Figure 2.1.8 shows.

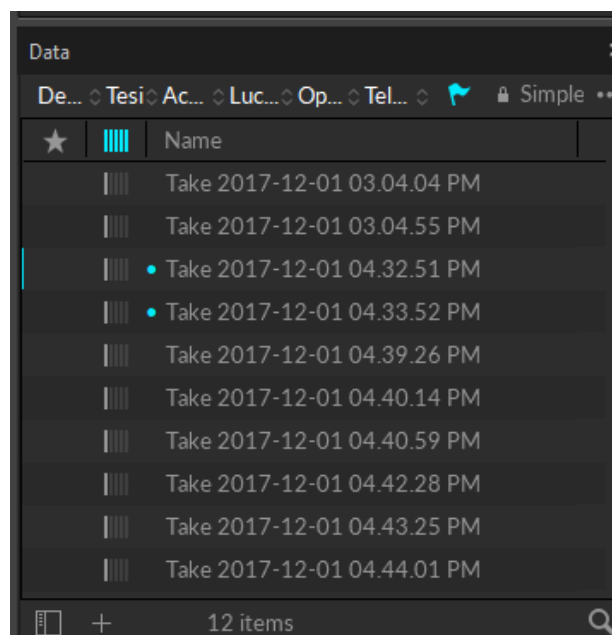


Figure 2.1.8\_An example of several takes grouped in a single session folder.

In Motive it is possible to monitor and assess the tracking data by using two different view modes: the Perspective View mode and the Camera Preview mode. The first one shows the reconstruction of 3D data within the calibrated 3D space and allows to analyze markers positions. The second one shows 2D images from each camera in the setup and enables to mask certain pixel regions in order to exclude them from the post-processing. The two following figures (Figure 2.1.9 and Figure 2.1.10) show the Perspective view and the Camera view modes, respectively:

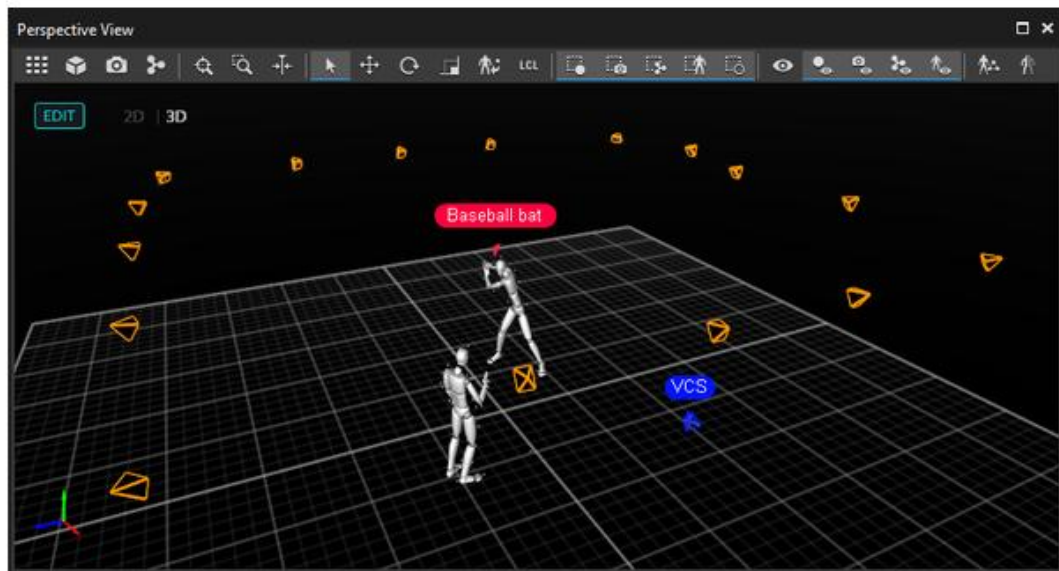


Figure 2.1.9\_The perspective view mode.

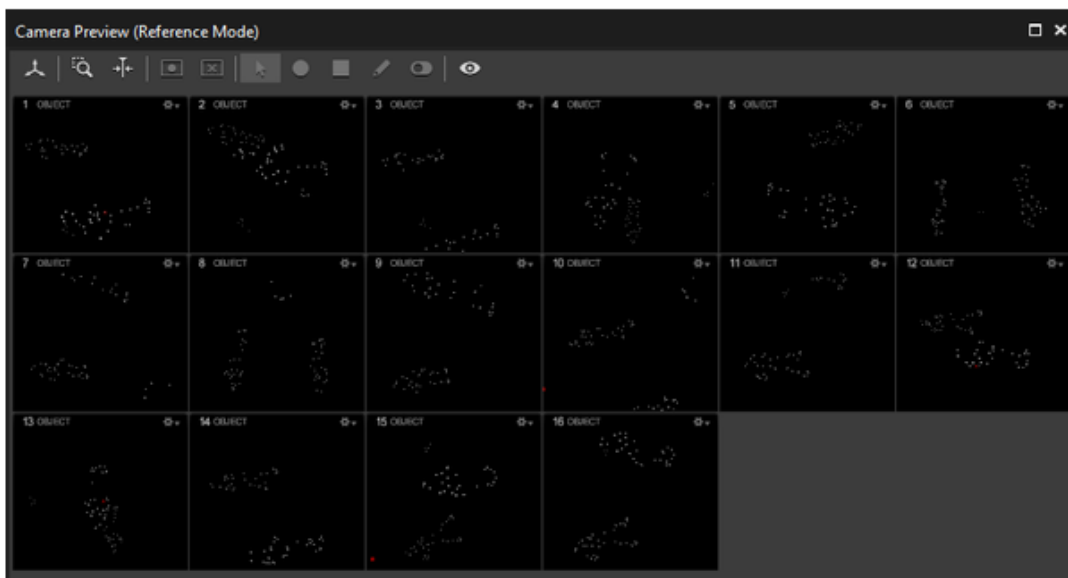


Figure 2.1.10\_The camera preview mode.

In Motive there are two primary operating modes: Live mode and Edit mode. In the Live mode, all cameras are active and the system is ready for recording the data. In the Edit mode, instead, the cameras are not active and Motive is processing pre-recorded Take files. The two following figures (Figure 2.1.11 and Figure 2.1.12) show the difference between the two Motive operating modes:

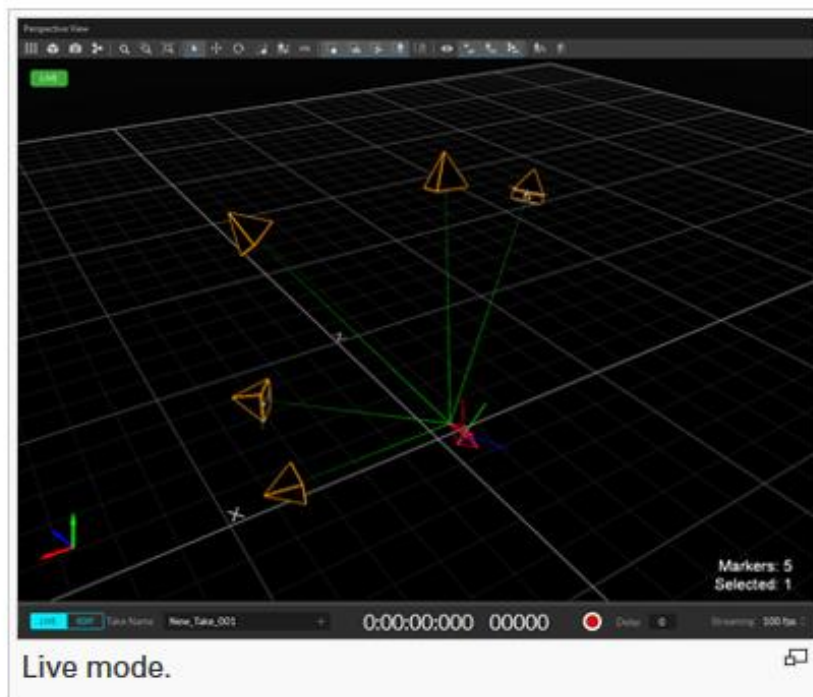


Figure 2.1.11\_Motive live mode: all the cameras are active.

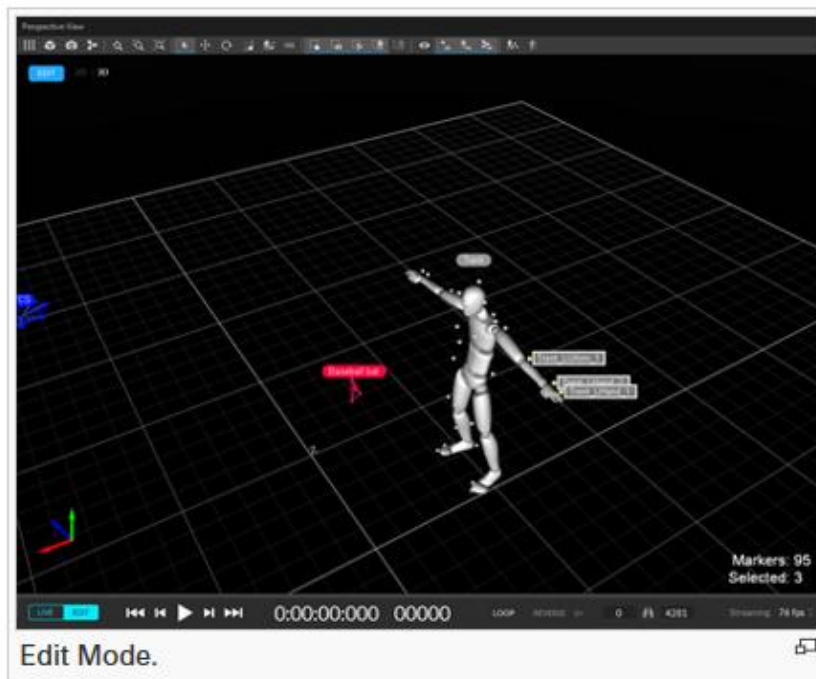


Figure 2.1.12\_Motive edit mode: the cameras are not active.

After having recorded data with Live mode, it is possible to select the Edit mode and to open a Take file previously obtained. The first step consists of the label the markers. Marker labels are software tags assigned to trajectories of reconstructed markers. In this way they can be referenced for tracking individual markers, rigid bodies or skeletons. There are two methods for labeling markers in Motive: auto-labeling and manual labeling. Sometimes the auto-labeling makes some mistakes and manual labeling is necessary. In both cases, it is fundamental to create groups of markers through markersets. Once a markerset asset is created, new marker labels can be added. For example, inside the markerset “Right foot” it is possible to insert the marker labels “Right toe”, “Right heel” and “Right malleolus”. As the Figure 2.1.13 shows, a way to simplify the process of labeling consists in giving different colours to labels:

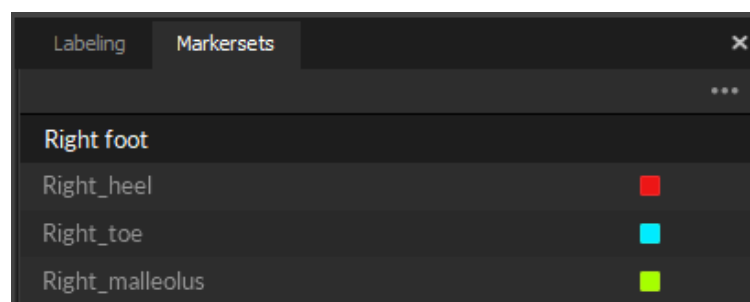


Figure 2.1.13\_An example of Markerset Pane with different colours for labels.

At this point it is necessary to assign, remove and edit marker labels through the Labeling Pane. For a given frame, all labels are colour-coded: white for assigned marker labels and red for labels without reconstructions. The Figure 2.1.14 shows an example of Labeling Pane:

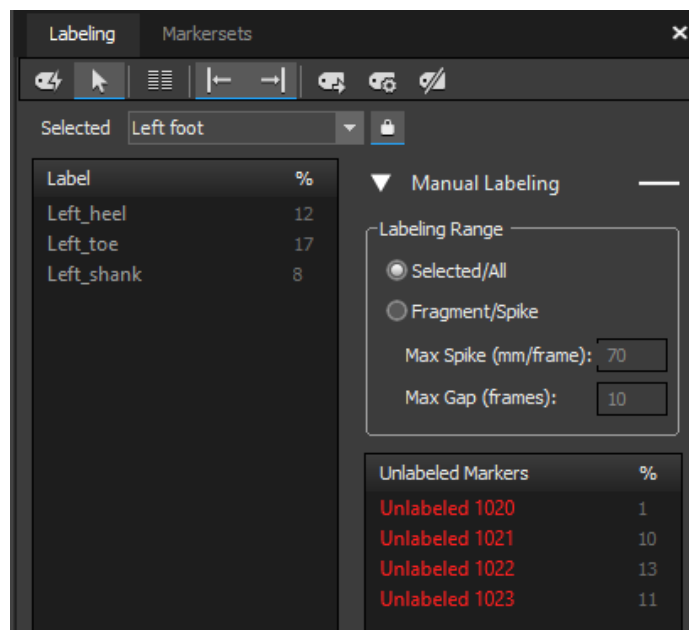


Figure 2.1.14\_An example of labeling pane for markers labeling.

Once the phase of markers labeling has ended, it is possible to export the Take file in two formats: C3D and CSV. In particular, the data from the CSV files can be imported on Excel files and analysed. The following Figure 2.1.15 shows an example of an Excel file with the data imported from Motive and elaborated. It is possible to observe that for each marker there are three columns of data: one for x, one for y and one for z coordinate. It is important to underline that these coordinates are the ones of the V120:Trio bar reference system.

The local system of the bar is centred in the central camera and is composed in this way:

- the axis z is perpendicular to the bar itself;
- the axis y is perpendicular to the plane on which the bar is positioned;
- the axis x forms a right-handed triplet with the other two.

	A	B	C	D	E	F	G
1		Take Name	Take 2018-02-19 03.0	Capture Frame Rate	120	Export Frame Rate	120
2							
3		Marker	Marker	Marker	Marker	Marker	Marker
4		Right foot_Right toe			Left foot_Left toe		
5		3EBA13A21E2211E86	3EBA13A21E2211E86	3EBA13A21E2211E86	45E5B0221E2211E86A	45E5B0221E2211E86A	45E5B0221E2211E86A
6		Position	Position	Position	Position	Position	Position
7	Time	X	Y	Z	X	Y	Z
8	0				1,25068	0,834622	3,253192
9	0,008333				1,247365	0,82746	3,25584
10	0,016667				1,246441	0,82202	3,260081
11	0,024999				1,2438	0,817827	3,259699
12	0,033332				1,242665	0,815383	3,26167
13	0,041665				1,242538	0,812717	3,263679
14	0,049998				1,242303	0,810562	3,263604
15	0,058331				1,242279	0,808657	3,264362
16	0,066664				1,241812	0,806769	3,264151
17	0,074997	1,552708	0,735788	3,123181	1,241423	0,805305	3,264174
18	0,08333	1,526723	0,736704	3,124044	1,240845	0,80397	3,263225
19	0,091663	1,49902	0,737096	3,123962	1,24037	0,802752	3,262542
20	0,099996	1,46949	0,737081	3,122537	1,239988	0,802089	3,262196
21	0,108329	1,440345	0,737631	3,123531	1,239636	0,801604	3,261624
22	0,116662	1,410445	0,73754	3,123471	1,23937	0,801332	3,261253
23	0,124995	1,380336	0,737462	3,123904	1,239149	0,801306	3,26094

Figure 2.1.15\_An example of Excel file with the data imported from Motive after the label of markers.

## 2.2 Inertial Measurement Units: Xsens

### 2.2.1 Inertial sensors

Inertial sensors are devices which combine accelerometers and gyroscopes. They use the property of bodies to maintain constant translational and rotational velocity, unless disturbed by forces or torques respectively. The first natural three-dimensional inertial sensor is the vestibular system, which is situated in the inner ear. It is considered as such because it can sense angular motion and linear acceleration of the human head. In this way it has represented a biologic model to follow in order to realize artificial inertial sensors.

However, the most important technological advancement for the creation of small inertial sensors has been the introduction of Micro Electro Mechanical Systems (MEMS). Thanks to them, it has been possible to obtain Inertial Measurement Units (IMU). These inertial sensor devices are small enough to be attached to subjects. As a result, when they move in the space the IMUs can provide changes in position relative to an initial reference or a starting point. They do not require a camera or another recording device, but they involve specialized software for interpretation of outcome.

Commercial optical systems such as Optitrack or Vicon can guarantee accurate position information and, consequently, can be often adopted as a gold standard for the human movement analysis. However, they have some important restrictions: problems of markers occlusion, high costs, limited measurement volumes and the need of a specialized laboratory with fixed instruments

The last disadvantage makes them not adequate for many applications, like control of prosthetics or monitoring of daily life activities. The increased necessity to monitor patients in their own environment has promoted a large development of inertial sensors in clinical context. In fact, they are highly portable, easily wearable and not invasive systems (Xsens, 2000). The IMU provides kinematic measurements thanks to both an accelerometer and a gyroscope of the micron order.

As the following Figure 2.2.1 shows, a typical inertial sensor contains a tri-axial accelerometer and a tri-axial gyroscope:

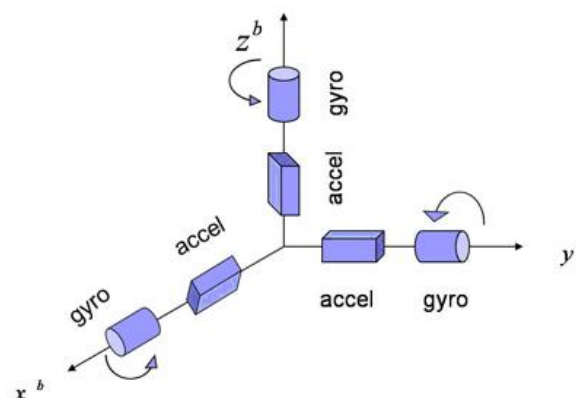


Figure 2.2.1\_The scheme of an IMU.

An accelerometer is a device that allows the direct measure of acceleration (Figure 2.2.2). It is attached to an object and it measures the acceleration of the object itself in the point of attachment. This device can be very small and light. The smallest accelerometers are  $2\text{ mm} \times 2\text{ mm} \times 1\text{ mm}$ .

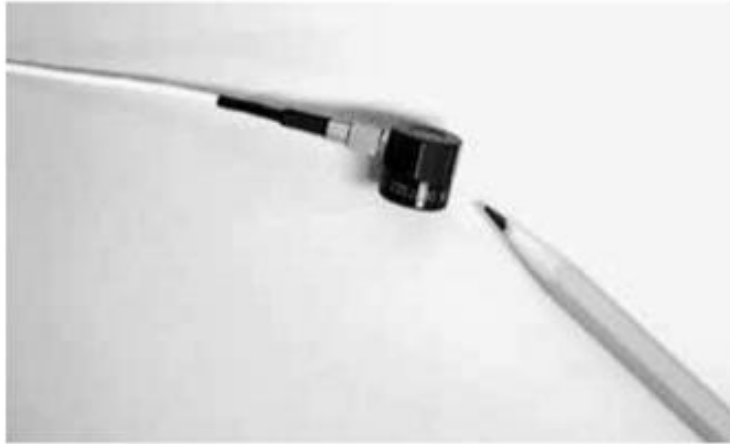


Figure 2.2.2\_An example of an accelerometer (McGinnis, 2013).

Accelerometers measure acceleration in precise directions. An accelerometer that returns acceleration in only one direction along a specific axis is called uniaxial or one-dimensional. An accelerometer that provides three accelerations along three different axes of a Cartesian triad is called triaxial or three-dimensional. The orientation of the accelerometer is very important, because it defines the direction of the acceleration. If the accelerometer is attached to a foot that moves in the space, then the direction of the measured acceleration changes according to the change of foot orientation (McGinnis, 2013).

A uniaxial accelerometer is simply made up of a mass suspended by a spring inside a housing, as the Figure 2.2.3 shows.

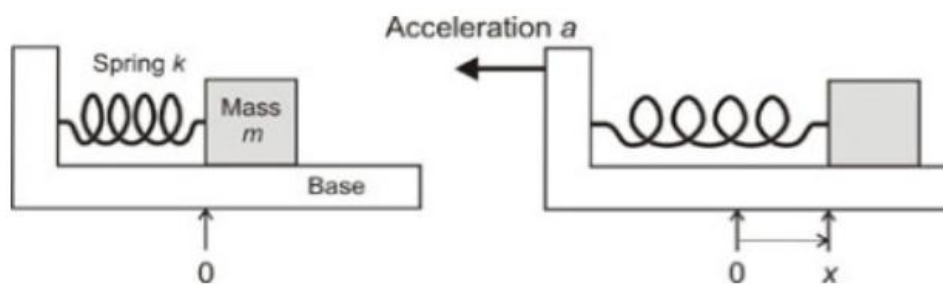


Figure 2.2.3\_The scheme of a system mass-spring (Xsens, 2000).

In their linear region springs are governed by a physical principle called Hooke's law. According to this principle, the restoring force generated by a spring is proportional to the amount of expansion or compression it has endured.

The equation that represents the concept is:

$$F = kx$$

where  $k$  is the constant of proportionality between the displacement  $x$  and the force  $F$ .

The second fundamental physical principle about mass is Newton's second law of motion. A force that acts on a mass which is accelerated will have a magnitude explained by this equation:

$$F = ma$$

This force produces an expansion or a compression of the mass on the spring. As a result, it is possible to obtain this new equation, which correlates the two previous ones:

$$ma = kx$$

A displacement of  $x$  implies an acceleration of the mass of  $a = kx/m$  as well as an acceleration causes a displacement of the mass of  $x = ma/k$ . In this way, the measurement of the acceleration has been simplified and converted into the measurement of the displacement of a mass connected to a spring. In order to obtain a triaxial accelerometer, it is necessary to duplicate this system along each of the axes. (Xsens, 2000)

Gyroscopes are instruments implied for the measurement of angular motion, because they maintain their rotation axis in a fixed direction. Mechanical gyroscopes work according to the conservation of angular momentum, because they sense the change in direction of an angular momentum. The Figure 2.2.4 shows the scheme of a gyroscope, with all its parts.

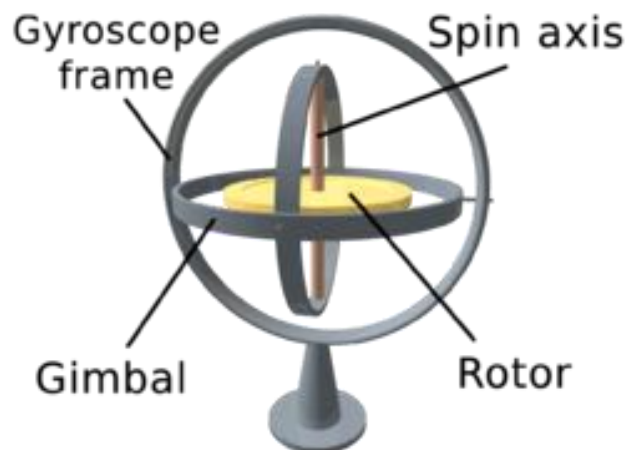


Figure 2.2.4\_The scheme of a system mass-spring (McGinnis, 2013).

A gyroscope consists of a wheel mounted in two or three supports called *gimbals*. They promote the rotation of the wheel about a single axis. When the gyroscope has two gimbals, the outer one is called the *gyroscope frame*: it has one degree of rotational freedom, whereas its axis possesses none. The inner gimbal, which has two degrees of rotational freedom, is mounted in order to have an axis that is always perpendicular to the pivotal axis.

The central wheel is also called *rotor* and possesses three degrees of rotational freedom. Its axis of rotation is called *spin axis*: it is always perpendicular to the axis of the inner gimbal and it has two degrees of rotational freedom.

Newton's second law establishes that the angular momentum of a body will be unchanged unless a torque acts on it. The behaviour of the gyroscope is described by this equation:

$$\tau = \frac{dL}{dt} = \frac{d(I\omega)}{dt} = I\alpha$$

Where:

- the vectors  $\tau$  and  $L$  are respectively the torque on the gyroscope and its angular momentum
- the scalar  $I$  is its moment of inertia
- the vector  $\omega$  is its angular velocity
- the vector  $\alpha$  is its angular acceleration

Both a tri-axial accelerometer and a tri-axial gyroscope are usually situated inside an inertial measurement unit. In this way, the device can measure both the acceleration and the angular velocity of the body to which it is attached.

### 2.2.2 Xsens Xbus Kit

Since its foundation in 2000, Xsens is involved in sensor and software research and development and represents a leader in inertial human motion capture solutions.

One of the many Xsens technologies is the Xbus Kit, which contains:

- 7 MTx's (Motion Trackers)
- 1 Xbus Master
- 1 MT Manager and software development kit
- Accessories:
  - 7 Xbus cables
  - 1 Xbus Master Cable USB
  - 1 power adapter
  - 4 AA rechargeable batteries
  - 1 belt
  - 1 Bluetooth Transceiver USB
  - MVN straps for easy sensors fixation

The Figure 2.2.5 shows the components of the Xsens Xbus Kit:



Figure 2.2.5\_The Xsens Xbus Kit.

The Xbus Kit supplies a completely ambulatory measurement of human motion. It is composed of a set of MTx's, an Xbus Master and a wireless transceiver. The MTx's are powered and controlled by the Xbus Master and they produce 3D acceleration, 3D rate of turn and earth magnetic field. Then, the Xbus Master samples and sends synchronous digital data from the MTx units to the PC. The transmitted data are recorded by using the software MT Manager.

This kit can be implied in many fields, such as biomechanics, rehabilitation, virtual reality and sport science. It has many qualities:

- It connects multiple Motion Trackers by the Xbus Master.
- It allows synchronous sampling of multiple MTx's at adjustable frequencies up to 512 Hz.
- It has an ergonomic design.
- It allows external triggering and notification of trigger moment available for synchronization.
- It is compatible with PC via USB cable or wireless Bluetooth.

The most important components of the Xbus Kit are the Motion Trackers. The MTx is a small and accurate 3DOF inertial Orientation Tracker. It provides drift-free 3D orientation as well as kinematic data: 3D acceleration, 3D rate of turn (rate gyro) and 3D earth magnetic field. Both the accelerometers and the rate of turn sensors are MEMS solid state, whereas the magnetometer is a thin magnetoresistive film. All calibrated sensor readings (accelerations, rate of turn, earth magnetic field) are in the right handed Cartesian coordinate system. This reference system is fixed to the device and is defined as the sensor coordinate system (S). In particular, it is aligned to the external housing of the MTx, as the Figure 2.2.6 shows.

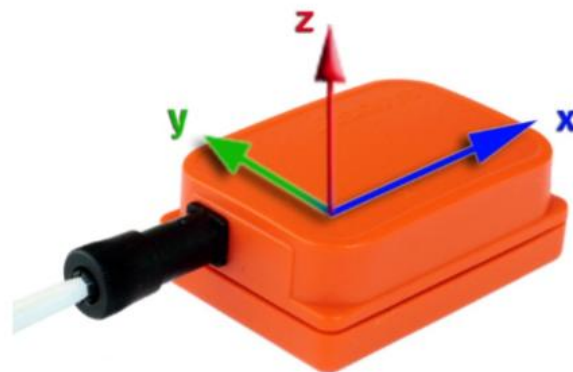


Figure 2.2.6\_MTx with sensor-fixed co-ordinate system overlaid (S).

The units of the MTx calibrated data output are presented in the following Table 2.2.1. It is important to notice that the linear 3D accelerometer measures all accelerations, including the acceleration due to gravity. Therefore, if there is the necessity to use the 3D linear accelerations output to estimate the “free” acceleration, gravity first must be subtracted.

Vector	Unit
Acceleration	m/s <sup>2</sup>
Angular velocity (rate of turn)	rad/s
Magnetic field	a.u. (arbitrary units) normalized to earth field strength

Table 2.2.1\_The units of the MTx calibrated data.

The technical specifications of MTx are reported in the following Table 2.2.2:

TECHNICAL SPECIFICATIONS	
Width	38 mm
Height	21 mm
Length	53 mm
Weight	30 g
Rate of turn performances	Dimensions: 3 axes
	Full scale: $\pm 1200$ deg/s
	Bandwidth: 40 Hz
Acceleration performances	Dimensions: 3 axes
	Full scale: $\pm 50$ m/s <sup>2</sup>
	Bandwidth: 30 Hz
Magnetic field performances	Dimensions: 3 axes
	Full scale: $\pm 750$ mGauss
	Bandwidth: 10 Hz
Orientation performances	Dynamic range: all angles in 3D
	Angular resolution: 0.05 deg
Max update rate	512 Hz (calibrated sensor data)
	120 Hz (orientation data)
Operating voltage	4,5-30 V
Power consumption	350 mW
Temperature operating range	-20°-55°
Housing material	Plastic
	Dust resistant
	Light weight

Table 2.2.2\_The technical specifications of Xsens MTx's.

The following Figure 2.2.7 shows the MTx's technical drawings:

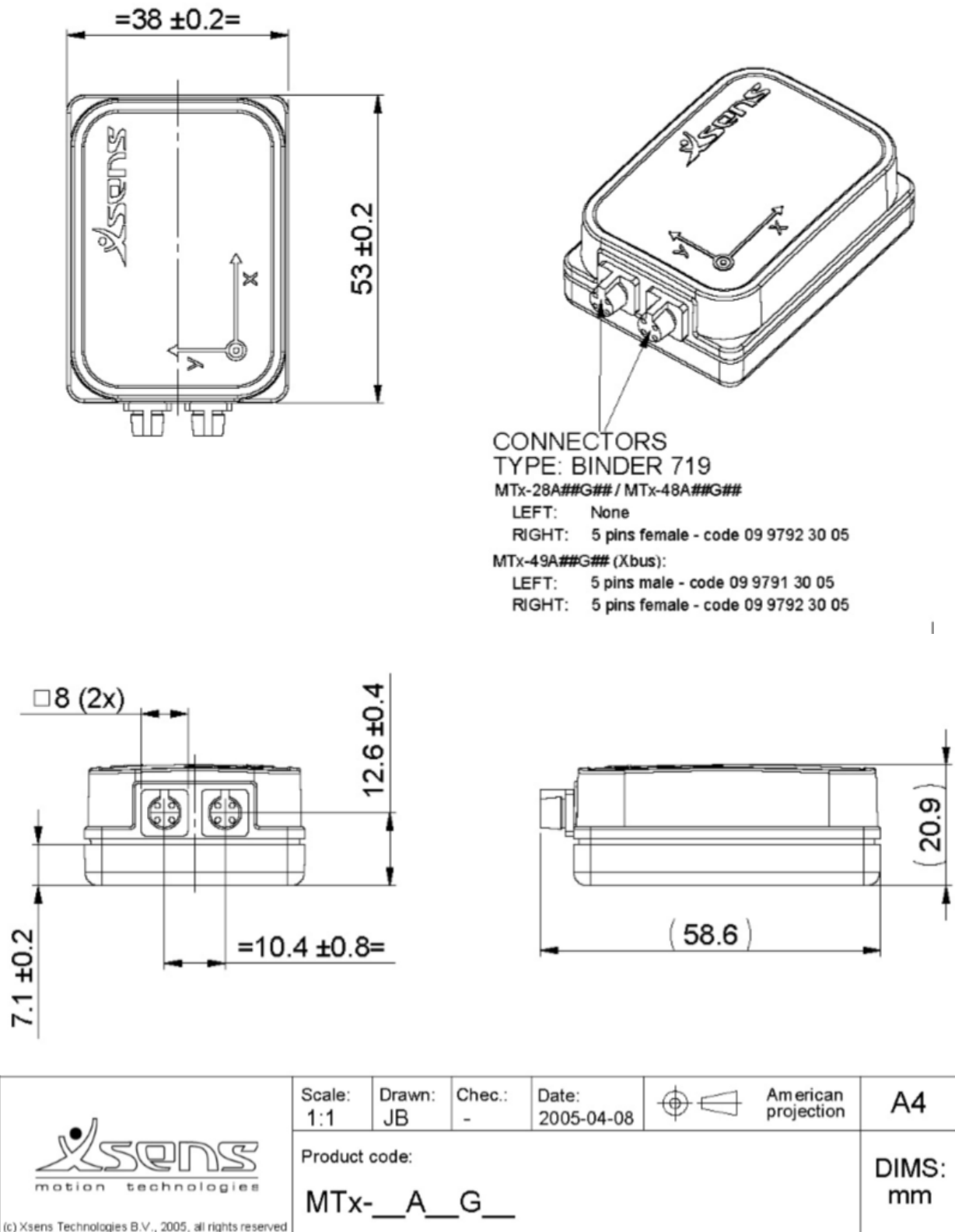


Figure 2.2.7\_MTx technical drawings.

A part from the Motion Trackers, the other very important component of the Xbus Kit is the Xbus Master. It interconnects multiple MTx Motion Trackers via an Xbus cable. It delivers power to the connected Motion Trackers and receives their data while they are sampled synchronously. The obtained data are transmitted by a USB cable or wireless Bluetooth link to a PC. The Xbus Master works on batteries or external power supply and has an ergonomic design with its belts.

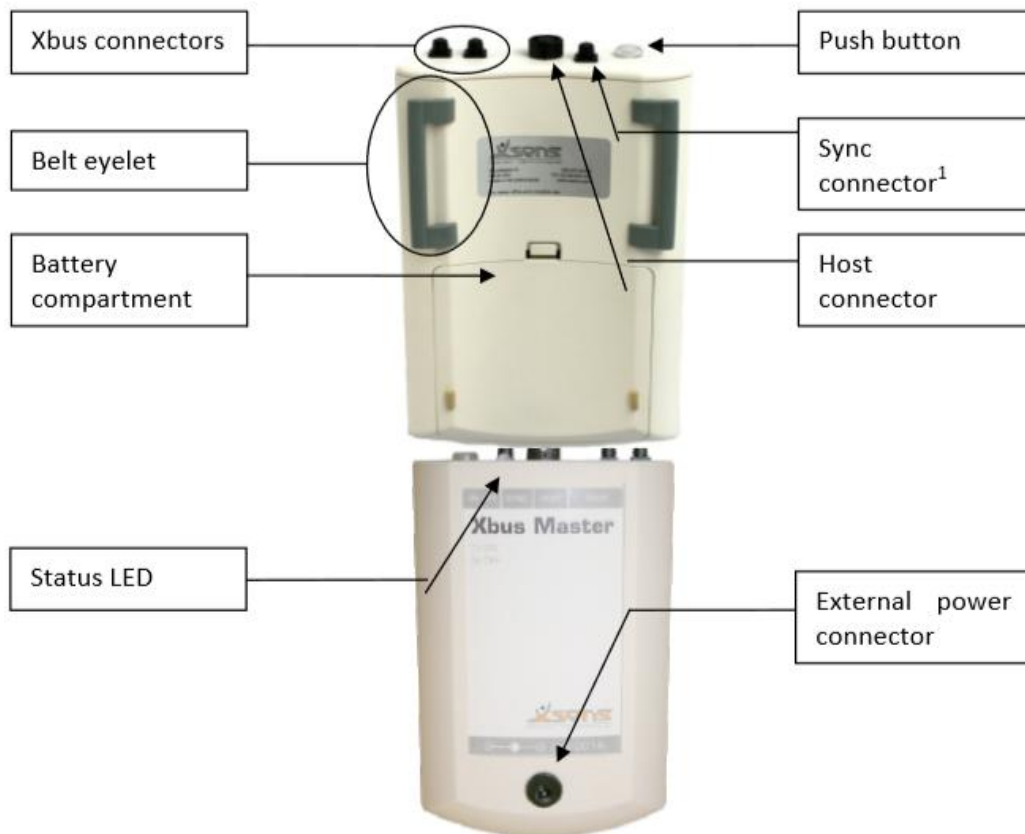


Figure 2.2.8\_Xbus Master overview.

As the Figure 2.2.8 shows, the Xbus Master has many components:

- The Xbus connector connects a string or a chain of Motion Trackers with the Xbus Master.
- The eyelets are used to attach the Xbus Master to the supplied belt in order to fix it around the waist of the subjects.
- The battery compartment accommodates four AA type batteries for Xbus power.
- The status LED is useful to visualize the Xbus Master status because it shows both the current state and the current mode.
- The current state is viewed using a specific flash sequence of the LED: off for power down, solid for configuration state, two short flashes for measurement state waiting for trigger and one flash for measurement state sending data.

- The current mode is visualized using a specific colour of LED: green for serial mode, blue for Bluetooth mode, purple for host not found, yellow for low battery mode and red for fault mode.
- The push button controls the power state of the Xbus Master. The button must be pressed once to switch the Xbus Master on, 3 consecutive times to switch it off.
- The sync connector can be used for synchronization with other devices or another Xbus Master.
- The host connector connects the Xbus Master to a host using the standard USB communication port.
- The external power connector allows to connect the power adapter for using the Xbus Master without batteries.

The following Figure 2.2.9 shows an example of Xsens MTx configuration with the Xbus Master at waist level in Bluetooth mode:



Figure 2.2.9\_A photo of an example of MTx configuration with the Xbus Master at waist level in Bluetooth mode.

### 2.2.3 MT Manager software

MT Manager is a software compatible with all Xsens Motion Trackers and the Xbus Master. Its icon is represented in Figure 2.2.10. An example of a software typical screen is shown in the Figure 2.1.11.

MT Manager software allows to:

- View 3D orientation in real time
- View inertial and magnetic sensor data in real time
- View latitude, longitude and altitude plots in real time
- Export log files to other formats like ASCII
- Change and view various device setting and properties



Figure 2.2.10\_The icon of MT Manager Software.

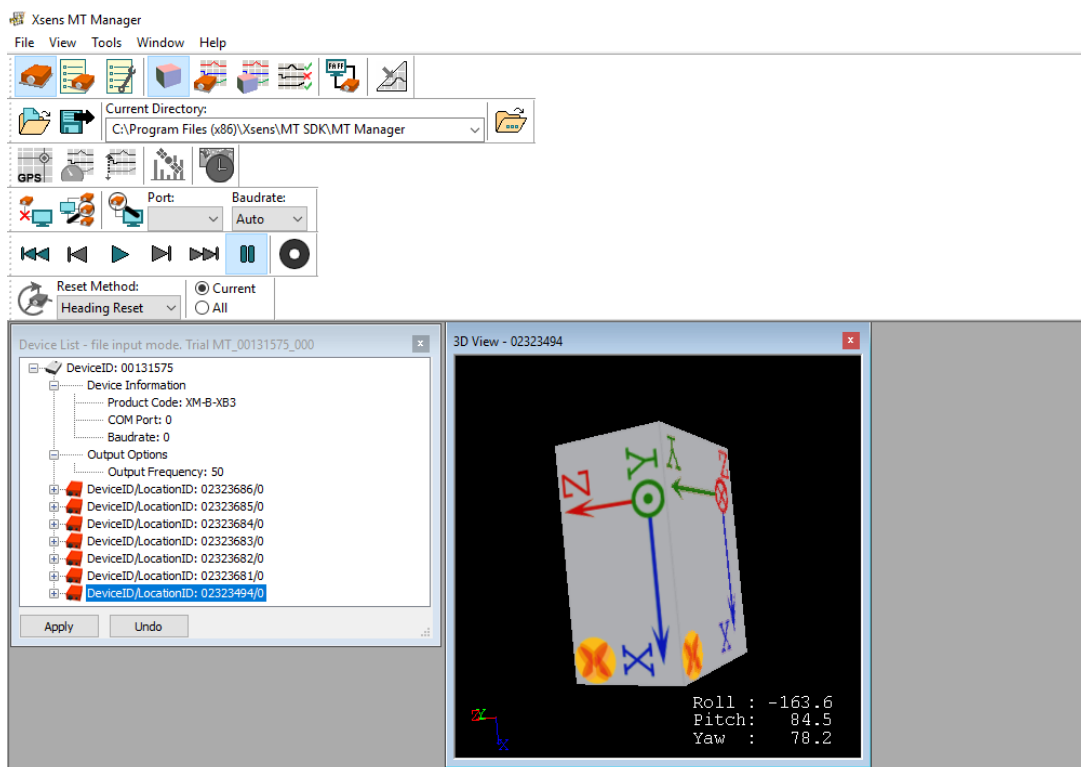


Figure 2.2.11\_An example of a typical MT Manager screen.

Once the Xbus Master is turned on and connected to the PC, the MTx used are displayed in the Device List with the respective unique device ID number (Figure 2.2.12).

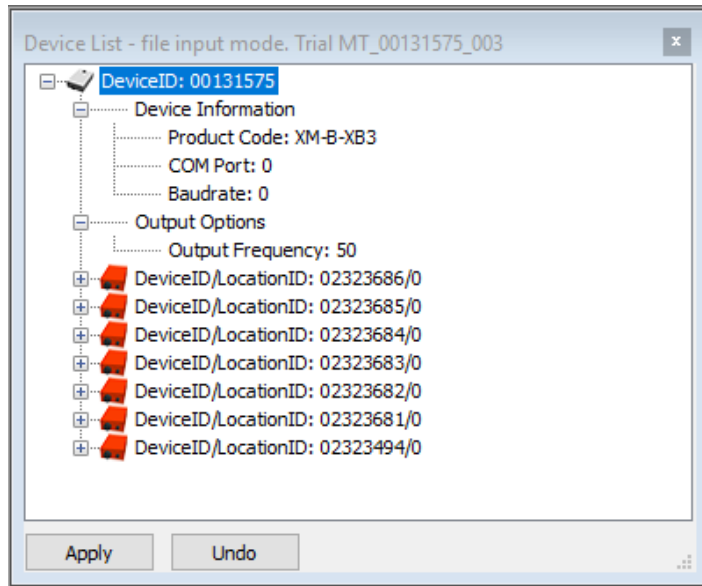


Figure 2.2.12\_An example of device list with seven MTx connected to the Xbus Master.

When all the necessary MTx are connected, it is possible to record an acquisition, creating binary files with format “.MTB” (MT Binary Communication Protocol). They contain recorded output log-files from all Motion Trackers. Then, the software can input these binary files in order to visualize them. By selecting Calibrated Data View and clicking on Play, the software allows to reproduce the acquisition (Figure 2.2.13).

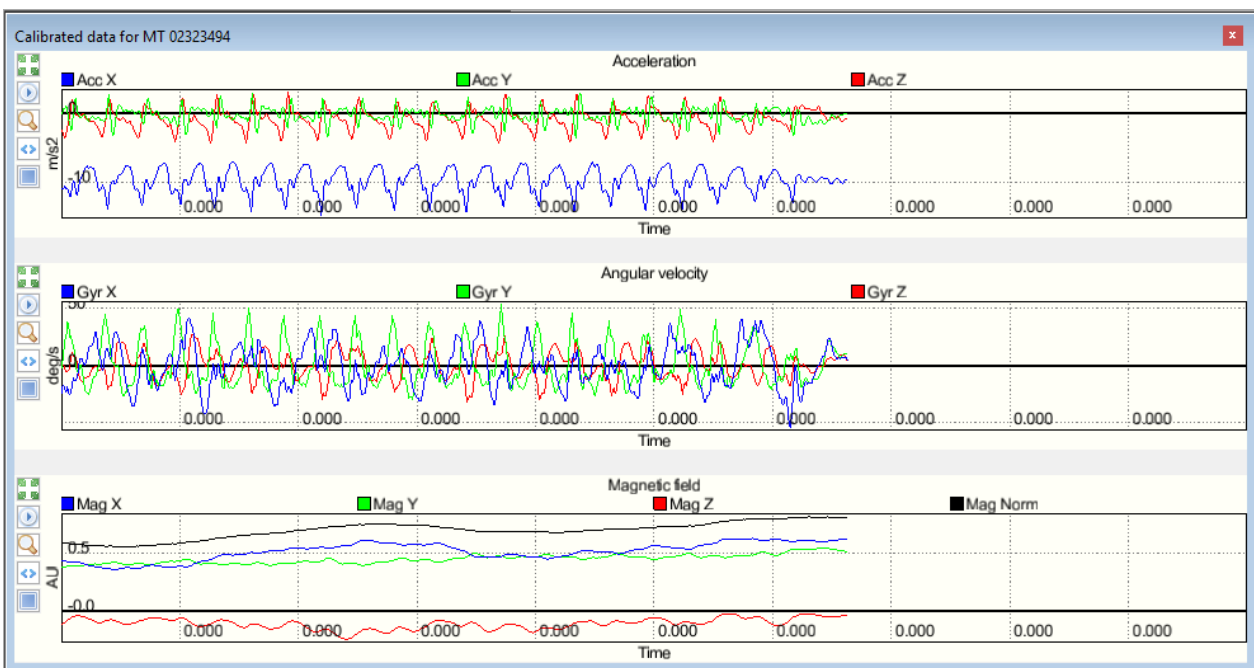


Figure 2.2.13\_An example of calibrated data produced by a MTx located on trunk.

As the Table 2.2.3 shows, each colour corresponds to a specific direction axis:

Colour	Corresponding axis
Red	Acceleration, angular velocity (roll) and normalized magnetic field in X direction
Green	Acceleration, angular velocity (pitch) and normalized magnetic field in Y direction
Blue	Acceleration, angular velocity (yaw) and normalized magnetic field in Z direction
Black	Total acceleration, angular velocity and magnetic field, if available

**Table 2.2.3\_The colours of MT Manager with their correspondences to different direction axes.**

The MT Manager can also export data logged in .MTB files to ASCII format, which can be imported in Excel or Matlab. The export file can contain a sample counter, calibrated sensor data (3D acceleration, rate of turn, magnetic field) and orientation data. The output orientation can be presented in different conventions:

- Unit normalized Quaternions or Euler parameters
- Euler angles (roll, pitch, yaw)
- Rotation Matrix (Direction Cosine Matrix)

The Figure 2.2.14 shows an example of Excel screen with data imported from MT Manager:

	A	B	C	D	E	F	G	H	I	J	K	L	M	
1	// Start Time: 0													
2	// Sample rate: 50.0Hz													
3	// Scenario: 5.9													
4	// Firmware Version: 2.6.1													
5														
6	Counter	Acc_X	Acc_Y	Acc_Z	Gyr_X	Gyr_Y	Gyr_Z	Mag_X	Mag_Y	Mag_Z	Roll	Pitch	Yaw	
7		12743	-9,144673	0,295518	0,726611	0,318217	0,050514	-0,014288	0,734412	0,170225	-0,316479	-89,72543	86,187027	110,313469
8		12744	-9,241616	0,56082	0,49075	0,244419	0,044501	0,034525	0,734265	0,168511	-0,315801	-90,103074	86,223406	109,653098
9		12745	-9,282496	0,574866	0,029781	0,151209	0,042107	0,094857	0,734014	0,16595	-0,316108	-90,619307	86,323394	108,964012
10		12746	-9,27829	0,241186	-0,391245	0,084111	0,078	0,121788	0,732355	0,161944	-0,31417	-91,870965	86,457453	107,612747
11		12747	-9,178208	-0,145195	-0,561106	0,049186	0,127913	0,131142	0,734474	0,160518	-0,312282	-94,283146	86,593203	105,139832
12		12748	-9,262029	-0,271128	-0,66866	0,022828	0,150002	0,097377	0,734031	0,15837	-0,310626	-97,230347	86,683905	102,161252
13		12749	-9,400373	-0,228073	-0,733361	-0,025663	0,184153	0,044069	0,735321	0,156367	-0,30803	-100,912243	86,694869	98,50262
14		12750	-9,740215	0,195898	-1,112542	-0,103315	0,204433	-0,002291	0,735645	0,157489	-0,305232	-104,806052	86,638557	94,719487
15		12751	-9,893517	0,442056	-0,883158	-0,168612	0,231751	-0,000323	0,736722	0,15974	-0,300483	-109,17433	86,557114	90,53623
16		12752	-9,744088	0,577832	-0,778477	-0,184897	0,21234	0,002915	0,737958	0,161856	-0,296576	-112,999699	86,471312	86,916725
17		12753	-10,022242	0,15649	-1,077585	-0,235417	0,172284	-0,001394	0,737296	0,162252	-0,292231	-116,043576	86,386002	84,137243
18		12754	-10,507399	-0,499872	-1,53056	-0,299959	0,150483	-0,026947	0,736352	0,164211	-0,287719	-118,431447	86,27879	82,09013
19		12755	-10,670618	-0,64785	-1,751082	-0,294963	0,159643	-0,047342	0,737371	0,16648	-0,285759	-120,679242	86,139997	80,174696
20		12756	-10,543739	-0,584775	-1,870369	-0,181129	0,202162	-0,011508	0,738629	0,167176	-0,282429	-123,524573	86,005805	77,53141
21		12757	-10,191959	-0,796483	-1,990446	-0,115376	0,227845	-0,003887	0,737965	0,168711	-0,278209	-126,54009	85,850265	74,639538
22		12758	-10,209316	-0,423814	-1,059948	-0,154932	0,151393	-0,028182	0,738117	0,169396	-0,274017	-128,212946	85,71976	73,141602
23		12759	-12,097178	-0,755384	-1,351232	-0,03648	-0,193992	0,191532	0,737085	0,168406	-0,275682	-127,608954	86,027409	73,788087

**Figure 2.2.14\_An example of Excel file with data imported from an ASCII file exported from MT Manager.**



### 3. Preliminary tests

#### 3.1 Preliminary tests with Optitrack

The setting chosen for the experiment was a mechanical laboratory with two Optitrack V120:Trio bars located opposite each other so as to view both sides of the subject (Figure 3.1.1).



Figure 3.1.1\_Location of the two Optitrack v120:Trio.

In order to capture as many steps as possible, the bars were 6.5 meters away from each other, whereas the length of the walk was 6 meters. The 3.5 central meters represented the acquisition volume of the cameras (Figure 3.1.2). Each bar had a local reference system, according to which:

- the axis z was perpendicular to the bar itself;
- the axis y was perpendicular to the plane on which the bar was positioned;
- the axis x formed a right-handed triplet with the other two.

As the Figure 3.1.3 shows, the origin of this local reference system was in the middle of the bar, in correspondence of the central camera.

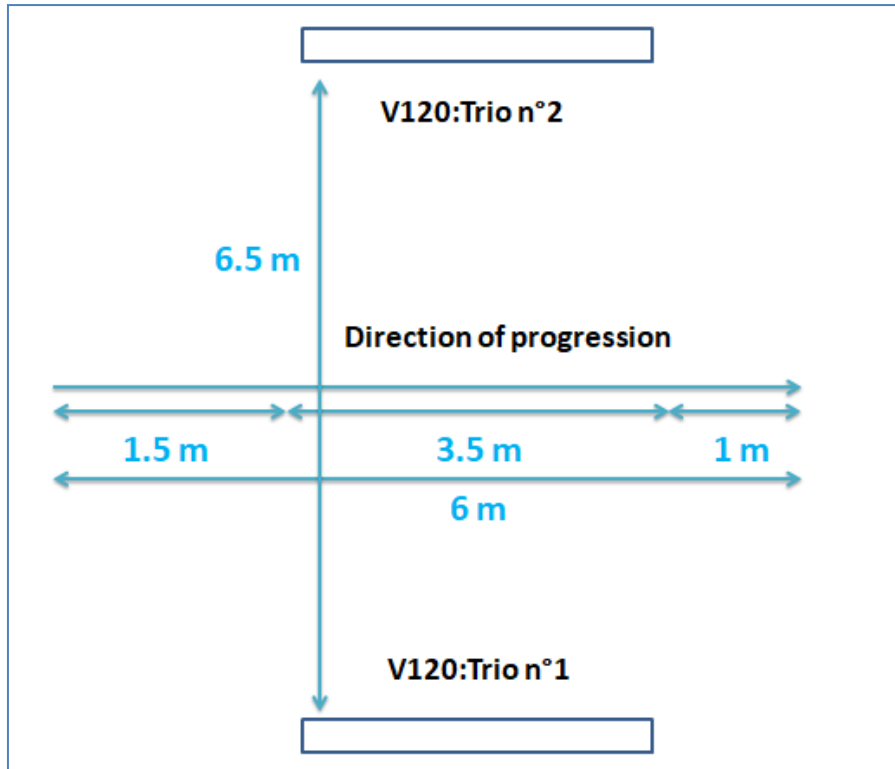


Figure 3.1.2\_Setting with distances.

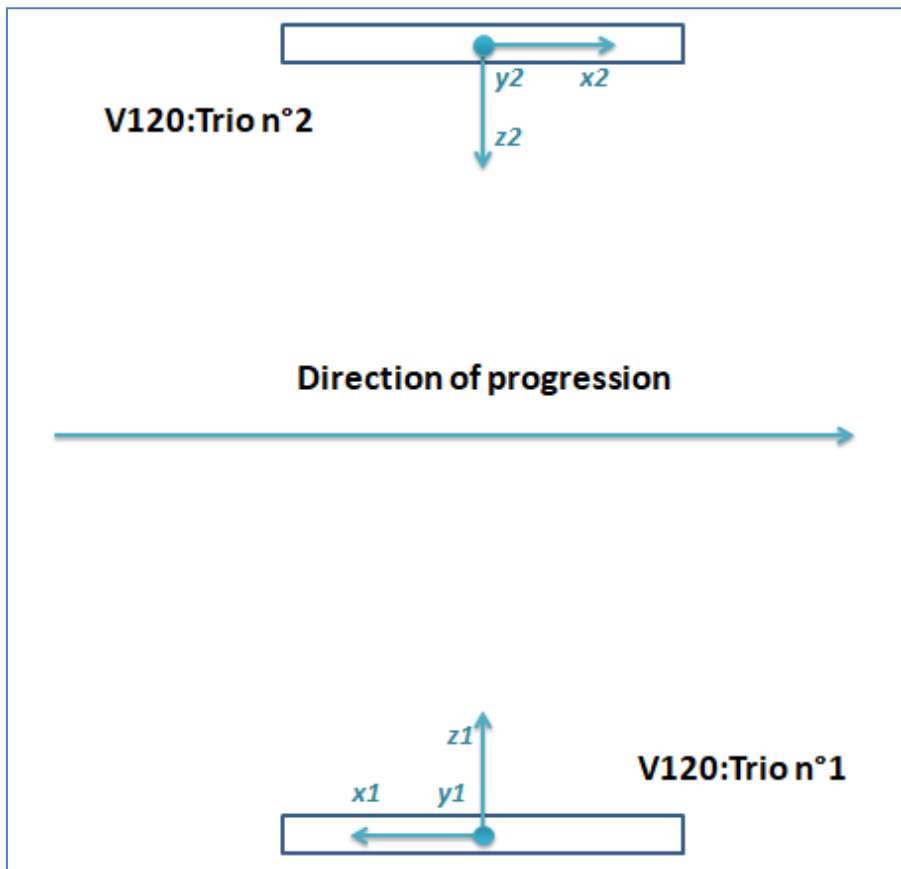


Figure 3.1.3\_Top view of V120:Trio bars and their local reference systems.

Before the test, the problem of data transformation was addressed. Three fixed markers were located inside the acquisition volume on paper cones. After a static acquisition with the software Motive, it was possible to rename the markers as A, B and C and to build a reference system which allowed to convert the data from one bar's system into the other's one. The new system had its origin in B: the X axis was calculated as the distance of A from B; the axis of support S was calculated as the distance of C from B; the Y axis was obtained as the vector product of X and S; the Z axis was obtained as the vector product of X and Y. The Figure 3.1.4 shows this configuration:

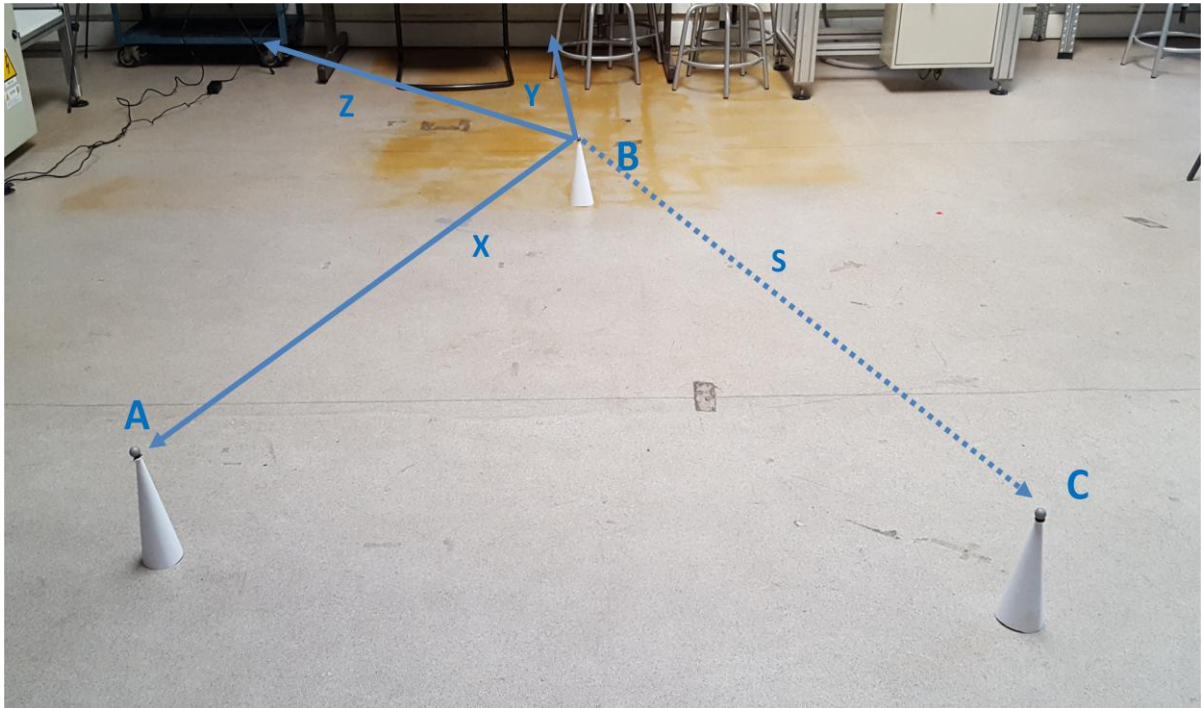


Figure 3.1.4\_ Configuration of fixed markers for the creation of the transformation matrix.

When the coordinates of A, B and C were defined and the new reference system was built, it was possible to construct the transformation matrix which allowed to convert the data from one bar's reference system into the other's one.

First, it was recommended to calculate the transformation matrices which converted the data from the local reference systems of the bars into the new reference system. The first three columns indicated the orientation of the local axes in the base reference; the fourth column indicated the coordinates of the origin of the tern B. For the bar n°1 this matrix was:

$${}^1M_{ABC} = \begin{bmatrix} x1_X & y1_X & z1_X & B1_X \\ x1_Y & y1_Y & z1_Y & B1_Y \\ x1_Z & y1_Z & z1_Z & B1_Z \\ 0 & 0 & 0 & 1 \end{bmatrix}$$

For the bar n°2 this matrix was:

$${}^2M_{ABC} = \begin{bmatrix} x2_x & y2_x & z2_x & B2_x \\ x2_y & y2_y & z2_y & B2_y \\ x2_z & y2_z & z2_z & B2_z \\ 0 & 0 & 0 & 1 \end{bmatrix}$$

Since in this case the need was to convert the data into the reference system of the Optitrack bar n°1, the inverse of the transformation matrix of the bar n°2 was obtained as follows:

$${}^{ABC}M_2 = \left[ \begin{array}{ccc|c} {}^2M_{ABC}^T & & & - {}^2M_{ABC}^T \cdot pB2 \\ \hline 0 & 0 & 0 & 1 \end{array} \right]$$

Finally, the matrix which enabled to convert the data from the reference system of the bar n°2 into the reference system of the bar n°1 was:

$${}^1M_2 = {}^1M_{ABC} \cdot {}^{ABC}M_2$$

After obtaining these data, the fixed markers were removed from the acquisition volume.

Another important problem to solve before asking the subject to walk was that of temporal synchronization of the two bars. The first attempt was to place a fixed marker in the visual field and to make sure it was seen from both bars. When both the acquisitions of the two bars had already started, this marker was covered with a paper cone. During the phase of post-processing, the frame in which the marker disappeared was considered the instant zero for both bars.

The subject chosen for the test was a healthy man of 25 years old. As the Figure 3.1.5 and the Figure 3.1.6 show, the markers positioned on the subject were eight:

- two on the heels
- two on the shanks
- two on the malleolus
- two on the toes

All the markers were fixed with the adhesive tape as symmetrically as possible. Furthermore, they were positioned on anatomic landmarks, in correspondence of the bones. It was important to check if there were at least four steps and so two complete strides inside the volume of acquisition of both bars. The subject was asked to walk in front of cameras without recording: in this way it was possible to verify the number of steps from both the PC. In order to record steps when the subject was already walking, the start of the route was situated before the acquisition volume of the cameras. Similarly, the end of the walk was identified after the acquisition volume of the cameras.



Figure 3.1.5\_Markers on right and left heels.

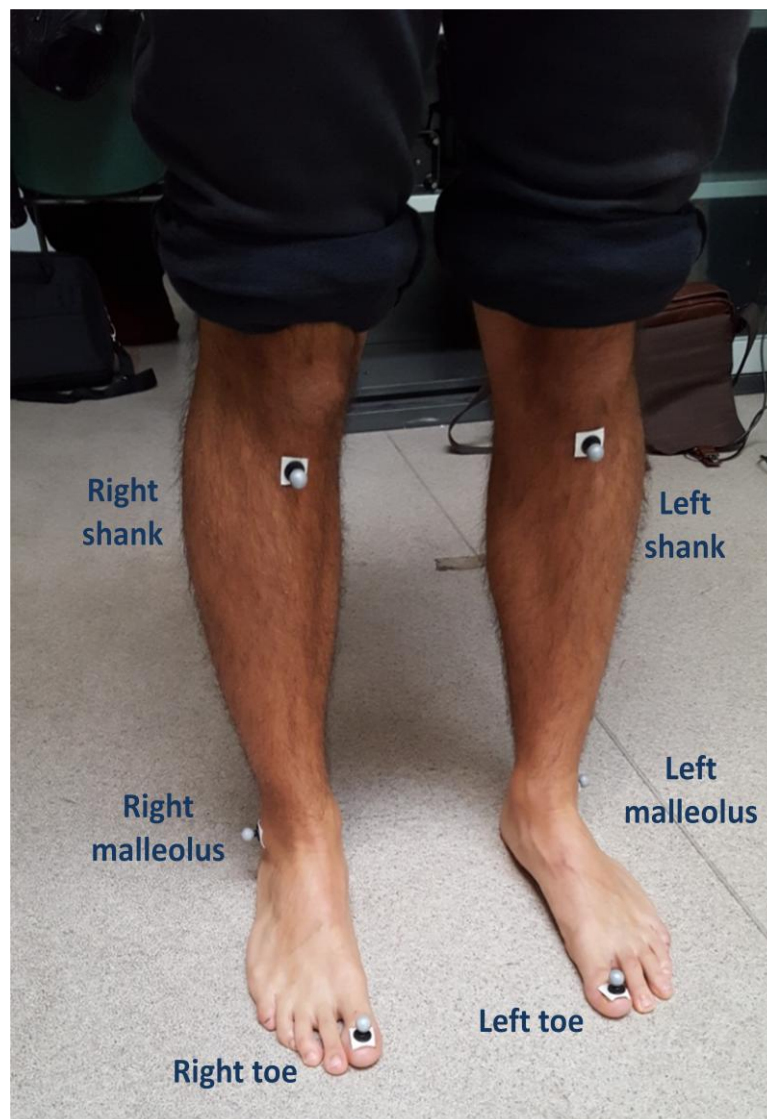


Figure 3.1.6\_Markers configuration on shanks, toes and malleolus.

The subject was asked to walk barefoot along the diagonal on the floor for four times, as the Figure 3.1.7 shows. The test was repeated three times at three different speeds: normal, fast and slow. A total of sixteen acquisitions were recorded.



**Figure 3.1.7**\_An example of acquisition with the subject walking at normal speed.

After the acquisitions, the software Motive allowed the labeling of markers. The frame corresponding to the disappearance of the fixed marker was considered the instant zero. After the temporal synchronization, there were some steps to take:

- First, it was necessary to create in the Asset Pane two new assets corresponding respectively to right and left leg.
- Then, in the Markerset Pane it was possible to insert the names of markers and to give them specific colours (Figure 3.1.8).
- Finally, as the Figure 3.1.9 shows, for all the frames of the acquisitions it was required to label the markers assigning them to the corresponding label. The markers on the malleolus were very important in order to distinguish right from left leg. In fact, the marker on the right malleolus was visible only from the cameras of the bar which was nearest to the right leg, whereas it was occluded for the other one. For the left malleolus was the same but with the opposite bar.

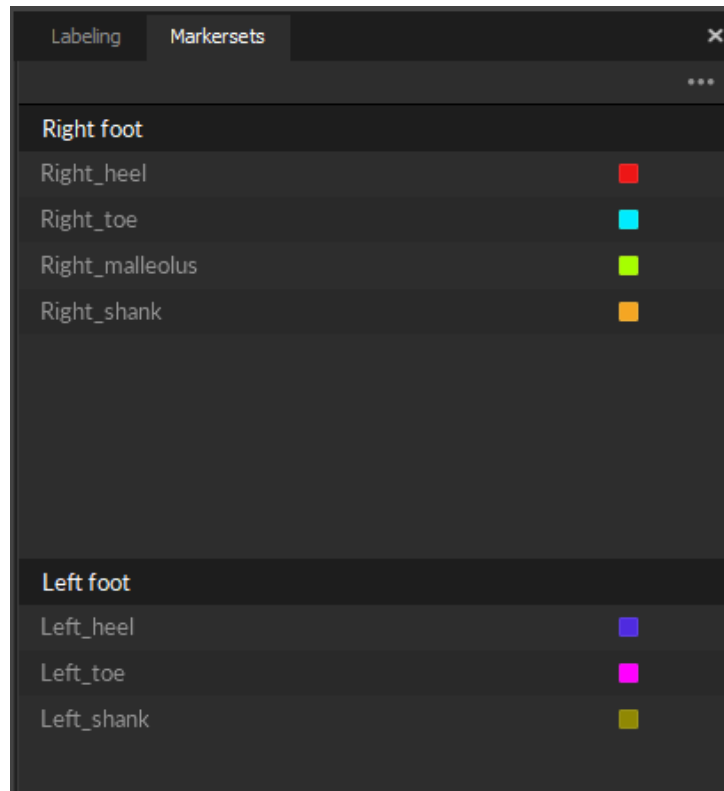


Figure 3.1.8\_The Markersets pane with the names of the labels.

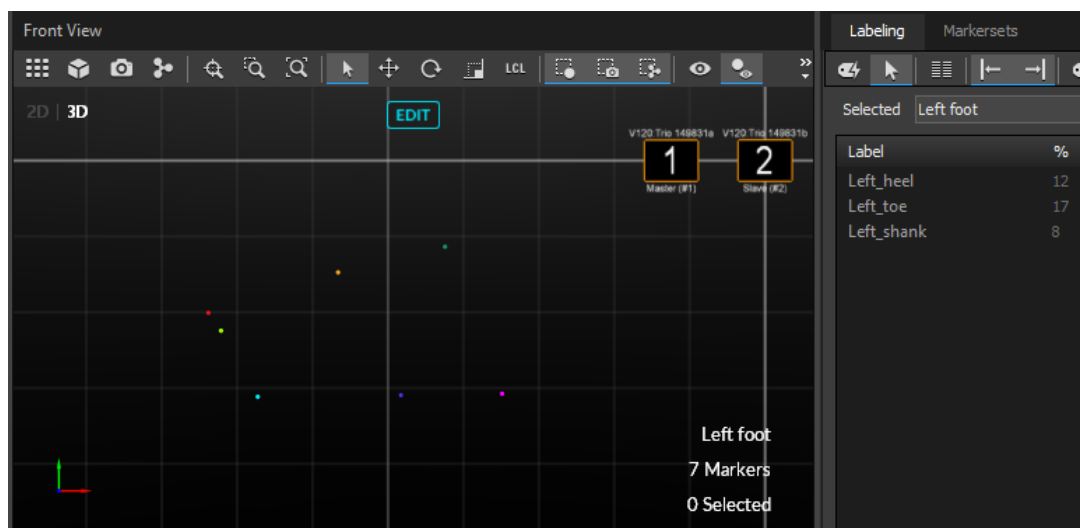


Figure 3.1.9\_The phase of labeling.

Once the labeling phase ended, it was essential to check if the transformation matrices obtained from the fixed markers worked. This was made for example for the right toe: the whole coordinate  $x$  of the right toe in the reference system of the bar n°2 was pre-multiplied by the transformation matrix. The coordinate  $x$  in the reference system of the bar n°1 and the same coordinate obtained from the transformation were superimposable, as the Figure 3.1.10 shows. This demonstrated that the transformation matrices previously calculated was mathematically correct.

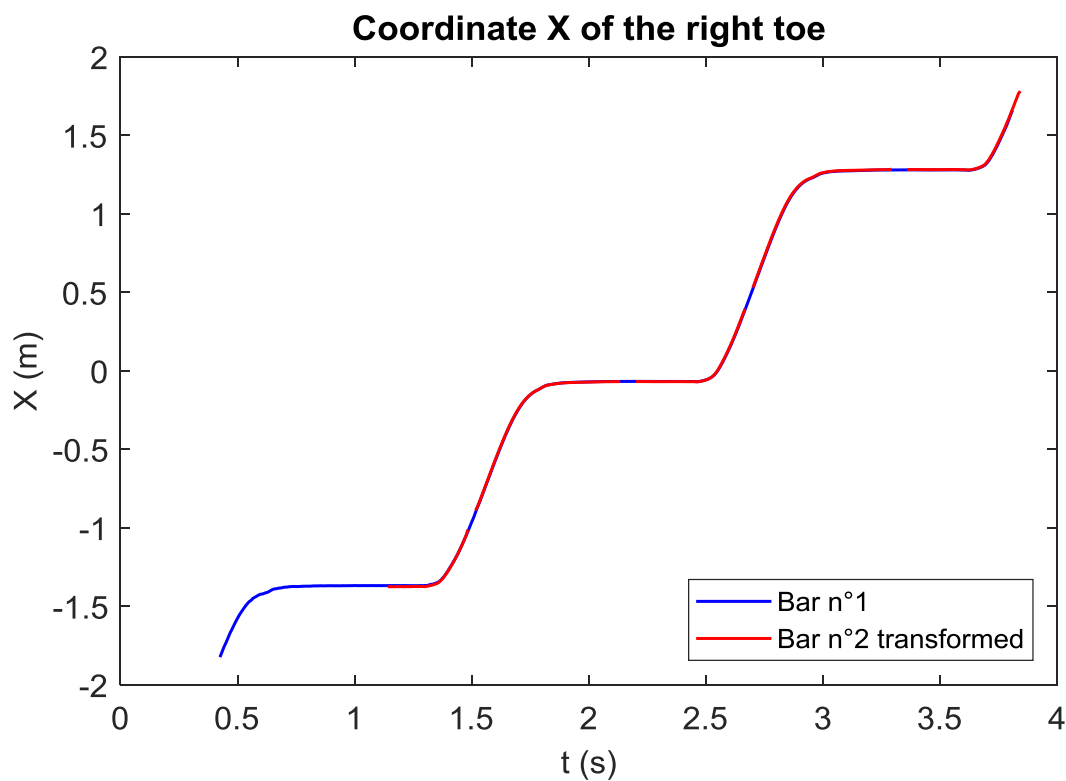


Figure 3.1.10\_Coordinates X of both bars for the right toe.

One transition in front of cameras at normal speed was analyzed. The data elaborated on Motive were exported and then imported on Matlab. In this way it became easier to create scripts which automatically identified gait events. According to work of Veilleux of 2016, gait events were easy to find in the antero-posterior trajectories of heels and toes (L. Veilleux, 2016):

- The toe-off is defined as the first frame where the toe marker changes direction in the anterior-posterior axis (Figure 3.1.11).
- The heel-strike is defined as the frame before the horizontal trajectory of the heel marker change of direction (Figure 3.1.12).

In order to control that these events were correct, the heel-strike and the toe-off were also searched for in the vertical coordinates of markers as the lowest points (Figure 3.1.13 and Figure 3.1.14).

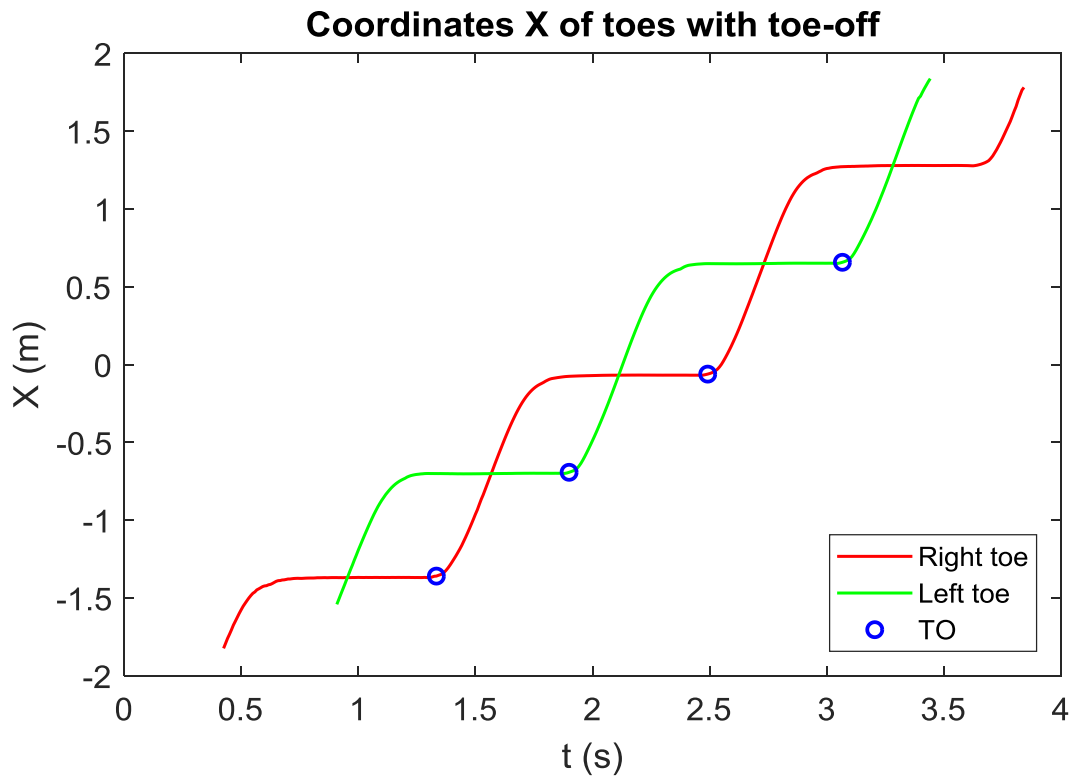


Figure 3.1.11\_Coordinates X of toes with toe-off (TO).

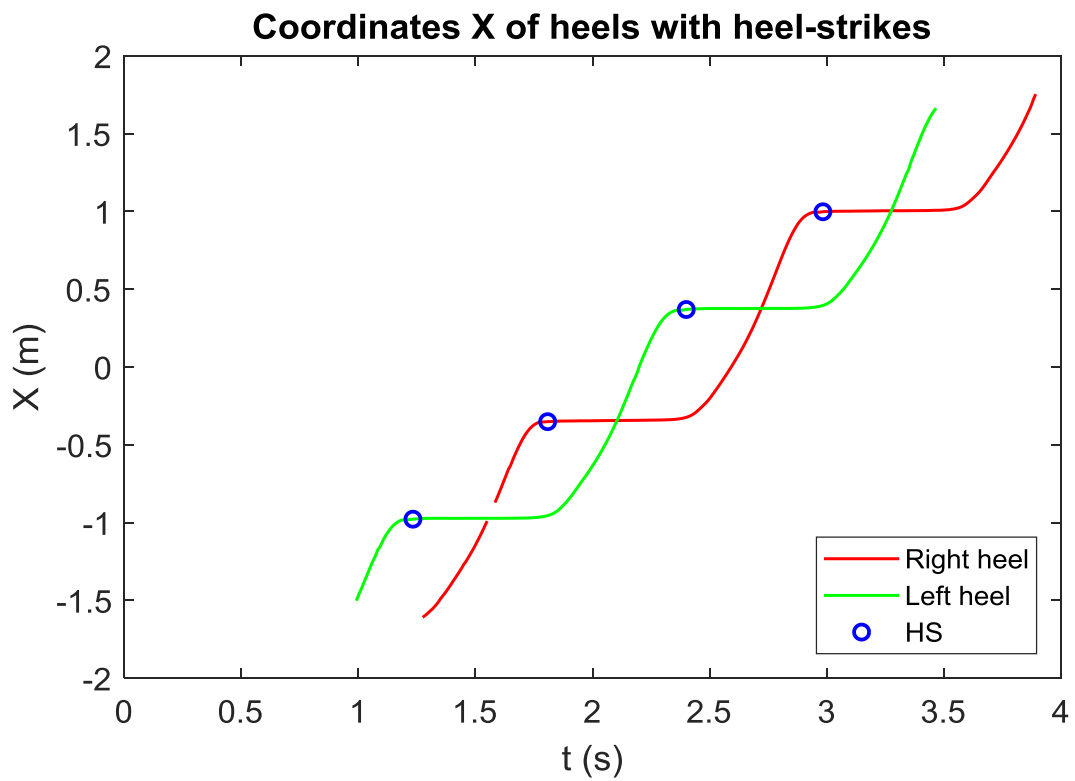


Figure 3.1.12\_Coordinate X of heels with heel-strikes (HS).

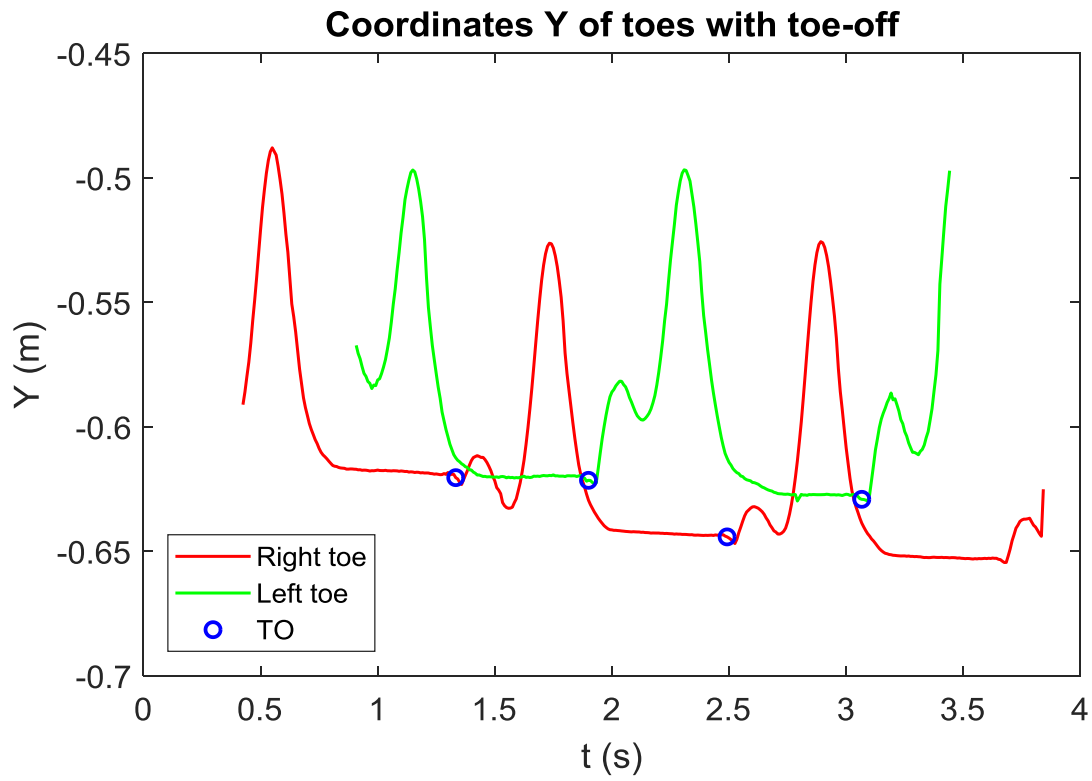


Figure 3.1.13\_Coordinates Y of toes with toe-off (TO).

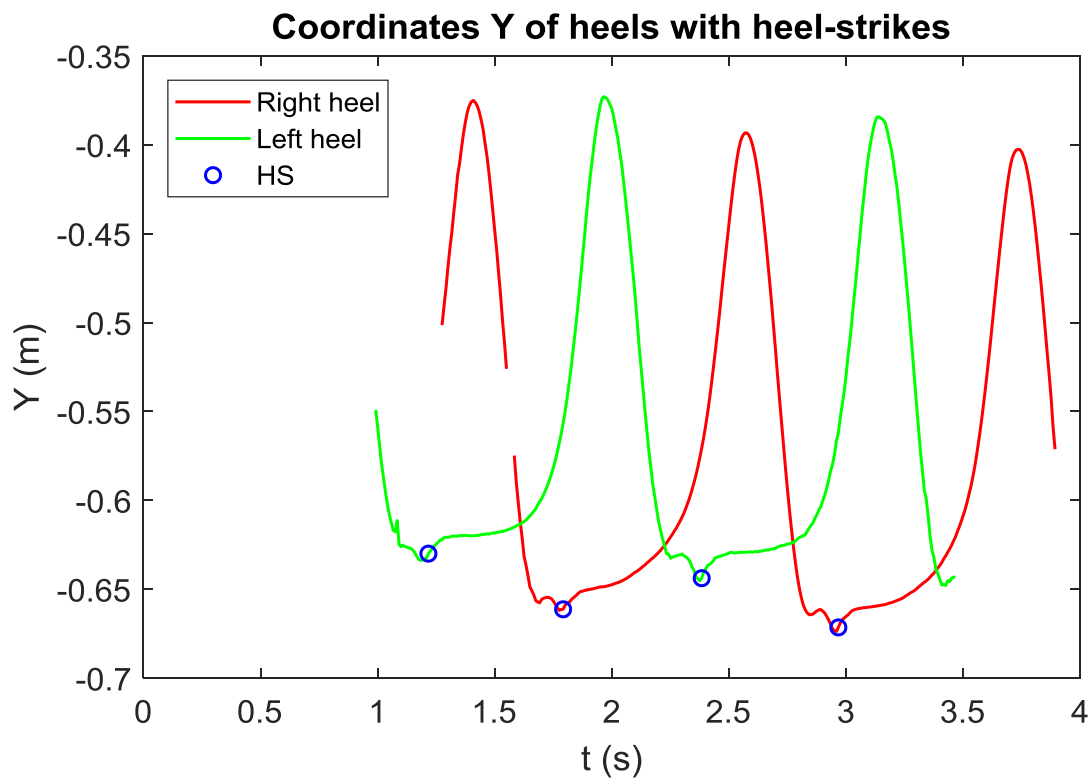


Figure 3.1.14\_Coordinates Y of heels with heel-strikes (HS).

On the basis of these gait events, it was possible to obtain the following Table 3.1.1 with the values of spatio-temporal parameters averaged between right and left sides:

<b>Spatio-temporal parameters</b>	<b>Mean values</b>
<b>Stride time (s)</b>	1,18
<b>Stride frequency (Hz)</b>	0,85
<b>Step time (s)</b>	0,58
<b>Step frequency (Hz)</b>	1,74
<b>Foot symmetry (%GC)</b>	0,49
<b>Stance time (s)</b>	0,68
<b>Swing time (s)</b>	0,49
<b>Single support time (s)</b>	0,5
<b>Double support time (s)</b>	0,19
<b>Limp index (right/left)</b>	1,03
<b>Stride length (m)</b>	1,35
<b>Stride length/height (%)</b>	87,04
<b>Step length (m)</b>	0,63
<b>Step length/height (%)</b>	40,44
<b>Step width (m)</b>	0,25
<b>Walking speed (m/s)</b>	1,15
<b>Speed/height (%)</b>	74,08
<b>Cadence (strides/min)</b>	51

Table 3.1.1\_Mean values of spatio-temporal parameters of the test subject.

In order to verify if these data are plausible or not, they were compared with spatio-temporal parameters obtained in literature through optical motion capture systems.

The Table 3.1.2 shows the spatio-temporal parameters of the preliminary test compared with those found in literature. The parameters obtained with Optitrack V120:Trio are of the same order of magnitude of those presented in literature with different optical motion capture systems.

<b>Spatio-temporal parameters</b>	<b>Pre-test</b>	<b>(F. Bugané, 2012)</b>	<b>(C. P. Meena, 2015)</b>	<b>(F. Kluge, 2017)</b>
<b>Stride time (s)</b>	1,18	1,09		1,13
<b>Stride frequency (Hz)</b>	0,85			
<b>Step time (s)</b>	0,58	0,54		0,72
<b>Step frequency (Hz)</b>	1,74			
<b>Foot symmetry (%GC)</b>	49	50		
<b>Stance time (s)</b>	0,68		0,8	
<b>Swing time (s)</b>	0,49		0,37	0,41
<b>Single support time (s)</b>	0,5			
<b>Double support time (s)</b>	0,19			
<b>Limp index (right/left)</b>	1,03			
<b>Stride length (m)</b>	1,35	1,38	1,09	1,45
<b>Stride length/height (%)</b>	87,04	80		
<b>Step length (m)</b>	0,63	0,69	0,54	
<b>Step length/height (%)</b>	40,44			
<b>Step width (m)</b>	0,25			
<b>Walking speed (m/s)</b>	1,15	1,29	1,17	1,34
<b>Speed/height (%)</b>	74,08	74,95		
<b>Cadence (strides/min)</b>	51	56		

Table 3.1.2\_Comparison between the spatio-temporal parameters obtained with the preliminary test and those found in literature.

### 3.2 Preliminary tests with Xsens

The setting chosen for the experiment was a corridor of 15 meters. All the seven Xsens MTx were positioned in two different configurations. According to the first one (Figure 3.2.1):

- n°681 → right foot
- n°682 → left foot
- n°683 → right thigh
- n°684 → right shank
- n°685 → left thigh
- n°686 → left shank
- n°494 → trunk

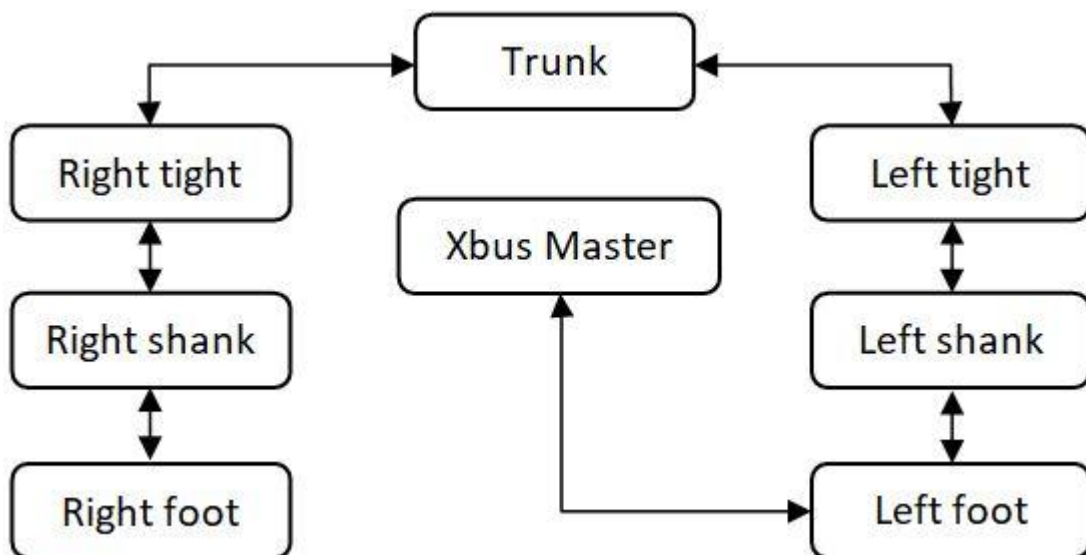


Figure 3.2.1\_First configuration of Xsens MTx.

According to the second one (Figure 3.2.2):

- n°681 → right foot
- n°682 → left foot
- n°683 → right shank
- n°684 → right heel
- n°685 → left shank
- n°686 → left heel
- n°494 → trunk

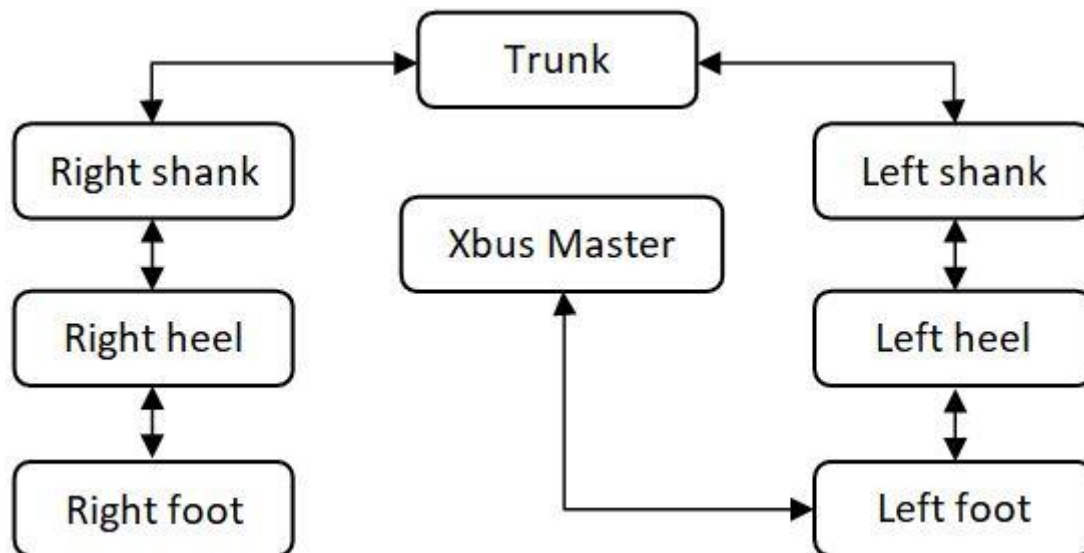


Figure 3.2.2\_Second configuration of Xsens MTx.

The subject chosen for the test was a healthy female of 24 years old wearing her shoes. The following four figures (from Figure 3.2.3 to Figure 3.2.6) show the configurations of inertial sensors with their local axes.

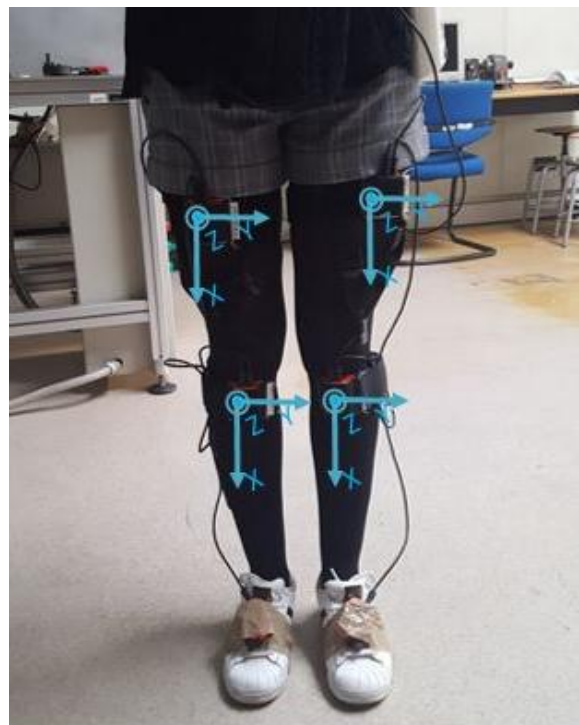


Figure 3.2.3\_The inertial sensors MTx on the tights and on the shanks with their local reference systems.



Figure 3.2.4\_The inertial sensor MTx on the trunk with its local reference system.

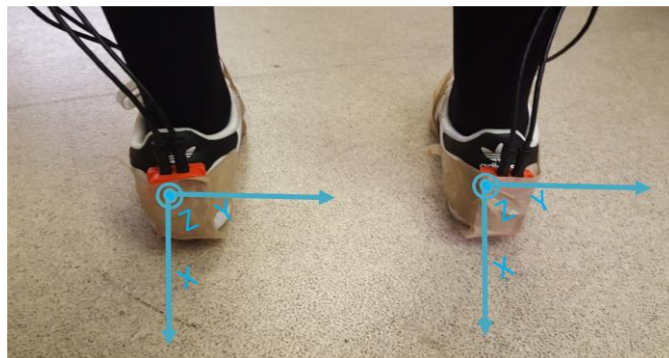


Figure 3.2.5\_The inertial sensors MTx on the heels with their local reference systems.



Figure 3.2.6\_The inertial sensors MTx on the feet with their local reference systems.

Since all the seven inertial sensors were used, the sampling frequency could be at most 50 Hz. For both configurations, the subject was asked to walk along the corridor always in the same direction at three different speeds: normal, fast and slow. For each speed the test was repeated five times. There were in total fifteen acquisitions. The Figure 3.2.7 shows the subject walking along the corridor.



**Figure 3.2.7**\_An example of acquisition with the subject walking at normal speed.

One acquisition at normal speed was analyzed. In order to consider the signal when the subject was already walking, the first two steps were not examined. In the same way, also the last two steps were discarded. The analysis was focused on ten steps, so on five complete strides.

The data of each sensor were exported with the software MT Manager and then imported on Excel and Matlab. The axes of all the sensors were rotated and overturned in order to obtain a Cartesian triad with x-axis pointing upward, y-axis pointing to the right side of the subject and z-axis pointing in the same direction of the gait.

The signals recorded were plotted in order to make comparisons with previous literature articles and works. The first similarity was noticed between the trunk acceleration along the sensor Z-axis and the trunk acceleration in the antero-posterior direction obtained by Zijlstra in 2004 (Figure 3.2.8).

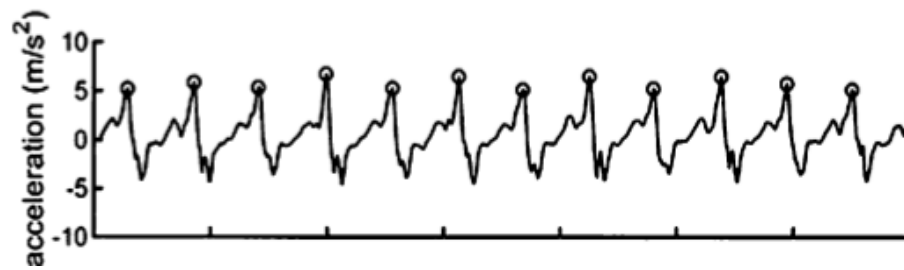


Figure 3.2.8\_The antero-posterior acceleration measured by Zijlstra in his work (Zijlstra, 2004).

Since the similarity of the two trends was evident, it was possible to identify the heel-strikes as Zijlstra did in his work: they were found as the peaks preceding the zero-crossings from positive to negative. First it was necessary to build a Matlab function to find the zero-crossings from positive to negative: every time the function found a positive sample followed by two negative samples, a zero-crossing was identified. Then, the code calculated the maximum of the acceleration in the interval between two consecutive zero-crossing instants.

The Figure 3.2.9 shows the trunk acceleration along sensor Z-axis with the HS identified by circles:

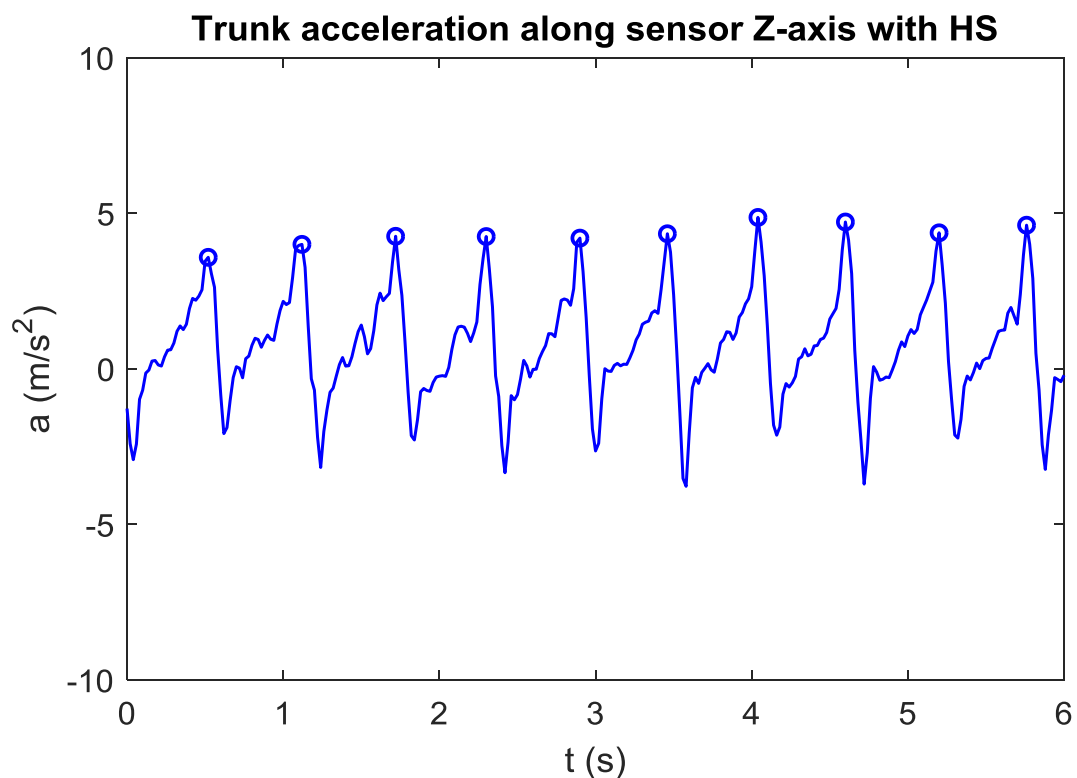


Figure 3.2.9\_The acceleration along the trunk sensor Z-axis with the HS identified with circles.

An interesting analysis was made with the acceleration along the trunk sensor Z-axis and the angular velocity around the same axis. It was noticed an alternation of sign of the angular velocity every time there was a peak in the acceleration. This alternation was used in order to distinguish between right and left steps. In Matlab the sum of the angular velocity in the interval between a peak and the next zero-crossing of the acceleration was made. Then, the sign of this sum was evaluated: when it was positive, the step was considered a right step; conversely, a negative sum indicated a left step. The Figure 3.2.10 shows the alternation of sign of the angular velocity every time a peak of acceleration occurs.

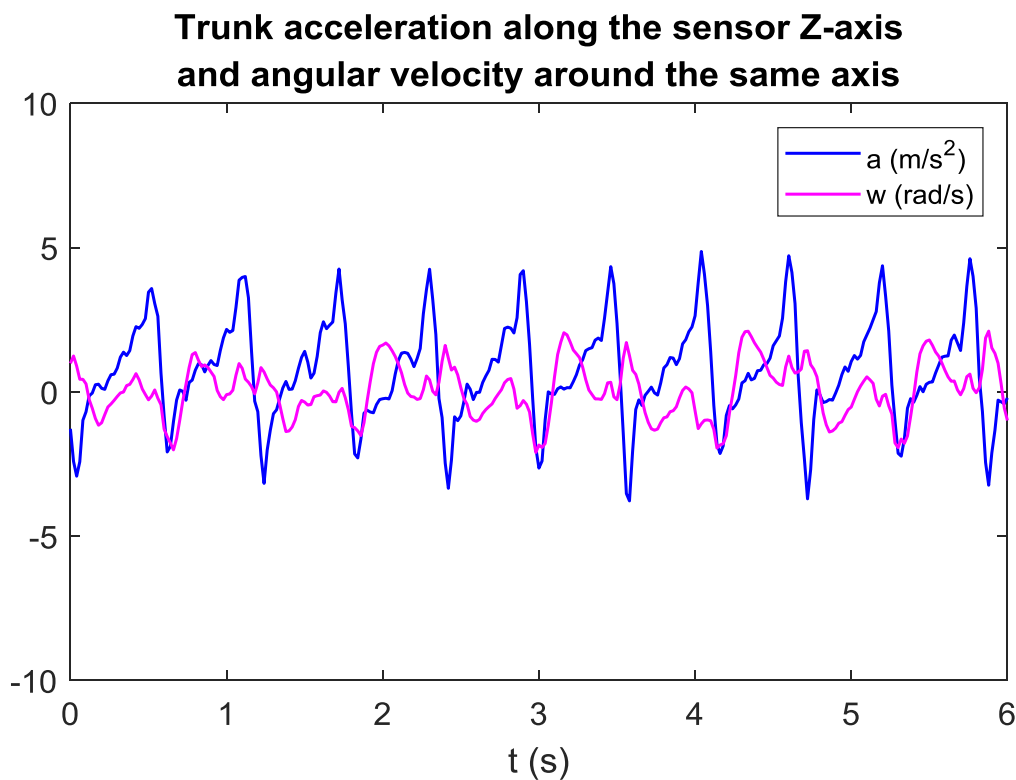


Figure 3.2.10\_Trunk acceleration along the sensor Z-axis and trunk angular velocity around the same axis.

In the Figure 3.2.11 it is possible to see the distinction between right and left steps through the sign of angular velocity around sensor Z-axis. The result was the pelvis acceleration along the sensors Z-axis with the alternation of red and green circles, the two colours corresponding respectively to right and left steps. In order to verify if this method of distinction between right and left steps was correct, the heels accelerations along sensors Z-axis were plotted, as it can be seen in Figure 3.2.12.

This algorithm for the distinction between right and left HS was considered correct, because the colours of the circles in the Figure 3.2.11 corresponded to the colours of the signals in the Figure 3.2.12.

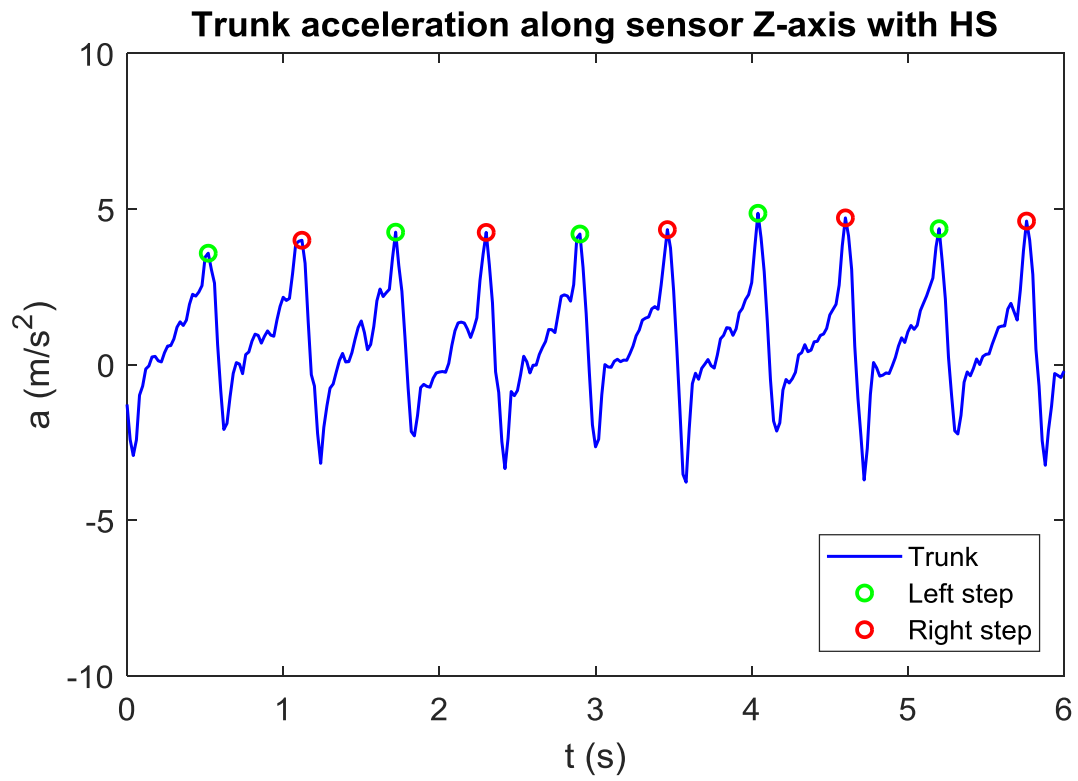


Figure 3.2.11\_Trunk acceleration along the sensor Z-axis with the distinction between right and left HS.

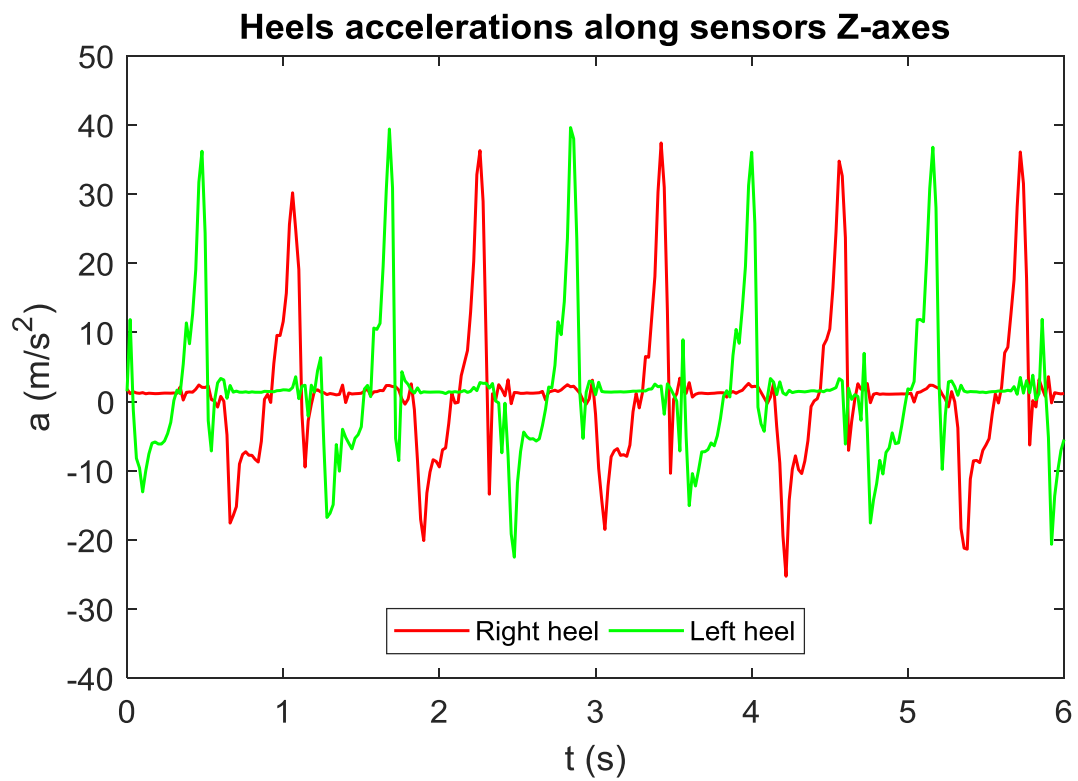


Figure 3.2.12\_Heels accelerations along the sensors Z-axes.

Another similarity was found between the acceleration along heels sensors Z-axes (Figure 3.2.13) and the acceleration along the accelerometer X-axis measured by Rampp and his colleagues in 2015 (Figure 3.2.14). In order to make a more effective comparison with literature, the acceleration was expressed with the same unit of the one presented by Rampp. According to this article, the HS were the acceleration minima after the zero-crossings from positive to negative.

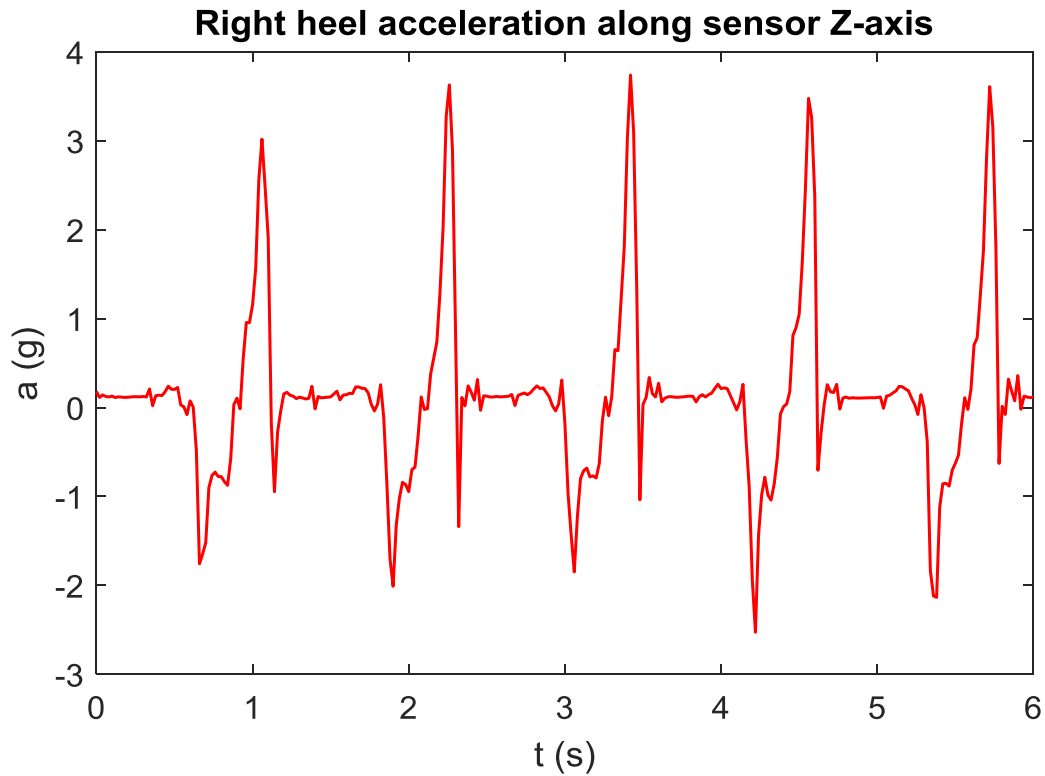


Figure 3.2.13\_Right heel acceleration along sensor Z-axis.

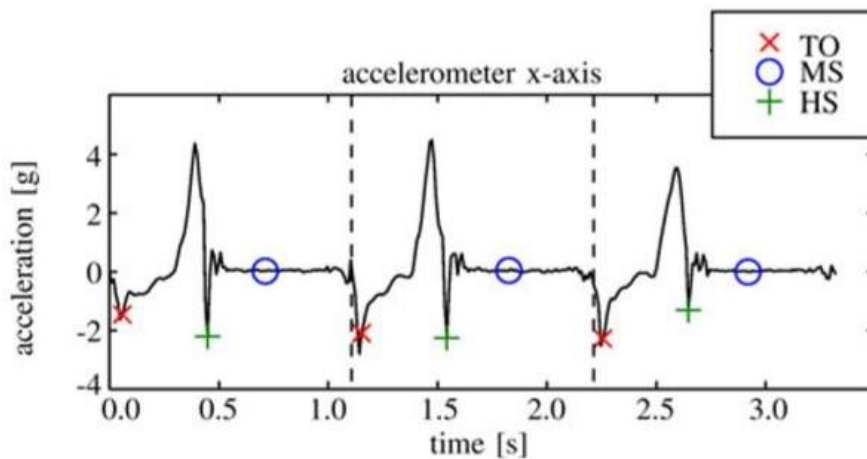


Figure 3.2.14\_The accelerometer X-axis measured by Rampp in his work (A. Rampp, 2015).

It was interesting to see if the method proposed by Zijlstra in 2004 and the one proposed by Ramp in 2015 identified as heel-strikes instants the same frames: the check consisted in plotting heel-strikes instants found with Zijlstra method on the heels accelerations.

As the Figure 3.2.15 shows, there was only a frame of difference: heel-strikes found in the trunk acceleration preceded the ones found in heels accelerations of a frame.

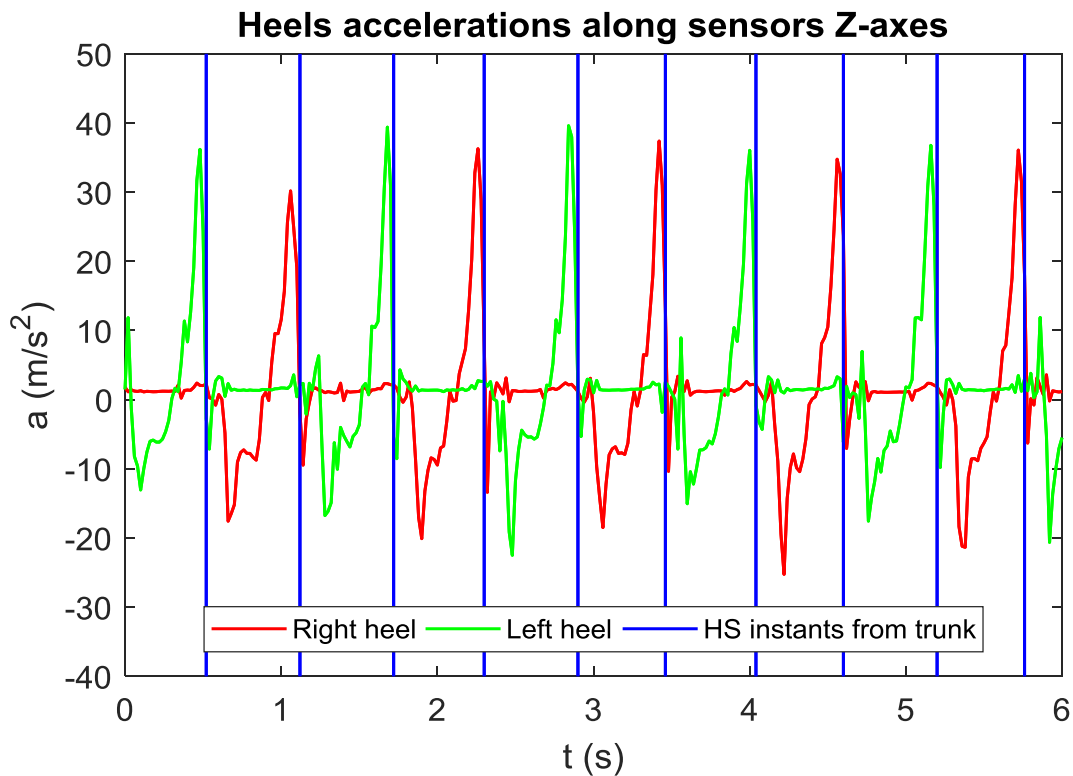


Figure 3.2.15\_Heels accelerations along sensors Z-axes with instants corresponding to the HS found in the trunk acceleration.

In the same way, the angular velocity around the heels sensors Y-axes was very similar to the angular velocity in the sagittal plane found by Misu and his colleagues in 2017 (Figure 3.2.16). They identified the toe-off as the time of the first maximum value after quiet standing and every other maximum (S. Misu, 2017). As before, the accelerations were expressed in the same unit of those used in the work analyzed. Since there was evident similarity, a Matlab code was created to find toe-off as the maxima of the heels angular velocities around sensors Y-axis. First, it was necessary to build a function that found every zero-crossing from negative to positive: when it identified a negative sample and five positive samples, it established the presence of a zero-crossing. Then, the code searched for every TO as the maximum between two consecutive zero-crossings from negative to positive. The Figure 3.2.17 shows the angular velocities of heels with the TO identified with circles.

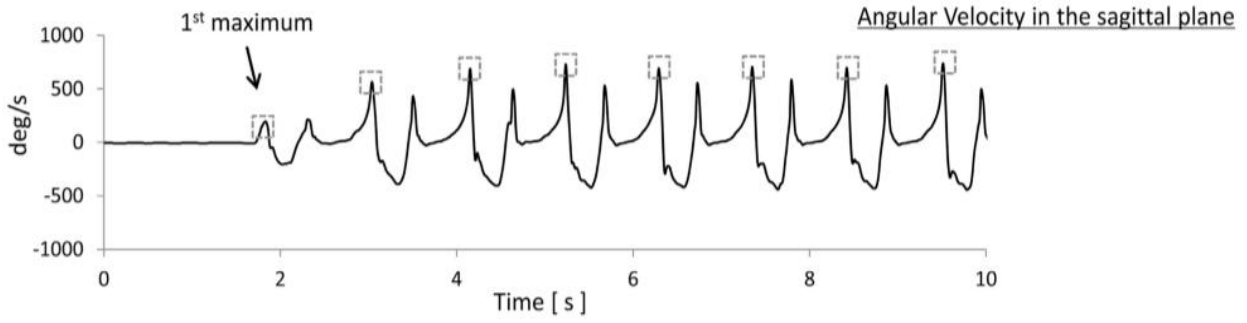


Figure 3.2.16\_The angular velocity in the sagittal plane measured by Misu in his work (S. Misu, 2017).

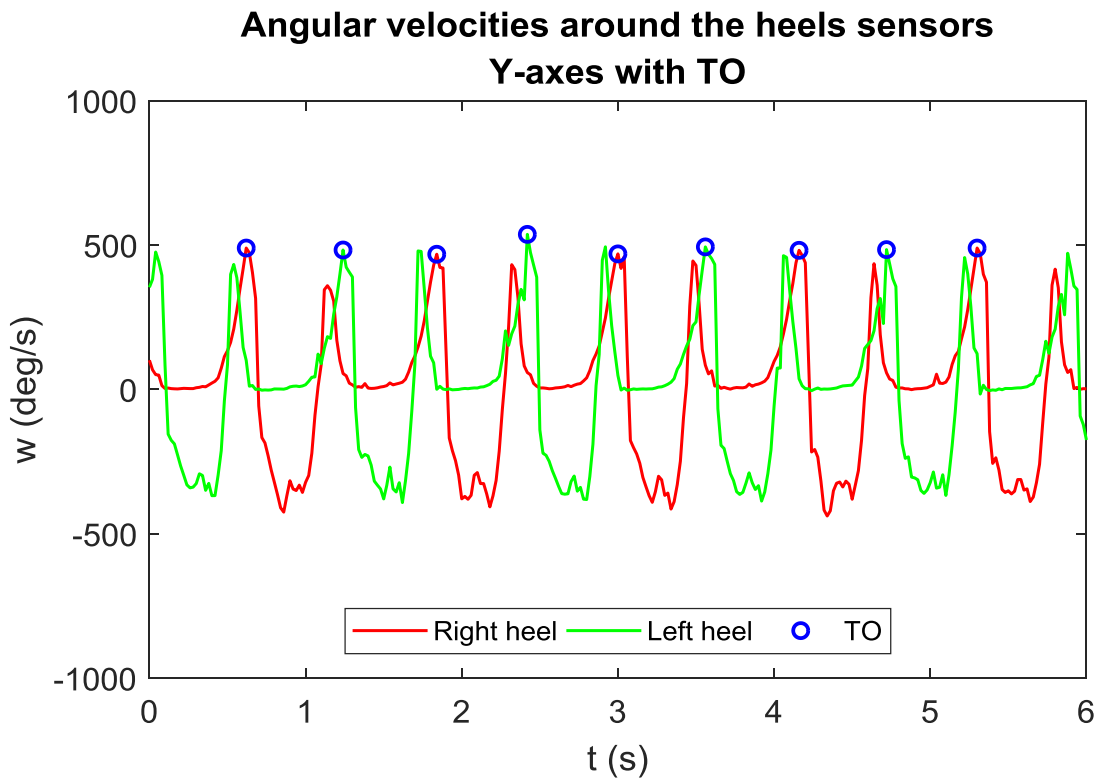


Figure 3.2.17\_The angular velocities around heels sensors Y-axes with the TO identified with circles.

Once the gait events were found, it was possible to estimate the spatio-temporal parameters, mediating ten strides. The Table 3.2.1 presents the mean values of the parameters:

<b>Spatio-temporal parameters</b>	<b>Mean values</b>
<b>Stride time (s)</b>	1,16
<b>Stride frequency (Hz)</b>	0,86
<b>Step time (s)</b>	0,58
<b>Step frequency (Hz)</b>	1,73
<b>Foot symmetry (%GC)</b>	50
<b>Stance time (s)</b>	0,68
<b>Swing time (s)</b>	0,48
<b>Single support time (s)</b>	0,51
<b>Double support time (s)</b>	0,20
<b>Limp index (right/left)</b>	1,03

**Table 3.2.1\_Mean values of the spatio-temporal parameters estimated with Xsens MTx.**

The Table 3.2.2 shows the spatio-temporal parameters of the preliminary test compared with those found in literature. The parameters obtained with Xsens inertial sensors are of the same order of magnitude of those presented in literature with different IMUs.

<b>Spatio-temporal parameters</b>	<b>Pre-test</b>	(S. Misu, 2017)	(F. Kluge, 2017)	(A. Rampp, 2015)
<b>Stride time (s)</b>	1,16	1,04	1,13	1,23
<b>Stride frequency (Hz)</b>	0,86			
<b>Step time (s)</b>	0,58	0,52		0,72
<b>Step frequency (Hz)</b>	1,73			
<b>Foot symmetry (%GC)</b>	50	50		
<b>Stance time (s)</b>	0,68	0,61	0,72	0,86
<b>Swing time (s)</b>	0,48	0,43	0,41	0,36
<b>Single support time (s)</b>	0,51			
<b>Double support time (s)</b>	0,20			
<b>Limp index (right/left)</b>	1,03			

Table 3.2.2\_Comparison between the spatio-temporal parameters obtained with the preliminary test and those found in literature.

### 3.3 Preliminary tests with Optitrack and Xsens not synchronized

The setting chosen for the experiment was the same laboratory used for the preliminary test with Optitrack V120:Trio. The cameras were placed as the same configuration and with the same distances of the experiment with the first subject. On the floor a guideline was created with scotch tape in order to establish the exact rectilinear path. Before the dynamic acquisitions, it was necessary to place three markers on the floor at different heights and to do a static acquisition. They consented to create a reference system used to transform the data from the system of one bar into the other's one (Figure 3.3.1).

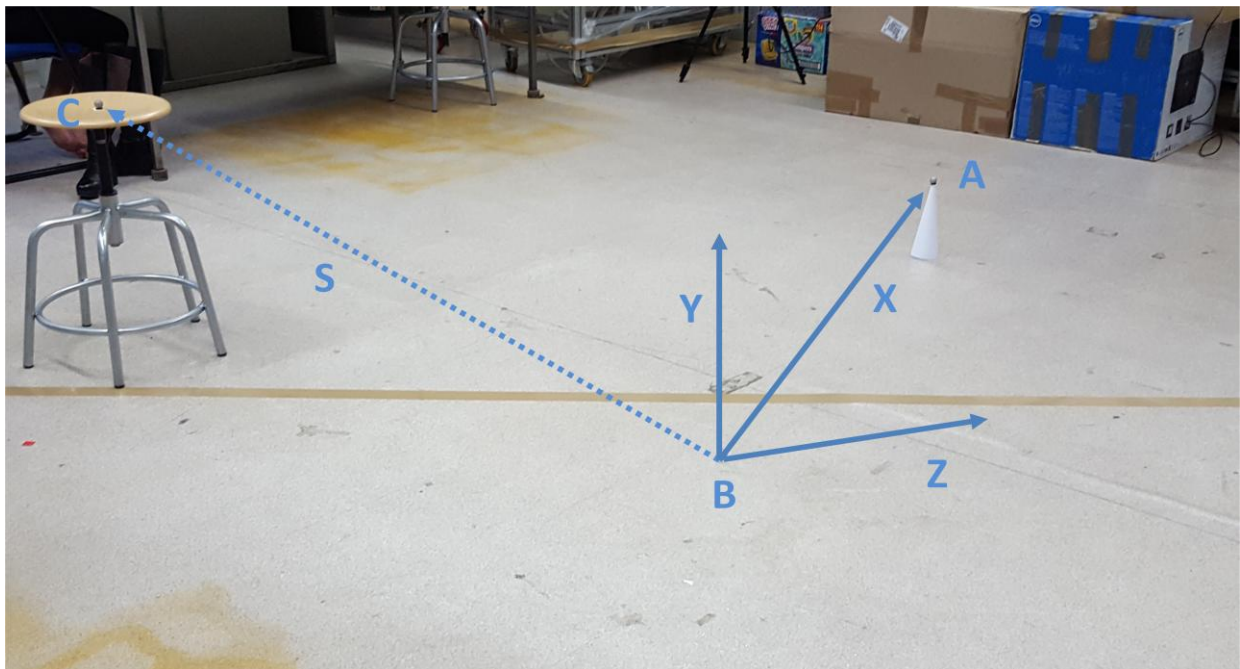


Figure 3.3.1\_Configuration of fixed markers for the creation of the transformation matrix.

Thanks to this new reference system, it was possible to build the transformation matrix. It pre-multiplied the data from one bar in order to fill the gap and to obtain better coordinates. Once this matrix was created and the data were multiplied, the same check of the first test was made: the coordinates of one bar were superimposable to those of the other bar transformed and so the matrix could be considered mathematically correct.

At this point it was necessary to place markers and inertial sensors on the subjects.

The subjects chosen were two: a healthy female of 54 years old and a healthy male of 24 years old, both barefoot. For each subject six markers were used: two on the toes, two on the heels and two on the malleolus. The markers on the shanks used in the first experiment were discarded, because all the spatio-temporal parameters were obtained only from the trajectories of heels and toes.

All the seven Xsens MTx were positioned according to a specific configuration, shown in Figure 3.3.2:

- n°681 → right foot
- n°682 → left foot
- n°683 → right shank
- n°684 → right heel
- n°685 → left shank
- n°686 → left heel
- n°494 → trunk

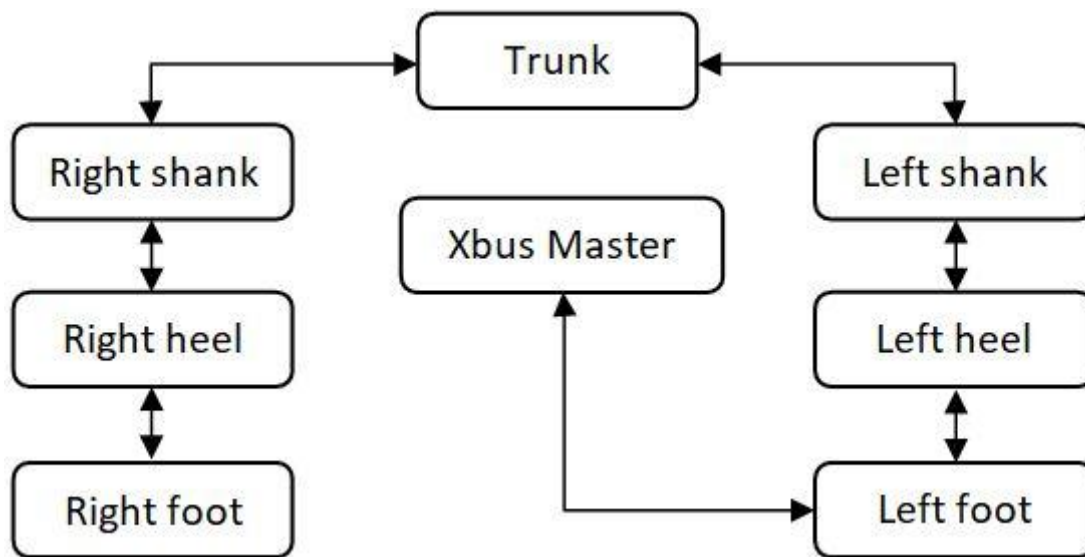


Figure 3.3.2\_Configuration of Xsens MTx.

The first configuration adopted in the first experiment was excluded, because the thighs do not produce interesting signals. The Xbus Master was located at waist level. The following six figures (from Figure 3.3.3 to Figure 3.3.8) show the MTx on both subjects.

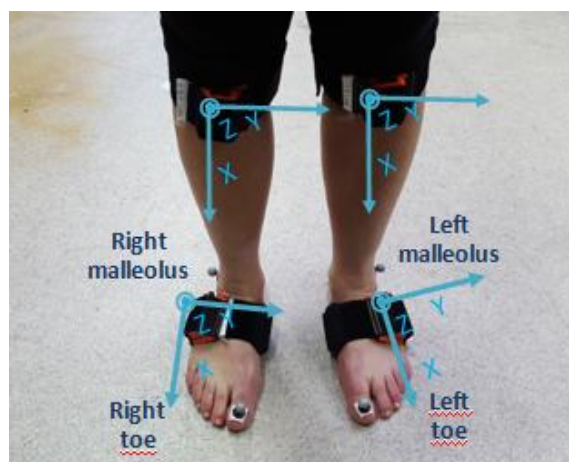


Figure 3.3.3\_Female subject: Xsens MTx on shanks and feet with their local reference systems; markers on malleolus and toes.

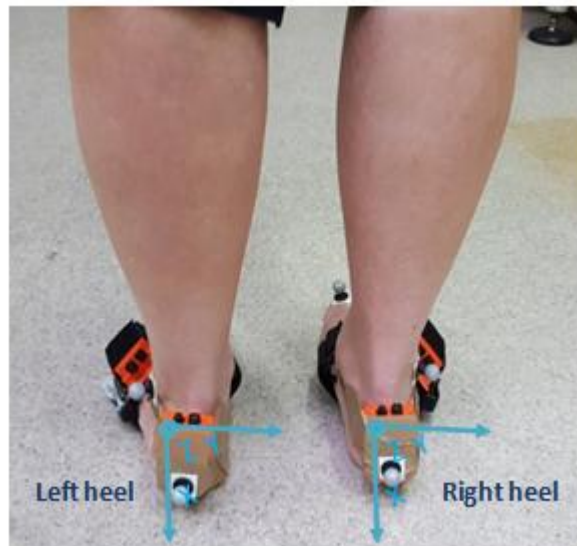


Figure 3.3.4\_Female subject: Xsens MTx on heels with their local reference systems; markers on heels.

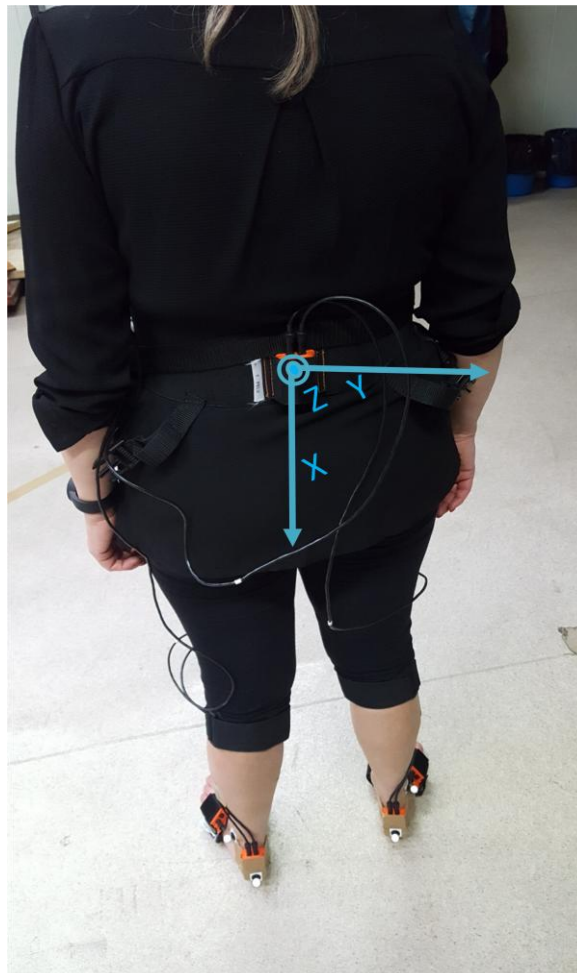


Figure 3.3.5\_Female subject: Xsens MTx on the trunk with its local reference system.

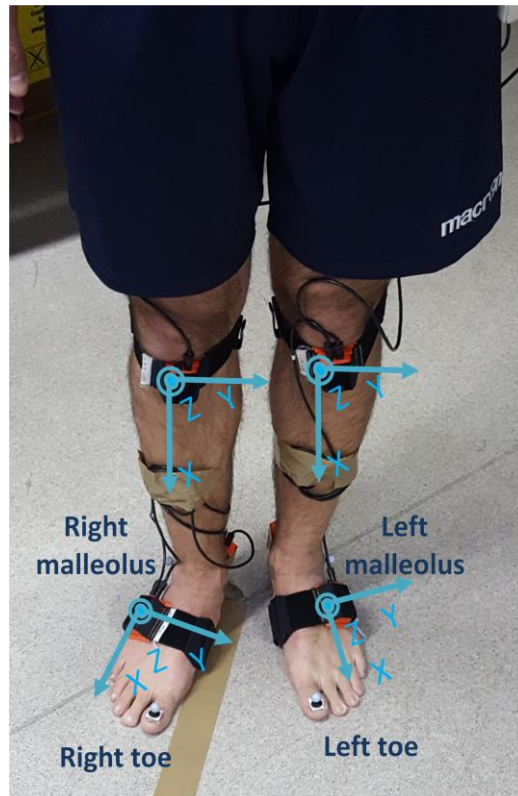


Figure 3.3.6\_ Male subject: Xsens MTx on shanks and feet with their local reference systems; markers on malleolus and toes.

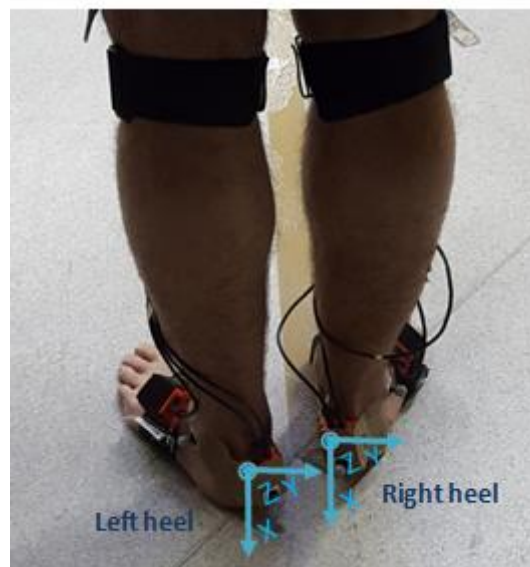


Figure 3.3.7\_ Male subject: Xsens MTx on heels with their local reference systems; markers on heels.



Figure 3.3.8\_ Male subject: Xsens MTx on the trunk with its local reference system.

The subjects were asked to walk barefoot following the guideline. The test was made at three different speeds: normal, fast and slow. The walk was made always in the same direction of progression. For each speed the test was repeated four times. For each subject there were in total 12 acquisitions. The Figure 3.3.9 shows the two subjects walking following the line on the floor.



Figure 3.3.9\_Examples of acquisitions with the subjects walking at normal speed.

After the test, for each subject one acquisition at normal speed was analysed. After having done the labeling of markers, the same transformation matrices calculated in subchapter 5.1 were used. In order to check if the transformation matrices were correct, the coordinate X of left toe of female subject was plotted (Figure 3.3.10).

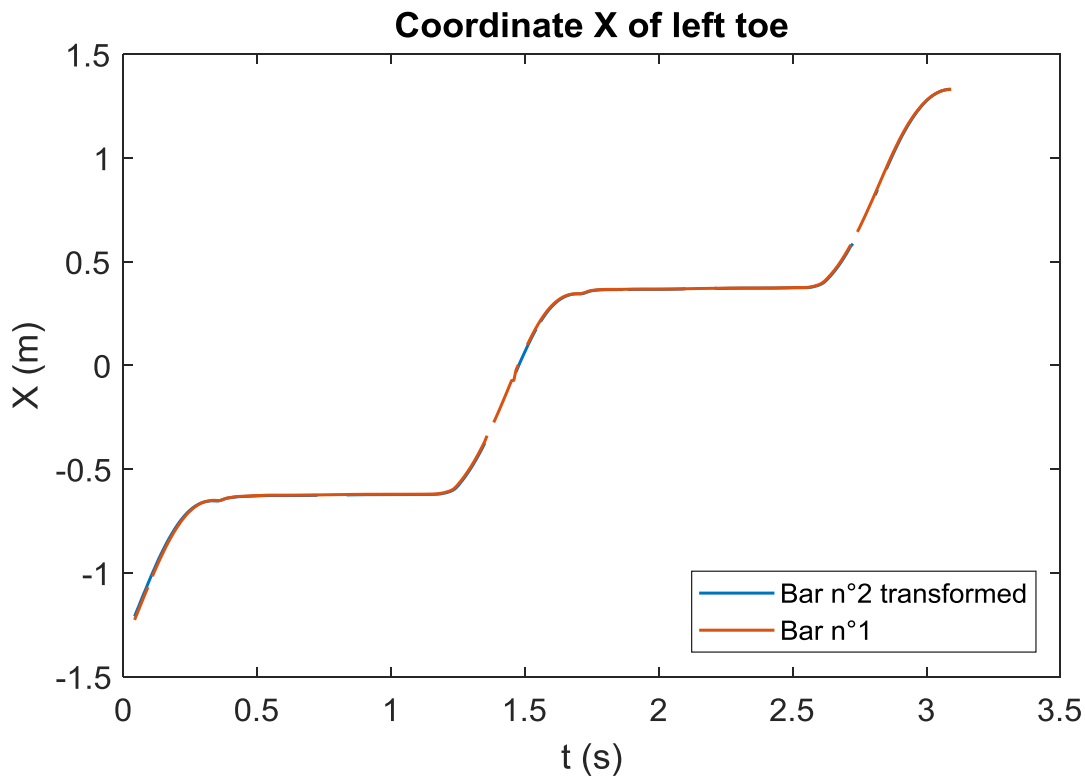


Figure 3.3.10\_ Female subject: coordinates X of the bar n°1 and of the bar n°2 transformed of the left toe.

As the Figure 3.3.10 shows, the data from bar n°1 and those from bar n°2 transformed were superimposable. This allowed to affirm that the transformation matrices were mathematically correct.

Next step consisted in searching for heel-strikes and toe-off in the horizontal coordinates. The HS were identified as the frames before the horizontal trajectory of the heel marker change of direction, whereas the TO were the first frames where the toes markers changed direction in the anterior-posterior axis (L. Veilleux, 2016). The positions of these gait events were also controlled in the vertical coordinates, verifying that they corresponded to the lowest frames.

The following eight figures (from Figure 3.3.11 to Figure 3.3.18) show the horizontal and the vertical coordinates of the markers of both subjects, with HS and TO identified with circles.

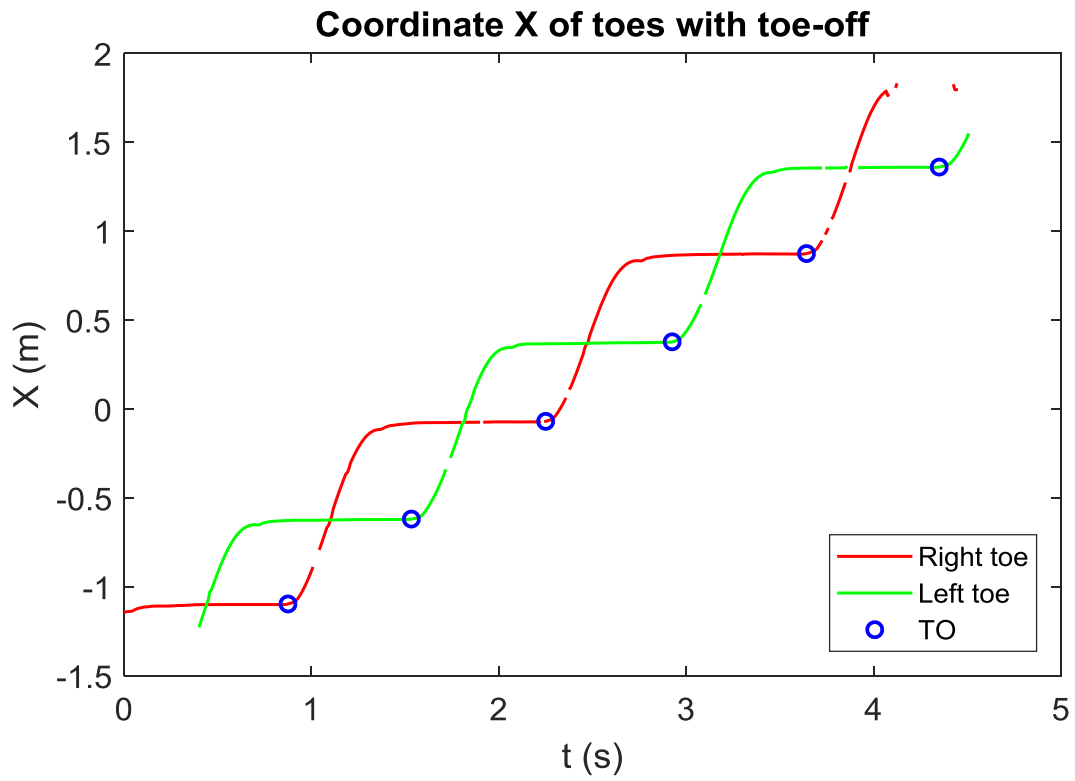


Figure 3.3.11\_Female subject: coordinate X of toes with toe-off (TO).

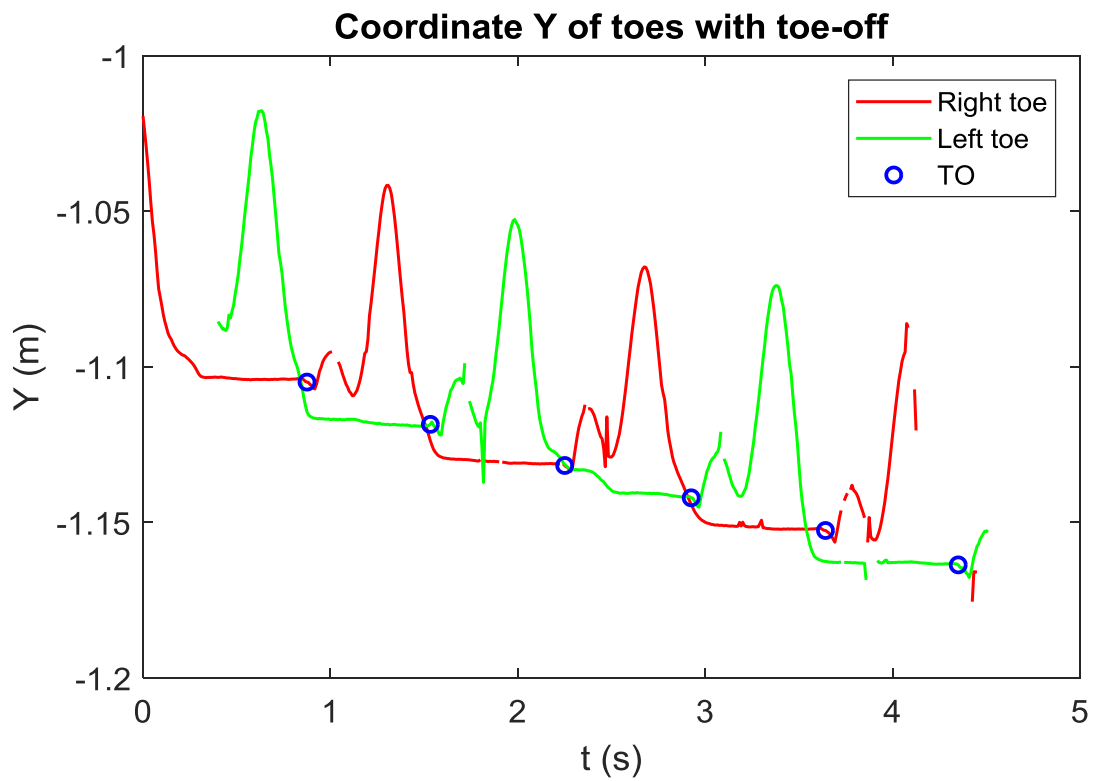


Figure 3.3.12\_Female subject: coordinate Y of toes with toe-off (TO).

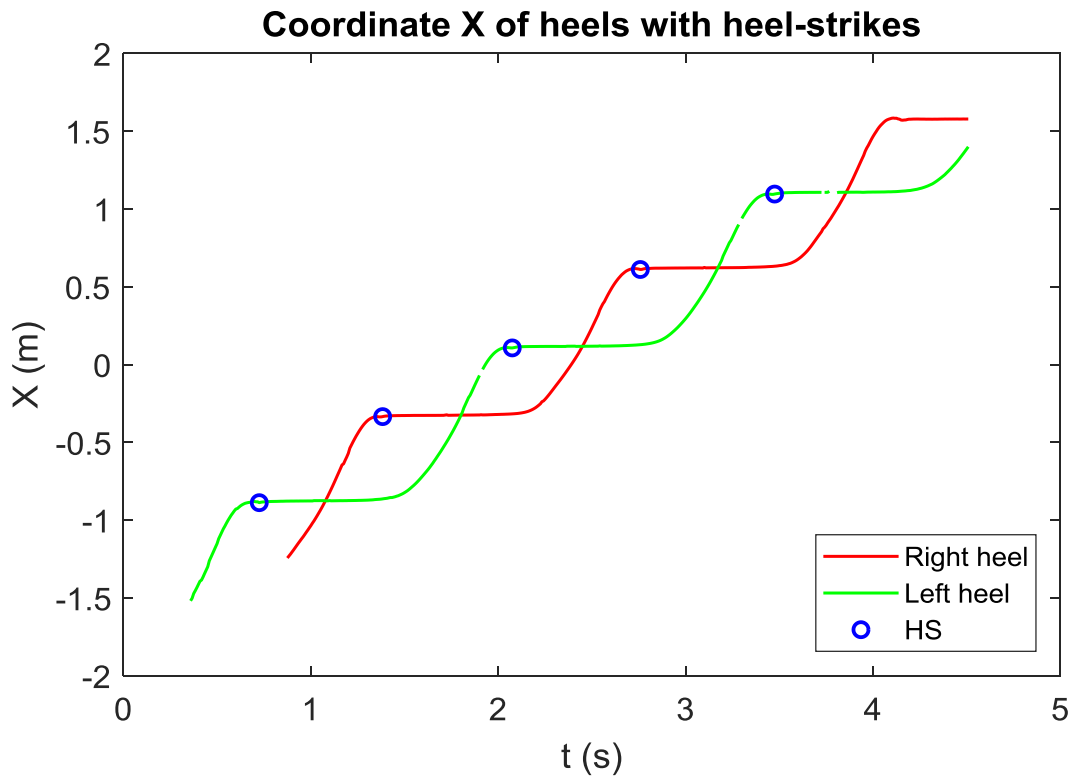


Figure 3.3.13\_Female subject: coordinate X of heels with heel-strikes (HS).

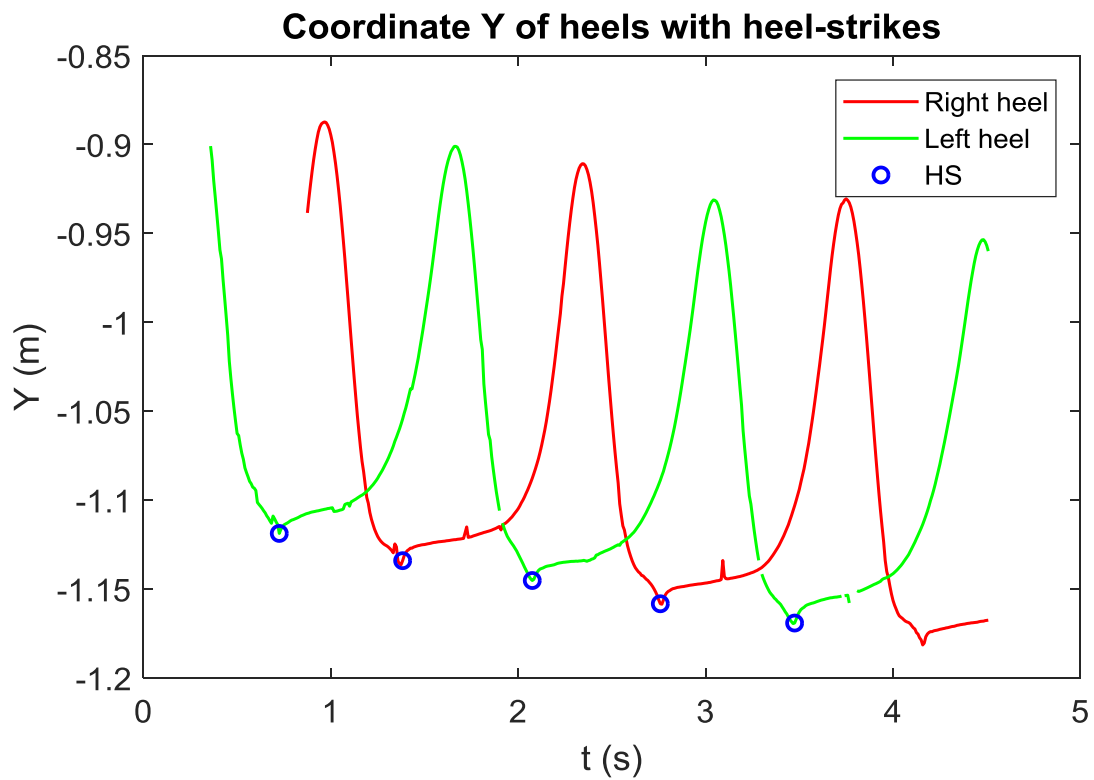


Figure 3.3.14\_Female subject: coordinate Y of heels with heel-strikes (HS).

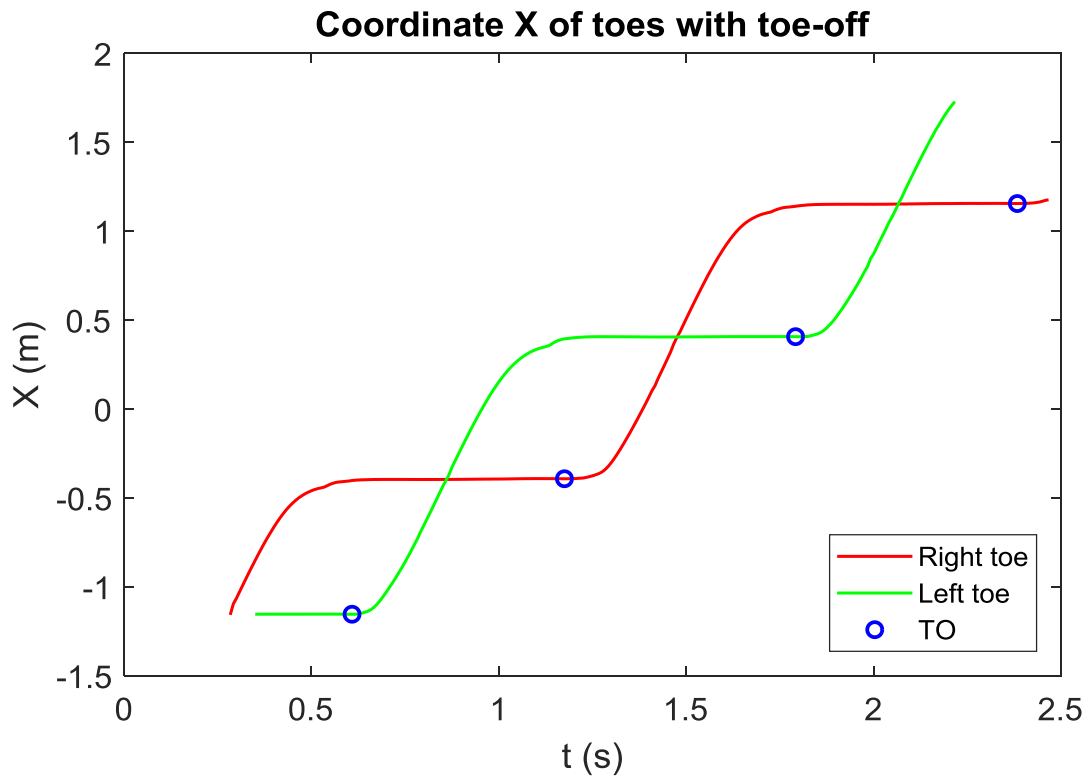


Figure 3.3.15\_Male subject: coordinate X of toes with toe-off (TO).

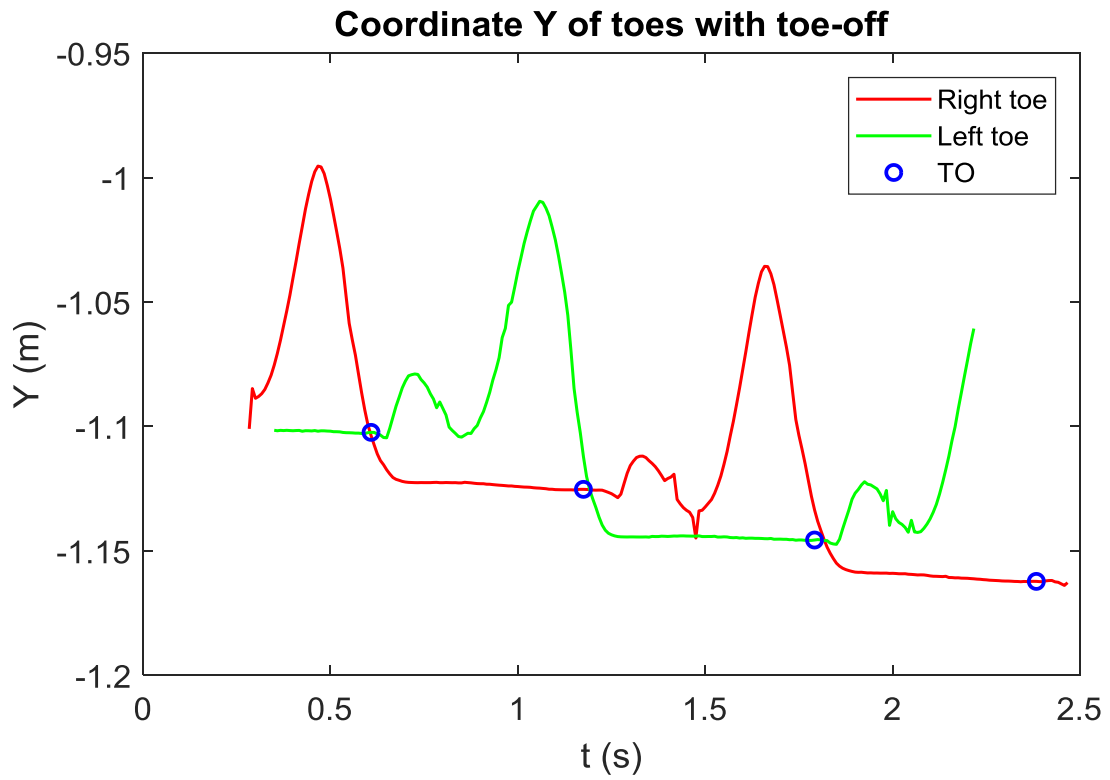


Figure 3.3.16\_Male subject: coordinate Y of toes with toe-off (TO).

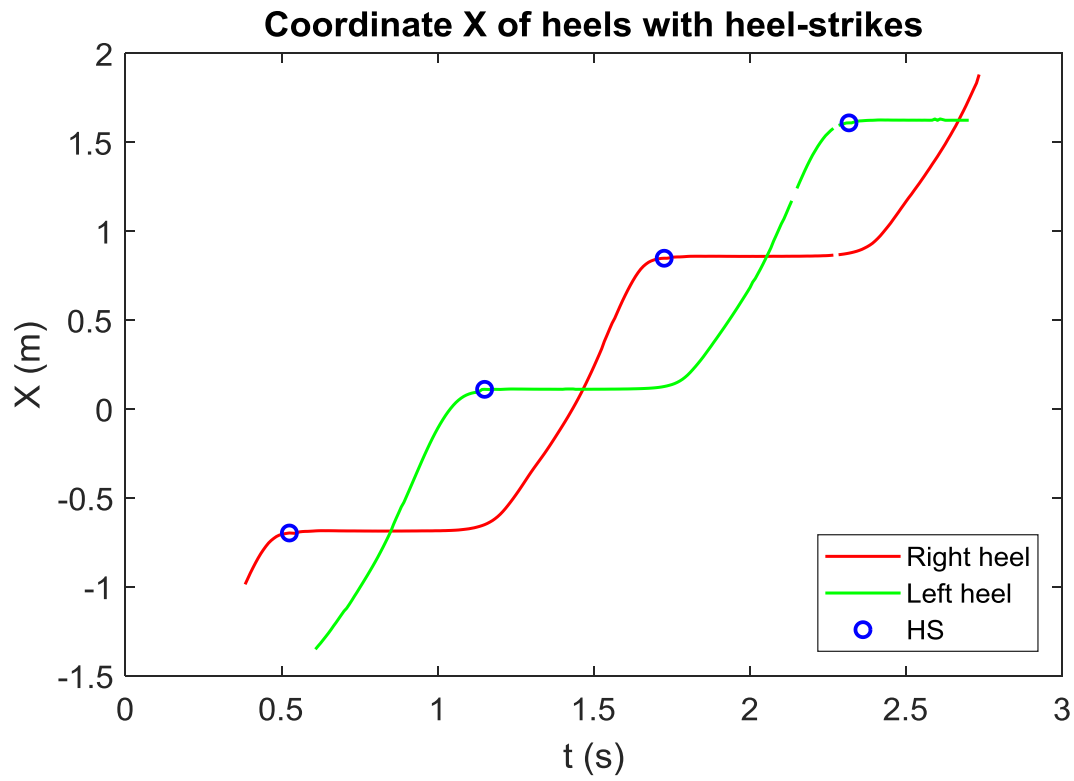


Figure 3.3.17\_Male subject: coordinate X of heels with heel-strikes (HS).

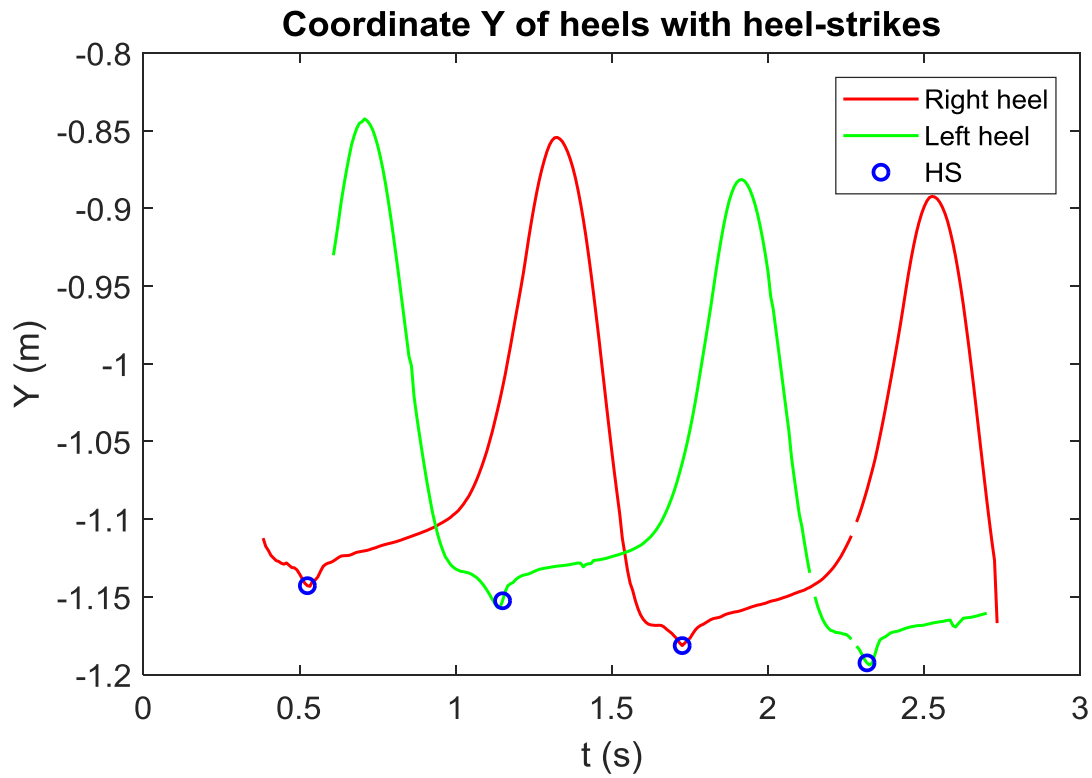


Figure 3.3.18\_Male subject: coordinate Y of heels with heel-strikes (HS).

After the identification of gait events in Optritrack trajectories, it was necessary to analyze the Xsens signals. The same procedure followed with the subject of the second test was applied for both subjects. The HS were identified as the peaks of trunk acceleration along the sensor Z-axis, distinguishing between right and left through the sign of angular velocity around the same axis. The TO were identified as the maxima of the heels angular velocities around sensors Y-axes. The same Matlab code and functions were used in order to identify gait events.

The four following figures (from Figure 3.3.19 to Figure 3.3.22) show the signals of both subjects with the gait events identified with circles.

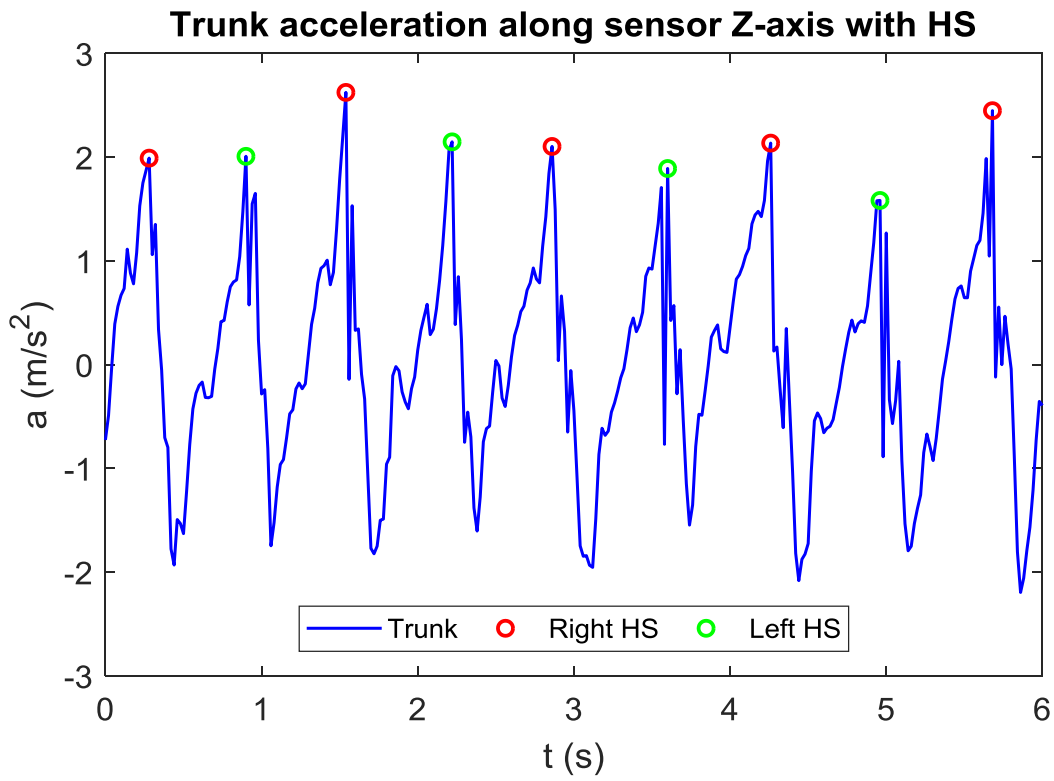


Figure 3.3.19\_ Female subject: trunk acceleration along sensor Z-axis with HS.

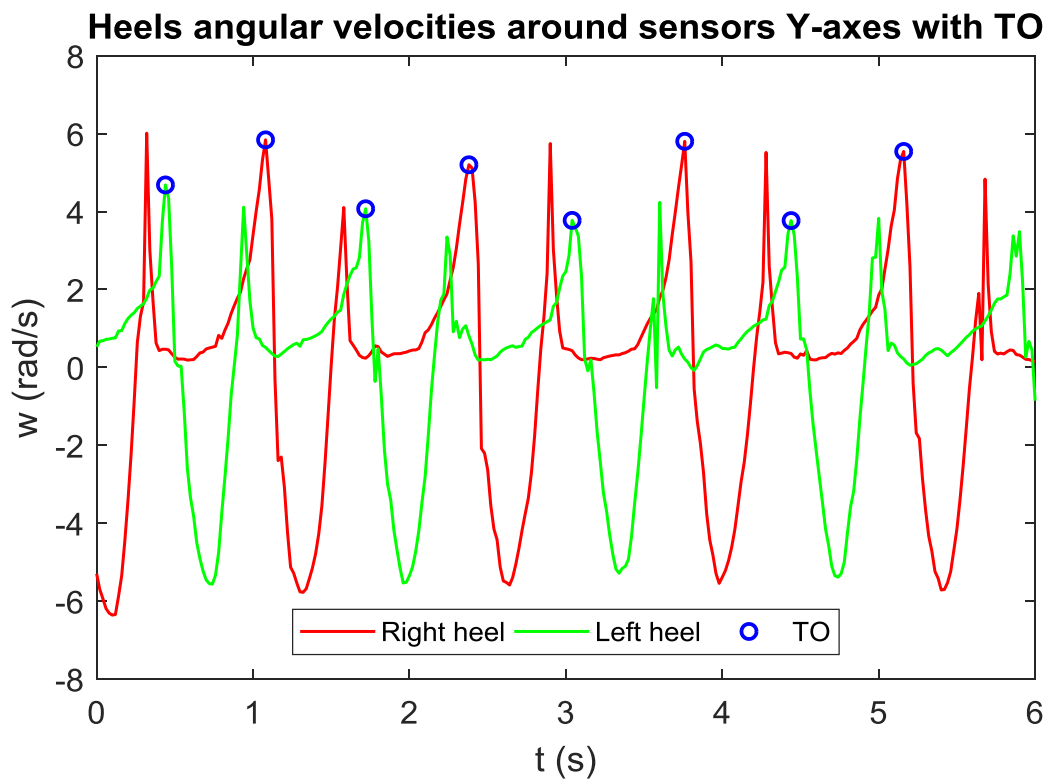


Figure 3.3.20\_ Female subject: heels angular velocities around sensors Y-axes with TO.

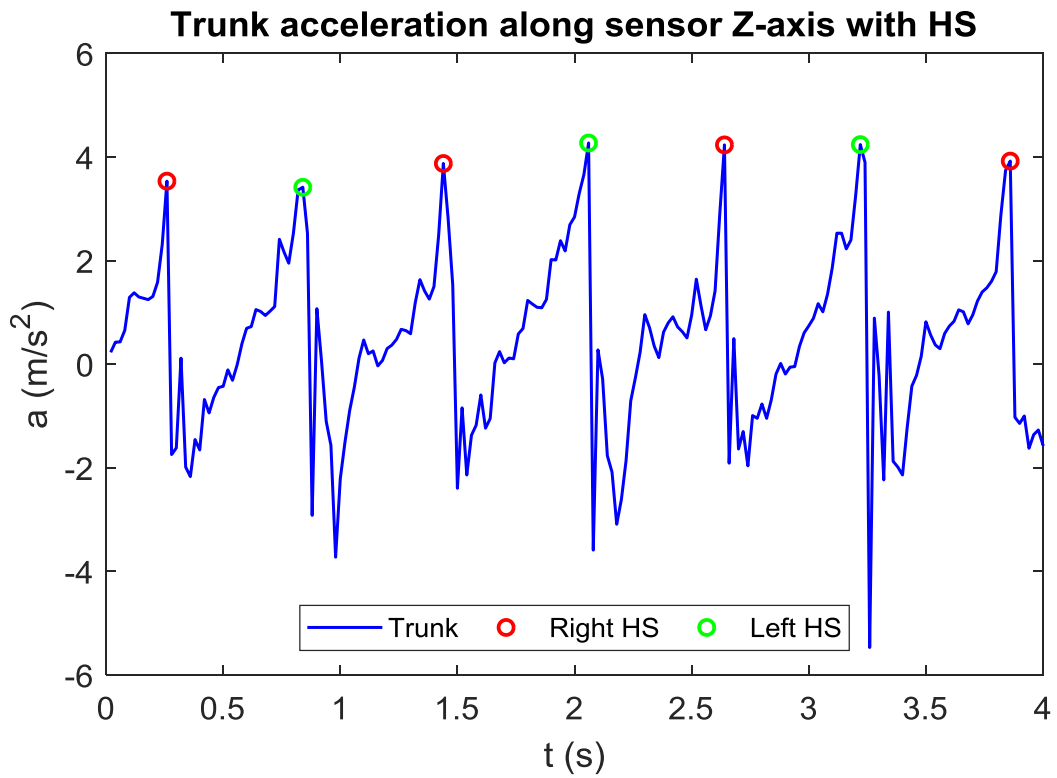


Figure 3.3.21\_ Male subject: trunk acceleration along sensor Z-axis with HS.

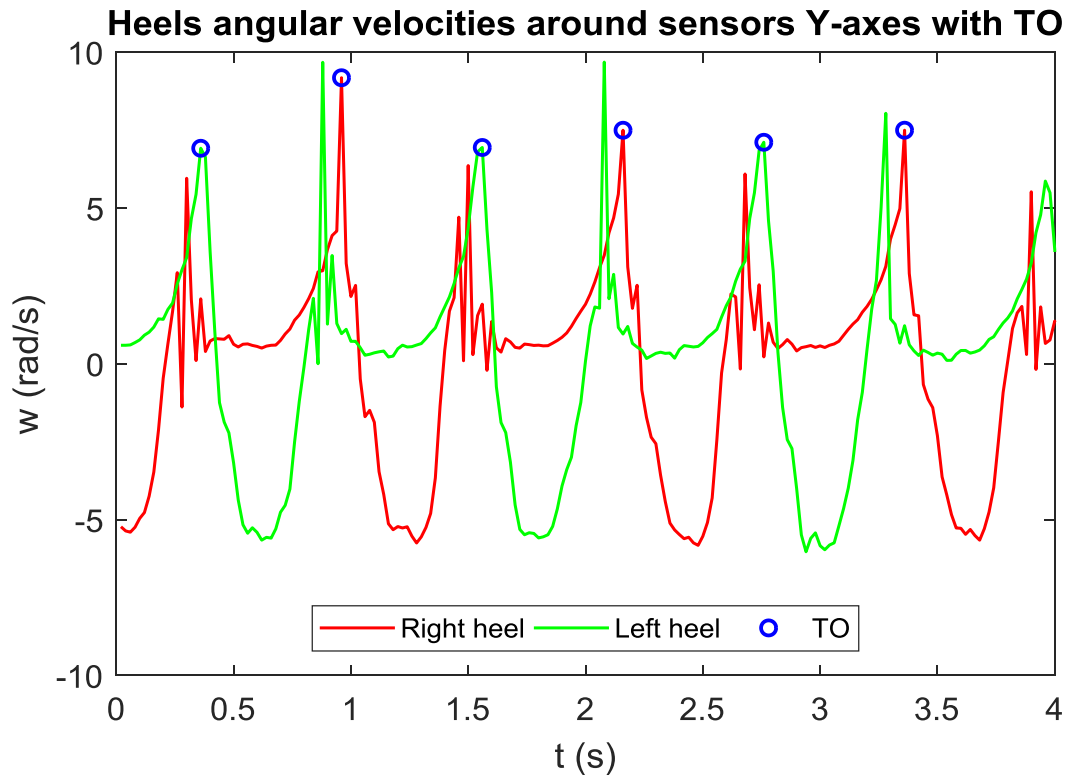


Figure 3.3.22\_ Male subject: heels angular velocities around sensors Y-axes with TO.

Once gait events were defined both with Optitrack and Xsens, spatio-temporal parameters were estimated from both methods and compared. The two following tables (Table 3.3.1 and Table 3.3.2) present the spatio-temporal parameters for both subjects:

<b>Female subject</b>		
<b>Spatio-temporal parameters</b>	<b>Optitrack</b>	<b>Xsens</b>
<b>Stride time (s)</b>	1,38	1,33
<b>Stride frequency (Hz)</b>	0,73	0,75
<b>Step time (s)</b>	0,67	0,65
<b>Step frequency (Hz)</b>	1,49	1,55
<b>Foot symmetry (%GC)</b>	0,49	0,49
<b>Stance time (s)</b>	0,88	0,83
<b>Swing time (s)</b>	0,50	0,50
<b>Single support time (s)</b>	0,55	0,55
<b>Double support time (s)</b>	0,37	0,33
<b>Limp index (right/left)</b>	1,06	1,04

Table 3.3.1\_Female subject: spatio-temporal parameters estimated both from Optitrack and Xsens.

<b>Male subject</b>		
<b>Spatio-temporal parameters</b>	<b>Optitrack</b>	<b>Xsens</b>
<b>Stride time (s)</b>	1,20	1,20
<b>Stride frequency (Hz)</b>	0,83	0,83
<b>Step time (s)</b>	0,58	0,59
<b>Step frequency (Hz)</b>	1,74	1,70
<b>Foot symmetry (%GC)</b>	0,48	0,49
<b>Stance time (s)</b>	0,65	0,70
<b>Swing time (s)</b>	0,55	0,50
<b>Single support time (s)</b>	0,54	0,51
<b>Double support time (s)</b>	0,10	0,20
<b>Limp index (right/left)</b>	1,03	1,03

Table 3.3.2\_Male subject: spatio-temporal parameters estimated both from Optitrack and Xsens.

### 3.4 Preliminary tests with Optitrack and Xsens synchronized

The test was performed in the same setting of the previous ones. Optitrack V120:Trio were positioned in the same configuration with the same distances. Before asking the subjects to walk, it was necessary to record a static acquisition with three markers on the floor. This time the global reference system was created according to the direction of progression: all the data were transformed from the local reference systems of the two bars into the global reference system (Figure 3.4.1). The latter had its origin in B: the X-axis was calculated as the distance of A from B; the axis of support S was calculated as the distance of C from B; the Y-axis was obtained as the vector product of S and X; the Z-axis was obtained as the vector product of X and Y.

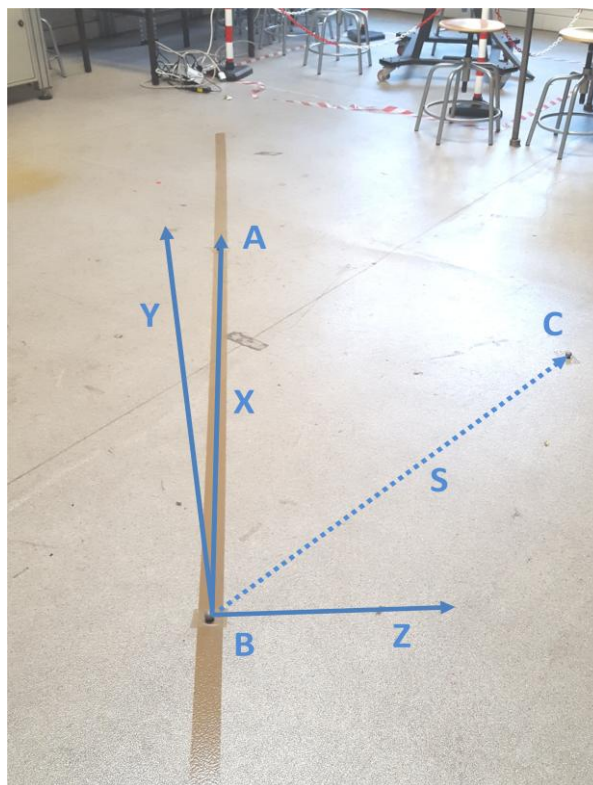


Figure 3.4.1\_The configuration of fixed markers and the global reference system.

Once this reference was created, it was possible to construct transformation matrices that allowed to convert the data from the local systems of the bars into the global one. First, it was recommended to calculate the transformation matrices to convert the data from the local reference systems of the bars to the new reference system. The first three columns indicated the orientation of the local axes in the base reference; the fourth column indicated the coordinates of the origin of the tern B.

The matrix for the bar n°1 is:

$${}^1M_0 = \begin{bmatrix} x1_X & y1_X & z1_X & B1_X \\ x1_Y & y1_Y & z1_Y & B1_Y \\ x1_Z & y1_Z & z1_Z & B1_Z \\ 0 & 0 & 0 & 1 \end{bmatrix}$$

The matrix for the bar n°2 is:

$${}^2M_0 = \begin{bmatrix} x2_X & y2_X & z2_X & B2_X \\ x2_Y & y2_Y & z2_Y & B2_Y \\ x2_Z & y2_Z & z2_Z & B2_Z \\ 0 & 0 & 0 & 1 \end{bmatrix}$$

Then it was necessary to invert these two matrices, obtaining the following two news matrices:

$${}^0M_1 = \begin{bmatrix} {}^1M_0^T & -{}^1M_0^T \cdot B1 \\ 0 & 0 & 0 & 1 \end{bmatrix}$$

$${}^0M_2 = \begin{bmatrix} {}^2M_0^T & -{}^2M_0^T \cdot B2 \\ 0 & 0 & 0 & 1 \end{bmatrix}$$

All the data from the cameras were pre-multiplied by the inverse matrices to obtain the information according to a single reference system.

The healthy subjects chosen for the experiment were three: a female of 27 years old, a female of 24 years old and a male of 24 years old.

They were asked to wear both markers and inertial sensors. The six passive reflective markers were fixed using double-sided adhesive tape directly on the skin of the subjects. The markers were positioned bilaterally on anatomical landmarks: two on the malleolus, two on the heels and two on the toes.

The configuration chosen for the five MTx sensors was the following one:

- n°683 → right thigh
- n°684 → right shank
- n°685 → left thigh
- n°686 → left shank
- n°494 → pelvis

There was also the Xbus Master with its belt at waist level. The inertial sensors were connected to each other and to the Xbus Master via cables. It was important to accommodate cables in such a way they did not hinder the subjects during the gait. The connection between the Xbus Master and the PC was guaranteed by Bluetooth.

The Figure 3.4.2 shows the configuration of Xsens MTx adopted for this test.

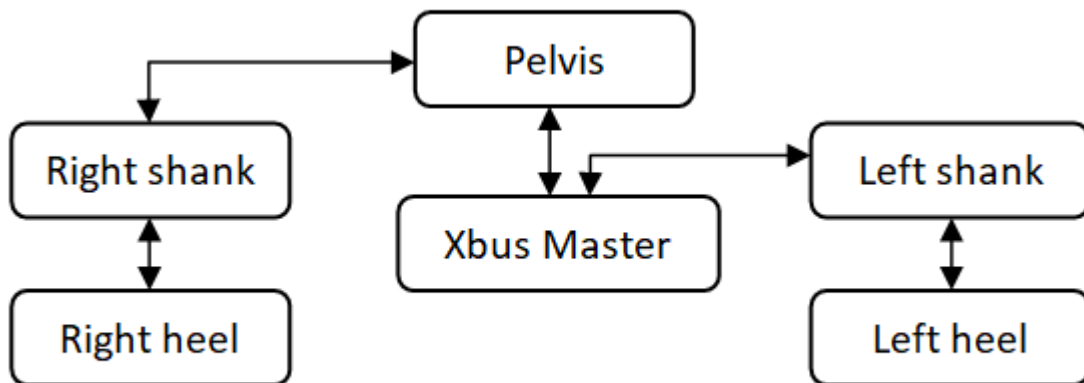


Figure 3.4.2\_The configuration Xsens MTx sensors.

The following six figures (from Figure 3.4.3 to Figure 3.4.8) show the configuration of markers and inertial sensors for all the three subjects.

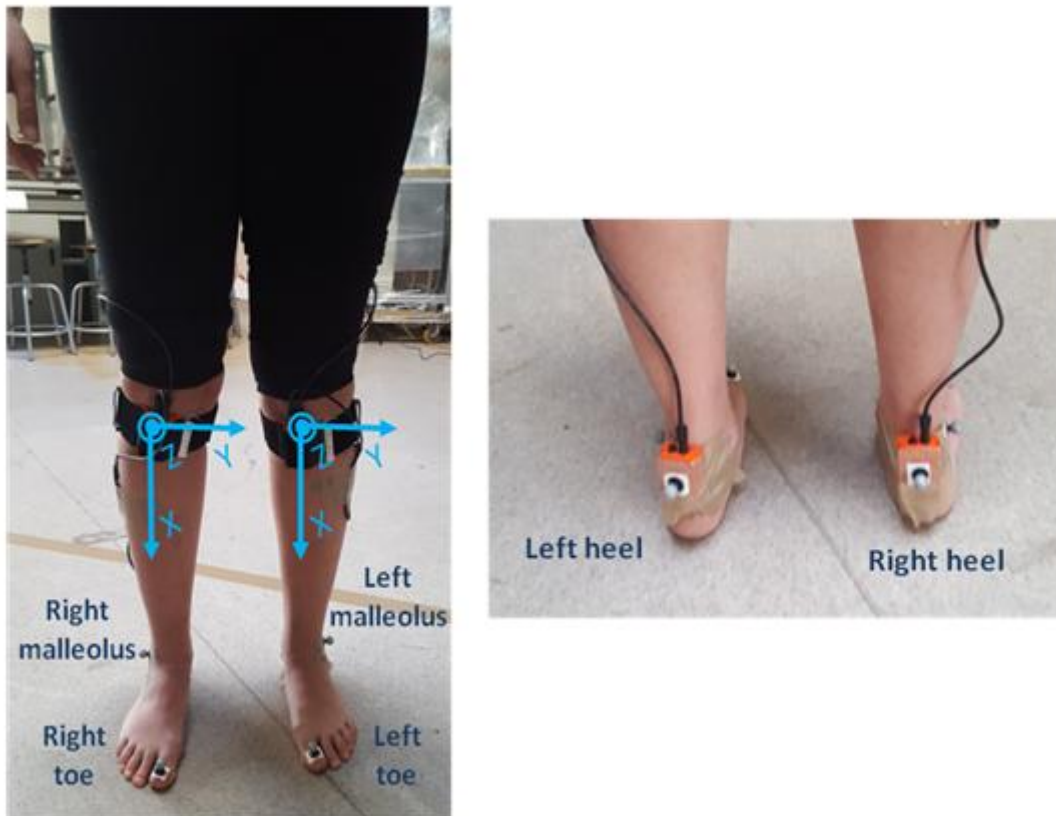


Figure 3.4.3\_The configuration of markers and inertial sensors on lower limbs for the first female subject.

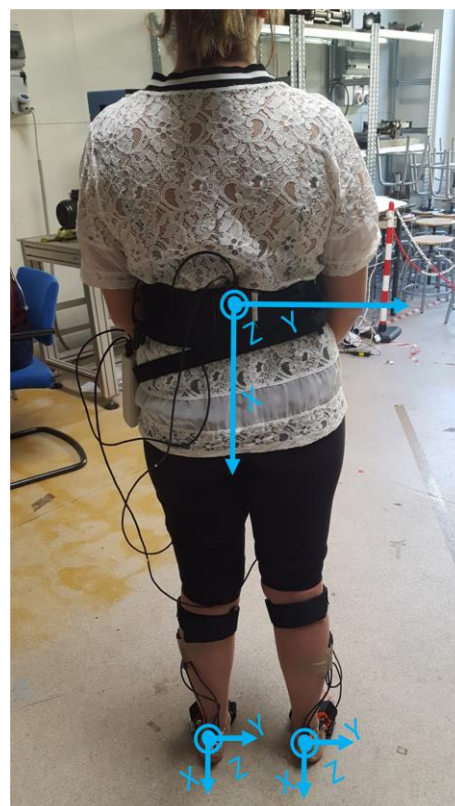


Figure 3.4.4\_The configuration of inertial sensors on heels and trunk for the first female subject.

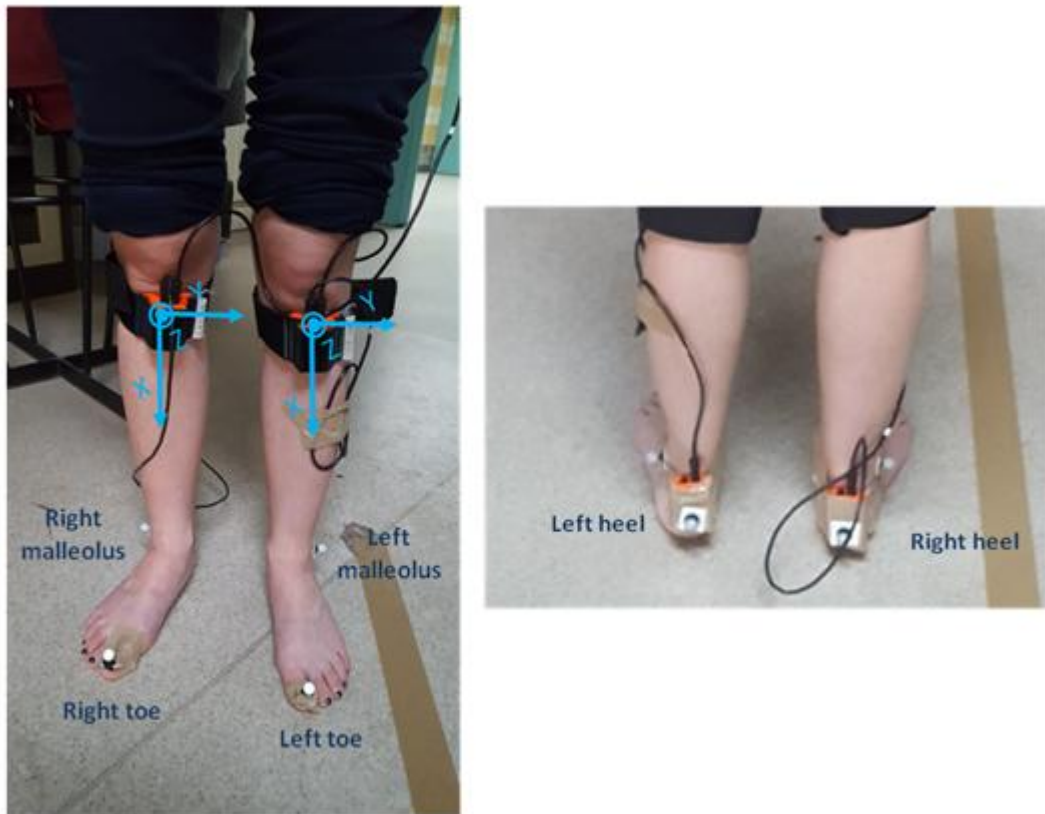


Figure 3.4.5\_ The configuration of markers and inertial sensors on lower limbs for the second female subject.

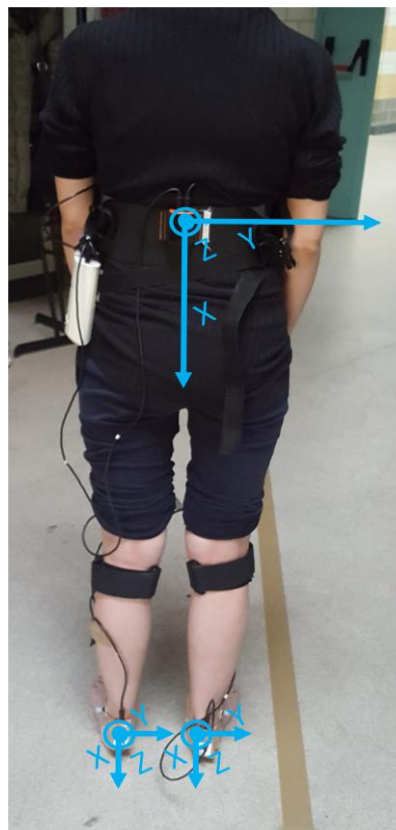


Figure 3.4.6\_ The configuration of inertial sensors on heels and trunk for the second female subject.

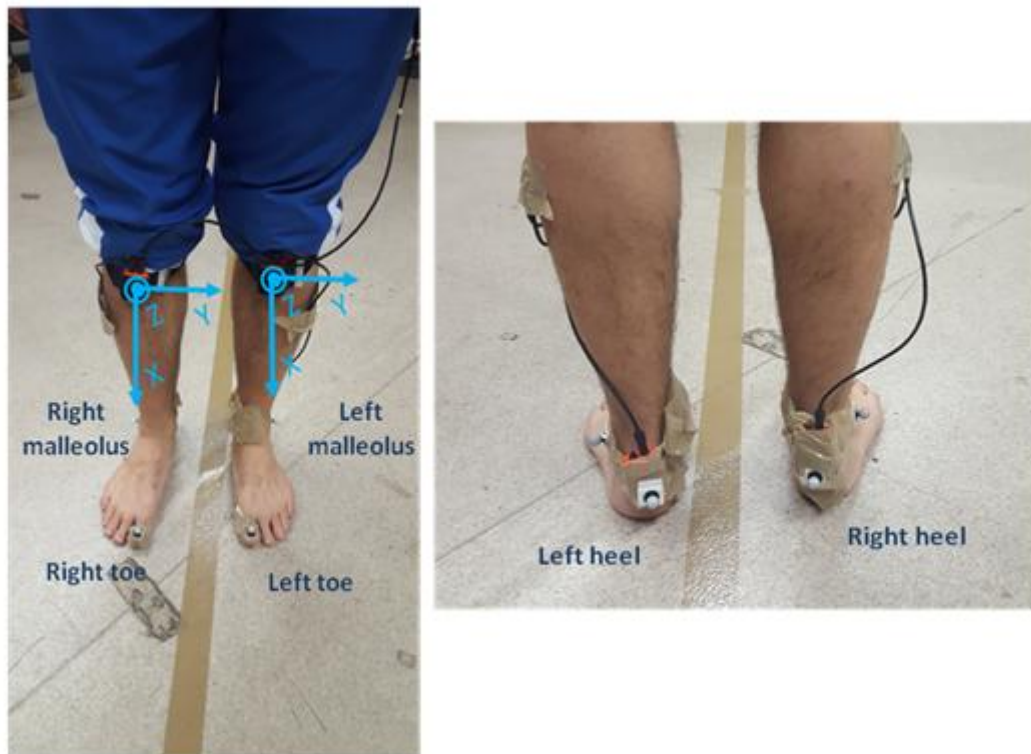


Figure 3.4.7\_The configuration of markers and inertial sensors on lower limbs for the male subject.

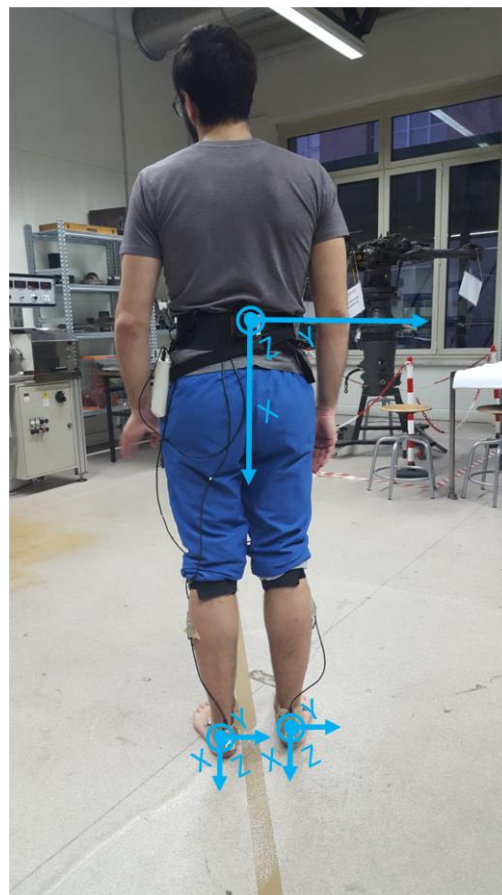


Figure 3.4.8\_The configuration of inertial sensors on heels and trunk for the male subject.

The subjects were asked to walk following the direction defined by a line on the floor (Figure 3.4.9). The test was repeated at three different speeds: preferred, fast and slow. For each speed there were six transitions in front of cameras. For each subject there were in total 18 acquisitions.



Figure 3.4.9\_The three subjects walking along the line on the floor.

There was the necessity to temporally synchronize together the motion capture system and the inertial sensors, in order to identify repeatable events of sensors signals associated to heel-strike and toe-off and to estimate the temporal parameters with the two instrumentations from the same steps. The most engineering method to synchronize two different instrumentations is to use a trigger. The instant in which the trigger is sent can be considered the instant zero for both the instrumentations. Even if this method would have been more precise, it was not applicable in this case; indeed, it was not guaranteed that the trigger sent to the two Optitrack bars and to an Xsens sensor would produce the same delay. Furthermore the two bars were independent one from the other and they were connected to two different PC, which increased the possibility of different delays. For all these reasons, the easiest solution to temporally synchronize the two bars and the inertial sensors consisted of an external event. Once the two Motive recordings and the MT Manager recording had started, the subjects entered the acquisition volume of the cameras and hit the right foot on the floor. Then they returned to the starting point and walked along the line. During the post-processing phase on Motive, the instant corresponding to the lowest point of the vertical coordinate of the right heel marker was considered the instant zero for both bars. For the Xsens MTx, the instant zero was the one corresponding to the peak of the vertical acceleration of the right heel (Figure 3.4.10).

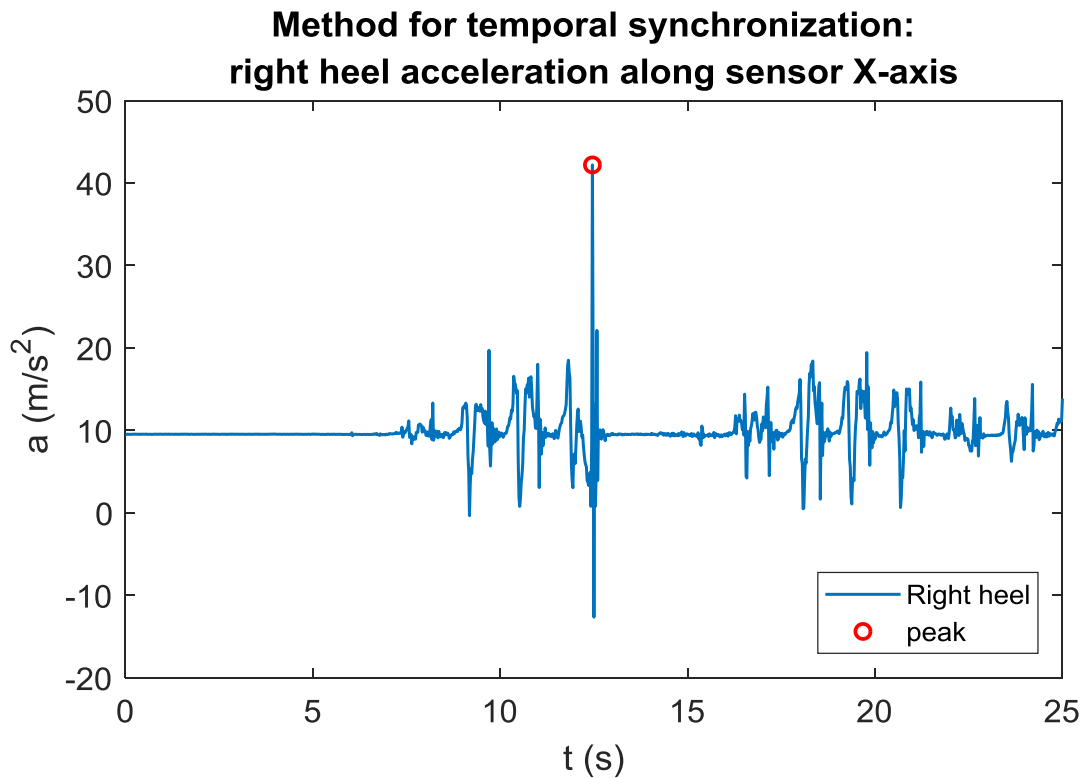


Figure 3.4.10\_The method of synchronization with an external event for the right heel MTx sensor.

Once the temporal synchronization was completed, it was possible to verify its correctness with the two bars plotting the same coordinate of the same marker. For example, if the coordinate X of the left toe marker from bar n°1 and those from bar n°2 were stackable, the temporal synchronization could be considered correct. This method allowed also to verify the correctness of the transformation matrices. The following three figures (from Figure 3.4.11 to Figure 3.4.13) represent the superimposition of the coordinates from the two bars after the transformation. Every figure refers to a specific marker of one subject and to a specific speed.

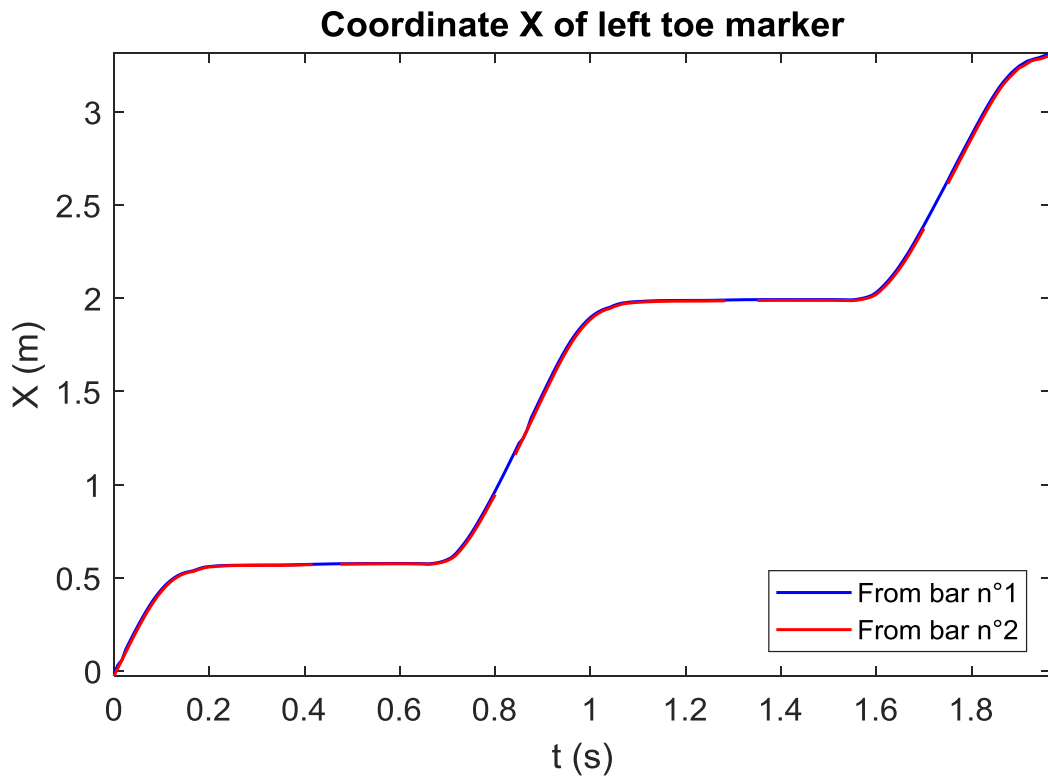


Figure 3.4.11\_First female subject: coordinate X of left toe marker of an acquisition at fast speed.

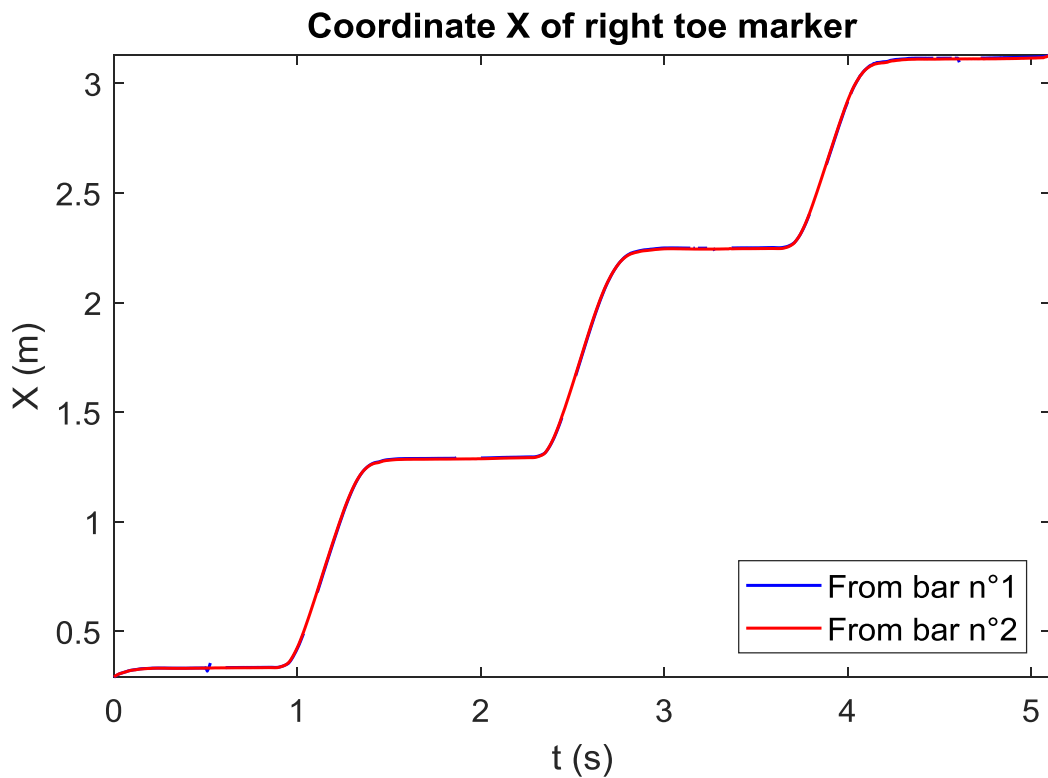


Figure 3.4.12\_Second female subject: coordinate X of right toe marker of an acquisition at normal speed.

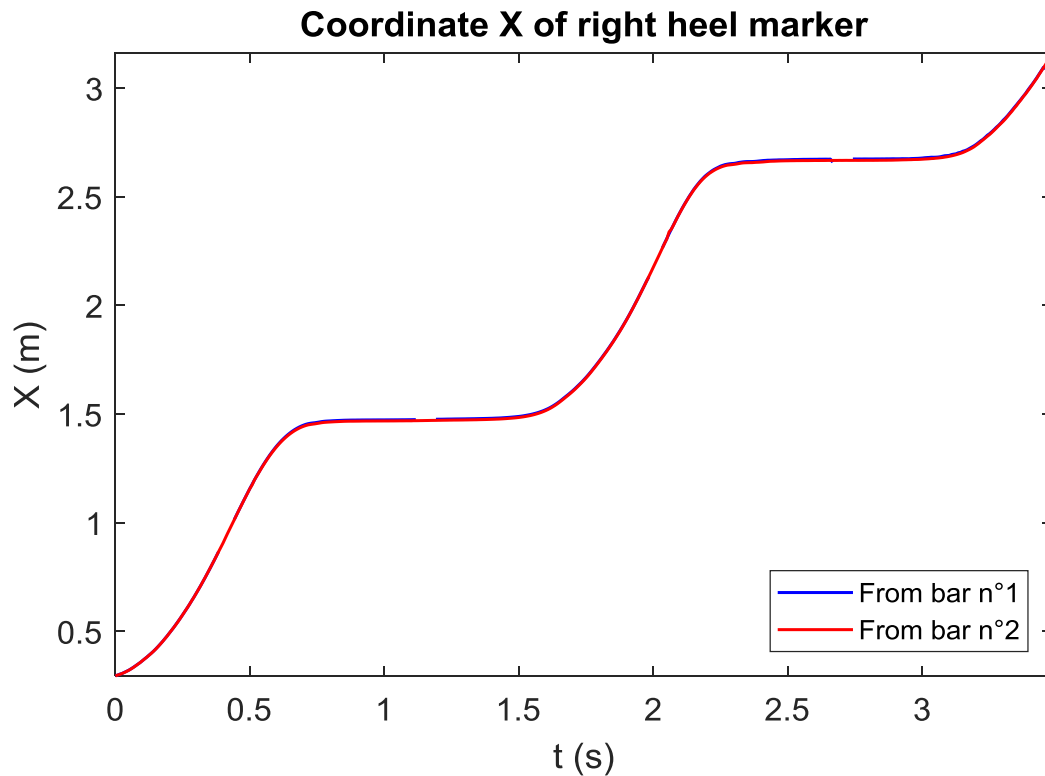


Figure 3.4.13\_ Male subject: coordinate X of right heel marker of an acquisition at slow speed.

The analysis of data focused on three acquisitions per subject: one for the preferred speed, one for the fast speed and one for the slow speed. The algorithm used to identify gait events in the marker trajectories was the same way adopted in the previous preliminary tests. The heel-strike was identified as the frame before the horizontal trajectory of the heel marker change of direction, whereas the toe-off was defined as the first frame where the toe marker changed direction in the anterior-posterior axis (L. Veilleux, 2016). For each marker, a Matlab routine found gait events on the horizontal trajectory and defined a temporal window of sixteen samples, eight before and eight after the frame corresponding to the heel-strike or the toe-off. Then, it verified if this point corresponded exactly to the minima of this window in the vertical trajectory and eventually shifted it.

In the following pages there are the plots of the marker coordinates for each subject (from Figure 3.4.14 to Figure 3.4.19): in every page there is the same marker trajectory for all the three subjects and for one specific walking speed.

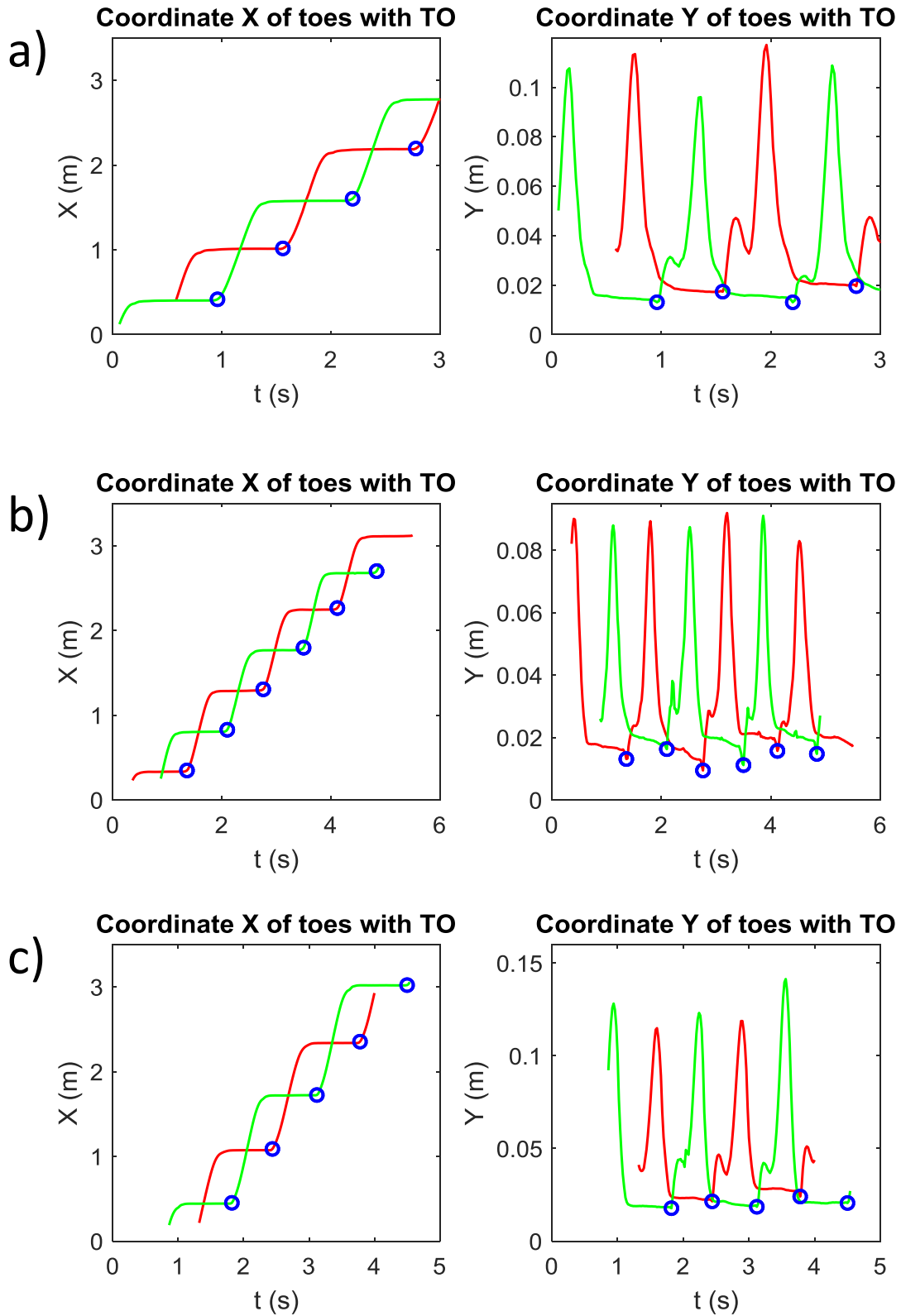


Figure 3.4.14\_Coordinates X and Y of toes markers at normal speed. a) First female b) Second female c) Male. The red line is the trajectory of the right toe, whereas the green one is the trajectory of left toe. The blue circles are the instants of toe-off for both toes.

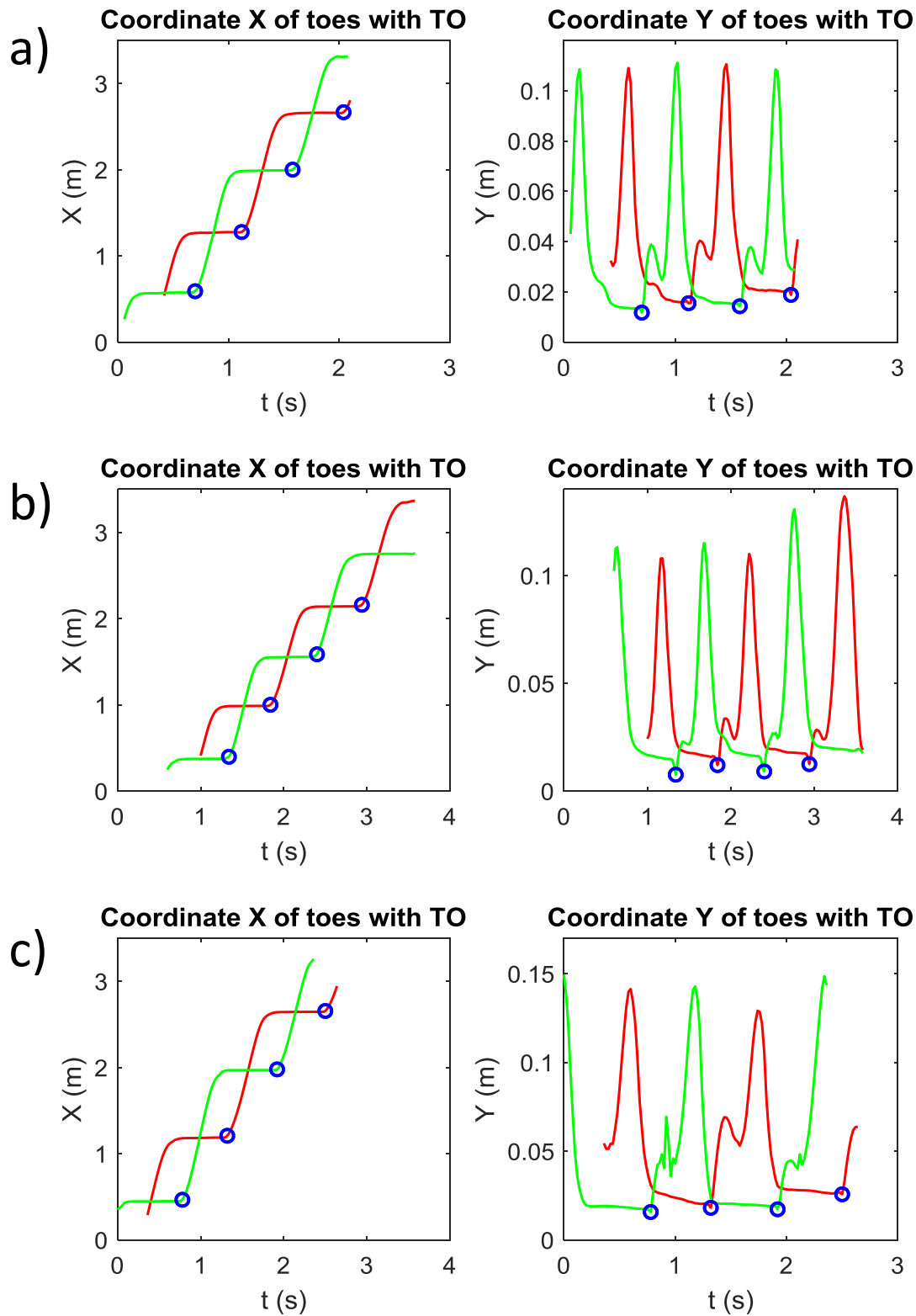
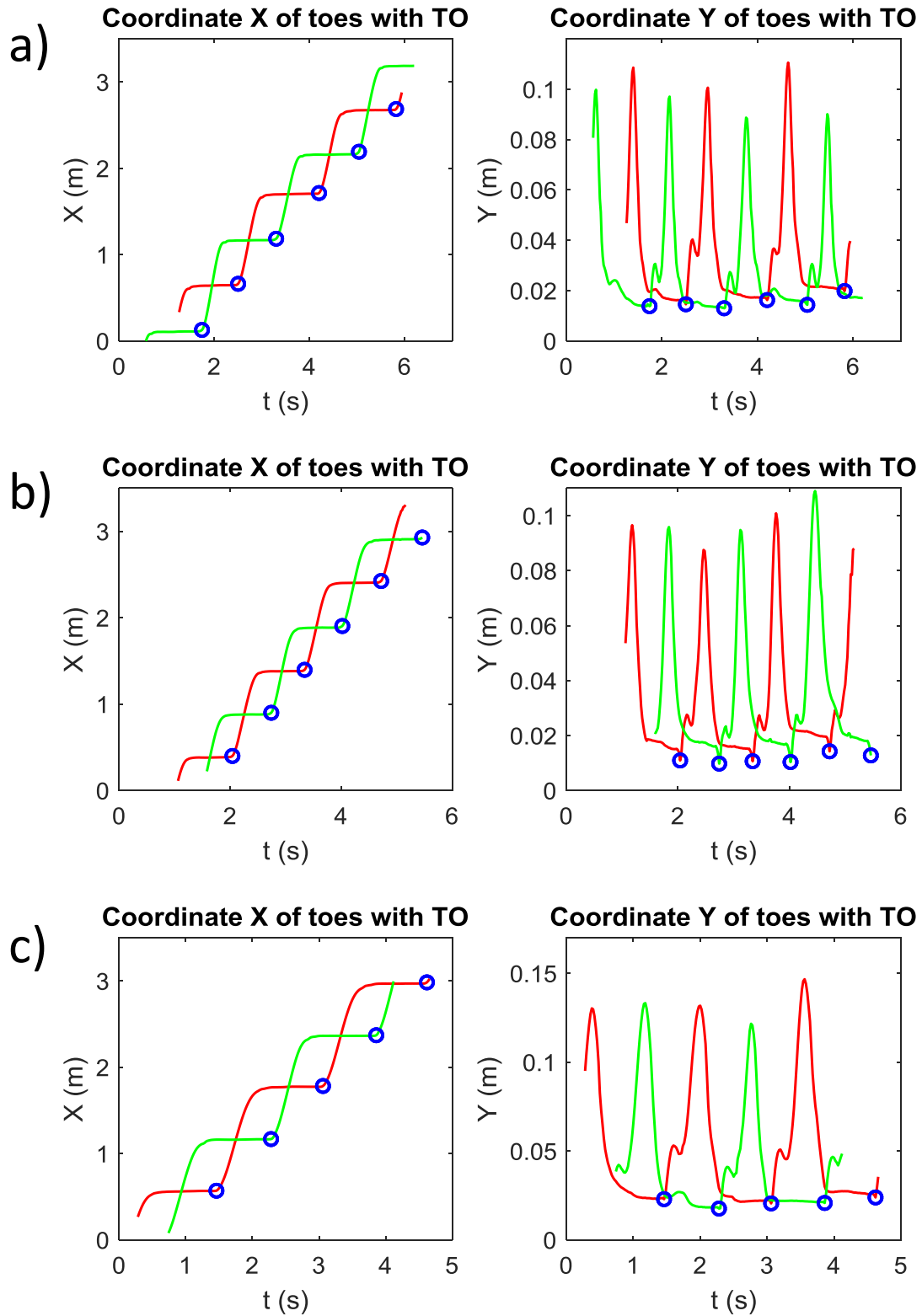


Figure 3.4.15\_Coordinates X and Y of toes markers at fast speed. a) Fist female b) Second female c) Male. The red line is the trajectory of the right toe, whereas the green one is the trajectory of left toe. The blue circles are the instants of toe-off for both toes.



**Figure 3.4.16\_Coordinates X and Y of toes markers at slow speed. a) First female b) Second female c) Male. The red line is the trajectory of the right toe, whereas the green one is the trajectory of left toe. The blue circles are the instants of toe-off for both toes.**

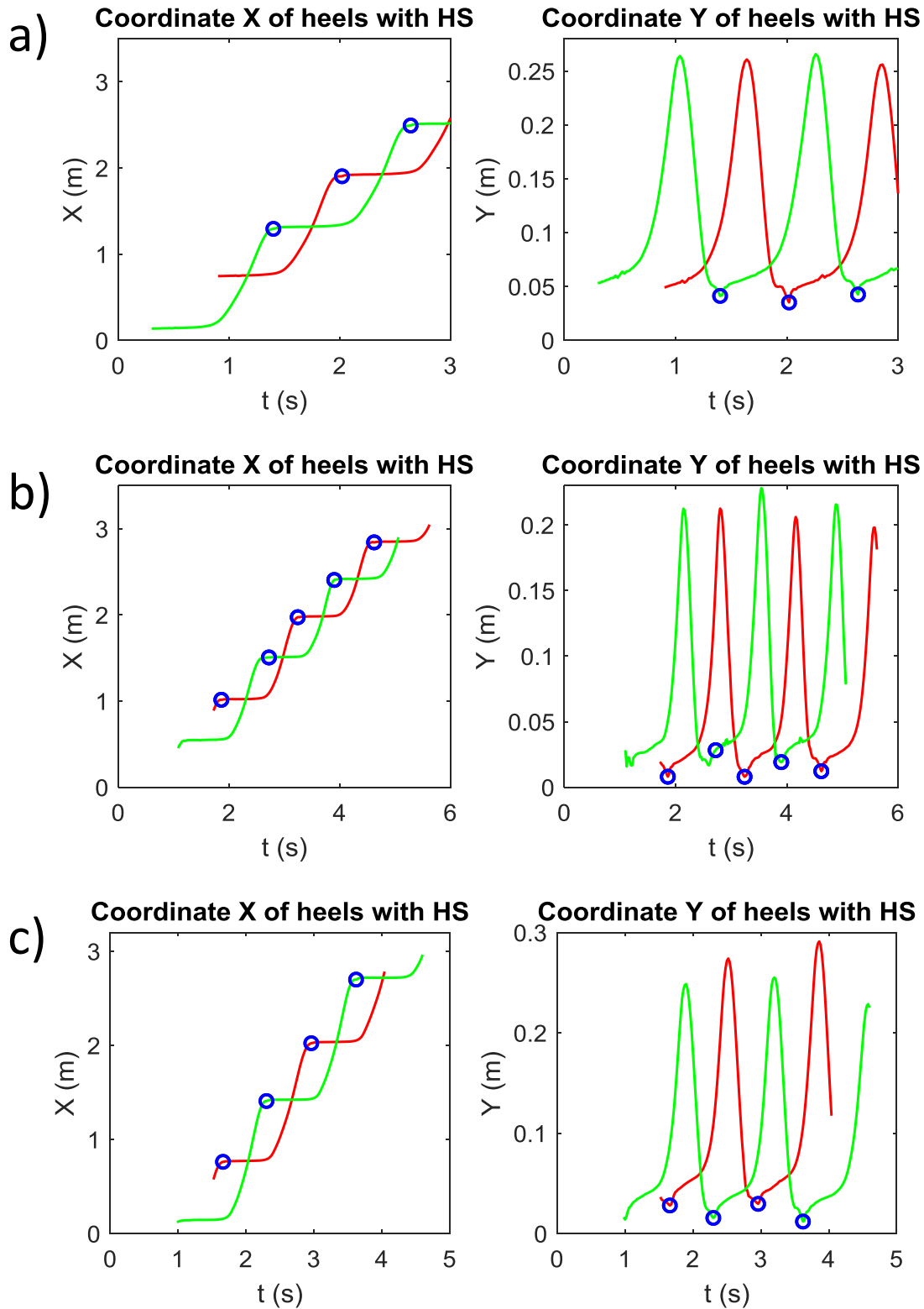


Figure 3.4.17\_Coordinates X and Y of heels markers at normal speed. a) First female b) Second female c) Male. The red line is the trajectory of the right heel, whereas the green one is the trajectory of left heel. The blue circles are the instants of heel-strikes for both heels.

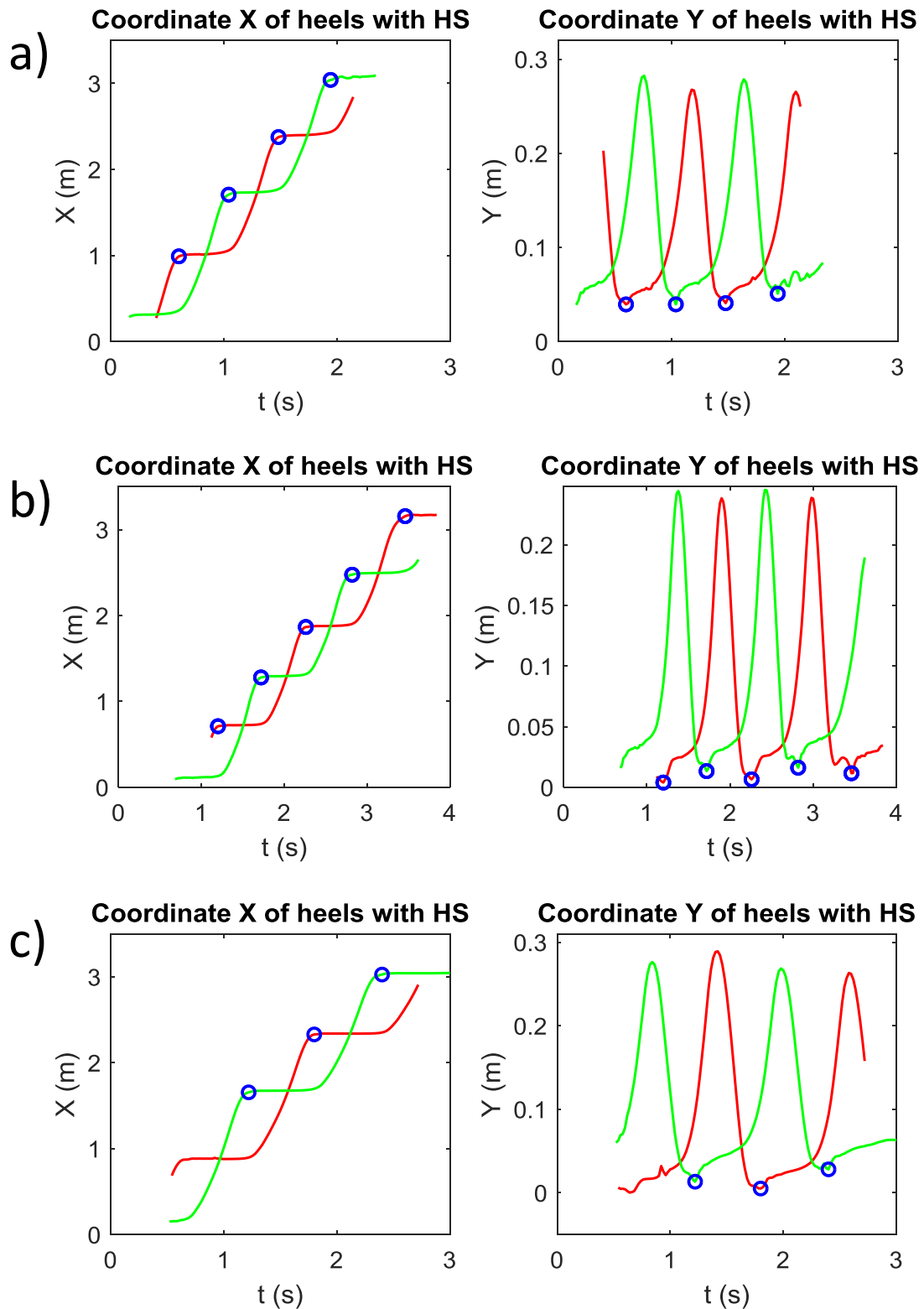


Figure 3.4.18\_Coordinates X and Y of heels markers at fast speed. a) Fist female b) Second female c) Male. The red line is the trajectory of the right heel, whereas the green one is the trajectory of left heel. The blue circles are the instants of heel-strikes for both heels.

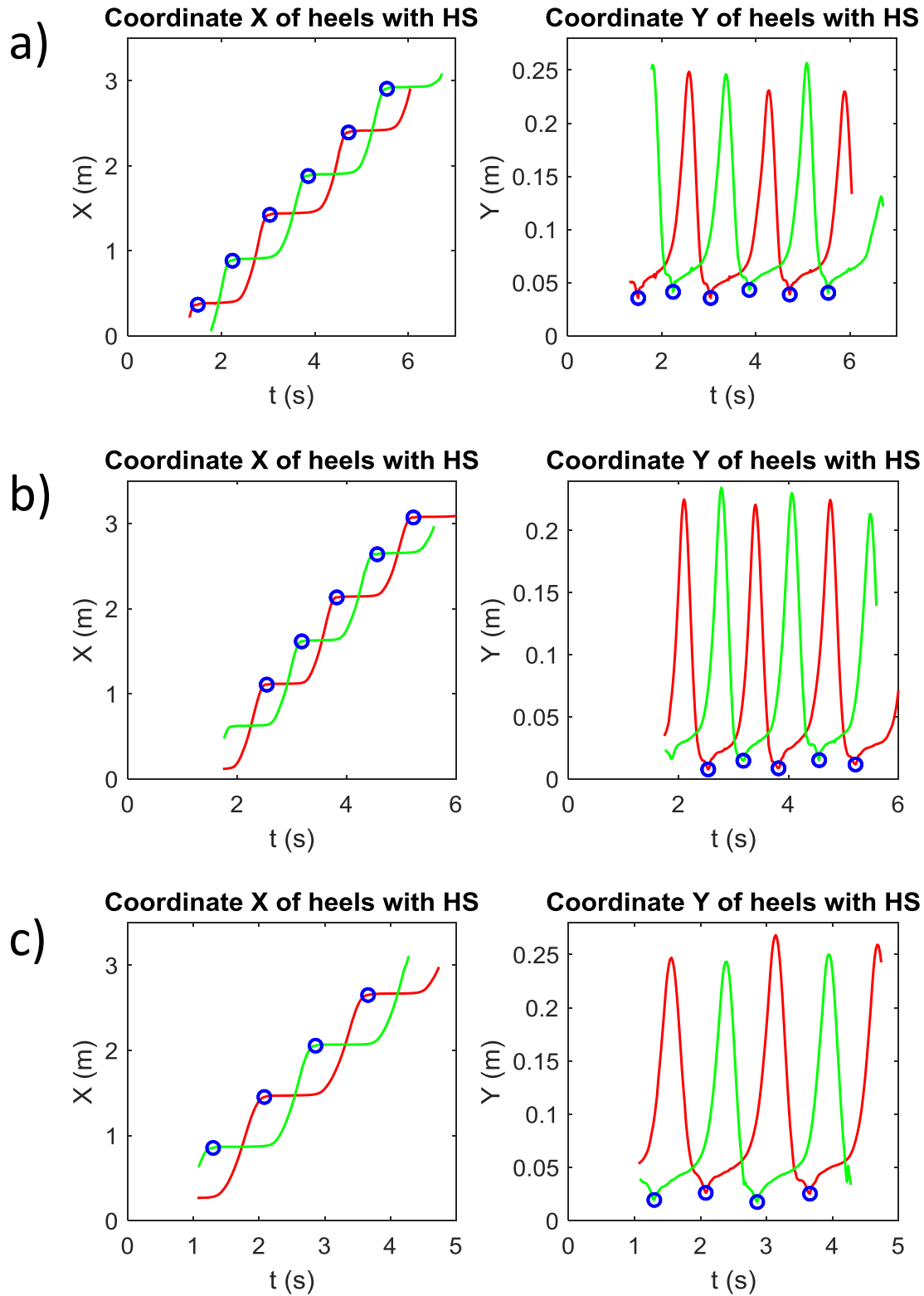


Figure 3.4.19\_Coordinates X and Y of heels markers at slow speed. a) Fist female b) Second female c) Male.  
 The red line is the trajectory of the right heel, whereas the green one is the trajectory of left heel.  
 The blue circles are the instants of heel-strikes for both heels.

Once the analysis of marker trajectories was ended, the research of gait events in inertial sensors signals started. The algorithms implemented from literature were two:

The first one used the acceleration of trunk along the sensor Z-axis. The HS and the TO were identified, respectively, as the maximum and the minimum peaks of this signal, as Zijlstra proposed in 2004. The Matlab code previously used for the identification of peaks was maintained. However, the distinction between right and left sides was different: the signal used was not the trunk angular velocity around the Z-axis, but that around the X-axis. The change of signal was due to the fact that the angular velocity around the vertical axis had a more evident alternation of sign. When it was positive the code recognised a right HS, whereas on the contrary the code recognised a left HS. The distinction between right and left TO was established on the basis of the HS. In fact, in a healthy gait, a right TO follows a left HS and a left TO follows a right HS.

The second used the angular velocities of heels around the sensors Y-axis. Following the work of Misu of 2017, the TO and the HS were identified, respectively, as the maxima and the peaks among the maxima of this signals. The Matlab code for the TO was the same used for the test with Optitrack and Xsens not synchronized. The HS were found writing a code that found the maxima among the TO previously identified.

In the following pages there are six figures (from Figure 3.4.20 to Figure 3.4.25) with the inertial sensors signals. In each page there are the signals of all the subjects with the same algorithm proposed to find gait events.

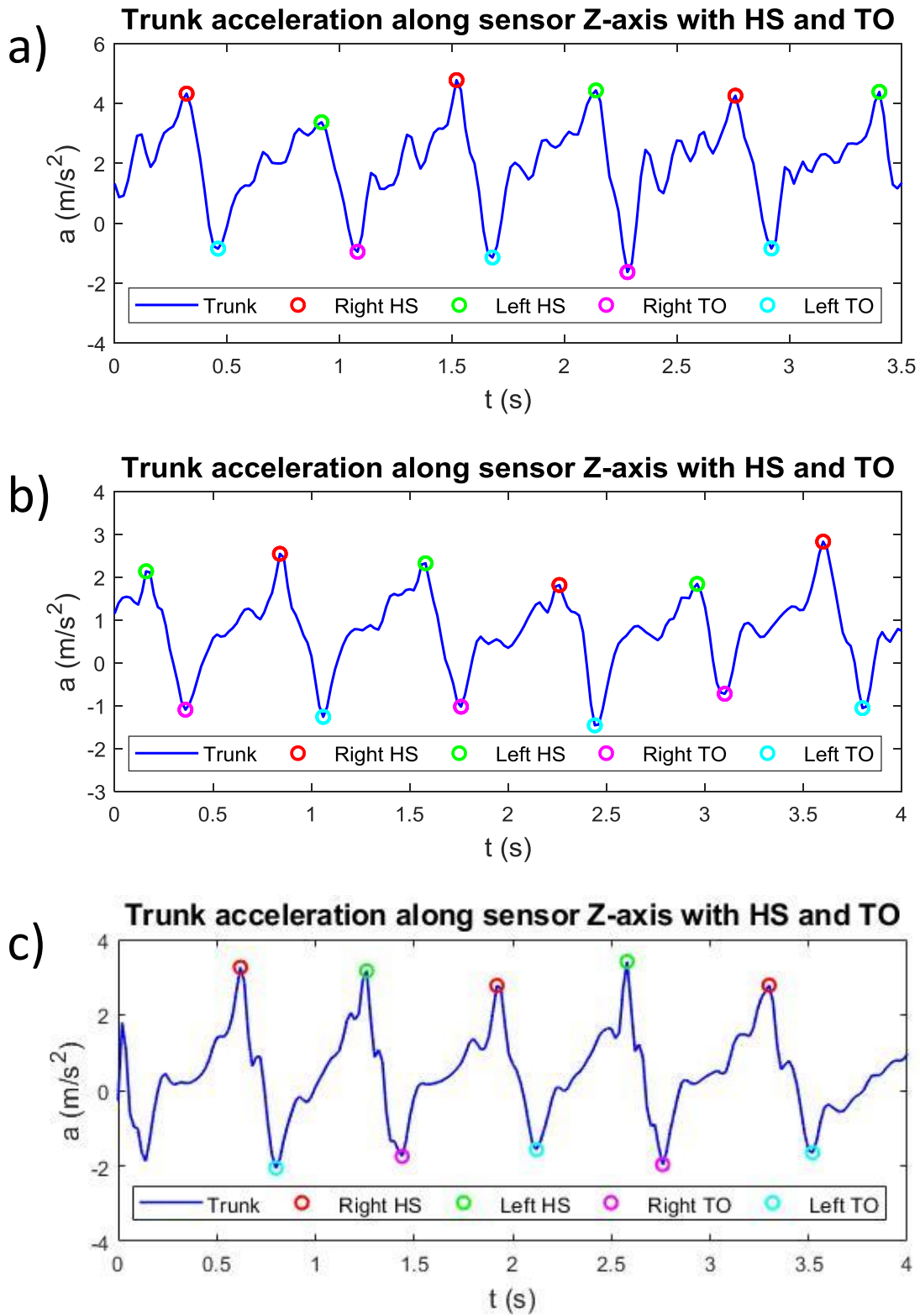


Figure 3.4.20\_Trunk acceleration along sensor Z-axis at normal speed with HS and TO identified with circles. a) Fist female b) Second female c) Male.

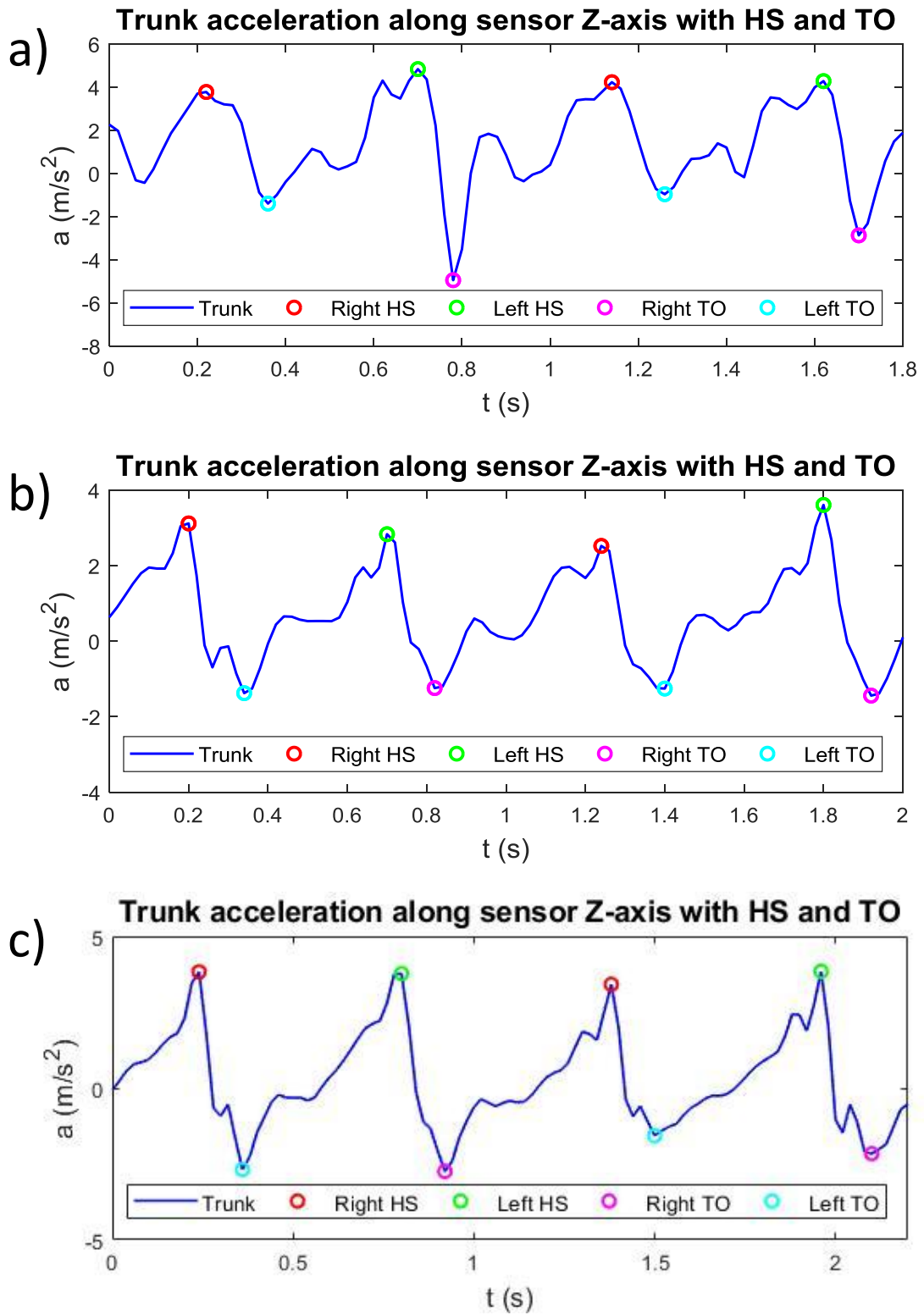


Figure 3.4.21\_Trunk acceleration along sensor Z-axis at fast speed with HS and TO identified with circles. a) Fist female b) Second female c) Male.

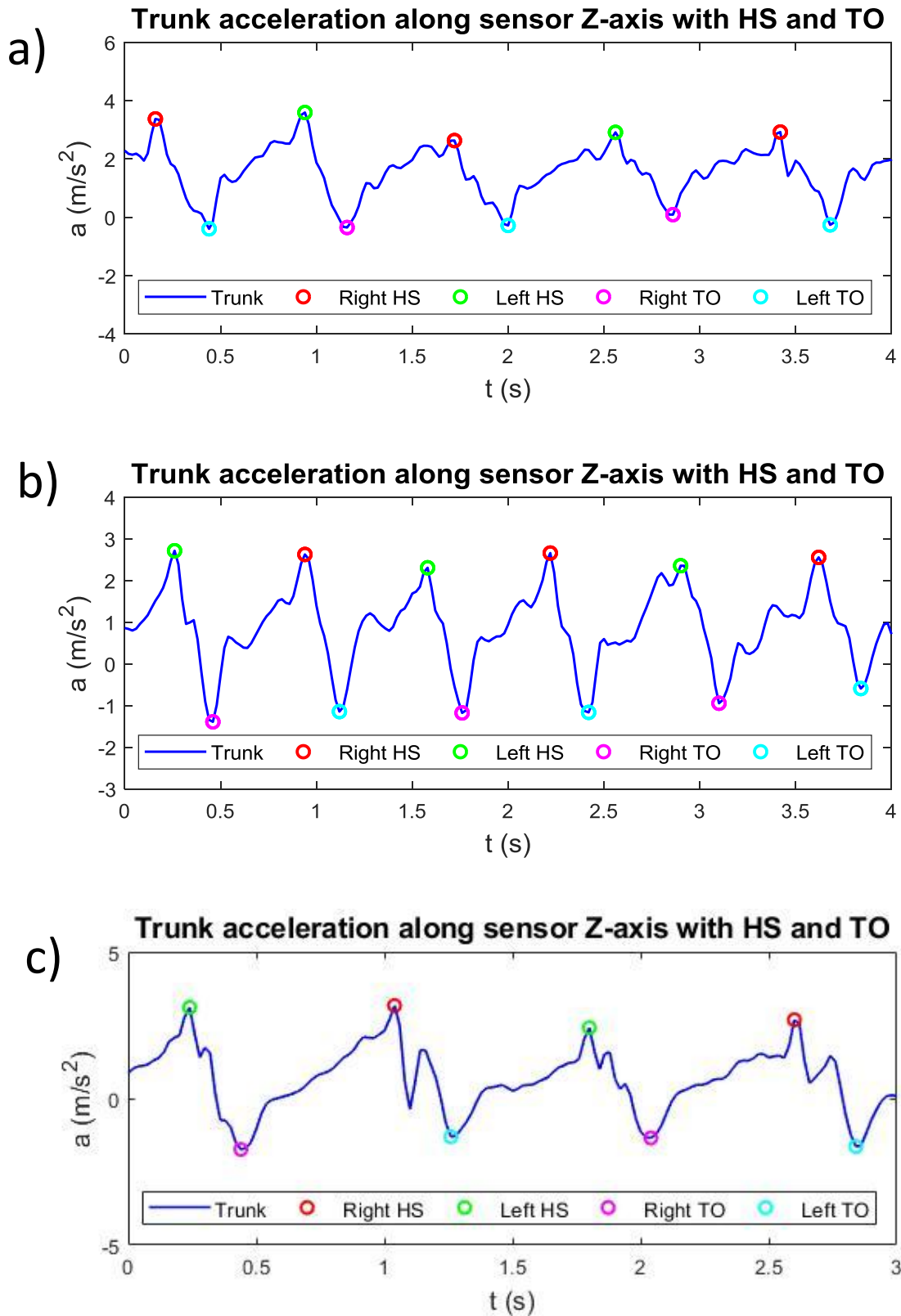


Figure 3.4.22\_Trunk acceleration along sensor Z-axis at slow speed with HS and TO identified with circles. a) Fist female b) Second female c) Male.

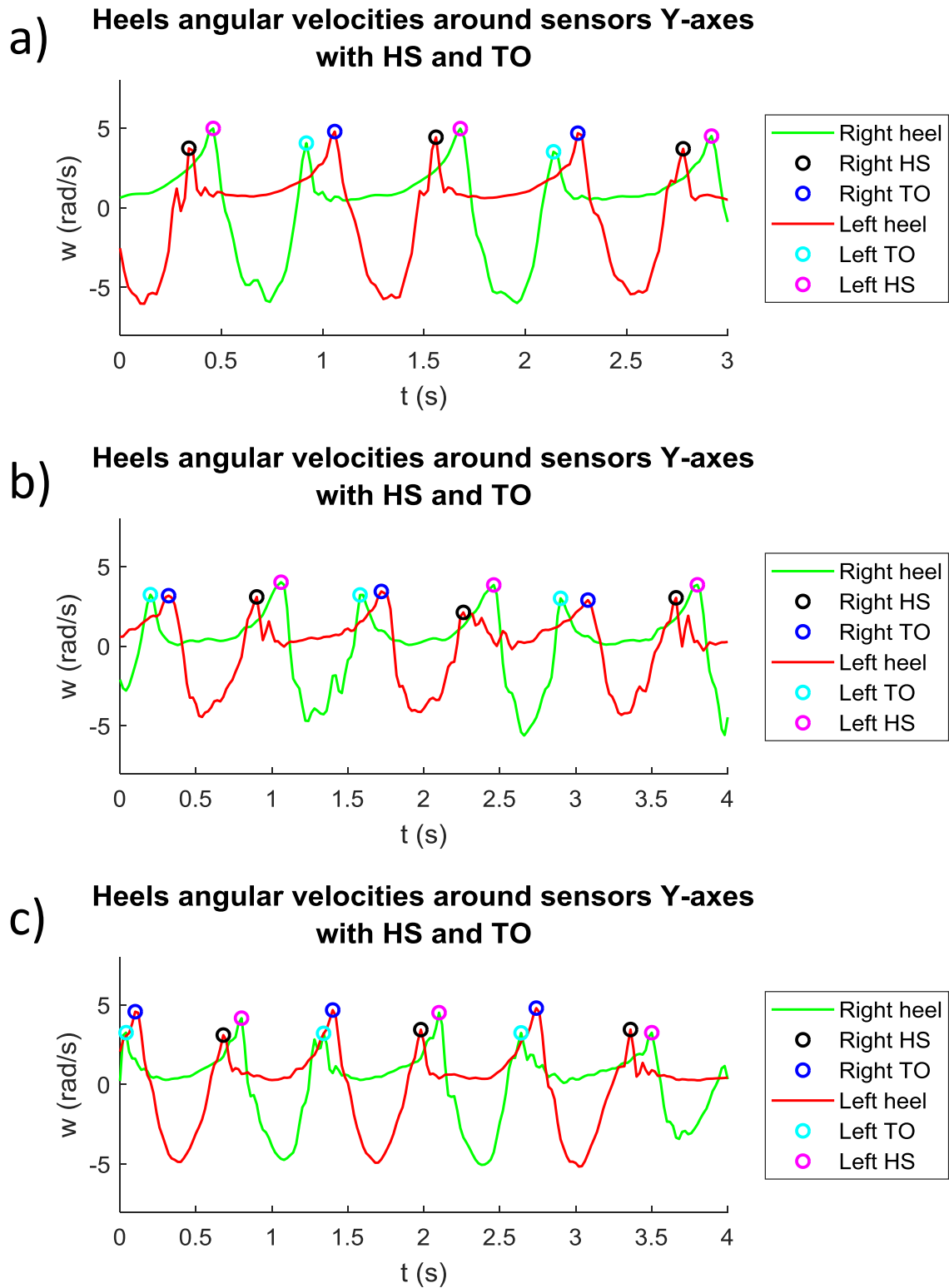
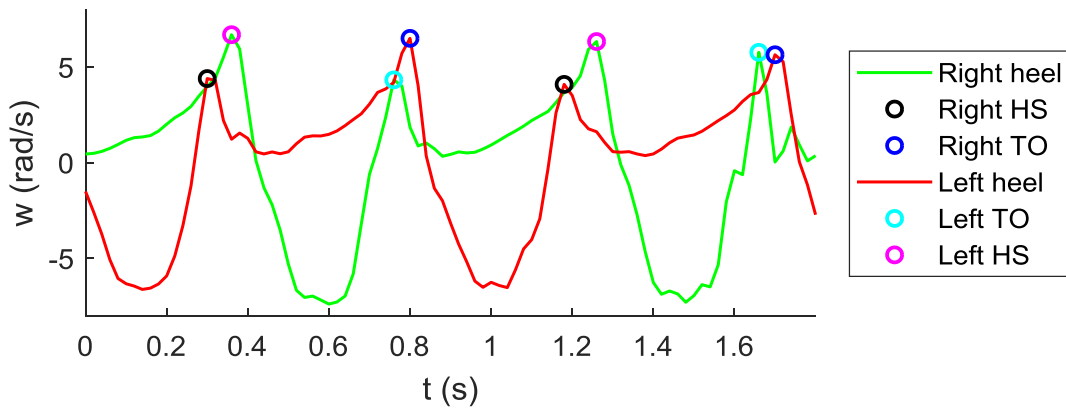
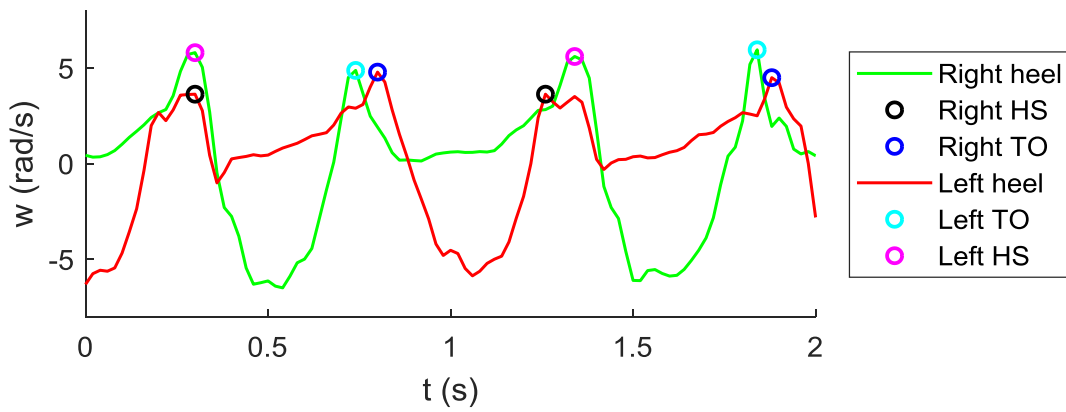


Figure 3.4.23\_Heels angular velocities around the sensors Y-axis at normal speed with HS and TO identified with circles. a) Fist female b) Second female c) Male.

a) Heels angular velocities around sensors Y-axes with HS and TO



b) Heels angular velocities around sensors Y-axes with HS and TO



c) Heels angular velocities around sensors Y-axes with HS and TO

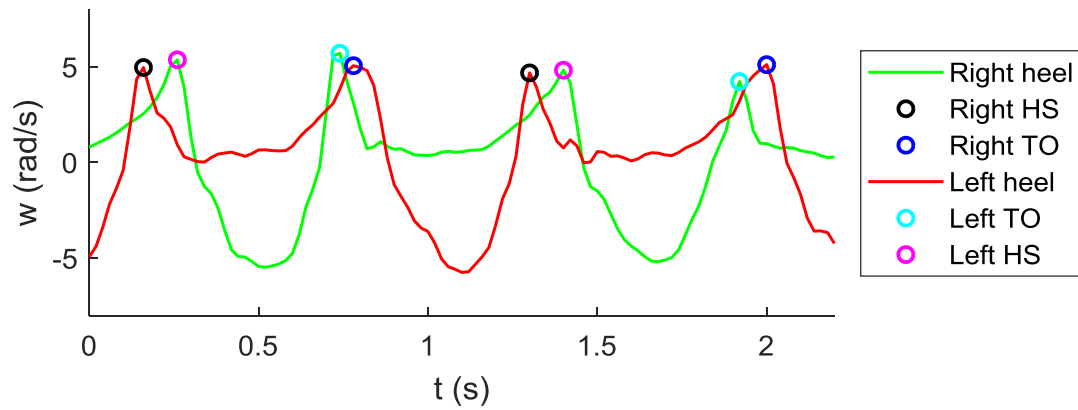


Figure 3.4.24\_Heels angular velocities around the sensors Y-axis at fast speed with HS and TO identified with circles. a) Fist female b) Second female c) Male.

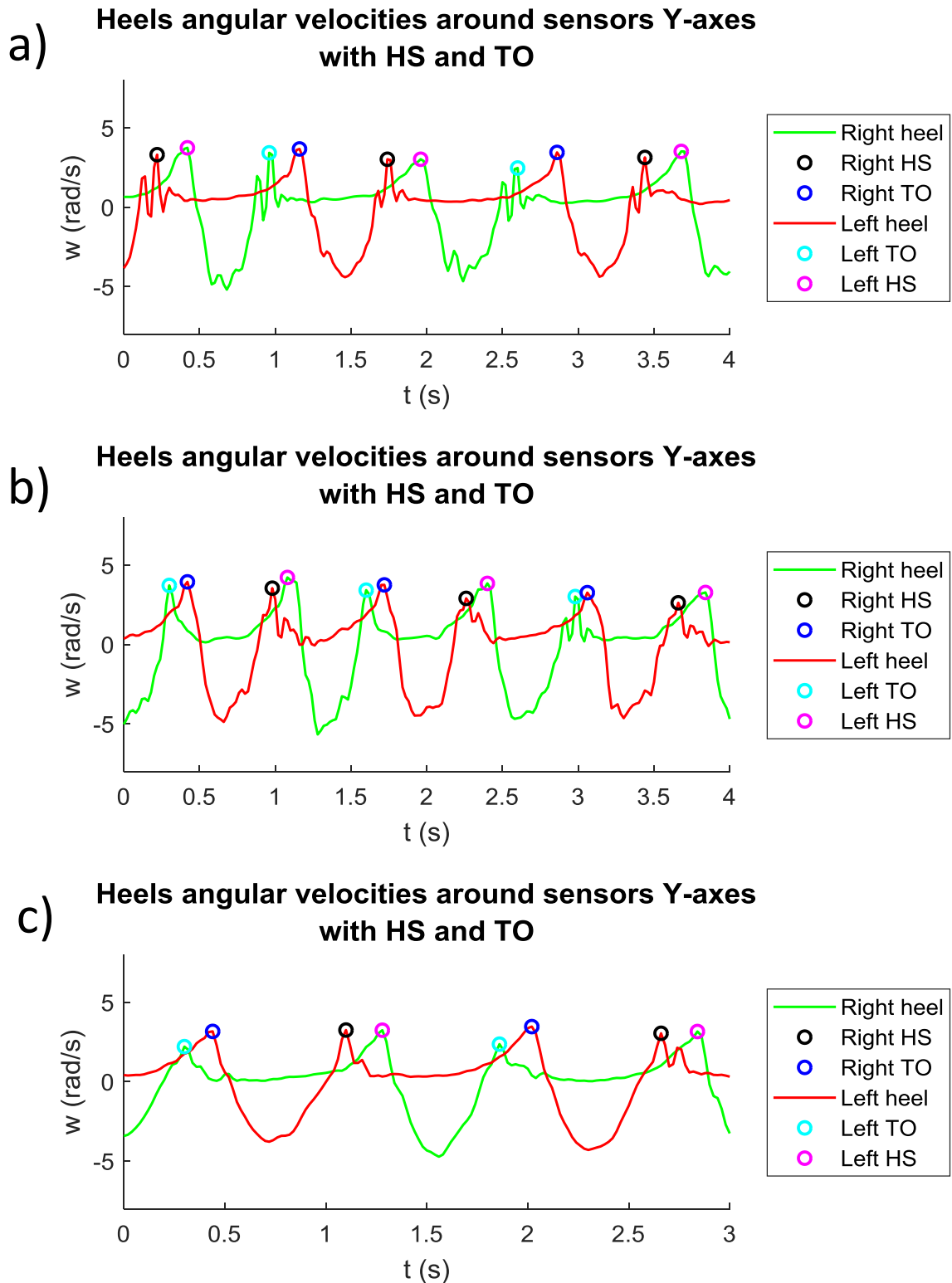


Figure 3.4.25\_Heels angular velocities around the sensors Y-axis at slow speed with HS and TO identified with circles. a) Fist female b) Second female c) Male.

The following eighteen tables (from Table 3.4.1 to Table 3.4.18) contain mean values of spatio-temporal parameters estimated from Optitrack, Xsens algorithm with trunk and Xsens algorithm with heels. Every table is related to a subject and a speed.

<b>First female subject _ normal speed</b>				
<b>Spatio-temporal parameters</b>	<b>Optitrack</b>		<b>Xsens from trunk</b>	
	<b>Right</b>	<b>Left</b>	<b>Right</b>	<b>Left</b>
<b>Stride time (s)</b>	1,22	1,24	1,24	1,22
<b>Step time (s)</b>	0,62	0,62	0,60	0,62
<b>Stance time (s)</b>	0,76	0,80	0,76	0,76
<b>Stance duration (%GC)</b>	62,30	64,52	61,29	62,30
<b>Swing time (s)</b>	0,46	0,44	0,44	0,46
<b>Swing duration (%GC)</b>	37,70	35,48	35,48	37,70
<b>Single support time (s)</b>	0,44	0,46	0,46	0,44
<b>SS duration (%GC)</b>	36,07	37,10	37,10	36,07
<b>Double support time (s)</b>	0,30	0,36	0,32	0,30
<b>DS duration (%GC)</b>	24,59	29,03	25,81	24,59
<b>Foot symmetry (%GC)</b>	50,82	50,00	48,39	50,82
<b>Limp index (right/left)</b>	0,95	0,95	1,00	1,00

Table 3.4.1\_First female subject at normal speed: spatio-temporal parameters from Optitrack and Xsens from trunk.

<b>First female subject _ normal speed</b>				
<b>Spatio-temporal parameters</b>	<b>Optitrack</b>		<b>Xsens from heels</b>	
	<b>Right</b>	<b>Left</b>	<b>Right</b>	<b>Left</b>
<b>Stride time (s)</b>	1,22	1,24	1,22	1,22
<b>Step time (s)</b>	0,62	0,62	0,64	0,58
<b>Stance time (s)</b>	0,76	0,80	0,72	0,76
<b>Stance duration (%GC)</b>	62,30	64,52	59,02	62,30
<b>Swing time (s)</b>	0,46	0,44	0,50	0,46
<b>Swing duration (%GC)</b>	37,70	35,48	40,98	37,70
<b>Single support time (s)</b>	0,44	0,46	0,46	0,50
<b>SS duration (%GC)</b>	36,07	37,10	37,70	40,98
<b>Double support time (s)</b>	0,30	0,36	0,22	0,30
<b>DS duration (%GC)</b>	24,59	29,03	18,03	24,59
<b>Foot symmetry (%GC)</b>	50,82	50,00	52,46	47,54
<b>Limp index (right/left)</b>	0,95	0,95	0,95	0,95

Table 3.4.2\_First female subject at normal speed: spatio-temporal parameters from Optitrack and Xsens from heels.

Second female subject _ normal speed				
Spatio-temporal parameters	Optitrack		Xsens from trunk	
	Right	Left	Right	Left
Stride time (s)	1,38	1,30	1,38	1,40
Step time (s)	0,64	0,74	0,68	0,72
Stance time (s)	0,90	0,90	0,88	0,88
Stance duration (%GC)	65,22	69,23	63,74	62,85
Swing time (s)	0,48	0,50	0,49	0,52
Swing duration (%GC)	34,78	38,46	35,56	37,15
Single support time (s)	0,50	0,48	0,52	0,49
SS duration (%GC)	36,23	36,92	37,71	35,02
Double support time (s)	0,42	0,40	0,39	0,36
DS duration (%GC)	30,43	30,77	28,18	25,70
Foot symmetry (%GC)	46,38	56,92	49,32	51,42
Limp index (right/left)	1,00	1,00	1,00	1,00

Table 3.4.3\_Second female subject at normal speed: spatio-temporal parameters from Optitrack and Xsens from trunk.

Second female subject _ normal speed				
Spatio-temporal parameters	Optitrack		Xsens from heels	
	Right	Left	Right	Left
Stride time (s)	1,38	1,30	1,38	1,35
Step time (s)	0,64	0,74	0,69	0,66
Stance time (s)	0,90	0,90	0,82	0,87
Stance duration (%GC)	65,22	69,23	59,43	64,49
Swing time (s)	0,48	0,50	0,56	0,48
Swing duration (%GC)	34,78	38,46	40,57	35,51
Single support time (s)	0,50	0,48	0,48	0,56
SS duration (%GC)	36,23	36,92	34,75	41,47
Double support time (s)	0,42	0,40	0,26	0,39
DS duration (%GC)	30,43	30,77	18,87	28,99
Foot symmetry (%GC)	46,38	56,92	50,00	48,88
Limp index (right/left)	1,00	1,00	0,94	0,94

Table 3.4.4\_Second female subject at normal speed: spatio-temporal parameters from Optitrack and Xsens from heels.

Male subject _ normal speed				
Spatio-temporal parameters	Optitrack		Xsens from trunk	
	Right	Left	Right	Left
Stride time (s)	1,30	1,32	1,30	1,32
Step time (s)	0,66	0,64	0,66	0,64
Stance time (s)	0,78	0,82	0,82	0,86
Stance duration (%GC)	60,00	62,12	63,08	65,15
Swing time (s)	0,52	0,48	0,48	0,46
Swing duration (%GC)	40,00	36,36	36,92	34,85
Single support time (s)	0,48	0,52	0,46	0,48
SS duration (%GC)	36,92	39,39	35,38	36,36
Double support time (s)	0,26	0,34	0,34	0,40
DS duration (%GC)	20,00	25,76	26,15	30,30
Foot symmetry (%GC)	50,77	48,48	50,77	48,48
Limp index (right/left)	0,95	0,95	0,95	0,95

Table 3.4.5\_Male subject at normal speed: spatio-temporal parameters from Optitrack and Xsens from trunk.

Male subject _ normal speed				
Spatio-temporal parameters	Optitrack		Xsens from heels	
	Right	Left	Right	Left
Stride time (s)	1,30	1,32	1,30	1,30
Step time (s)	0,66	0,64	0,64	0,66
Stance time (s)	0,78	0,82	0,72	0,76
Stance duration (%GC)	60,00	62,12	55,38	58,46
Swing time (s)	0,52	0,48	0,58	0,54
Swing duration (%GC)	40,00	36,36	44,62	41,54
Single support time (s)	0,48	0,52	0,54	0,58
SS duration (%GC)	36,92	39,39	41,54	44,62
Double support time (s)	0,26	0,34	0,14	0,22
DS duration (%GC)	20,00	25,76	10,77	16,92
Foot symmetry (%GC)	50,77	48,48	49,23	50,77
Limp index (right/left)	0,95	0,95	0,95	0,95

Table 3.4.6\_Male subject at normal speed: spatio-temporal parameters from Optitrack and Xsens from heels.

First female subject _ fast speed				
Spatio-temporal parameters	Optitrack		Xsens from trunk	
	Right	Left	Right	Left
Stride time (s)	0,88	0,90	0,92	0,92
Step time (s)	0,44	0,44	0,44	0,48
Stance time (s)	0,52	0,54	0,56	0,56
Stance duration (%GC)	59,09	60,00	60,87	60,87
Swing time (s)	0,36	0,34	0,36	0,34
Swing duration (%GC)	40,91	37,78	39,13	36,96
Single support time (s)	0,34	0,36	0,34	0,36
SS duration (%GC)	38,64	40,00	36,96	39,13
Double support time (s)	0,16	0,20	0,20	0,22
DS duration (%GC)	18,18	22,22	21,74	23,91
Foot symmetry (%GC)	50,00	48,89	47,83	52,17
Limp index (right/left)	0,96	0,96	1,04	1,04

Table 3.4.7\_First female subject at fast speed: spatio-temporal parameters from Optitrack and Xsens from trunk.

First female subject _ fast speed				
Spatio-temporal parameters	Optitrack		Xsens from heels	
	Right	Left	Right	Left
Stride time (s)	0,88	0,90	0,88	0,90
Step time (s)	0,44	0,44	0,42	0,46
Stance time (s)	0,52	0,54	0,50	0,50
Stance duration (%GC)	59,09	60,00	56,82	55,56
Swing time (s)	0,36	0,34	0,38	0,40
Swing duration (%GC)	40,91	37,78	43,18	44,44
Single support time (s)	0,34	0,36	0,40	0,38
SS duration (%GC)	38,64	40,00	45,45	42,22
Double support time (s)	0,16	0,20	0,12	0,10
DS duration (%GC)	18,18	22,22	13,64	11,11
Foot symmetry (%GC)	50,00	48,89	47,73	51,11
Limp index (right/left)	0,96	0,96	1,00	0,95

Table 3.4.8\_First female subject at fast speed: spatio-temporal parameters from Optitrack and Xsens from heels.

Second female subject _ fast speed				
Spatio-temporal parameters	Optitrack		Xsens from trunk	
	Right	Left	Right	Left
Stride time (s)	1,06	1,10	1,04	1,10
Step time (s)	0,54	0,52	0,54	0,50
Stance time (s)	0,64	0,68	0,62	0,70
Stance duration (%GC)	60,38	61,82	59,62	63,64
Swing time (s)	0,42	0,38	0,42	0,36
Swing duration (%GC)	39,62	34,55	40,38	32,73
Single support time (s)	0,38	0,42	0,36	0,42
SS duration (%GC)	35,85	38,18	34,62	38,18
Double support time (s)	0,22	0,30	0,20	0,34
DS duration (%GC)	20,75	27,27	19,23	30,91
Foot symmetry (%GC)	50,94	47,27	51,92	45,45
Limp index (right/left)	0,94	0,94	0,89	0,89

Table 3.4.9\_Second female subject at fast speed: spatio-temporal parameters from Optitrack and Xsens from trunk.

Second female subject _ fast speed				
Spatio-temporal parameters	Optitrack		Xsens from heels	
	Right	Left	Right	Left
Stride time (s)	1,06	1,10	0,96	1,04
Step time (s)	0,54	0,52	0,52	0,44
Stance time (s)	0,64	0,68	0,50	0,60
Stance duration (%GC)	60,38	61,82	52,08	57,69
Swing time (s)	0,42	0,38	0,46	0,44
Swing duration (%GC)	39,62	34,55	47,92	42,31
Single support time (s)	0,38	0,42	0,44	0,46
SS duration (%GC)	35,85	38,18	45,83	44,23
Double support time (s)	0,22	0,30	0,04	0,16
DS duration (%GC)	20,75	27,27	4,17	15,38
Foot symmetry (%GC)	50,94	47,27	54,17	42,31
Limp index (right/left)	0,94	0,94	0,83	0,83

Table 3.4.10\_Second female subject at fast speed: spatio-temporal parameters from Optitrack and Xsens from heels.

Male subject _ fast speed				
Spatio-temporal parameters	Optitrack		Xsens from trunk	
	Right	Left	Right	Left
Stride time (s)	1,16	1,18	1,02	1,16
Step time (s)	0,58	0,58	0,45	0,56
Stance time (s)	0,68	0,70	0,70	0,70
Stance duration (%GC)	58,62	59,32	69,82	60,34
Swing time (s)	0,48	0,44	0,32	0,44
Swing duration (%GC)	41,38	37,29	30,18	37,93
Single support time (s)	0,44	0,48	0,44	0,46
SS duration (%GC)	37,93	40,68	38,60	39,66
Double support time (s)	0,20	0,26	0,22	0,26
DS duration (%GC)	17,24	22,03	19,30	22,41
Foot symmetry (%GC)	50,00	49,15	43,22	48,28
Limp index (right/left)	0,97	0,97	0,97	0,97

Table 3.4.11\_Male subject at fast speed: spatio-temporal parameters from Optitrack and Xsens from trunk.

Male subject _ fast speed				
Spatio-temporal parameters	Optitrack		Xsens from heels	
	Right	Left	Right	Left
Stride time (s)	1,16	1,18	1,14	1,14
Step time (s)	0,58	0,58	0,56	0,58
Stance time (s)	0,68	0,70	0,62	0,66
Stance duration (%GC)	58,62	59,32	54,39	57,89
Swing time (s)	0,48	0,44	0,52	0,48
Swing duration (%GC)	41,38	37,29	45,61	42,11
Single support time (s)	0,44	0,48	0,48	0,52
SS duration (%GC)	37,93	40,68	42,11	45,61
Double support time (s)	0,20	0,26	0,10	0,18
DS duration (%GC)	17,24	22,03	8,77	15,79
Foot symmetry (%GC)	50,00	49,15	49,12	50,88
Limp index (right/left)	0,97	0,97	0,94	0,94

Table 3.4.12\_Male subject at fast speed: spatio-temporal parameters from Optitrack and Xsens from heels.

First female subject _ slow speed				
Spatio-temporal parameters	Optitrack		Xsens from trunk	
	Right	Left	Right	Left
Stride time (s)	1,61	1,65	1,63	1,65
Step time (s)	0,83	0,78	0,82	0,81
Stance time (s)	1,08	1,12	1,07	1,09
Stance duration (%GC)	66,99	67,84	65,58	66,05
Swing time (s)	0,53	0,53	0,56	0,53
Swing duration (%GC)	33,01	32,10	34,42	32,10
Single support time (s)	0,53	0,53	0,53	0,56
SS duration (%GC)	32,90	32,14	32,50	33,95
Double support time (s)	0,55	0,59	0,51	0,56
DS duration (%GC)	33,98	35,74	31,16	33,95
Foot symmetry (%GC)	51,57	47,24	50,29	49,07
Limp index (right/left)	0,96	0,96	0,98	0,98

Table 3.4.13\_First female subject at slow speed: spatio-temporal parameters from Optitrack and Xsens from trunk.

First female subject _ slow speed				
Spatio-temporal parameters	Optitrack		Xsens from heels	
	Right	Left	Right	Left
Stride time (s)	1,61	1,65	1,52	1,64
Step time (s)	0,83	0,78	0,78	0,74
Stance time (s)	1,08	1,12	0,94	1,00
Stance duration (%GC)	66,99	67,84	61,84	60,98
Swing time (s)	0,53	0,53	0,58	0,64
Swing duration (%GC)	33,01	32,10	38,16	39,02
Single support time (s)	0,53	0,53	0,64	0,58
SS duration (%GC)	32,90	32,14	42,11	35,37
Double support time (s)	0,55	0,59	0,36	0,36
DS duration (%GC)	33,98	35,74	23,68	21,95
Foot symmetry (%GC)	51,57	47,24	51,32	45,12
Limp index (right/left)	0,96	0,96	0,94	0,94

Table 3.4.14\_First female subject at slow speed: spatio-temporal parameters from Optitrack and Xsens from heels.

Second female subject _ slow speed				
Spatio-temporal parameters	Optitrack		Xsens from trunk	
	Right	Left	Right	Left
Stride time (s)	1,34	1,35	1,34	1,32
Step time (s)	0,66	0,69	0,66	0,66
Stance time (s)	0,85	0,86	0,85	0,85
Stance duration (%GC)	63,39	63,77	63,46	64,39
Swing time (s)	0,49	0,49	0,47	0,47
Swing duration (%GC)	36,67	36,23	35,18	35,61
Single support time (s)	0,49	0,49	0,47	0,47
SS duration (%GC)	36,47	36,33	35,11	35,61
Double support time (s)	0,36	0,37	0,38	0,38
DS duration (%GC)	26,72	27,54	28,28	28,79
Foot symmetry (%GC)	49,42	51,05	49,42	50,00
Limp index (right/left)	0,99	0,99	1,00	1,00

Table 3.4.15\_Second female subject at slow speed: spatio-temporal parameters from Optitrack and Xsens from trunk.

Second female subject _ slow speed				
Spatio-temporal parameters	Optitrack		Xsens from heels	
	Right	Left	Right	Left
Stride time (s)	1,34	1,35	1,32	1,34
Step time (s)	0,66	0,69	0,67	0,67
Stance time (s)	0,85	0,86	0,77	0,79
Stance duration (%GC)	63,39	63,77	58,31	58,99
Swing time (s)	0,49	0,49	0,55	0,55
Swing duration (%GC)	36,67	36,23	41,69	41,01
Single support time (s)	0,49	0,49	0,55	0,55
SS duration (%GC)	36,47	36,33	41,64	41,10
Double support time (s)	0,36	0,37	0,22	0,24
DS duration (%GC)	26,72	27,54	16,62	17,97
Foot symmetry (%GC)	49,42	51,05	50,78	49,93
Limp index (right/left)	0,99	0,99	0,97	0,97

Table 3.4.16\_Second female subject at slow speed: spatio-temporal parameters from Optitrack and Xsens from heels.

Male subject _ slow speed				
Spatio-temporal parameters	Optitrack		Xsens from trunk	
	Right	Left	Right	Left
Stride time (s)	1,58	1,56	1,56	1,56
Step time (s)	0,78	0,78	0,80	0,76
Stance time (s)	0,98	0,98	1,00	1,02
Stance duration (%GC)	62,03	62,82	64,10	65,38
Swing time (s)	0,62	0,58	0,60	0,54
Swing duration (%GC)	39,24	37,18	38,46	34,62
Single support time (s)	0,58	0,62	0,54	0,60
SS duration (%GC)	36,71	39,74	34,62	38,46
Double support time (s)	0,36	0,40	0,40	0,48
DS duration (%GC)	22,78	25,64	25,64	30,77
Foot symmetry (%GC)	49,37	50,00	51,28	48,72
Limp index (right/left)	1,00	1,00	0,98	0,98

Table 3.4.17\_Male subject at slow speed: spatio-temporal parameters from Optitrack and Xsens from trunk.

Male subject _ slow speed				
Spatio-temporal parameters	Optitrack		Xsens from heels	
	Right	Left	Right	Left
Stride time (s)	1,58	1,56	1,58	1,56
Step time (s)	0,78	0,78	0,80	0,76
Stance time (s)	0,98	0,98	0,92	0,98
Stance duration (%GC)	62,03	62,82	58,23	62,82
Swing time (s)	0,62	0,58	0,66	0,58
Swing duration (%GC)	39,24	37,18	41,77	37,18
Single support time (s)	0,58	0,62	0,58	0,66
SS duration (%GC)	36,71	39,74	36,71	42,31
Double support time (s)	0,36	0,40	0,26	0,40
DS duration (%GC)	22,78	25,64	16,46	25,64
Foot symmetry (%GC)	49,37	50,00	50,63	48,72
Limp index (right/left)	1,00	1,00	0,96	0,96

Table 3.4.18\_Male subject at slow speed: spatio-temporal parameters from Optitrack and Xsens from heels.

The average values of gait parameters estimated with the three motion capture setups and algorithms are similar to those presented in literature studies. Considering the different velocities, the temporal parameters such as stride time, step time, stance time, swing time, single support time and double support time increased at lower speed. On the contrary they reduced at higher speed. The foot symmetry and the limp index were always about 50% and 1, respectively.

The following two tables (Table 3.4.19 and Table 3.4.20) contain the errors of the two Xsens algorithms. They were estimated as the modulus of the difference between the Optitrack values and the Xsens ones.

Spatio-temporal parameters	Errors Optitrack - Xsens trunk		
	Normal speed	Slow speed	Fast speed
Stride time (s)	0,02	0,00	0,01
Step time (s)	0,00	0,00	0,00
Stance time (s)	0,01	0,01	0,01
Stance duration (%GC)	1,85	0,42	0,62
Swing time (s)	0,01	0,00	0,00
Swing duration (%GC)	0,09	0,12	0,61
Single support time (s)	0,01	0,00	0,00
SS duration (%GC)	0,07	0,11	0,63
Double support time (s)	0,02	0,01	0,01
DS duration (%GC)	1,76	0,30	1,23
Foot symmetry (%GC)	0,70	0,08	0,05
Limp index (right/left)	0,02	0,01	0,01

Table 3.4.19\_Xsens trunk: errors estimated as differences between Optitrack and Xsens.

Spatio-temporal parameters	Errors Optitrack - Xsens heels		
	Normal speed	Slow speed	Fast speed
Stride time (s)	0,00	0,02	0,04
Step time (s)	0,01	0,02	0,02
Stance time (s)	0,05	0,08	0,06
Stance duration (%GC)	4,05	4,28	4,13
Swing time (s)	0,04	0,05	0,04
Swing duration (%GC)	3,02	4,07	5,67
Single support time (s)	0,04	0,05	0,04
SS duration (%GC)	3,07	4,16	5,70
Double support time (s)	0,09	0,13	0,11
DS duration (%GC)	7,07	8,35	9,81
Foot symmetry (%GC)	0,75	0,36	0,16
Limp index (right/left)	0,02	0,03	0,03

Table 3.4.20\_Xsens heels: errors estimated as differences between Optitrack and Xsens.

Considering the differences between Optitrack and IMUs, for all parameters and for all speeds the average errors from the trunk algorithm resulted lower compared with the heels one. For the parameters such as step time, stride time, stance time, swing time, single support time and double support time, the differences underlined negligible errors, generally around 10-40 ms. For all duration parameters related to the gait cycle (%GC), errors revealed higher values. The heels algorithm showed less accurate parameters detection. Local and undesirable movements might affect the heels sensors positions during the gait performance. The continuous changes of local axes orientations may be another cause of differences in TO and HS instants detection. In both cases, the different sample frequency for the data acquisition might partly cause the discrepancy of gait events detection. The increase of gait speed seemed to influence the parameter estimation. Indeed, for the fast velocity, the differences between system setups increased.

## 4. Test on healthy elderly subjects

### 4.1 Materials and methods

#### 4.1.1 Participants

Nine subjects were included in the experiment, six females and four males. The fundamental criteria for the participants' inclusion were two:

- age over 64 years
- absence of neurological and musculoskeletal disorders

All the subjects gave their written informed consent before the beginning of the test. They were informed about the methods, about the purpose of the experiment and about the absence of the invasiveness during the test.

The following Table 4.1.1 shows the main anthropometric data of the nine volunteers. Data are presented as average and standard deviation of the total number of subjects.

<b>Subjects</b>	<b>Mean <math>\pm</math> SD</b>
Age (years)	67.4 $\pm$ 5.1
Height (cm)	164.2 $\pm$ 12.3
Body mass (Kg)	71.7 $\pm$ 15.5
BMI	26.4 $\pm$ 2.9

**Table 4.1.1\_Anthropometric data of participants: age, height, body mass and BMI.**

#### 4.1.2 Instruments

The instrumentation included three MTx Xsens inertial sensors sampling at 50 Hz and two Optitrack V120:Trio bars sampling at 120 Hz.

The sensors of Xsens Bus Kit and the passive reflective markers visible from Optitrack V120:Trio were positioned at the same time on the bodies of the participants.

Three inertial sensors were fixed on the subjects. Two of them were positioned on the heels using a self-adhesive gauze, which was well stretched so as to keep them still. The third sensor was placed medially on the trunk through an elastic band supplied in the kit.

All the three IMUs were oriented with the local vertical axis pointing downward (x-axis), the local medio-lateral axis directed to the right side of the participants (y-axis) and the local anterior-posterior axis pointing in the opposite direction to that of the gait (z-axis).

The inertial sensors were connected to each other and to the Xbus Master via cables. It was important to accommodate cables in such a way they did not hinder the subjects during the gait. The connection between the Xbus Master and the PC was guaranteed by Bluetooth.

Six passive reflective markers were fixed using double-sided adhesive tape directly on the skin of the subjects. The markers were positioned bilaterally on anatomical landmarks: two on the malleolus, two on the heels and two on the toes. The markers on the heels were placed on the corresponding inertial sensors, paying attention to position them as low as possible.

The arrangement of markers and sensors is showed in Figure 4.1.1:

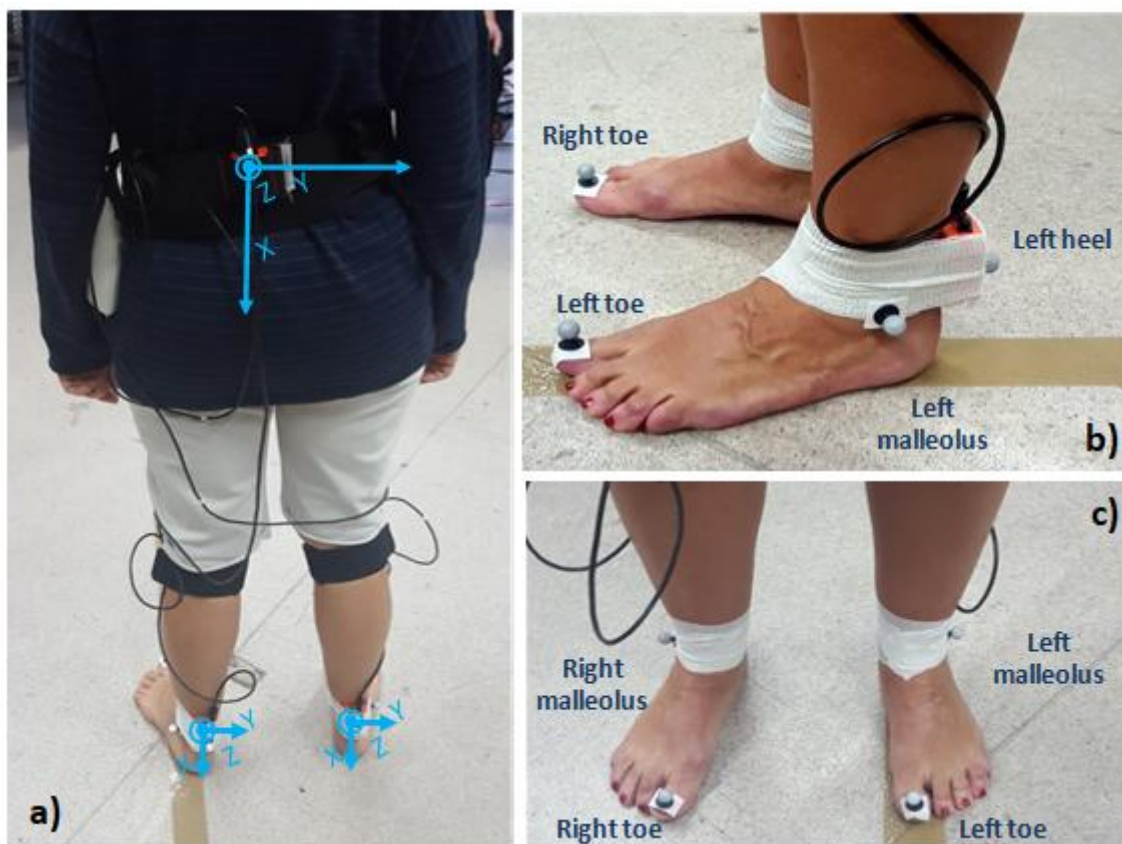


Figure 4.1.1\_a) Three inertial sensors on heels and trunk with their local axes. b) and c) Six reflective passive markers on heels, toes and malleolus.



The dual-task consisted in asking subjects about their life, their habits and their interests, in order to distract them from the first task.



Figure 4.1.3\_One of the nine subjects during the test.

In order to temporally synchronize the signals from IMUs and the markers coordinates from both bars, it was necessary to use an external event. Before walking, the subjects were asked to impact their right heel on the ground. This gesture was used to identify the instant zero for both the inertial sensors and the two bars.

#### 4.1.4 Signal processing and data analysis

The first step was the labeling of markers with the software Motive. The use of different colours for every marker made this task easier. Furthermore, the markers on the malleolus were useful to distinguish between right and left sides. Afterwards, it was necessary to calculate the transformation matrices from the coordinates of the three fixed markers on the floor recorded by both the Optitrack bars. The transformation matrices were the same introduced in Chapter 3.4 for the preliminary tests. Once the coordinates of markers were expressed in a unique global reference system, the next step was to temporally synchronize the two bars.

The frame corresponding to the minima of the right heel marker vertical coordinate was considered the instant zero for both bars.

At this point the most important thing to do was to identify gait events. The identification of heel-strike (HS) and toe-off (TO) from markers was made following the algorithm proposed by Veilleux in 2016. The heel-strike is defined as the frame before the horizontal trajectory of the heel marker change of direction. The toe-off is defined as the first frame where the toe marker changes direction in the anterior-posterior axis (L. Veilleux, 2016).

For each marker, a Matlab routine found gait events on the horizontal trajectory and defined a temporal window of sixteen samples, eight before and eight after the frame corresponding to the heel-strike or the toe-off. Then, it verified if this point corresponded exactly to the minima of this window in the vertical trajectory and eventually shifted it.

The Figure 4.1.4 shows an example of identification of GE from both horizontal and vertical trajectories.

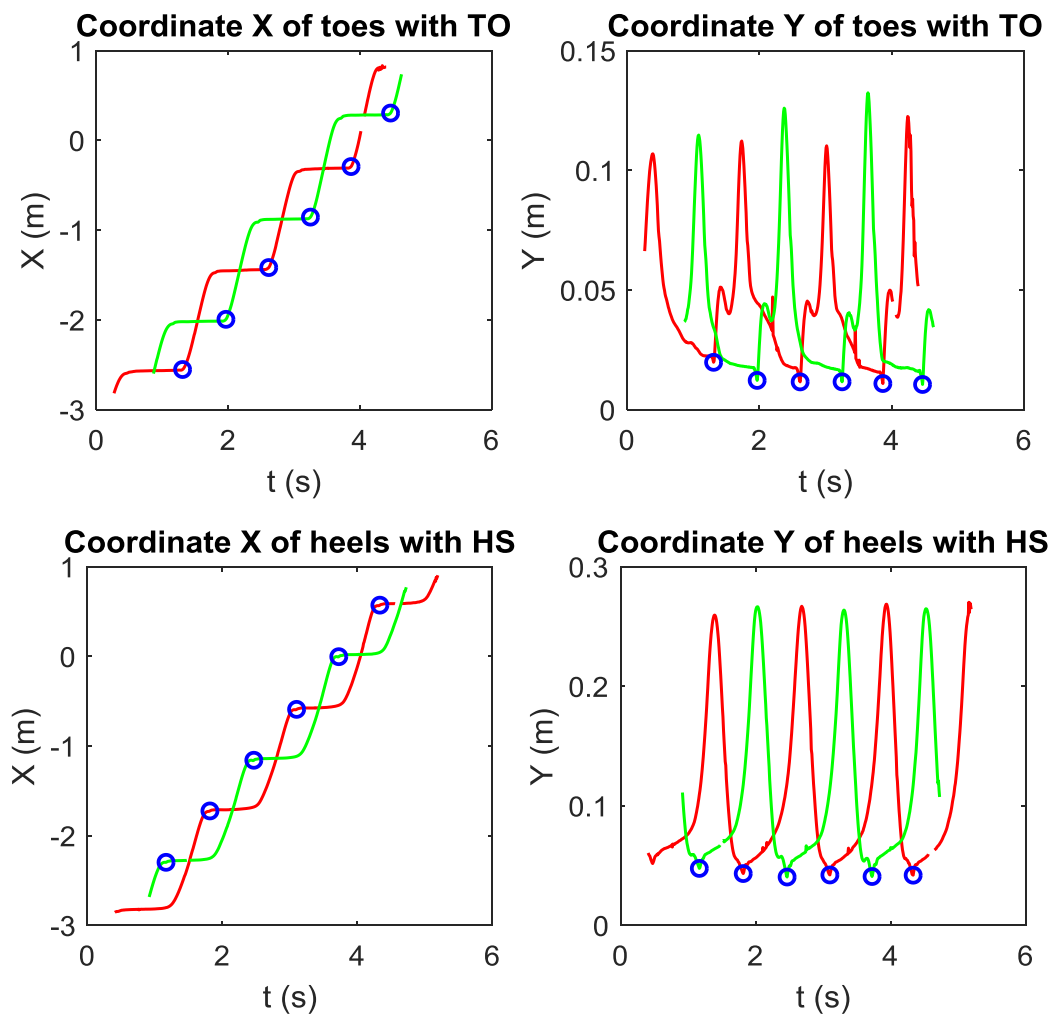


Figure 4.1.4. An example of identification of gait events from horizontal and vertical trajectories of toes and heels. Red colour is associated to right foot, green colour to left foot. Blue circles are respectively toe-off and heel-strikes.

Hereafter, also the inertial sensors signals were processed. When too much corrupted by noise, they were filtered using a low pass 4<sup>th</sup> order Butterworth filter with a cut-off frequency of 30 Hz. This frequency was chosen on the basis of the power spectral density of the signals. The axes were rotated and overturned in order to obtain a Cartesian triad with x-axis pointing upward, y-axis pointing to the right side of the subjects and z-axis pointing in the same direction of the gait. The temporal synchronization between the Optitrack bars and Xsens inertial sensors was obtained with the external event. The instant corresponding to zero for the IMUs signals was chosen as the one corresponding to the maximum peaks of the right heel vertical acceleration. Then, two different Matlab functions were created: one for the identification of gait events from the anterior-posterior acceleration of the trunk and one for the identification of gait events from the sagittal angular velocity of heels. The first algorithm was taken from the work of Zijlstra of 2004. The heel-strikes were identified as the maximum peaks of the anterior-posterior acceleration of the trunk. Furthermore, the sign of the trunk angular velocity around the vertical axis was used to distinguish between right (positive sign) and left (negative sign). The toe-off were identified as the minimum peaks of the same signal. The distinction between right and left TO was guaranteed by the alternation of heel-strikes. After a right HS there was a left TO and after a left HS there was a right TO. The Figure 4.1.5 shows an example of identification of gait events from the anterior-posterior acceleration of the trunk sensor:

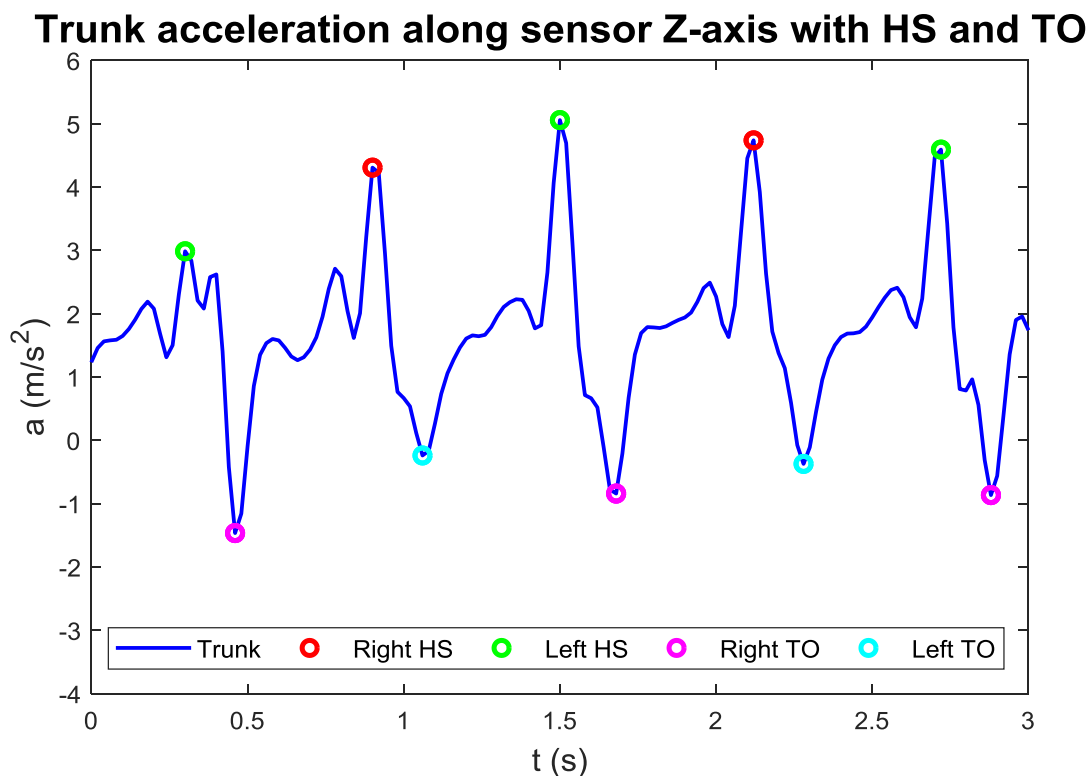
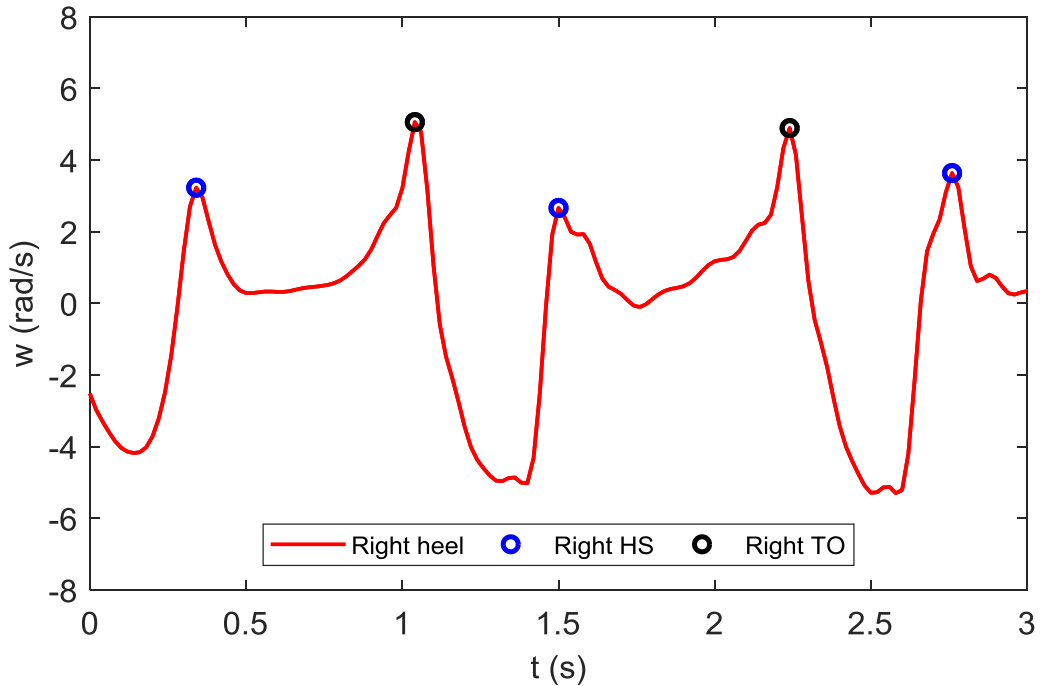


Figure 4.1.5\_An example of identification of GE from anterior-posterior acceleration of trunk sensor.

The second algorithm was taken from the work of Misu and his colleagues of 2017. The TO were searched for as the maximum peaks of the sagittal angular velocity of heels and the HS as the maxima among the TO. The Figure 4.1.6 shows an example of identification of GE from sagittal angular velocity of heels sensors.

a) **Right heel angular velocity around sensor Y-axis with HS and TO**



b) **Left heel angular velocity around sensor Y-axis with HS and TO**

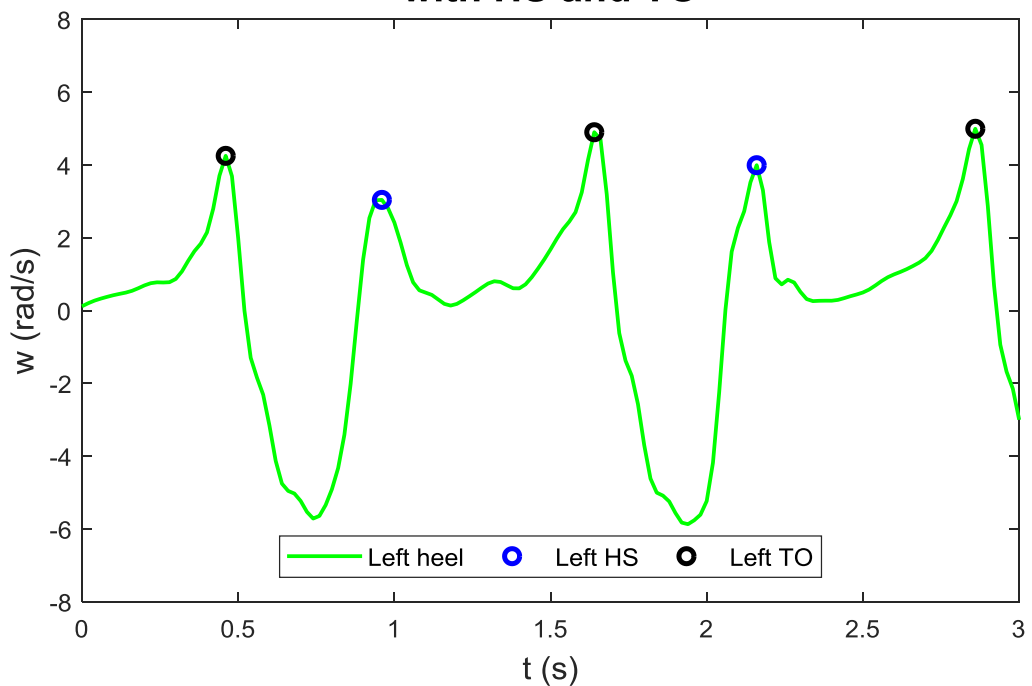


Figure 4.1.6\_An example of identification of GE from sagittal angular velocity of right (a) and left (b) heels sensors.

Once the gait events were identified both from markers coordinates and from inertial sensors signals, a Matlab function was written to estimate the following spatio-temporal parameters:

- Stride time (s)
- Stride frequency (Hz)
- Step time (s)
- Step frequency (Hz)
- Stance time (s)
- Stance duration (%GC)
- Swing time (s)
- Swing duration (%GC)
- Single support time (s)
- Single support duration (%GC)
- Double support time (s)
- Double support duration (%GC)
- Foot symmetry (%GC)
- Limp index

The foot symmetry was calculated as the ratio between the step time and the stride time, whereas the limp index was estimated as the ratio between right and left stance times.

All the spatio-temporal parameters were always estimated for both right and left sides. All calculations were always performed for Optitrack, Xsens algorithm with trunk and Xsens algorithm with heels.

Spatio-temporal parameters were obtained for each transition in front of the cameras. Then, mean and standard deviation values were evaluated for every subject. Fourteen tables were created, one for each parameter. The mean and the standard deviation values of each parameter for every subject were calculated respectively for: Optitrack, Xsens algorithm with trunk and Xsens algorithm with heels. The distinction between right and left sides was maintained.

The purpose was to compare the spatio-temporal parameters obtained with Xsens inertial sensors signals with those obtained with the Optitrack bars, used as gold standard. In particular, the attention was paid to the comparison between the two different algorithms used with the inertial sensors signals. The results, presented in the following subchapter 4.2, were produced both for the trials with single-task and for those with dual-task. The data were presented in two different ways: tables of errors obtained by differences and Bland-Altman plots.

The errors were evaluated doing a difference between the real value obtained with Optitrack and the value obtained with Xsens. The differences were always calculated for both the Xsens algorithms tested. A set of fourteen tables was realized, each of them for a single spatio-temporal parameter. In the first column there are the nine subjects. In the second and third columns there are the errors of the algorithm of trunk both for right and left sides. In the fourth and fifth columns there are the errors of the algorithm of heels for both sides.

The Bland-Altman plots are scatter diagrams generally used in order to compare two methods. On the ordinates there is the difference of two measures, whereas on the abscissas there is the arithmetic mean of the same two measures. The horizontal lines represent respectively the mean of differences and the mean of differences  $\pm 1.96 \times SD$ , where SD is the standard deviation. The mean of differences allows to estimate if one method provides an overestimation or an underestimation of the parameter with respect to the other method. The other two lines define the Limit of Agreement. If the points in the graph are within these two lines, the two methods are considered to give congruent results. The points outside the two lines are cases in which the two methods are not congruent with each other. Bland-Altman plots were evaluated for every parameter comparing the two Xsens algorithms with respect to the gold standard Optitrack. The difference of right and left sides was maintained, but it was not expressed graphically. In this way, in every plot there are eighteen points of the same colour, nine for the right side and nine for the left side. The only exceptions are the double support time and the double support duration, for which there is no difference between right and left sides. Consequently, in these two cases the points in the Bland-Altman plots are only nine. In order to distinguish between the two Xsens algorithms, two different colours were used: red for algorithm with trunk and blue for algorithm with heels.

Subsequently, also the comparison between the trials with single-task and those with dual-task was made. Two tables were realized, one for the single-task and one for the dual-task. Mean and standard deviation values were calculated among all the nine subjects for all parameters and with the three methods: Optitrack, Xsens with trunk acceleration and Xsens with heels angular velocity. Then, fourteen bar diagrams were obtained, each of them for a single spatio-temporal parameter. Every bar diagram has six columns: the first and the second present data from Optitrack, the third and the fourth present the data from Xsens with the sensor on the trunk and the fifth and the sixth present the data from Xsens with the sensors on the heels. The first, the third and the fifth columns are related to the single-task, whereas the second, the fourth and the sixth ones are related to the dual-task.

Finally, the paired t-test was applied for statistical analysis of single-task and dual-task data. It is a statistical procedure useful to compare two different conditions applied to the same subjects, because it can determine the amount of mean difference between two observations sets. The paired t-test is used when the subjects are the same in both conditions and the two sets of measures can be coupled, as in this case. This procedure works with two hypotheses:

- the null hypothesis provides that the average of difference between a series of paired observations is equal to zero.
- the alternative hypothesis provides that the difference between the two sets does not have a mean equal to zero.

Another important factor is the p-value, proposed by R. Fisher in 1920s to measure the force of a scientific result. He defined the p-value as an indicator of discrepancy between the data and the null hypothesis. It is necessary to compare the p-value with the significance level, in order to establish if the difference between the population means is statistically significant. The conditions are two:

1. When the p-value is  $\leq \alpha$ , the difference between the means is statistically significant. For this reason the null hypothesis is rejected.
2. When the p-value is  $> \alpha$ , the difference between the means is not statistically significant. For this reason the null hypothesis is not rejected.

Choosing a 95% of confidence interval, the t-test was made by using a Matlab function called *ttest*, which produces the p-values as outputs. Each spatio temporal parameter was considered as a single independent variable. When all the p-values were obtained, a table with three columns was realized: the first column is related to Optitrack, the second column is related to Xsens with trunk and the third one is related to Xsens with heels.

The Table 4.1.2 presents a summary of all the materials and methods of this study:

<b>Materials and methods</b>	
<b>Participants</b>	Nine subjects over 64 years old and with no neurological or musculoskeletal disorders.
<b>Instruments</b>	<ul style="list-style-type: none"> <li>- Three Xsens IMUs: two on the heels and one on the trunk.</li> <li>- Two Optitrack V120:Trio bars and six reflective markers: two on the malleolus, two on the heels and two on the toes.</li> </ul>
<b>Protocol</b>	<ul style="list-style-type: none"> <li>- Static acquisition with three fixed markers for the creation of the global reference system.</li> <li>- 3 trials at preferred normal speed with single-task, each of them composed of 8 transitions in front of cameras.</li> <li>- 3 trials at preferred normal speed with dual-task, each of them composed of 8 transitions in front of cameras.</li> </ul>
<b>Data analysis and post-processing</b>	<ul style="list-style-type: none"> <li>- Creation of transformation matrices in order to obtain all the data from markers in the same global reference system.</li> <li>- Temporal synchronization:                             <ul style="list-style-type: none"> <li>o Optitrack: minimum of the vertical coordinate of the right heel marker.</li> <li>o Xsens: maximum of the right heel vertical acceleration.</li> </ul> </li> <li>- Algorithms:                             <ul style="list-style-type: none"> <li>o Optitrack: horizontal trajectories of heels and toes markers. HS as the frame before the change of direction, TO as the first frame of the change of direction. Verification of the correspondence of the GE with the minima of the vertical trajectory (L. Veilleux, 2016).</li> <li>o Xsens: anterior-posterior acceleration of trunk. HS as maximum peaks, TO as minimum peaks (Zijlstra, 2004). Distinction between right and left sides through the sign of the trunk angular velocity around vertical axis.</li> <li>o Xsens: sagittal angular velocity of heels. TO as maximum peaks, HS as maxima among TO (S. Misu, 2017).</li> </ul> </li> </ul>

**Table 4.1.2\_Summary of materials and methods adopted for the experiment.**

## 4.2 Results

### 4.2.1 Normal speed with single-task

The following fourteen tables (from Table 4.2.1 to Table 4.2.14) present the spatio-temporal parameters obtained for every subject with the three methods adopted: Optitrack, Xsens algorithm with trunk acceleration and Xsens algorithm with heels angular velocity.

Subjects	Stride time (s)											
	Optitrack				Algorithm from trunk				Algorithm from heels			
	Right		Left		Right		Left		Right		Left	
	Mean	SD	Mean	SD	Mean	SD	Mean	SD	Mean	SD	Mean	SD
1	1,06	0,03	1,06	0,03	1,05	0,02	1,06	0,02	1,06	0,02	1,06	0,03
2	1,07	0,05	1,08	0,02	1,07	0,03	1,08	0,03	1,06	0,03	1,08	0,03
3	1,06	0,03	1,05	0,03	1,07	0,04	1,06	0,04	1,06	0,04	1,06	0,04
4	1,14	0,03	1,15	0,03	1,15	0,08	1,16	0,04	1,15	0,03	1,14	0,04
5	1,24	0,02	1,26	0,03	1,25	0,02	1,26	0,03	1,24	0,03	1,24	0,03
6	1,19	0,05	1,20	0,05	1,20	0,09	1,20	0,05	1,19	0,05	1,19	0,04
7	1,22	0,05	1,23	0,05	1,21	0,07	1,23	0,06	1,23	0,05	1,22	0,05
8	1,23	0,03	1,24	0,03	1,24	0,03	1,24	0,03	1,24	0,03	1,23	0,04
9	1,23	0,03	1,24	0,03	1,23	0,05	1,25	0,03	1,24	0,04	1,24	0,03

Table 4.2.1\_Mean and standard deviation values for stride time.

Subjects	Stride frequency (Hz)											
	Optitrack				Algorithm from trunk				Algorithm from heels			
	Right		Left		Right		Left		Right		Left	
	Mean	SD	Mean	SD	Mean	SD	Mean	SD	Mean	SD	Mean	SD
1	0,95	0,02	0,94	0,02	0,95	0,02	0,94	0,02	0,95	0,02	0,95	0,02
2	0,93	0,04	0,93	0,02	0,94	0,03	0,93	0,02	0,94	0,02	0,93	0,03
3	0,95	0,03	0,95	0,03	0,94	0,03	0,94	0,03	0,95	0,04	0,94	0,04
4	0,87	0,02	0,87	0,02	0,87	0,06	0,87	0,03	0,87	0,02	0,87	0,03
5	0,81	0,02	0,80	0,02	0,80	0,02	0,79	0,02	0,81	0,02	0,81	0,02
6	0,84	0,03	0,84	0,03	0,84	0,06	0,83	0,03	0,84	0,03	0,84	0,03
7	0,82	0,03	0,81	0,03	0,83	0,05	0,82	0,04	0,82	0,03	0,82	0,03
8	0,81	0,02	0,81	0,02	0,81	0,02	0,81	0,02	0,81	0,02	0,81	0,03
9	0,81	0,02	0,81	0,02	0,81	0,03	0,80	0,02	0,81	0,02	0,81	0,02

Table 4.2.2\_Mean and standard deviation values for stride frequency.

Subjects	Step time (s)											
	Optitrack				Algorithm from trunk				Algorithm from heels			
	Right		Left		Right		Left		Right		Left	
	Mean	SD	Mean	SD	Mean	SD	Mean	SD	Mean	SD	Mean	SD
1	0,54	0,02	0,52	0,01	0,53	0,02	0,53	0,01	0,53	0,01	0,53	0,02
2	0,54	0,05	0,54	0,03	0,54	0,02	0,54	0,02	0,53	0,01	0,54	0,02
3	0,53	0,02	0,53	0,01	0,53	0,02	0,53	0,03	0,54	0,03	0,52	0,02
4	0,57	0,01	0,57	0,02	0,58	0,04	0,58	0,05	0,57	0,02	0,58	0,02
5	0,62	0,01	0,64	0,02	0,63	0,02	0,63	0,01	0,60	0,03	0,64	0,03
6	0,58	0,03	0,61	0,02	0,61	0,05	0,59	0,04	0,59	0,03	0,60	0,02
7	0,59	0,03	0,64	0,03	0,59	0,04	0,63	0,04	0,59	0,02	0,64	0,03
8	0,62	0,02	0,62	0,02	0,62	0,02	0,62	0,02	0,62	0,02	0,62	0,02
9	0,62	0,02	0,61	0,02	0,62	0,03	0,62	0,02	0,62	0,03	0,61	0,02

Table 4.2.3\_Mean and standard deviation values for step time.

Subjects	Step frequency (Hz)											
	Optitrack				Algorithm from trunk				Algorithm from heels			
	Right		Left		Right		Left		Right		Left	
	Mean	SD	Mean	SD	Mean	SD	Mean	SD	Mean	SD	Mean	SD
1	1,86	0,06	1,91	0,05	1,90	0,05	1,88	0,05	1,90	0,05	1,89	0,06
2	1,86	0,13	1,88	0,17	1,87	0,08	1,86	0,08	1,89	0,05	1,85	0,08
3	1,90	0,08	1,89	0,05	1,90	0,09	1,88	0,09	1,87	0,10	1,91	0,09
4	1,74	0,04	1,75	0,06	1,76	0,14	1,74	0,17	1,77	0,07	1,73	0,06
5	1,62	0,04	1,58	0,04	1,59	0,05	1,59	0,03	1,67	0,08	1,57	0,08
6	1,72	0,08	1,64	0,06	1,67	0,14	1,70	0,13	1,70	0,08	1,67	0,06
7	1,70	0,07	1,57	0,06	1,70	0,12	1,61	0,11	1,71	0,06	1,57	0,08
8	1,62	0,05	1,61	0,05	1,62	0,04	1,62	0,05	1,63	0,06	1,62	0,07
9	1,60	0,05	1,65	0,08	1,62	0,07	1,61	0,06	1,61	0,07	1,63	0,05

Table 4.2.4\_Mean and standard deviation values for step frequency.

Subjects	Stance time (s)											
	Optitrack				Algorithm from trunk				Algorithm from heels			
	Right		Left		Right		Left		Right		Left	
	Mean	SD	Mean	SD	Mean	SD	Mean	SD	Mean	SD	Mean	SD
1	0,65	0,02	0,65	0,02	0,68	0,03	0,68	0,02	0,61	0,02	0,60	0,02
2	0,66	0,02	0,65	0,02	0,64	0,03	0,64	0,03	0,60	0,03	0,60	0,02
3	0,67	0,02	0,66	0,02	0,68	0,03	0,68	0,02	0,62	0,03	0,62	0,03
4	0,70	0,03	0,71	0,02	0,72	0,05	0,73	0,03	0,66	0,02	0,66	0,03
5	0,77	0,02	0,78	0,02	0,80	0,02	0,79	0,03	0,74	0,02	0,73	0,03
6	0,78	0,04	0,78	0,04	0,76	0,05	0,78	0,03	0,70	0,03	0,70	0,03
7	0,79	0,04	0,79	0,04	0,83	0,14	0,85	0,04	0,72	0,04	0,72	0,04
8	0,76	0,03	0,78	0,03	0,76	0,03	0,75	0,03	0,69	0,03	0,68	0,03
9	0,80	0,03	0,79	0,02	0,79	0,03	0,79	0,02	0,70	0,02	0,73	0,03

Table 4.2.5\_Mean and standard deviation values for stance time.

Subjects	Stance duration (%GC)											
	Optitrack				Algorithm from trunk				Algorithm from heels			
	Right		Left		Right		Left		Right		Left	
	Mean	SD	Mean	SD	Mean	SD	Mean	SD	Mean	SD	Mean	SD
1	61,46	1,63	61,42	1,40	64,61	2,61	64,34	1,46	57,30	1,11	56,66	0,86
2	61,32	2,80	60,21	1,79	59,61	2,46	59,24	2,09	56,75	2,06	55,76	1,56
3	63,48	0,95	62,83	0,88	63,41	1,20	63,73	1,30	58,27	1,77	58,63	0,84
4	61,58	1,43	61,75	0,92	62,53	3,75	63,14	2,86	57,44	1,33	57,90	1,51
5	61,90	0,97	61,72	0,98	63,50	1,42	63,09	1,63	59,97	1,52	58,49	1,73
6	65,31	1,81	65,31	1,18	64,04	2,73	64,78	1,98	58,63	1,50	58,84	1,26
7	64,22	1,07	64,48	1,39	68,47	11,24	69,71	2,44	58,90	1,20	58,98	1,71
8	61,57	0,91	62,73	0,89	61,67	1,86	61,00	1,43	55,95	1,22	55,69	1,28
9	65,01	0,90	64,34	1,86	64,34	1,73	63,82	1,03	56,83	1,36	58,98	1,49

Table 4.2.6\_Mean and standard deviation values for stance duration.

Subjects	Swing time (s)											
	Optitrack				Algorithm from trunk				Algorithm from heels			
	Right		Left		Right		Left		Right		Left	
	Mean	SD	Mean	SD	Mean	SD	Mean	SD	Mean	SD	Mean	SD
1	0,41	0,02	0,41	0,01	0,38	0,02	0,38	0,02	0,45	0,01	0,46	0,01
2	0,42	0,05	0,43	0,03	0,43	0,02	0,44	0,02	0,46	0,02	0,47	0,02
3	0,39	0,02	0,39	0,01	0,39	0,02	0,38	0,02	0,44	0,02	0,44	0,02
4	0,44	0,01	0,44	0,02	0,43	0,04	0,43	0,04	0,49	0,02	0,48	0,02
5	0,48	0,01	0,48	0,02	0,46	0,02	0,46	0,02	0,50	0,02	0,52	0,02
6	0,42	0,02	0,42	0,02	0,43	0,04	0,42	0,03	0,49	0,02	0,49	0,02
7	0,44	0,02	0,44	0,02	0,38	0,10	0,37	0,04	0,50	0,01	0,50	0,02
8	0,47	0,01	0,46	0,02	0,47	0,02	0,48	0,02	0,54	0,02	0,55	0,02
9	0,44	0,02	0,44	0,02	0,44	0,02	0,45	0,02	0,53	0,02	0,51	0,02

Table 4.2.7\_Mean and standard deviation values for swing time.

Subjects	Swing duration (%GC)											
	Optitrack				Algorithm from trunk				Algorithm from heels			
	Right		Left		Right		Left		Right		Left	
	Mean	SD	Mean	SD	Mean	SD	Mean	SD	Mean	SD	Mean	SD
1	38,58	1,17	38,48	1,14	35,64	1,84	36,04	1,70	42,78	1,04	43,43	0,94
2	38,84	3,91	40,27	2,35	39,84	1,69	40,50	1,87	43,07	1,79	44,13	1,20
3	36,70	0,86	37,12	0,80	36,41	0,97	36,20	1,26	41,77	1,65	41,41	0,89
4	38,71	1,17	38,66	0,99	37,65	3,32	37,01	2,92	42,74	1,17	42,11	1,40
5	38,10	0,89	38,37	0,80	36,73	1,16	36,96	1,59	40,25	1,58	41,76	1,83
6	34,87	1,73	34,79	1,24	35,98	2,54	35,27	2,21	41,56	1,46	41,18	1,24
7	35,71	0,92	35,53	1,12	31,16	7,48	30,65	2,85	41,13	1,14	41,01	1,24
8	38,41	0,71	37,32	1,56	38,15	1,32	38,93	1,43	43,82	1,01	44,19	1,31
9	35,37	1,20	35,96	1,38	35,73	1,46	36,38	1,23	43,18	1,44	41,17	1,30

Table 4.2.8\_Mean and standard deviation values for swing duration.

Subjects	Single support time (s)											
	Optitrack				Algorithm from trunk				Algorithm from heels			
	Right		Left		Right		Left		Right		Left	
	Mean	SD	Mean	SD	Mean	SD	Mean	SD	Mean	SD	Mean	SD
1	0,41	0,01	0,41	0,02	0,38	0,02	0,38	0,02	0,46	0,01	0,45	0,01
2	0,43	0,02	0,42	0,03	0,44	0,03	0,43	0,02	0,47	0,01	0,47	0,02
3	0,39	0,01	0,39	0,01	0,39	0,02	0,39	0,02	0,44	0,02	0,44	0,02
4	0,44	0,01	0,44	0,01	0,43	0,04	0,43	0,04	0,48	0,02	0,49	0,01
5	0,48	0,01	0,48	0,01	0,46	0,02	0,46	0,02	0,51	0,02	0,50	0,02
6	0,42	0,01	0,42	0,02	0,43	0,04	0,43	0,04	0,49	0,02	0,49	0,02
7	0,44	0,02	0,44	0,01	0,38	0,06	0,38	0,10	0,50	0,02	0,50	0,01
8	0,46	0,02	0,47	0,01	0,48	0,01	0,47	0,02	0,55	0,02	0,54	0,02
9	0,44	0,02	0,44	0,02	0,45	0,02	0,44	0,02	0,51	0,02	0,53	0,02

Table 4.2.9\_Mean and standard deviation values for single support time.

Subjects	Single support duration (%GC)											
	Optitrack				Algorithm from trunk				Algorithm from heels			
	Right		Left		Right		Left		Right		Left	
	Mean	SD	Mean	SD	Mean	SD	Mean	SD	Mean	SD	Mean	SD
1	38,35	1,21	38,72	1,21	35,57	1,54	35,64	1,84	43,22	0,83	42,79	0,90
2	40,15	2,32	38,86	1,76	40,66	2,00	39,84	1,67	44,03	1,21	43,67	1,66
3	37,02	0,71	36,74	0,81	36,38	0,92	36,41	0,97	41,47	0,91	41,65	1,43
4	38,48	0,80	38,60	1,13	37,03	2,43	37,47	3,18	42,30	1,14	42,62	0,86
5	38,26	0,72	38,14	0,86	36,76	1,39	36,73	1,16	41,33	1,69	40,56	1,50
6	34,81	0,91	34,89	1,39	35,46	1,67	35,98	2,54	41,01	0,95	41,35	1,16
7	35,62	1,04	35,71	1,02	30,71	4,45	31,16	7,48	40,98	1,17	41,13	1,17
8	37,50	1,55	38,26	0,69	38,79	1,15	38,15	1,32	44,34	0,98	43,90	0,93
9	35,48	1,37	35,42	1,16	36,00	0,91	35,73	1,46	41,53	1,36	42,66	1,45

Table 4.2.10\_Mean and standard deviation values for single support duration.

Subjects	Double support time (s)											
	Optitrack				Algorithm from trunk				Algorithm from heels			
	Right		Left		Right		Left		Right		Left	
	Mean	SD	Mean	SD	Mean	SD	Mean	SD	Mean	SD	Mean	SD
1	0,24	0,02	0,24	0,02	0,30	0,03	0,30	0,03	0,15	0,02	0,15	0,02
2	0,23	0,04	0,23	0,04	0,21	0,03	0,21	0,03	0,14	0,02	0,14	0,02
3	0,28	0,02	0,28	0,02	0,29	0,02	0,29	0,02	0,18	0,02	0,18	0,02
4	0,26	0,01	0,26	0,01	0,29	0,04	0,29	0,05	0,17	0,02	0,17	0,02
5	0,29	0,02	0,29	0,02	0,33	0,03	0,33	0,03	0,22	0,03	0,22	0,03
6	0,36	0,03	0,36	0,03	0,35	0,04	0,35	0,04	0,21	0,02	0,21	0,02
7	0,35	0,03	0,35	0,03	0,46	0,10	0,46	0,10	0,22	0,03	0,22	0,03
8	0,30	0,03	0,30	0,03	0,28	0,03	0,28	0,03	0,15	0,02	0,15	0,02
9	0,35	0,02	0,35	0,02	0,35	0,02	0,35	0,02	0,19	0,03	0,19	0,03

Table 4.2.11\_Mean and standard deviation values for double support time.

Subjects	Double support duration (%GC)											
	Optitrack				Algorithm from trunk				Algorithm from heels			
	Right		Left		Right		Left		Right		Left	
	Mean	SD	Mean	SD	Mean	SD	Mean	SD	Mean	SD	Mean	SD
1	22,94	1,62	22,94	1,62	28,32	3,04	28,32	3,04	13,79	1,34	13,79	1,34
2	20,89	3,60	20,89	3,60	19,66	3,04	19,66	3,04	13,09	2,16	13,09	2,16
3	26,18	1,36	26,18	1,36	27,40	1,37	27,40	1,37	16,83	1,87	16,83	1,87
4	22,64	1,04	22,64	1,04	25,28	3,93	25,52	4,04	15,16	1,59	15,16	1,59
5	23,53	1,07	23,53	1,07	26,30	2,04	26,30	2,04	18,00	2,60	18,00	2,60
6	30,35	1,95	30,35	1,95	28,75	3,26	28,75	3,26	17,26	1,72	17,26	1,72
7	28,76	1,70	28,76	1,70	38,19	8,51	38,19	8,51	17,86	1,98	17,86	1,98
8	24,27	1,66	24,27	1,66	22,92	1,80	22,92	1,80	11,99	1,34	11,99	1,34
9	28,67	1,40	28,67	1,40	27,89	1,89	27,89	1,89	15,65	1,92	15,65	1,92

Table 4.2.12\_Mean and standard deviation values for double support duration.

Subjects	Foot symmetry (%GC)											
	Optitrack				Algorithm from trunk				Algorithm from heels			
	Right		Left		Right		Left		Right		Left	
	Mean	SD	Mean	SD	Mean	SD	Mean	SD	Mean	SD	Mean	SD
1	50,43	1,44	49,33	0,93	49,57	0,88	50,04	1,26	49,75	1,17	50,03	0,88
2	49,76	2,30	49,42	4,93	50,47	2,06	50,48	1,98	49,43	1,76	50,74	1,58
3	50,06	0,96	50,28	1,05	49,81	1,76	50,33	1,74	50,64	1,86	49,57	1,99
4	49,73	1,16	49,65	0,98	49,54	4,71	50,30	3,55	49,10	1,61	50,19	1,53
5	49,16	0,90	50,79	0,96	49,66	0,88	49,86	1,17	48,24	2,76	51,71	2,19
6	48,50	1,31	51,07	1,23	50,25	3,87	49,48	2,80	49,36	1,11	50,46	1,59
7	47,94	0,79	51,92	0,72	48,03	3,50	51,09	2,37	47,80	0,78	52,24	0,87
8	49,71	1,06	50,12	0,83	50,30	1,14	49,98	0,87	50,13	1,64	50,27	1,22
9	50,32	1,16	49,18	1,61	49,61	1,84	50,04	1,45	50,31	1,49	49,67	1,76

Table 4.2.13\_Mean and standard deviation values for foot symmetry.

Subjects	Limp index											
	Optitrack				Algorithm from trunk				Algorithm from heels			
	Right		Left		Right		Left		Right		Left	
	Mean	SD	Mean	SD	Mean	SD	Mean	SD	Mean	SD	Mean	SD
1	1,00	0,03	1,00	0,03	0,99	0,04	0,99	0,04	1,01	0,03	1,01	0,03
2	1,02	0,05	1,02	0,05	1,00	0,03	1,00	0,03	1,01	0,05	1,01	0,05
3	1,02	0,03	1,02	0,03	1,00	0,04	1,00	0,04	0,99	0,05	0,99	0,05
4	1,00	0,04	1,00	0,04	0,99	0,09	1,00	0,08	1,00	0,06	1,00	0,06
5	0,99	0,03	0,99	0,03	1,00	0,03	1,00	0,03	1,03	0,05	1,03	0,05
6	1,00	0,04	1,00	0,04	0,98	0,07	0,98	0,07	1,00	0,04	1,00	0,04
7	0,99	0,03	0,99	0,03	0,97	0,16	0,97	0,16	1,00	0,03	1,00	0,03
8	0,98	0,03	0,98	0,03	1,01	0,05	1,01	0,05	1,01	0,04	1,01	0,04
9	1,01	0,03	1,01	0,03	1,00	0,04	1,00	0,04	0,97	0,04	0,97	0,04

Table 4.2.14\_Mean and standard deviation values for limp index.

The following fourteen tables (from Table 4.2.15 to Table 4.2.28) show the differences calculated between the mean values obtained from Optitrack and those obtained from the two Xsens algorithms.

Subjects	Stride time (s)			
	Errors algorithm trunk		Errors algorithm heels	
	Right	Left	Right	Left
1	0,01	0,00	0,00	0,00
2	0,00	-0,01	0,01	0,00
3	-0,01	-0,01	0,00	-0,01
4	-0,01	-0,01	0,00	0,00
5	-0,01	0,00	0,00	0,02
6	0,00	0,00	0,00	0,01
7	0,01	0,00	0,00	0,01
8	0,00	0,00	-0,01	0,01
9	0,00	-0,01	-0,01	0,00

Table 4.2.15\_Errors for stride time.

Subjects	Stride frequency (Hz)			
	Errors algorithm trunk		Errors algorithm heels	
	Right	Left	Right	Left
1	-0,01	0,00	0,00	0,00
2	0,00	0,00	-0,01	0,00
3	0,01	0,01	0,00	0,01
4	0,00	0,00	0,00	0,00
5	0,01	0,00	0,00	-0,01
6	0,00	0,00	0,00	-0,01
7	-0,01	0,00	0,00	-0,01
8	0,00	0,00	0,00	-0,01
9	0,00	0,01	0,00	0,00

Table 4.2.16\_Errors for stride frequency.

Subjects	Step time (s)			
	Errors algorithm trunk		Errors algorithm heels	
	Right	Left	Right	Left
1	0,01	-0,01	0,01	-0,01
2	0,00	-0,01	0,01	-0,01
3	0,00	-0,01	-0,01	0,00
4	0,00	-0,01	0,01	-0,01
5	-0,01	0,01	0,02	-0,01
6	-0,02	0,02	-0,01	0,01
7	-0,01	0,01	0,00	0,00
8	0,00	0,00	0,00	0,00
9	0,01	-0,01	0,00	0,00

Table 4.2.17\_Errors for step time.

Subjects	Step frequency (Hz)			
	Errors algorithm trunk		Errors algorithm heels	
	Right	Left	Right	Left
1	-0,04	0,03	-0,04	0,02
2	-0,01	0,03	-0,03	0,04
3	0,00	0,01	0,03	-0,02
4	-0,01	0,01	-0,02	0,02
5	0,03	-0,02	-0,05	0,01
6	0,05	-0,06	0,02	-0,03
7	0,00	-0,03	-0,01	0,01
8	0,01	-0,01	0,00	-0,01
9	-0,02	0,04	-0,01	0,02

Table 4.2.18\_Errors for step frequency.

Subjects	Stance time (s)			
	Errors algorithm trunk		Errors algorithm heels	
	Right	Left	Right	Left
1	-0,03	-0,03	0,04	0,05
2	0,02	0,01	0,05	0,05
3	0,00	-0,01	0,06	0,04
4	-0,01	-0,02	0,05	0,05
5	-0,03	-0,02	0,03	0,05
6	0,02	0,00	0,08	0,08
7	-0,04	-0,06	0,06	0,07
8	0,00	0,02	0,07	0,09
9	0,01	0,00	0,10	0,07

Table 4.2.19\_Errors for stance time.

Subjects	Stance duration (%GC)			
	Errors algorithm trunk		Errors algorithm heels	
	Right	Left	Right	Left
1	-3,16	-2,92	4,15	4,76
2	1,71	0,97	4,57	4,45
3	0,07	-0,89	5,21	4,21
4	-0,95	-1,39	4,15	3,85
5	-1,60	-1,38	1,94	3,22
6	1,27	0,53	6,68	6,47
7	-4,25	-5,22	5,32	5,50
8	-0,10	1,73	5,61	7,03
9	0,67	0,52	8,18	5,37

Table 4.2.20\_Errors for stance duration.

Subjects	Swing time (s)			
	Errors algorithm trunk		Errors algorithm heels	
	Right	Left	Right	Left
1	0,03	0,03	-0,04	-0,05
2	-0,01	0,00	-0,04	-0,04
3	0,00	0,01	-0,06	-0,05
4	0,01	0,02	-0,05	-0,04
5	0,02	0,02	-0,02	-0,04
6	-0,02	-0,01	-0,08	-0,07
7	0,06	0,06	-0,07	-0,07
8	0,00	-0,02	-0,07	-0,08
9	-0,01	-0,01	-0,10	-0,06

Table 4.2.21\_Errors for swing time.

Subjects	Swing duration (%GC)			
	Errors algorithm trunk		Errors algorithm heels	
	Right	Left	Right	Left
1	2,94	2,44	-4,20	-4,95
2	-1,01	-0,22	-4,23	-3,85
3	0,30	0,92	-5,06	-4,29
4	1,05	1,65	-4,03	-3,45
5	1,36	1,41	-2,15	-3,39
6	-1,11	-0,48	-6,69	-6,39
7	4,55	4,88	-5,43	-5,48
8	0,26	-1,61	-5,41	-6,87
9	-0,36	-0,42	-7,81	-5,21

Table 4.2.22\_Errors for swing duration.

Subjects	Single support time (s)			
	Errors algorithm trunk		Errors algorithm heels	
	Right	Left	Right	Left
1	0,03	0,03	-0,05	-0,04
2	-0,01	-0,01	-0,04	-0,05
3	0,00	0,00	-0,05	-0,05
4	0,01	0,01	-0,04	-0,05
5	0,02	0,02	-0,03	-0,03
6	-0,01	-0,02	-0,07	-0,08
7	0,06	0,06	-0,07	-0,07
8	-0,02	0,00	-0,08	-0,07
9	-0,01	-0,01	-0,08	-0,09

Table 4.2.23\_Errors for single support time.

Subjects	Single support duration (%GC)			
	Errors algorithm trunk		Errors algorithm heels	
	Right	Left	Right	Left
1	2,78	3,08	-4,87	-4,07
2	-0,51	-0,99	-3,88	-4,81
3	0,65	0,33	-4,45	-4,91
4	1,45	1,12	-3,82	-4,03
5	1,50	1,41	-3,06	-2,41
6	-0,66	-1,09	-6,20	-6,46
7	4,91	4,56	-5,36	-5,42
8	-1,28	0,12	-6,84	-5,63
9	-0,53	-0,31	-6,06	-7,24

Table 4.2.24\_Errors for single support duration.

Subjects	Double support time (s)			
	Errors algorithm trunk		Errors algorithm heels	
	Right	Left	Right	Left
1	-0,06	-0,06	0,10	0,10
2	0,01	0,01	0,08	0,08
3	-0,01	-0,01	0,10	0,10
4	-0,03	-0,04	0,09	0,09
5	-0,04	-0,04	0,07	0,07
6	0,02	0,02	0,16	0,16
7	-0,11	-0,11	0,13	0,13
8	0,02	0,02	0,15	0,15
9	0,01	0,01	0,16	0,16

Table 4.2.25\_Errors for double support time.

Subjects	Double support duration (%GC)			
	Errors algorithm trunk		Errors algorithm heels	
	Right	Left	Right	Left
1	-5,37	-5,37	9,15	9,15
2	1,23	1,23	7,80	7,80
3	-1,22	-1,22	9,35	9,35
4	-2,65	-2,88	7,48	7,48
5	-2,77	-2,77	5,53	5,53
6	1,60	1,60	13,08	13,08
7	-9,42	-9,42	10,91	10,91
8	1,35	1,35	12,28	12,28
9	0,77	0,77	13,02	13,02

Table 4.2.26\_Errors for double support duration.

Subjects	Foot symmetry (%GC)			
	Errors algorithm trunk		Errors algorithm heels	
	Right	Left	Right	Left
1	0,86	-0,71	0,68	-0,71
2	-0,71	-1,06	0,33	-1,31
3	0,25	-0,05	-0,59	0,71
4	0,19	-0,66	0,64	-0,54
5	-0,51	0,93	0,91	-0,92
6	-1,75	1,59	-0,86	0,61
7	-0,09	0,83	0,14	-0,32
8	-0,60	0,14	-0,42	-0,14
9	0,70	-0,87	0,01	-0,50

Table 4.2.27\_Errors for foot symmetry.

Subjects	Limp index			
	Errors algorithm trunk		Errors algorithm heels	
	Right	Left	Right	Left
1	0,00	0,00	-0,01	-0,01
2	0,02	0,02	0,01	0,01
3	0,01	0,01	0,03	0,03
4	0,01	0,00	0,00	0,00
5	-0,01	-0,01	-0,03	-0,03
6	0,01	0,01	0,00	0,00
7	0,02	0,02	-0,01	-0,01
8	-0,04	-0,04	-0,04	-0,04
9	0,01	0,01	0,04	0,04

Table 4.2.28\_Errors for limp index.

The following Table 4.2.29 presents the mean and the standard deviation values estimated among all the subjects from the errors reported in the previous fourteen tables (from Table 4.2.15 to Table 4.2.28).

Spatio-temporal parameters	Errors algorithm from trunk				Errors algorithm from heels			
	Right		Left		Right		Left	
	Mean	SD	Mean	SD	Mean	SD	Mean	SD
<b>Stride time (s)</b>	0,00	0,01	0,00	0,00	0,00	0,01	0,00	0,01
<b>Stride frequency (Hz)</b>	0,00	0,01	0,00	0,00	0,00	0,00	0,00	0,00
<b>Step time (s)</b>	0,00	0,01	0,00	0,01	0,00	0,01	0,00	0,01
<b>Step frequency (Hz)</b>	0,00	0,03	0,00	0,03	-0,01	0,03	0,01	0,02
<b>Stance time (s)</b>	-0,01	0,02	-0,01	0,02	0,06	0,02	0,06	0,02
<b>Stance duration (%)</b>	-0,70	2,00	-0,90	2,17	5,09	1,75	4,98	1,23
<b>Swing time (s)</b>	0,01	0,02	0,01	0,02	-0,06	0,02	-0,06	0,02
<b>Swing duration (%)</b>	0,89	1,86	0,95	1,94	-5,00	1,64	-4,87	1,24
<b>Single support time (s)</b>	0,01	0,02	0,01	0,02	-0,06	0,02	-0,06	0,02
<b>SS duration (%)</b>	0,92	1,99	0,91	1,88	-4,95	1,26	-5,00	1,43
<b>Double support time (s)</b>	-0,02	0,04	-0,02	0,04	0,12	0,04	0,12	0,04
<b>DS duration (%)</b>	-1,83	3,71	-1,86	3,72	9,85	2,66	9,85	2,66
<b>Foot symmetry (%)</b>	-0,18	0,81	0,02	0,93	0,09	0,61	-0,35	0,66
<b>Limp index (right/left)</b>	0,00	0,02	0,00	0,02	0,00	0,03	0,00	0,03

Table 4.2.29\_Mean and standard deviation values for errors of all the parameters among all the subjects.

In the following pages, the fourteen figures (from Figure 4.2.1 to Figure 4.2.14) show the Bland-Altman graphs for all the spatio-temporal parameters.

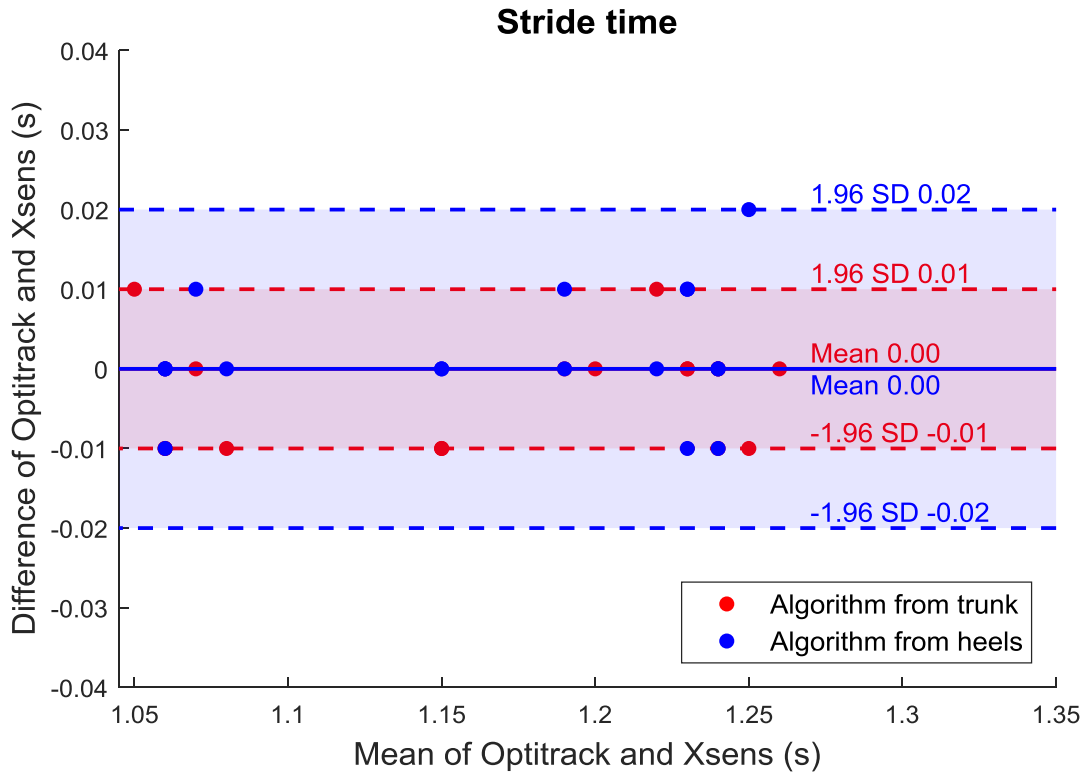


Figure 4.2.1\_Bland-Altman graph for stride time.

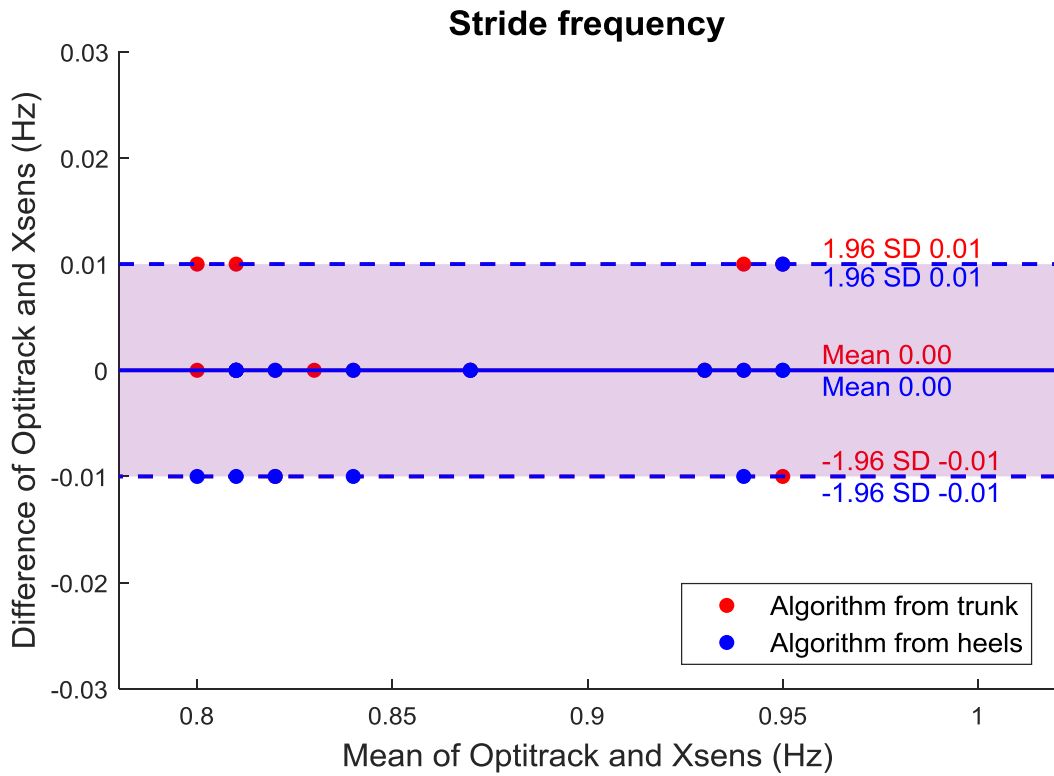


Figure 4.2.2\_Bland-Altman graph for stride frequency.

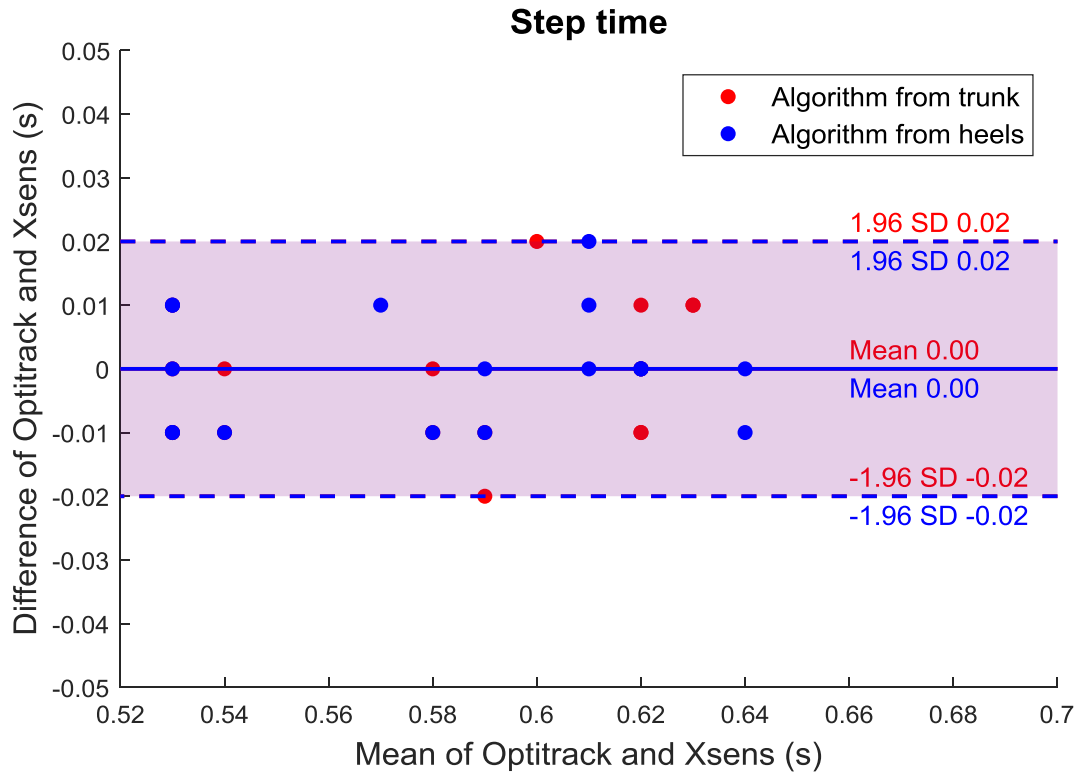


Figure 4.2.3\_Bland-Altman graph for step time.

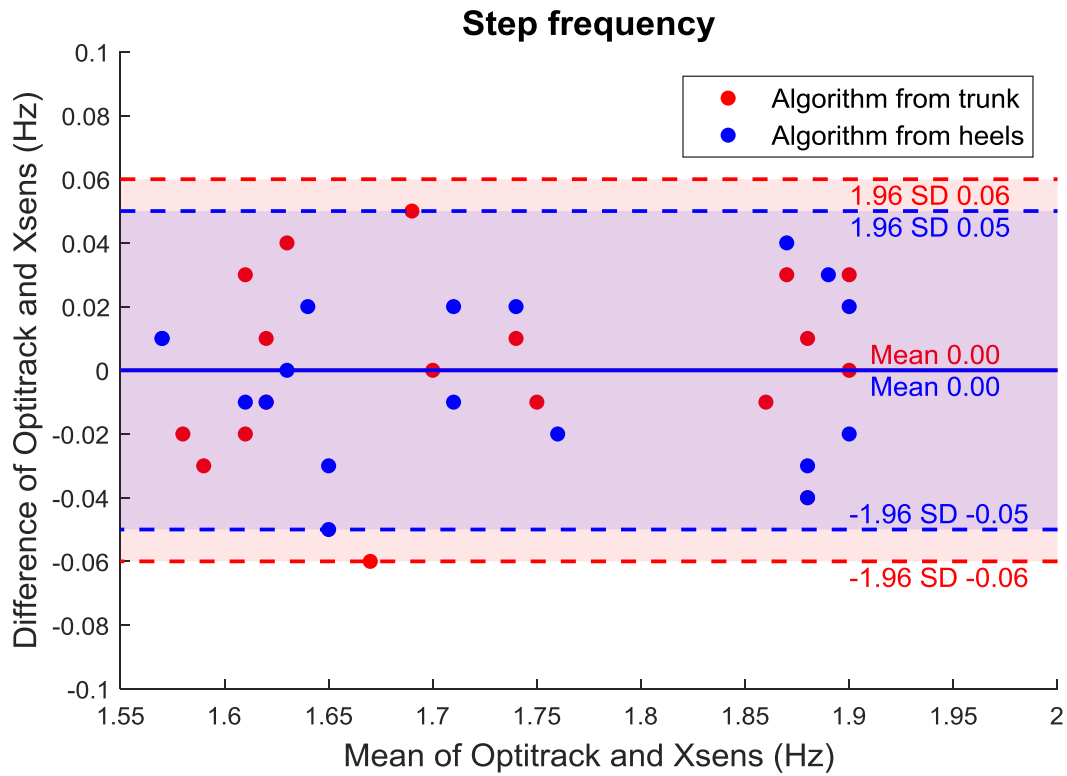


Figure 4.2.4\_Bland-Altman graph for step frequency.

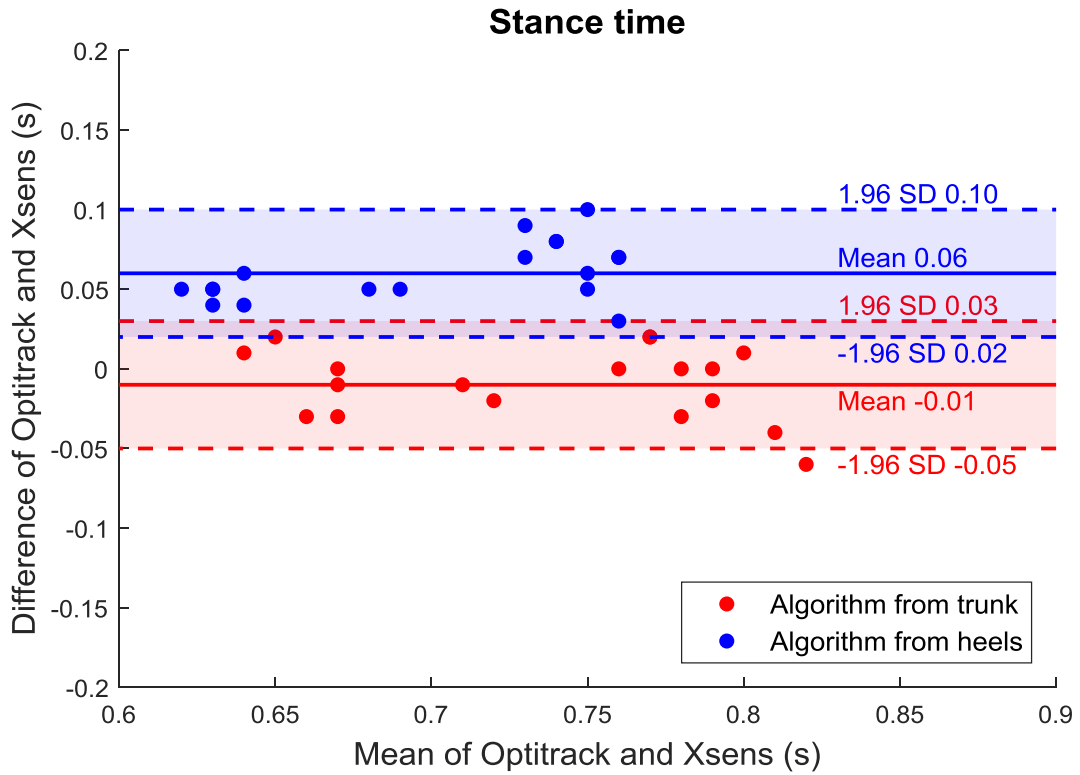


Figure 4.2.5\_Bland-Altman graph for stance time.

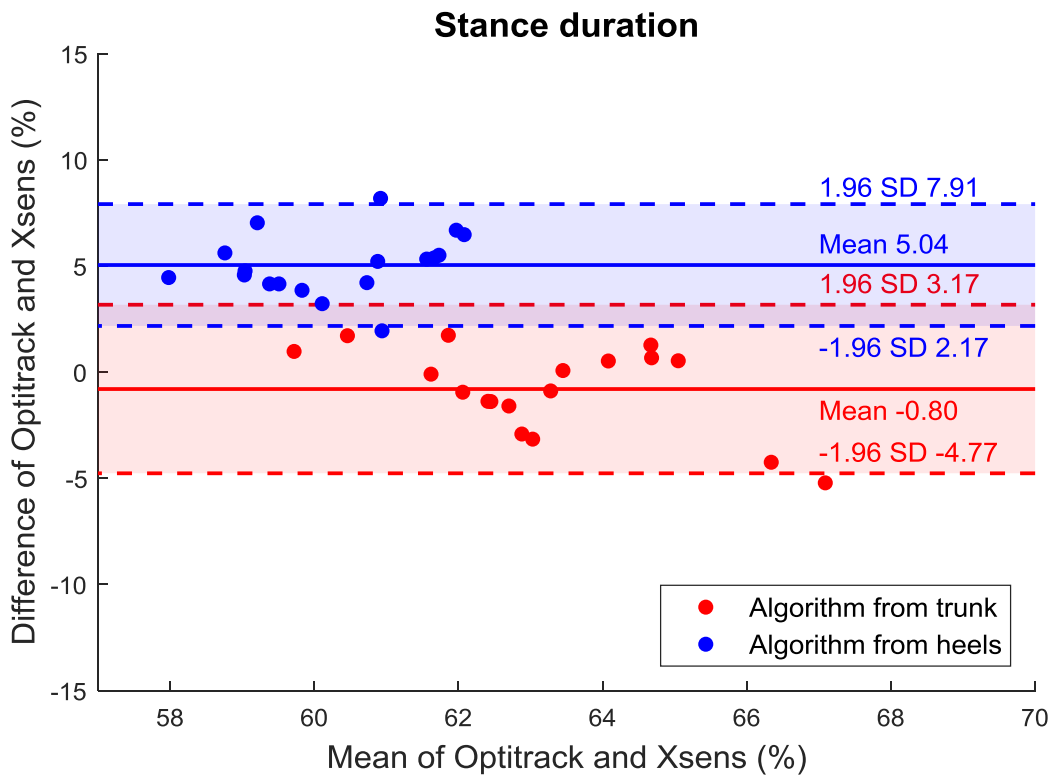


Figure 4.2.6\_Bland-Altman graph for stance duration.

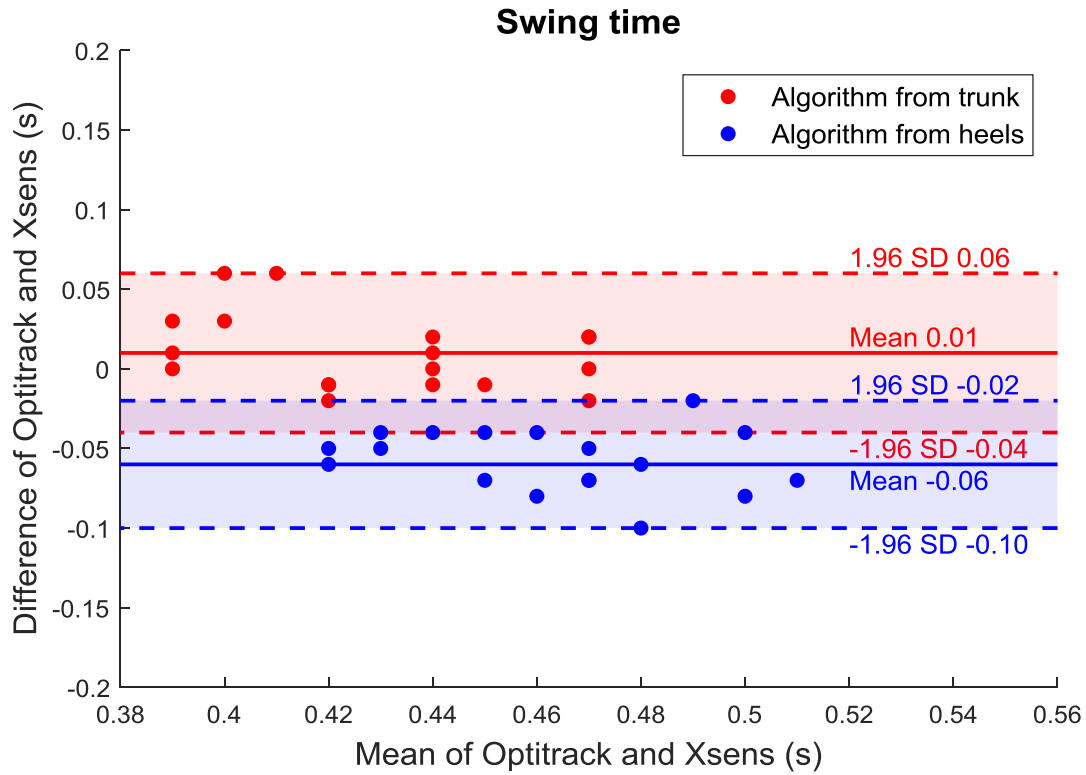


Figure 4.2.7\_Bland-Altman graph for swing time.

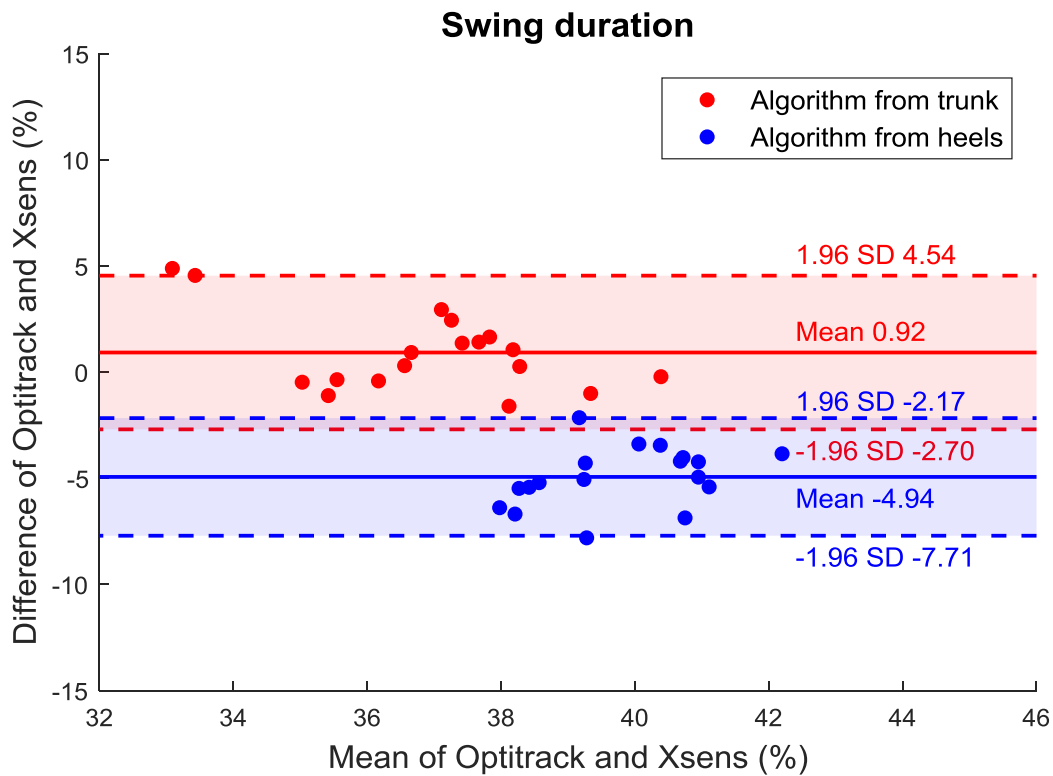


Figure 4.2.8\_Bland-Altman graph for swing duration.

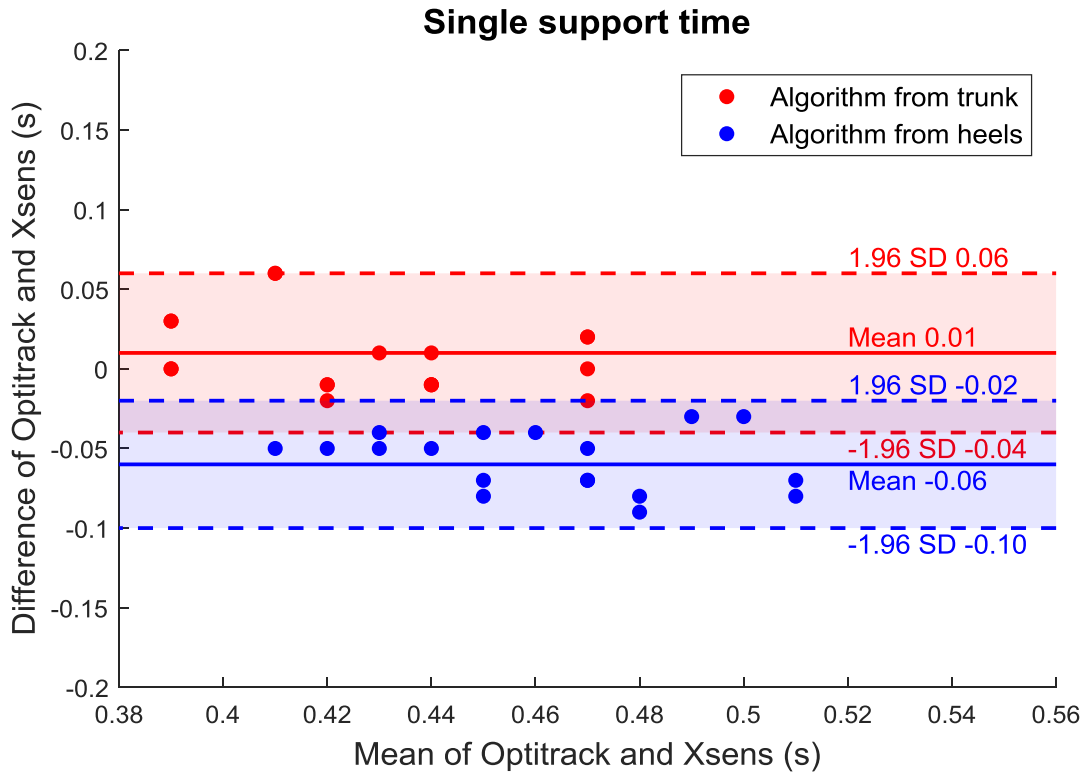


Figure 4.2.9\_Bland-Altman graph for single support time.

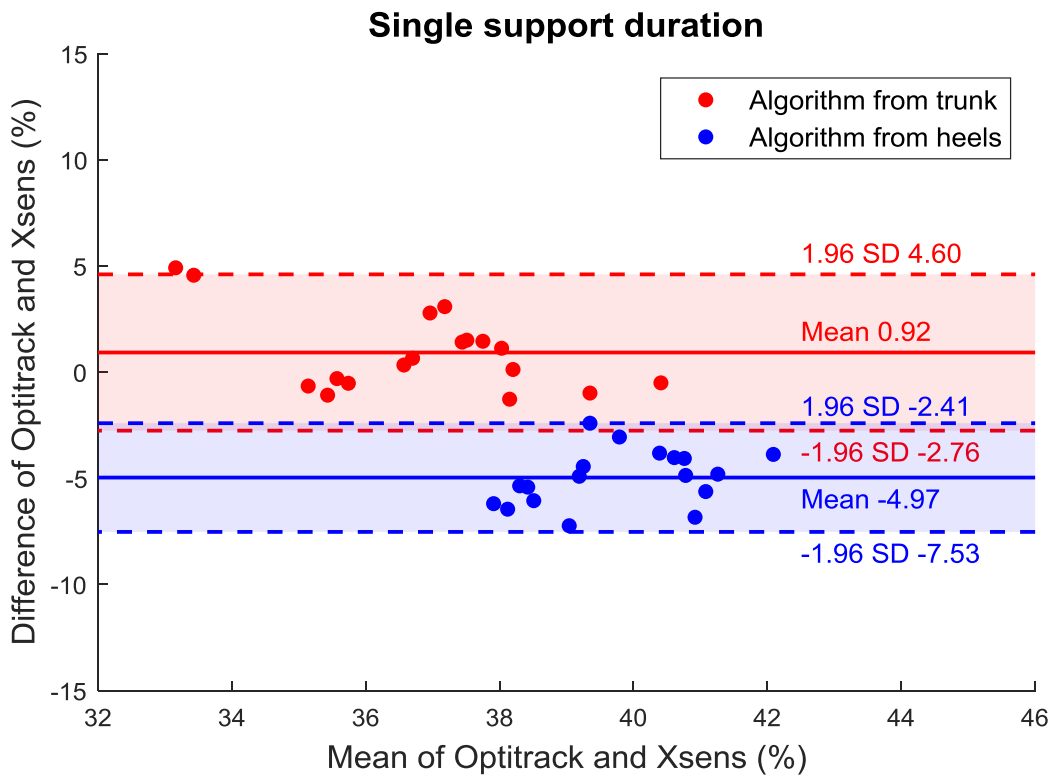


Figure 4.2.10\_Bland-Altman graph for single support duration.

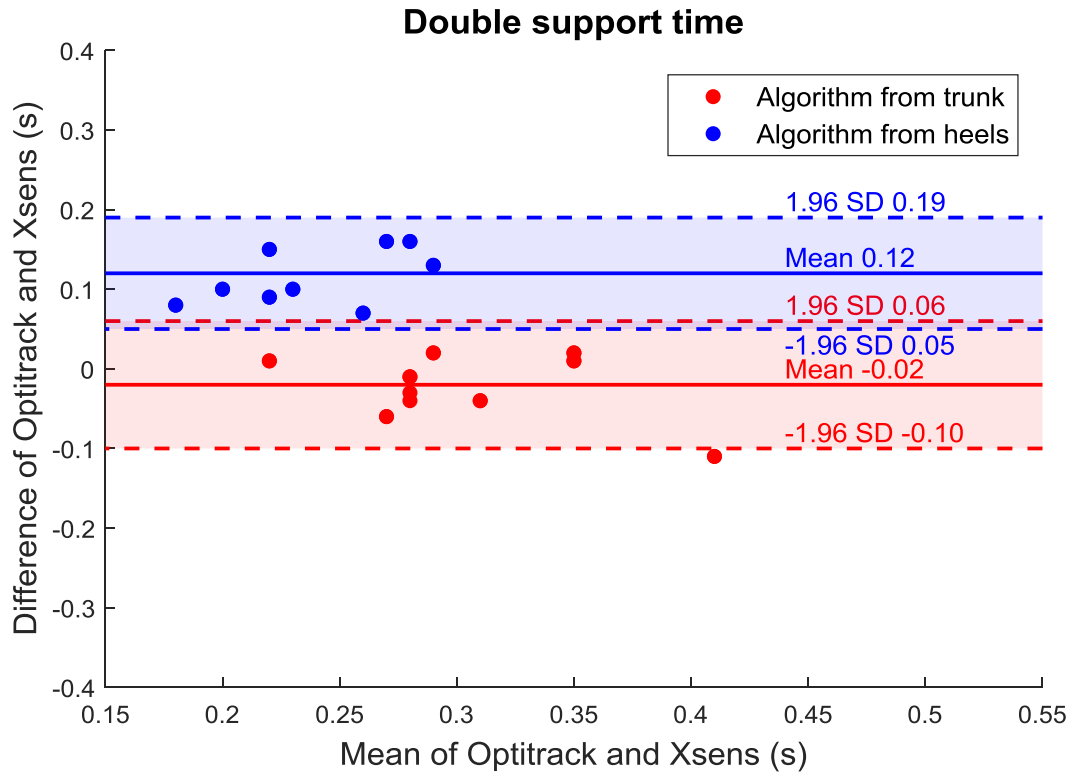


Figure 4.2.11\_Bland-Altman graph for double support time.

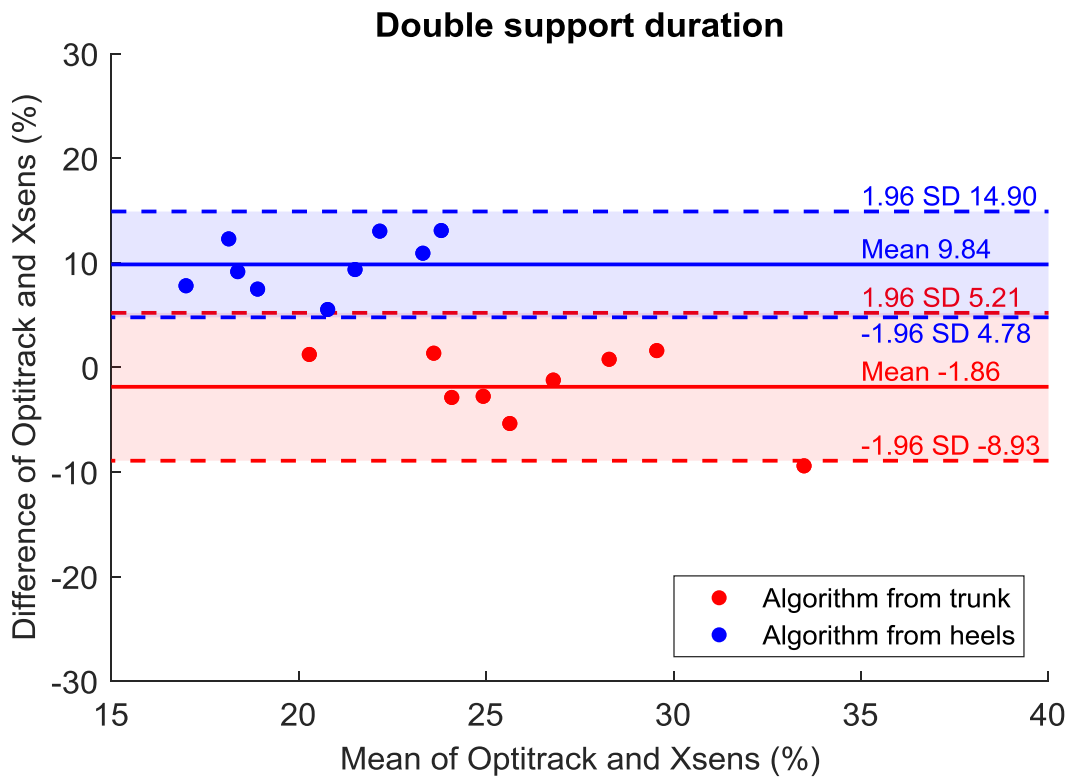


Figure 4.2.12\_Bland-Altman graph for double support duration.

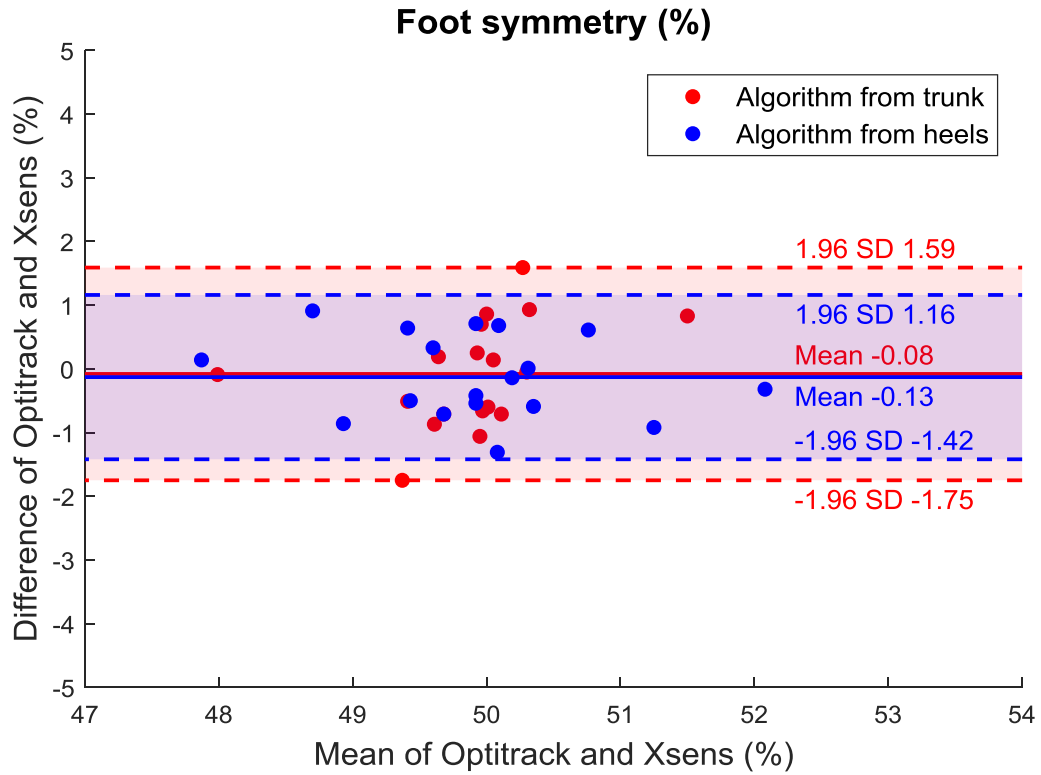


Figure 4.2.13\_Bland-Altman graph for foot symmetry.

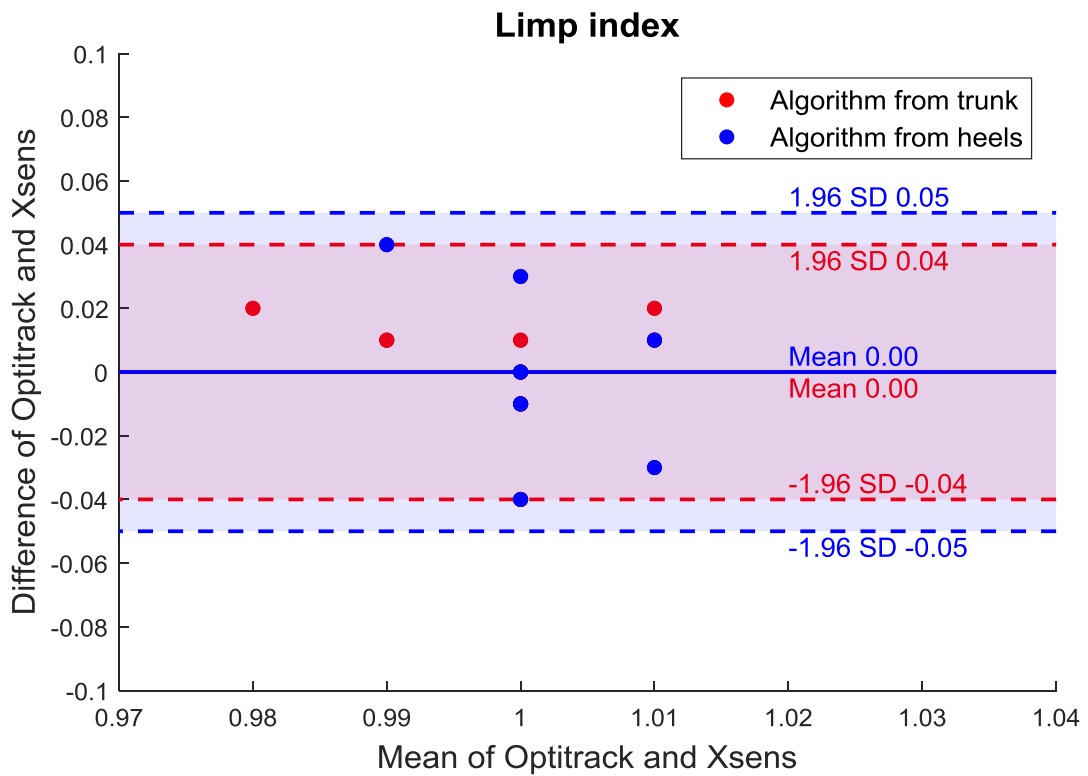


Figure 4.2.14\_Bland-Altman graph for limp index.

#### 4.1.2 Normal speed with dual-task

The following fourteen tables (from Table 4.2.30 to Table 4.2.43) present the spatio-temporal parameters obtained for every subject with the three methods adopted: Optitrack, Xsens algorithm with trunk acceleration and Xsens algorithm with heels angular velocity.

Subjects	Stride time (s)											
	Optitrack				Algorithm from trunk				Algorithm from heels			
	Right		Left		Right		Left		Right		Left	
	Mean	SD	Mean	SD	Mean	SD	Mean	SD	Mean	SD	Mean	SD
1	1,05	0,02	1,05	0,05	1,04	0,03	1,05	0,02	1,04	0,02	1,04	0,03
2	1,10	0,03	1,10	0,02	1,10	0,04	1,10	0,05	1,12	0,04	1,09	0,05
3	1,14	0,04	1,14	0,05	1,15	0,05	1,14	0,05	1,15	0,06	1,14	0,05
4	1,19	0,04	1,18	0,03	1,18	0,06	1,19	0,04	1,18	0,03	1,18	0,04
5	1,52	0,08	1,52	0,06	1,52	0,09	1,51	0,10	1,52	0,08	1,53	0,08
6	1,26	0,09	1,26	0,08	1,24	0,09	1,28	0,11	1,25	0,07	1,26	0,10
7	1,23	0,05	1,23	0,04	1,22	0,05	1,22	0,05	1,22	0,05	1,22	0,04
8	1,35	0,05	1,35	0,05	1,36	0,04	1,36	0,04	1,35	0,05	1,35	0,06
9	1,20	0,03	1,20	0,03	1,21	0,06	1,20	0,04	1,21	0,04	1,20	0,04

Table 4.2.30\_Mean and standard deviation values for stride time.

Subjects	Stride frequency (Hz)											
	Optitrack				Algorithm from trunk				Algorithm from heels			
	Right		Left		Right		Left		Right		Left	
	Mean	SD	Mean	SD	Mean	SD	Mean	SD	Mean	SD	Mean	SD
1	0,96	0,02	0,96	0,05	0,96	0,03	0,95	0,02	0,97	0,02	0,97	0,03
2	0,91	0,03	0,91	0,02	0,91	0,03	0,91	0,04	0,89	0,03	0,92	0,05
3	0,88	0,03	0,88	0,04	0,87	0,04	0,88	0,04	0,87	0,04	0,88	0,04
4	0,84	0,03	0,85	0,02	0,85	0,04	0,85	0,03	0,85	0,02	0,85	0,03
5	0,66	0,03	0,66	0,03	0,66	0,04	0,67	0,06	0,66	0,03	0,66	0,03
6	0,80	0,06	0,80	0,05	0,81	0,06	0,79	0,05	0,80	0,04	0,80	0,06
7	0,82	0,03	0,81	0,03	0,82	0,03	0,82	0,04	0,82	0,03	0,82	0,03
8	0,74	0,03	0,74	0,03	0,74	0,02	0,74	0,02	0,74	0,03	0,74	0,03
9	0,83	0,02	0,83	0,02	0,83	0,04	0,83	0,03	0,83	0,02	0,83	0,03

Table 4.2.31\_Mean and standard deviation values for stride frequency.

Subjects	Step time (s)											
	Optitrack				Algorithm from trunk				Algorithm from heels			
	Right		Left		Right		Left		Right		Left	
	Mean	SD	Mean	SD	Mean	SD	Mean	SD	Mean	SD	Mean	SD
1	0,53	0,03	0,52	0,03	0,51	0,02	0,54	0,02	0,53	0,02	0,51	0,01
2	0,55	0,02	0,56	0,01	0,55	0,03	0,55	0,03	0,55	0,02	0,55	0,04
3	0,56	0,02	0,57	0,03	0,57	0,03	0,57	0,03	0,59	0,03	0,56	0,04
4	0,59	0,02	0,59	0,03	0,61	0,06	0,57	0,07	0,59	0,03	0,59	0,02
5	0,73	0,05	0,78	0,03	0,76	0,05	0,75	0,07	0,71	0,06	0,81	0,04
6	0,63	0,05	0,63	0,04	0,64	0,06	0,63	0,06	0,62	0,05	0,64	0,04
7	0,61	0,03	0,62	0,03	0,60	0,03	0,62	0,03	0,58	0,03	0,64	0,02
8	0,67	0,03	0,68	0,03	0,68	0,02	0,68	0,03	0,67	0,03	0,68	0,03
9	0,61	0,02	0,59	0,03	0,60	0,04	0,60	0,03	0,60	0,02	0,60	0,02

Table 4.2.32\_Mean and standard deviation values for step time.

Subjects	Step frequency (Hz)											
	Optitrack				Algorithm from trunk				Algorithm from heels			
	Right		Left		Right		Left		Right		Left	
	Mean	SD	Mean	SD	Mean	SD	Mean	SD	Mean	SD	Mean	SD
1	1,91	0,12	1,93	0,10	1,97	0,08	1,86	0,06	1,91	0,07	1,95	0,05
2	1,84	0,08	1,80	0,04	1,82	0,07	1,82	0,08	1,81	0,08	1,89	0,29
3	1,78	0,07	1,75	0,08	1,75	0,10	1,76	0,09	1,70	0,08	1,80	0,11
4	1,69	0,06	1,70	0,08	1,66	0,20	1,79	0,24	1,71	0,09	1,69	0,07
5	1,37	0,10	1,28	0,06	1,32	0,08	1,42	0,50	1,41	0,11	1,24	0,07
6	1,60	0,12	1,61	0,12	1,59	0,12	1,60	0,17	1,63	0,12	1,58	0,10
7	1,65	0,07	1,61	0,08	1,66	0,08	1,63	0,09	1,73	0,07	1,56	0,06
8	1,50	0,07	1,47	0,07	1,48	0,05	1,47	0,05	1,49	0,06	1,47	0,07
9	1,65	0,04	1,69	0,08	1,67	0,11	1,67	0,09	1,66	0,07	1,66	0,07

Table 4.2.33\_Mean and standard deviation values for step frequency.

Subjects	Stance time (s)											
	Optitrack				Algorithm from trunk				Algorithm from heels			
	Right		Left		Right		Left		Right		Left	
	Mean	SD	Mean	SD	Mean	SD	Mean	SD	Mean	SD	Mean	SD
1	0,64	0,04	0,64	0,03	0,65	0,04	0,68	0,03	0,59	0,01	0,59	0,03
2	0,70	0,02	0,67	0,03	0,69	0,05	0,68	0,04	0,62	0,02	0,62	0,03
3	0,74	0,03	0,72	0,03	0,74	0,04	0,74	0,04	0,67	0,04	0,69	0,03
4	0,73	0,03	0,73	0,03	0,74	0,09	0,74	0,05	0,68	0,03	0,68	0,03
5	0,99	0,05	0,96	0,06	0,97	0,07	0,98	0,05	0,94	0,05	0,89	0,08
6	0,84	0,08	0,84	0,07	0,79	0,07	0,83	0,08	0,77	0,05	0,76	0,07
7	0,77	0,04	0,81	0,04	0,84	0,04	0,83	0,04	0,73	0,04	0,74	0,04
8	0,84	0,04	0,85	0,04	0,85	0,03	0,85	0,04	0,77	0,04	0,72	0,04
9	0,79	0,03	0,78	0,03	0,77	0,03	0,77	0,03	0,69	0,03	0,72	0,04

Table 4.2.34\_Mean and standard deviation values for stance time.

Subjects	Stance duration (%GC)											
	Optitrack				Algorithm from trunk				Algorithm from heels			
	Right		Left		Right		Left		Right		Left	
	Mean	SD	Mean	SD	Mean	SD	Mean	SD	Mean	SD	Mean	SD
1	60,82	3,98	60,74	3,04	62,39	2,69	64,40	2,22	56,88	0,92	57,33	1,28
2	63,12	1,19	60,68	2,62	62,72	3,34	61,97	2,76	55,84	1,67	57,02	4,33
3	64,67	1,26	63,61	1,48	63,93	1,88	64,71	1,84	58,36	2,22	60,29	1,59
4	61,01	1,32	61,92	1,72	62,36	5,43	62,56	4,14	57,46	2,04	57,99	1,29
5	65,14	2,15	63,38	2,51	64,21	1,95	65,07	5,42	62,11	2,05	57,89	3,23
6	66,68	3,26	66,74	2,14	63,70	1,93	64,48	2,10	61,46	2,09	60,69	2,37
7	62,98	1,53	65,46	1,04	69,14	2,46	68,11	1,76	59,71	2,24	60,99	1,19
8	62,49	1,38	62,95	1,37	62,71	1,43	62,32	1,61	56,62	1,34	52,84	1,48
9	65,39	1,44	64,97	1,24	63,73	1,94	64,28	2,20	57,06	1,59	60,19	1,46

Table 4.2.35\_Mean and standard deviation values for stance duration.

Subjects	Swing time (s)											
	Optitrack				Algorithm from trunk				Algorithm from heels			
	Right		Left		Right		Left		Right		Left	
	Mean	SD	Mean	SD	Mean	SD	Mean	SD	Mean	SD	Mean	SD
1	0,40	0,04	0,41	0,04	0,39	0,02	0,37	0,02	0,45	0,01	0,44	0,01
2	0,41	0,02	0,43	0,02	0,41	0,03	0,42	0,04	0,49	0,02	0,48	0,04
3	0,40	0,02	0,41	0,02	0,41	0,03	0,40	0,03	0,47	0,03	0,45	0,03
4	0,46	0,02	0,45	0,02	0,45	0,06	0,44	0,06	0,50	0,03	0,50	0,02
5	0,53	0,04	0,56	0,03	0,54	0,03	0,54	0,07	0,58	0,04	0,64	0,04
6	0,42	0,04	0,42	0,03	0,46	0,06	0,45	0,04	0,48	0,04	0,50	0,03
7	0,45	0,02	0,42	0,02	0,38	0,03	0,39	0,03	0,49	0,03	0,48	0,02
8	0,51	0,02	0,50	0,03	0,50	0,02	0,51	0,03	0,59	0,02	0,64	0,03
9	0,42	0,01	0,42	0,01	0,44	0,03	0,43	0,03	0,52	0,02	0,48	0,01

Table 4.2.36\_Mean and standard deviation values for swing time.

Subjects	Swing duration (%GC)											
	Optitrack				Algorithm from trunk				Algorithm from heels			
	Right		Left		Right		Left		Right		Left	
	Mean	SD	Mean	SD	Mean	SD	Mean	SD	Mean	SD	Mean	SD
1	38,45	3,75	39,08	2,92	37,29	2,34	35,74	2,35	43,13	0,98	42,62	1,37
2	36,90	1,05	39,21	2,16	36,73	2,85	37,71	2,87	44,56	2,51	43,00	3,19
3	35,42	1,41	36,26	1,21	35,68	1,64	35,11	1,85	41,16	1,78	39,53	1,63
4	38,98	1,15	38,22	1,47	37,99	5,06	36,88	4,67	42,79	1,64	42,35	1,41
5	34,74	1,69	36,67	2,38	35,97	2,61	35,13	4,19	38,06	1,85	42,29	3,03
6	33,05	2,74	33,39	2,18	35,75	2,44	35,24	2,21	38,41	2,00	39,42	1,81
7	37,04	1,69	34,49	0,98	30,83	1,94	32,06	1,72	40,18	2,05	39,16	0,90
8	37,60	0,96	37,29	1,37	37,08	1,24	37,58	1,66	43,51	1,11	47,22	1,39
9	34,69	1,41	35,30	1,15	36,37	1,61	35,98	2,48	43,06	1,65	39,86	1,60

Table 4.2.37\_Mean and standard deviation values for swing duration.

Subjects	Single support time (s)											
	Optitrack				Algorithm from trunk				Algorithm from heels			
	Right		Left		Right		Left		Right		Left	
	Mean	SD	Mean	SD	Mean	SD	Mean	SD	Mean	SD	Mean	SD
1	0,41	0,04	0,41	0,03	0,38	0,02	0,39	0,02	0,44	0,01	0,45	0,01
2	0,43	0,02	0,41	0,01	0,42	0,02	0,41	0,03	0,48	0,03	0,49	0,02
3	0,41	0,02	0,41	0,02	0,41	0,02	0,41	0,03	0,46	0,02	0,47	0,03
4	0,46	0,02	0,46	0,02	0,45	0,04	0,45	0,06	0,50	0,02	0,50	0,02
5	0,55	0,03	0,53	0,04	0,54	0,06	0,54	0,03	0,63	0,04	0,59	0,04
6	0,42	0,03	0,42	0,04	0,46	0,07	0,47	0,08	0,50	0,03	0,49	0,03
7	0,43	0,02	0,45	0,02	0,39	0,03	0,38	0,03	0,48	0,02	0,49	0,02
8	0,50	0,02	0,51	0,02	0,51	0,02	0,50	0,02	0,63	0,03	0,59	0,02
9	0,42	0,01	0,42	0,01	0,43	0,03	0,44	0,03	0,48	0,02	0,51	0,02

Table 4.2.38\_Mean and standard deviation values for single support time.

Subjects	Single support duration (%GC)											
	Optitrack				Algorithm from trunk				Algorithm from heels			
	Right		Left		Right		Left		Right		Left	
	Mean	SD	Mean	SD	Mean	SD	Mean	SD	Mean	SD	Mean	SD
1	39,09	2,91	39,22	2,88	36,22	1,74	37,27	2,35	42,85	1,04	43,09	0,89
2	38,86	1,83	37,58	0,85	37,97	1,87	37,07	2,75	43,37	2,75	44,84	2,26
3	36,11	1,21	35,65	1,12	35,55	1,14	35,68	1,64	40,34	1,48	41,02	1,75
4	38,44	1,34	38,70	0,93	37,51	3,20	37,99	5,06	42,34	1,37	42,45	1,29
5	36,16	1,73	34,82	1,77	35,22	3,48	35,97	2,61	41,63	2,82	38,90	1,54
6	33,27	1,85	33,11	2,71	36,10	2,06	36,21	2,82	39,46	1,80	38,69	1,08
7	34,94	0,90	36,64	1,13	31,60	1,38	30,90	1,87	39,13	1,03	39,91	1,81
8	37,19	0,93	37,61	0,96	37,49	1,12	37,08	1,24	46,22	1,27	43,84	1,17
9	35,16	1,00	34,76	1,13	35,91	1,47	36,37	1,61	40,16	1,65	42,10	1,61

Table 4.2.39\_Mean and standard deviation values for single support duration.

Subjects	Double support time (s)											
	Optitrack				Algorithm from trunk				Algorithm from heels			
	Right		Left		Right		Left		Right		Left	
	Mean	SD	Mean	SD	Mean	SD	Mean	SD	Mean	SD	Mean	SD
1	0,24	0,05	0,24	0,05	0,28	0,04	0,28	0,04	0,15	0,02	0,15	0,02
2	0,27	0,02	0,26	0,03	0,28	0,03	0,28	0,03	0,14	0,02	0,14	0,02
3	0,32	0,02	0,32	0,02	0,33	0,03	0,33	0,03	0,22	0,02	0,22	0,02
4	0,27	0,02	0,27	0,02	0,30	0,08	0,30	0,08	0,18	0,02	0,18	0,02
5	0,43	0,04	0,43	0,04	0,44	0,05	0,44	0,05	0,30	0,05	0,30	0,05
6	0,42	0,06	0,42	0,06	0,36	0,04	0,36	0,04	0,28	0,03	0,28	0,03
7	0,35	0,03	0,35	0,03	0,45	0,02	0,45	0,02	0,25	0,03	0,25	0,03
8	0,34	0,03	0,34	0,03	0,34	0,03	0,34	0,03	0,13	0,02	0,13	0,02
9	0,36	0,03	0,36	0,03	0,33	0,03	0,33	0,03	0,21	0,04	0,21	0,04

Table 4.2.40\_Mean and standard deviation values for double support time.

Subjects	Double support duration (%GC)											
	Optitrack				Algorithm from trunk				Algorithm from heels			
	Right		Left		Right		Left		Right		Left	
	Mean	SD	Mean	SD	Mean	SD	Mean	SD	Mean	SD	Mean	SD
1	22,46	4,65	22,46	4,65	26,97	3,44	26,97	3,44	14,25	2,06	14,25	2,06
2	24,27	1,87	24,04	2,05	25,22	2,85	25,22	2,85	12,44	1,99	12,44	1,99
3	28,32	1,95	28,32	1,95	29,22	1,83	29,22	1,83	19,31	1,87	19,31	1,87
4	22,80	1,09	22,80	1,09	25,13	6,33	25,13	6,33	14,86	1,30	14,86	1,30
5	28,59	2,07	28,59	2,07	28,90	2,78	28,90	2,78	19,65	3,05	19,65	3,05
6	33,56	3,82	33,56	3,82	28,50	3,04	28,50	3,04	22,17	1,65	22,17	1,65
7	28,47	1,34	28,47	1,34	37,11	2,21	37,11	2,21	20,66	2,30	20,66	2,30
8	25,11	1,58	25,11	1,58	25,34	1,82	25,34	1,82	9,26	1,48	9,26	1,48
9	30,00	2,02	30,00	2,02	27,65	2,10	27,65	2,10	17,08	2,74	17,08	2,74

Table 4.2.41\_Mean and standard deviation values for double support duration.

Subjects	Foot symmetry (%GC)											
	Optitrack				Algorithm from trunk				Algorithm from heels			
	Right		Left		Right		Left		Right		Left	
	Mean	SD	Mean	SD	Mean	SD	Mean	SD	Mean	SD	Mean	SD
1	50,06	2,59	49,23	2,31	48,25	1,47	51,19	1,54	50,56	1,74	49,48	1,26
2	49,55	1,24	50,59	0,81	50,65	2,12	50,39	1,81	50,17	1,94	49,22	3,77
3	49,92	0,84	50,57	1,12	50,51	1,90	50,06	1,78	51,69	1,80	48,98	2,36
4	50,16	2,01	49,82	1,83	52,93	6,76	48,85	4,65	49,52	2,39	50,34	1,82
5	48,54	2,29	51,72	1,99	50,43	2,16	49,24	4,51	46,79	2,54	52,94	2,51
6	49,89	2,40	50,01	1,91	50,56	3,90	50,07	2,85	49,24	1,93	50,81	2,45
7	49,30	1,49	50,39	1,84	49,25	1,59	50,42	1,34	47,49	1,14	52,67	1,00
8	49,27	2,02	50,30	1,26	49,97	1,10	50,31	1,03	49,46	1,89	50,20	1,20
9	50,53	1,50	49,40	1,34	49,63	2,93	49,74	2,23	49,91	1,54	49,99	1,78

Table 4.2.42\_Mean and standard deviation values for foot symmetry.

Subjects	Limp index											
	Optitrack				Algorithm from trunk				Algorithm from heels			
	Right		Left		Right		Left		Right		Left	
	Mean	SD	Mean	SD	Mean	SD	Mean	SD	Mean	SD	Mean	SD
1	1,00	0,07	1,00	0,07	0,96	0,06	0,96	0,06	0,99	0,05	0,99	0,05
2	1,04	0,03	1,05	0,05	1,02	0,11	1,02	0,11	1,01	0,05	1,01	0,05
3	1,02	0,04	1,02	0,04	1,00	0,06	1,00	0,06	0,97	0,06	0,97	0,06
4	1,00	0,05	1,00	0,05	1,00	0,15	1,00	0,15	1,00	0,07	1,00	0,07
5	1,03	0,06	1,03	0,06	1,00	0,05	1,00	0,05	1,07	0,07	1,07	0,07
6	1,00	0,07	1,00	0,07	0,96	0,06	0,96	0,06	1,01	0,07	1,01	0,07
7	0,96	0,04	0,96	0,04	1,02	0,05	1,02	0,05	0,98	0,04	0,98	0,04
8	0,99	0,03	0,99	0,03	1,01	0,05	1,01	0,05	1,07	0,05	1,07	0,05
9	1,01	0,04	1,01	0,04	1,00	0,05	1,00	0,05	0,96	0,04	0,96	0,04

Table 4.2.43\_Mean and standard deviation values for limp index.

The following fourteen tables (from Table 4.2.44 to Table 4.2.57) show the differences calculated between the mean values obtained from Optitrack and those obtained from the two Xsens algorithms.

Subjects	Stride time (s)			
	Errors algorithm trunk		Errors algorithm heels	
	Right	Left	Right	Left
1	0,01	0,00	0,01	0,01
2	0,00	0,00	-0,02	0,01
3	-0,01	0,00	-0,01	-0,01
4	0,01	-0,01	0,01	0,00
5	0,00	0,01	0,00	-0,01
6	0,02	-0,02	0,00	0,00
7	0,01	0,01	0,00	0,01
8	-0,01	-0,01	0,00	0,00
9	-0,01	0,00	-0,01	0,00

Table 4.2.44\_Errors for stride time.

Subjects	Stride frequency (Hz)			
	Errors algorithm trunk		Errors algorithm heels	
	Right	Left	Right	Left
1	-0,01	0,00	-0,01	-0,01
2	0,00	0,00	0,01	-0,01
3	0,01	0,00	0,00	0,01
4	-0,01	0,00	-0,01	0,00
5	0,00	-0,01	0,00	0,00
6	-0,01	0,01	0,00	0,00
7	0,00	-0,01	0,00	-0,01
8	0,01	0,00	0,00	0,00
9	0,00	0,00	0,00	0,00

Table 4.2.45\_Errors for stride frequency.

Subjects	Step time (s)			
	Errors algorithm trunk		Errors algorithm heels	
	Right	Left	Right	Left
1	0,02	-0,02	0,00	0,01
2	-0,01	0,01	-0,01	0,01
3	-0,01	0,00	-0,02	0,02
4	-0,02	0,02	0,01	0,00
5	-0,03	0,03	0,02	-0,02
6	-0,01	0,00	0,01	-0,01
7	0,00	0,01	0,03	-0,02
8	-0,01	0,00	0,00	0,00
9	0,00	-0,01	0,01	-0,01

Table 4.2.46\_Errors for step time.

Subjects	Step frequency (Hz)			
	Errors algorithm trunk		Errors algorithm heels	
	Right	Left	Right	Left
1	-0,06	0,07	0,00	-0,02
2	0,02	-0,03	0,03	-0,09
3	0,02	-0,01	0,07	-0,05
4	0,03	-0,09	-0,03	0,01
5	0,05	-0,14	-0,04	0,04
6	0,01	0,00	-0,03	0,03
7	-0,01	-0,01	-0,08	0,05
8	0,02	0,00	0,01	0,00
9	-0,02	0,02	-0,02	0,03

Table 4.2.47\_Errors for step frequency.

Subjects	Stance time (s)			
	Errors algorithm trunk		Errors algorithm heels	
	Right	Left	Right	Left
1	-0,01	-0,04	0,05	0,04
2	0,00	-0,02	0,07	0,05
3	0,00	-0,02	0,07	0,03
4	-0,01	-0,01	0,05	0,05
5	0,02	-0,01	0,05	0,08
6	0,05	0,02	0,07	0,08
7	-0,07	-0,02	0,04	0,06
8	-0,01	0,00	0,08	0,14
9	0,02	0,01	0,10	0,06

Table 4.2.48\_Errors for stance time.

Subjects	Stance duration (%GC)			
	Errors algorithm trunk		Errors algorithm heels	
	Right	Left	Right	Left
1	-1,57	-3,66	3,94	3,42
2	0,40	-1,30	7,28	3,65
3	0,74	-1,10	6,31	3,32
4	-1,35	-0,64	3,55	3,93
5	0,93	-1,70	3,02	5,49
6	2,98	2,26	5,22	6,05
7	-6,16	-2,65	3,27	4,46
8	-0,22	0,62	5,87	10,10
9	1,66	0,69	8,33	4,78

Table 4.2.49\_Errors for stance duration.

Subjects	Swing time (s)			
	Errors algorithm trunk		Errors algorithm heels	
	Right	Left	Right	Left
1	0,01	0,04	-0,04	-0,03
2	0,00	0,02	-0,08	-0,04
3	-0,01	0,01	-0,07	-0,04
4	0,01	0,01	-0,04	-0,05
5	-0,01	0,02	-0,05	-0,09
6	-0,04	-0,03	-0,07	-0,08
7	0,08	0,03	-0,04	-0,05
8	0,00	-0,01	-0,08	-0,14
9	-0,02	-0,01	-0,10	-0,06

Table 4.2.50\_Errors for swing time.

Subjects	Swing duration (%GC)			
	Errors algorithm trunk		Errors algorithm heels	
	Right	Left	Right	Left
1	1,16	3,35	-4,67	-3,54
2	0,17	1,50	-7,66	-3,79
3	-0,26	1,15	-5,75	-3,26
4	0,99	1,34	-3,80	-4,13
5	-1,24	1,54	-3,33	-5,62
6	-2,70	-1,85	-5,36	-6,02
7	6,21	2,43	-3,14	-4,67
8	0,51	-0,29	-5,92	-9,93
9	-1,68	-0,68	-8,37	-4,56

Table 4.2.51\_Errors for swing duration.

Subjects	Single support time (s)			
	Errors algorithm trunk		Errors algorithm heels	
	Right	Left	Right	Left
1	0,03	0,02	-0,03	-0,04
2	0,01	0,00	-0,05	-0,08
3	0,00	0,00	-0,05	-0,06
4	0,01	0,01	-0,04	-0,04
5	0,01	-0,01	-0,08	-0,06
6	-0,04	-0,05	-0,08	-0,07
7	0,04	0,07	-0,05	-0,04
8	-0,01	0,00	-0,12	-0,09
9	-0,01	-0,02	-0,06	-0,09

Table 4.2.52\_Errors for single support time.

Subjects	Single support duration (%GC)			
	Errors algorithm trunk		Errors algorithm heels	
	Right	Left	Right	Left
1	2,87	1,95	-3,76	-3,87
2	0,89	0,51	-4,52	-7,26
3	0,55	-0,02	-4,24	-5,37
4	0,93	0,71	-3,89	-3,75
5	0,95	-1,15	-5,47	-4,08
6	-2,82	-3,10	-6,19	-5,57
7	3,33	5,74	-4,20	-3,27
8	-0,30	0,53	-9,03	-6,23
9	-0,74	-1,62	-5,00	-7,34

Table 4.2.53\_Errors for single support duration.

Subjects	Double support time (s)			
	Errors algorithm trunk		Errors algorithm heels	
	Right	Left	Right	Left
1	-0,05	-0,05	0,09	0,09
2	-0,01	-0,01	0,13	0,13
3	-0,01	-0,01	0,10	0,10
4	-0,03	-0,03	0,09	0,09
5	0,00	0,00	0,13	0,13
6	0,06	0,06	0,15	0,15
7	-0,10	-0,10	0,10	0,10
8	0,00	0,00	0,21	0,21
9	0,03	0,03	0,15	0,15

Table 4.2.54\_Errors for double support time.

Subjects	Double support duration (%GC)			
	Errors algorithm trunk		Errors algorithm heels	
	Right	Left	Right	Left
1	-4,51	-4,51	8,21	8,21
2	-0,95	-1,18	11,82	11,60
3	-0,90	-0,90	9,01	9,01
4	-2,33	-2,33	7,94	7,94
5	-0,31	-0,31	8,95	8,95
6	5,05	5,05	11,38	11,38
7	-8,64	-8,64	7,81	7,81
8	-0,23	-0,23	15,85	15,85
9	2,35	2,35	12,93	12,93

Table 4.2.55\_Errors for double support duration.

Subjects	Foot symmetry (%GC)			
	Errors algorithm trunk		Errors algorithm heels	
	Right	Left	Right	Left
1	1,80	-1,95	-0,50	-0,24
2	-1,10	0,21	-0,61	1,38
3	-0,58	0,51	-1,76	1,59
4	-2,77	0,97	0,64	-0,52
5	-1,89	2,48	1,75	-1,21
6	-0,67	-0,06	0,65	-0,80
7	0,05	-0,03	1,81	-2,28
8	-0,70	0,00	-0,19	0,10
9	0,90	-0,34	0,62	-0,59

Table 4.2.56\_Errors for foot symmetry.

Subjects	Limp index			
	Errors algorithm trunk		Errors algorithm heels	
	Right	Left	Right	Left
1	0,04	0,04	0,01	0,01
2	0,03	0,03	0,03	0,04
3	0,02	0,02	0,05	0,05
4	0,00	0,00	0,00	0,00
5	0,03	0,03	-0,04	-0,04
6	0,04	0,04	-0,02	-0,02
7	-0,06	-0,06	-0,02	-0,02
8	-0,02	-0,02	-0,08	-0,08
9	0,01	0,01	0,05	0,05

Table 4.2.57\_Errors for limp index.

The following Table 4.2.58 presents the mean and the standard deviation values estimated among all the subjects from the errors reported in the previous fourteen tables (from Table 4.2.44 to Table 4.2.57).

Spatio-temporal parameters	Errors algorithm from trunk				Errors algorithm from heels			
	Right		Left		Right		Left	
	Mean	SD	Mean	SD	Mean	SD	Mean	SD
<b>Stride time (s)</b>	0,00	0,01	0,00	0,01	0,00	0,01	0,00	0,01
<b>Stride frequency (Hz)</b>	0,00	0,01	0,00	0,01	0,00	0,01	0,00	0,01
<b>Step time (s)</b>	-0,01	0,01	0,00	0,01	0,00	0,02	0,00	0,01
<b>Step frequency (Hz)</b>	0,01	0,03	-0,02	0,06	-0,01	0,04	0,00	0,05
<b>Stance time (s)</b>	0,00	0,03	-0,01	0,02	0,06	0,02	0,06	0,03
<b>Stance duration (%)</b>	-0,29	2,61	-0,83	1,81	5,20	1,89	5,02	2,12
<b>Swing time (s)</b>	0,00	0,03	0,01	0,02	-0,06	0,02	-0,06	0,03
<b>Swing duration (%)</b>	0,35	2,54	0,94	1,61	-5,33	1,83	-5,06	2,04
<b>Single support time (s)</b>	0,01	0,03	0,00	0,03	-0,06	0,03	-0,06	0,02
<b>SS duration (%)</b>	0,63	1,85	0,39	2,50	-5,14	1,65	-5,19	1,54
<b>Double support time (s)</b>	-0,01	0,05	-0,01	0,05	0,13	0,04	0,13	0,04
<b>DS duration (%)</b>	-1,16	3,89	-1,19	3,89	10,43	2,75	10,41	2,74
<b>Foot symmetry (%)</b>	-0,55	1,37	0,20	1,17	0,27	1,16	-0,29	1,21
<b>Limp index (right/left)</b>	0,01	0,03	0,01	0,03	0,00	0,04	0,00	0,04

Table 4.2.58\_Mean and standard deviation values for errors of all the parameters among all the subjects.

In the following pages, the fourteen figures (from Figure 4.2.15 to Figure 4.2.28) show the Bland-Altman graphs for all the spatio-temporal parameters.

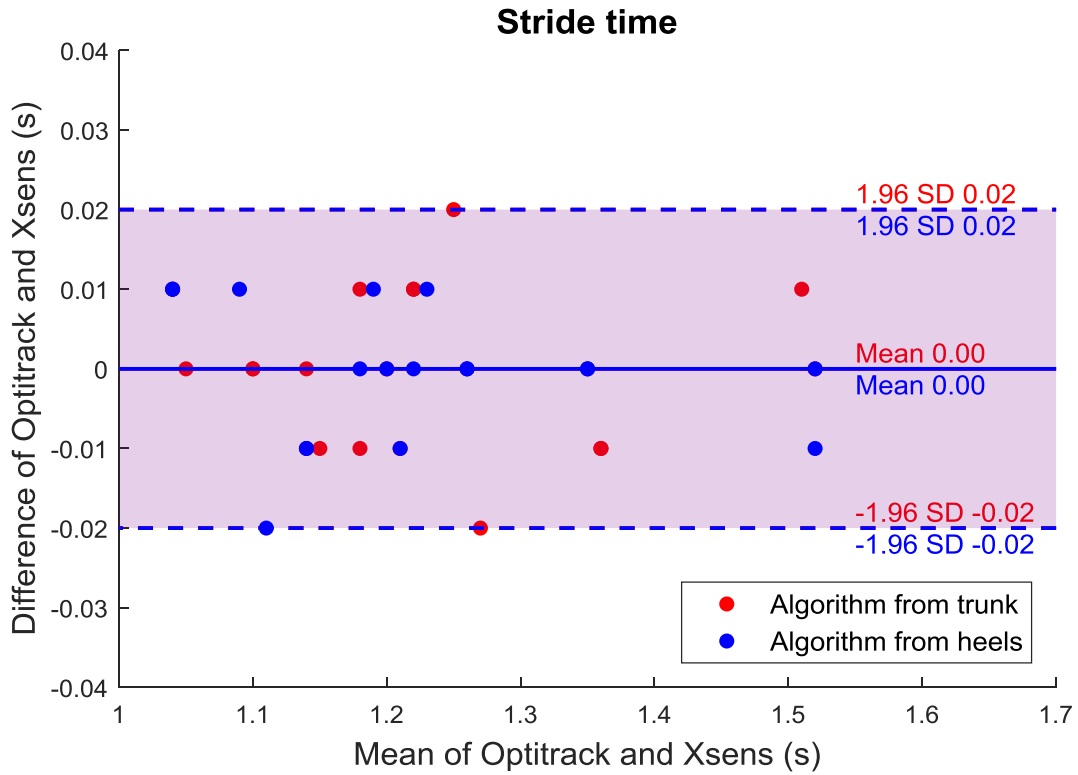


Figure 4.2.15\_Bland-Altman graph for stride time.

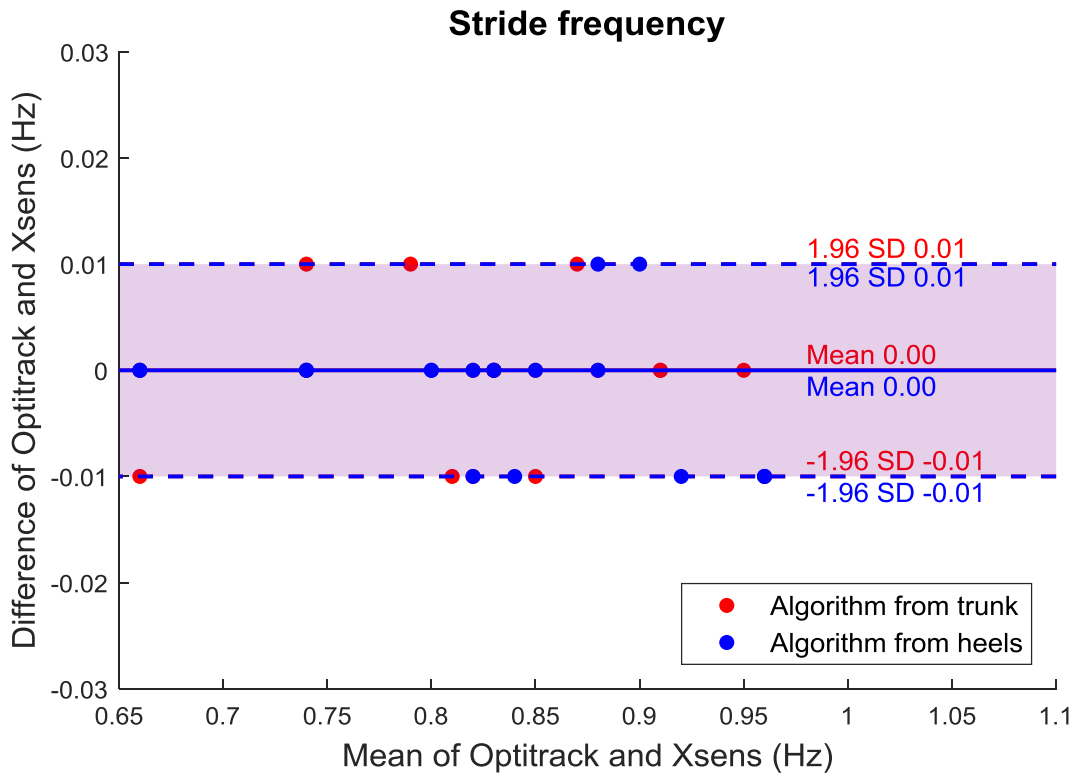


Figure 4.2.16\_Bland-Altman graph for stride frequency.

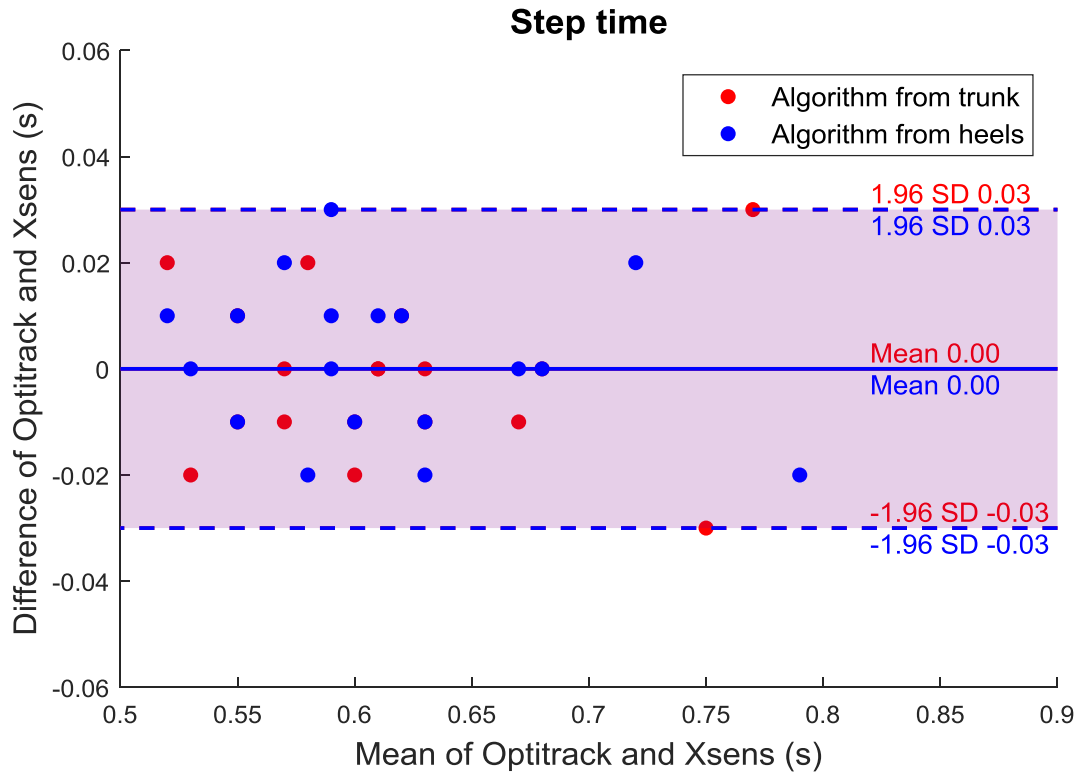


Figure 4.2.17\_Bland-Altman graph for step time.

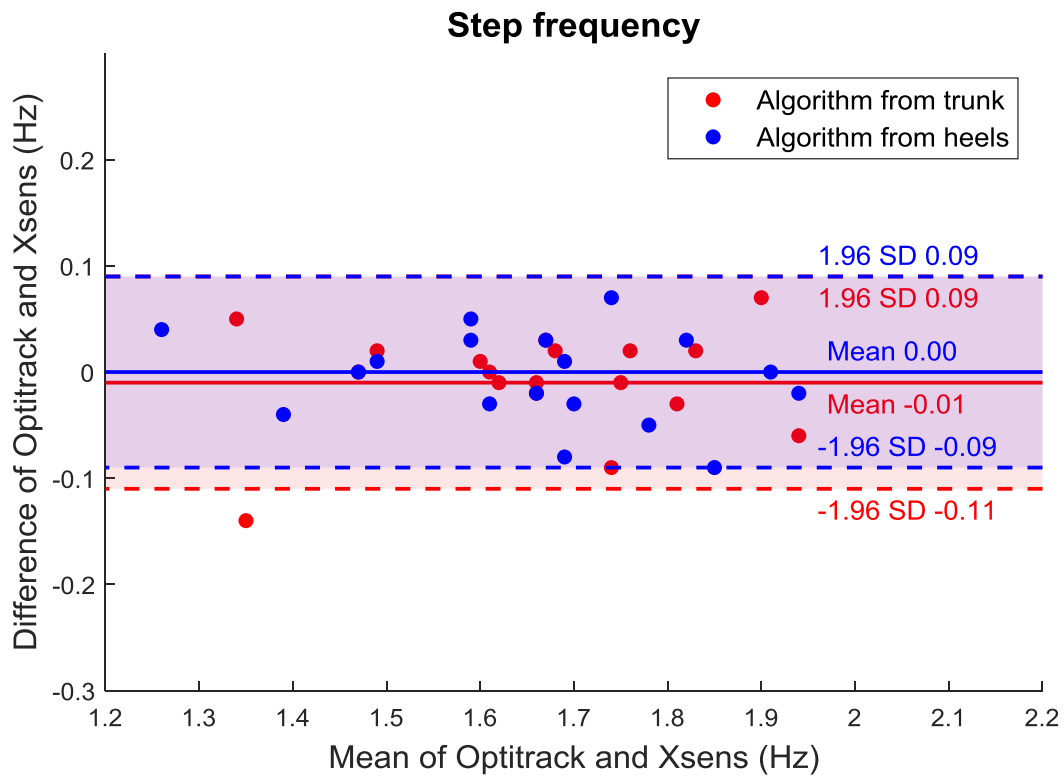


Figure 4.2.18\_Bland-Altman graph for step frequency.

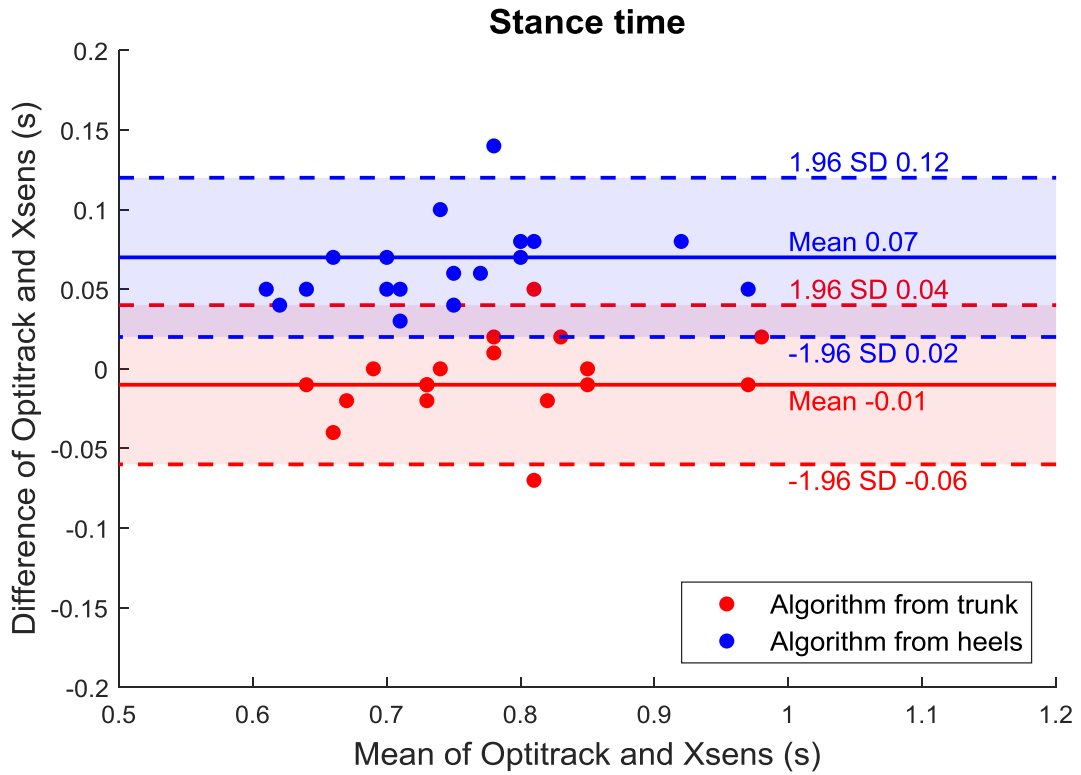


Figure 4.2.19\_Bland-Altman graph for stance time.

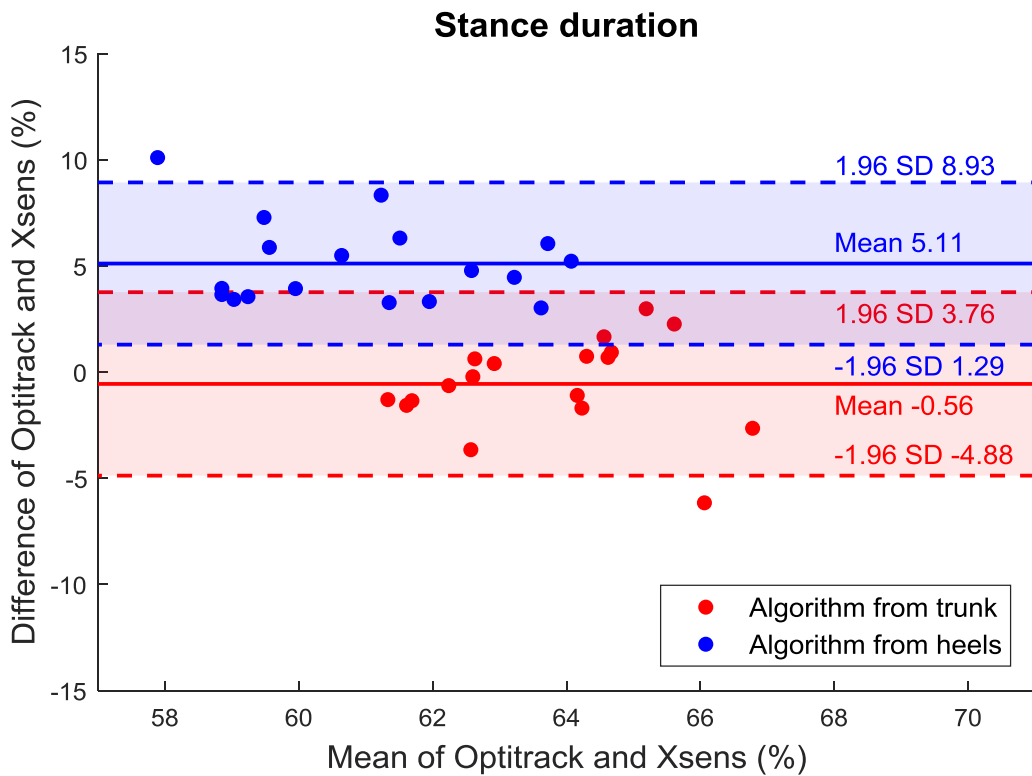


Figure 4.2.20\_Bland-Altman graph for stance duration.

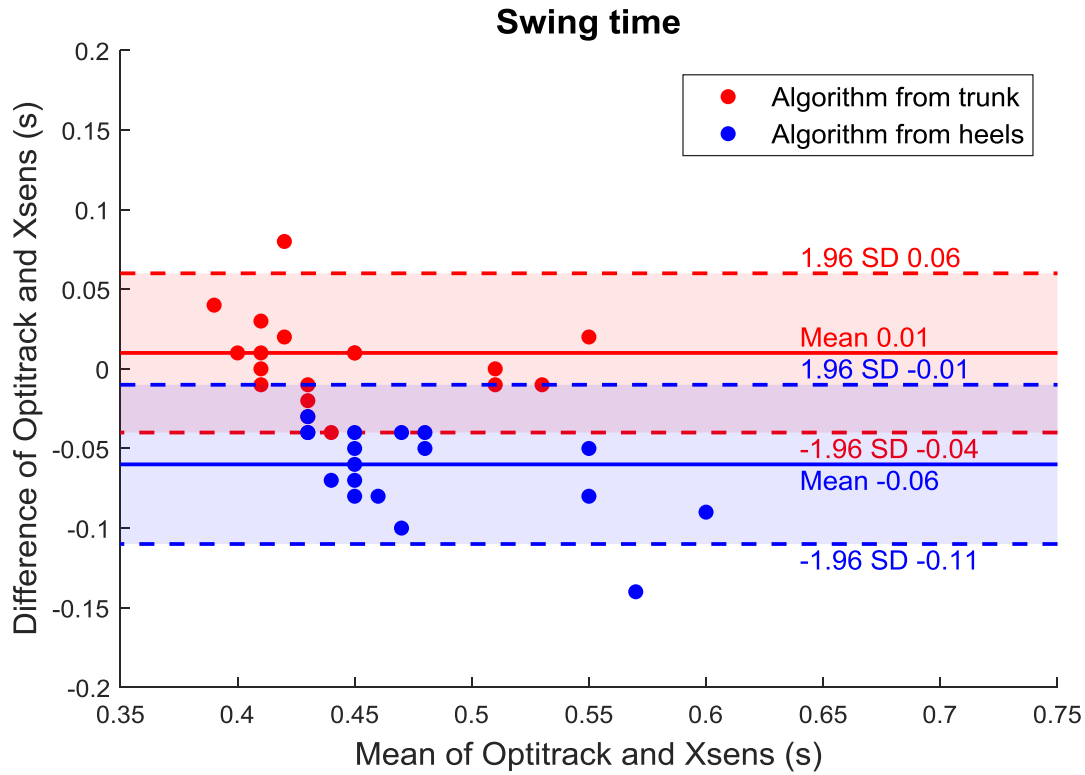


Figure 4.2.21\_Bland-Altman graph for swing time.

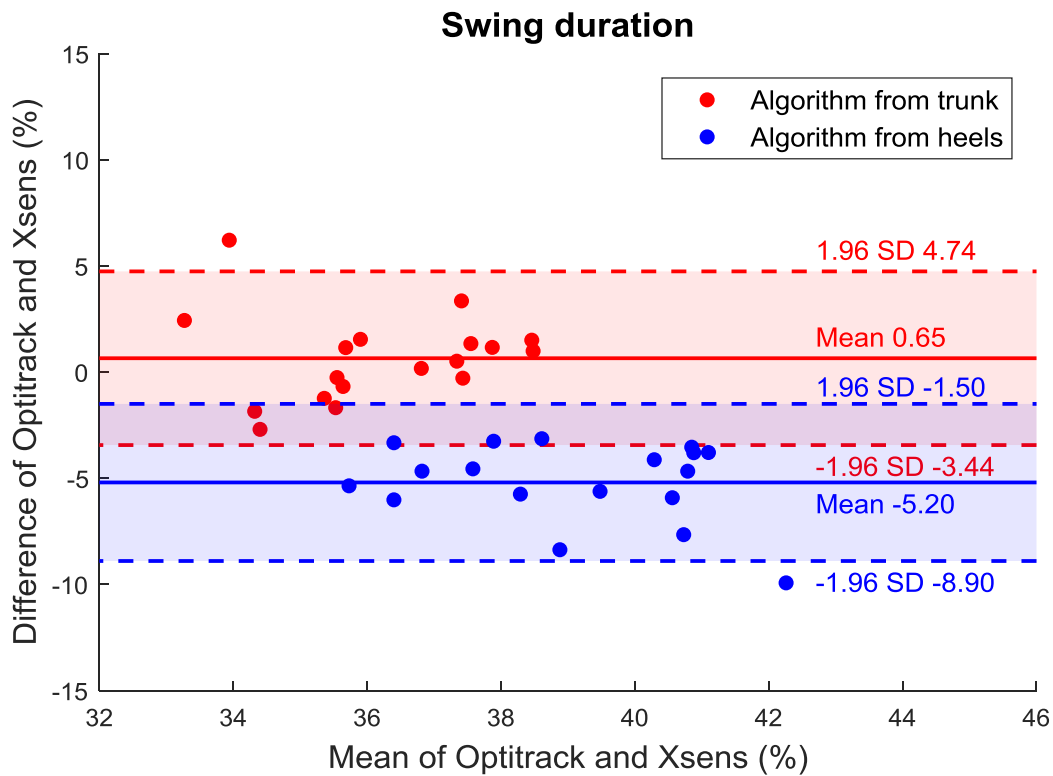


Figure 4.2.22\_Bland-Altman graph for swing duration.

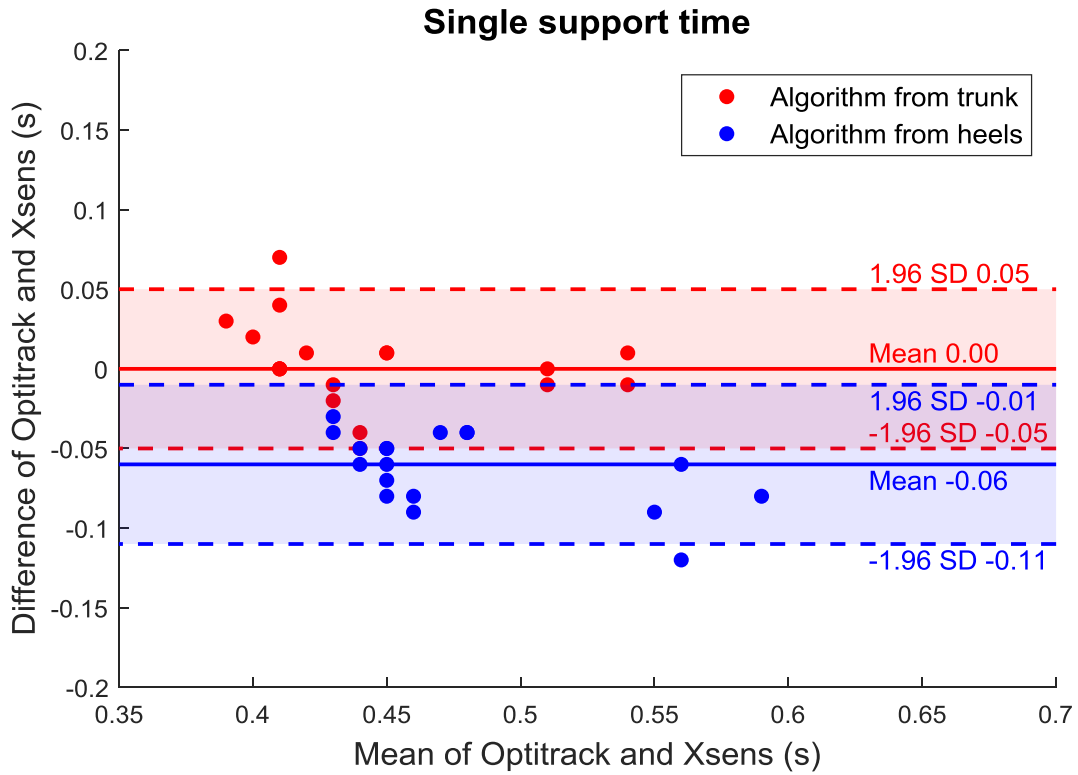


Figure 4.2.23\_Bland-Altman graph for single support time.

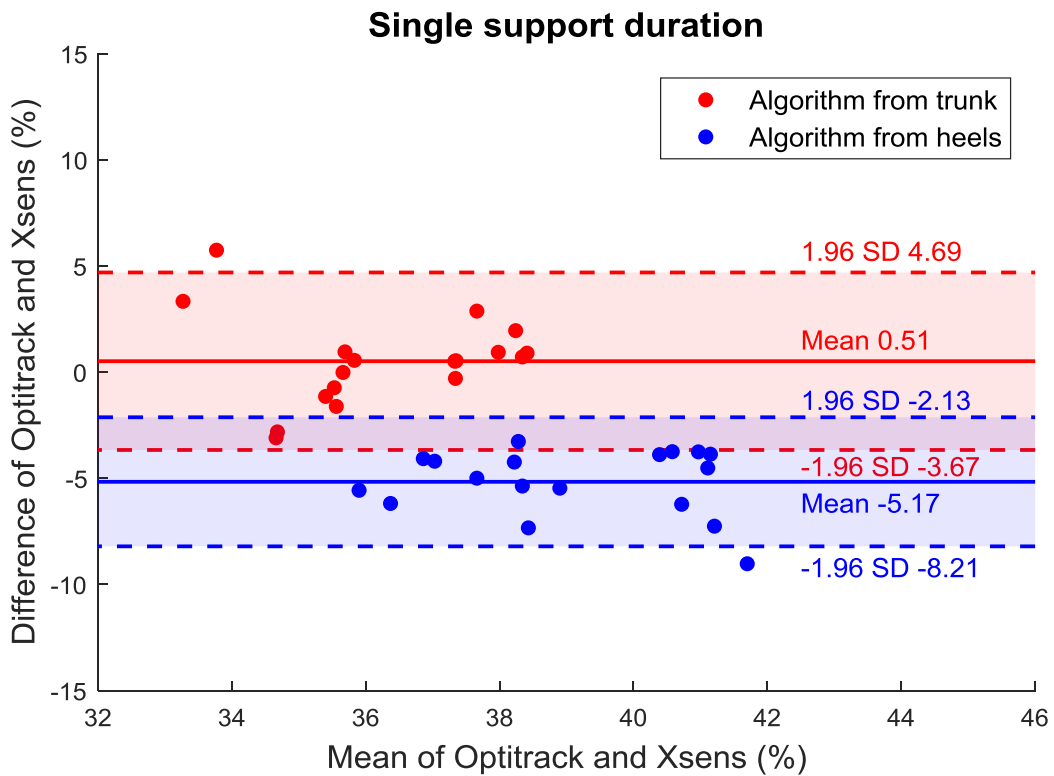


Figure 4.2.24\_Bland-Altman graph for single support duration.

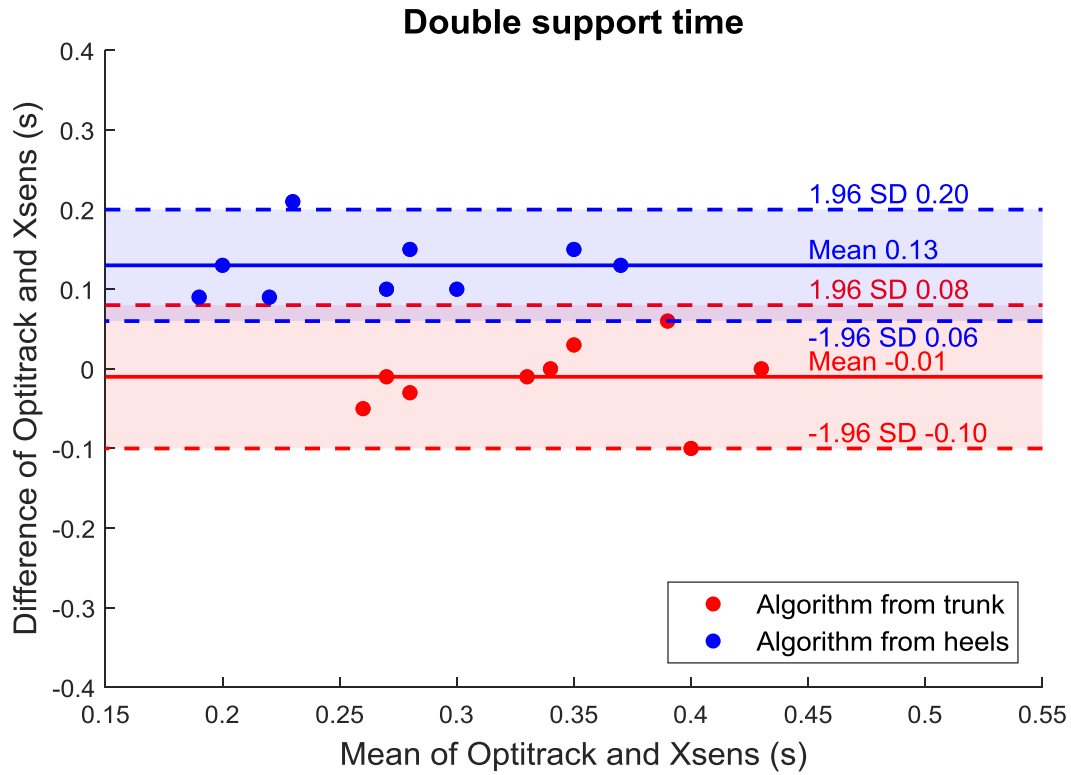


Figure 4.2.25\_Bland-Altman graph for double support time.

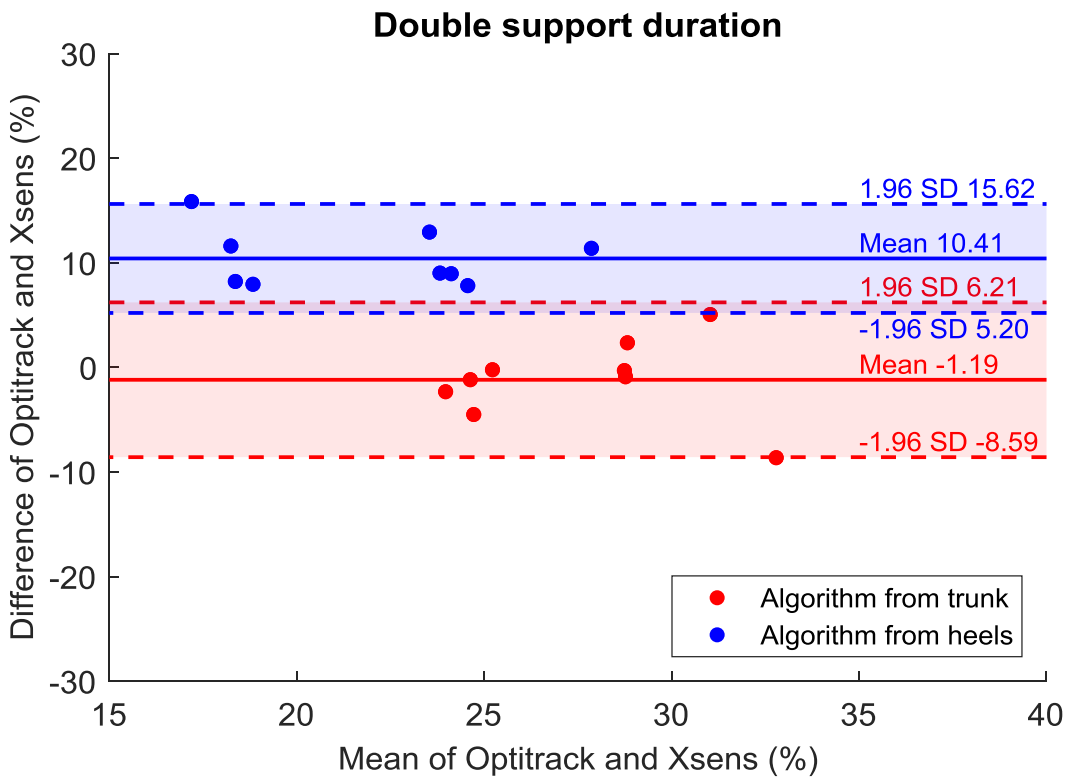


Figure 4.2.26\_Bland-Altman graph for double support duration.

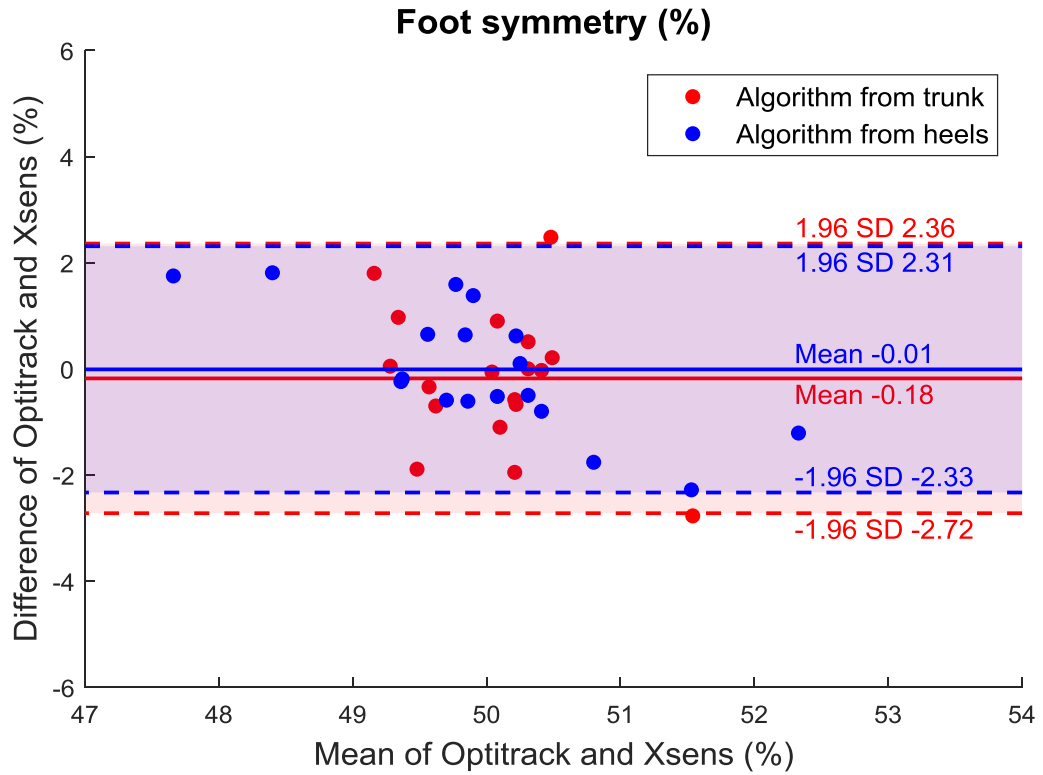


Figure 4.2.27\_Bland-Altman graph for foot symmetry.

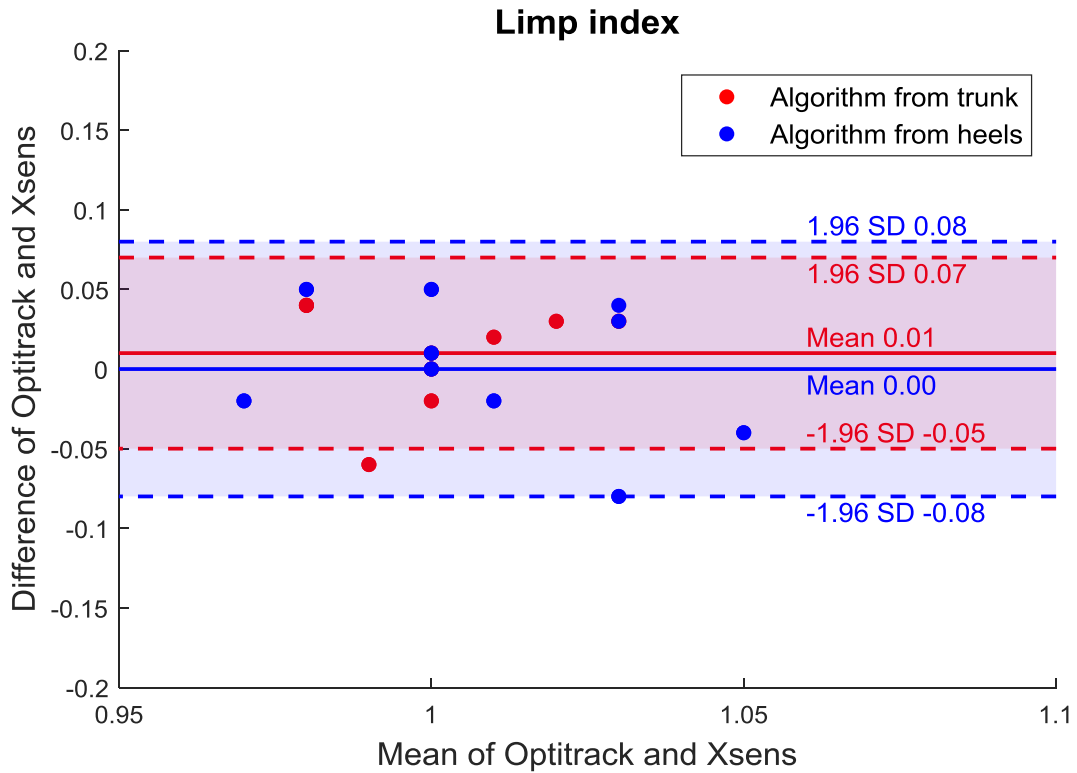


Figure 4.2.28\_Bland-Altman graph for limp index.

### 4.2.3 Normal speed with single-task and with dual-task

The following two tables (Table 4.2.59 and Table 4.2.60) show mean and standard deviation values of all the fourteen parameters among all the subjects for both the normal speed with single-task and the normal speed with dual-task. Furthermore, these values do not maintain the distinction between right and left sides.

Normal speed with single-task						
Spatio-temporal parameters	Optitrack		Xsens from trunk		Xsens from heels	
	Mean	SD	Mean	SD	Mean	SD
Stride time (s)	1,16	0,08	1,17	0,08	1,16	0,08
Stride frequency (Hz)	0,86	0,06	0,86	0,06	0,87	0,06
Step time (s)	0,58	0,04	0,58	0,04	0,58	0,04
Step frequency (Hz)	1,73	0,12	1,73	0,12	1,73	0,12
Stance time (s)	0,73	0,06	0,74	0,06	0,67	0,05
Stance duration (%)	62,81	1,61	63,61	2,57	57,78	1,27
Swing time (s)	0,43	0,03	0,42	0,04	0,49	0,03
Swing duration (%)	37,32	1,62	36,40	2,47	42,26	1,19
Single support time (s)	0,43	0,03	0,42	0,03	0,49	0,03
SS duration (%)	37,28	1,61	36,36	2,47	42,25	1,19
Double support time (s)	0,30	0,05	0,32	0,07	0,18	0,03
DS duration (%)	25,36	3,18	27,20	4,90	15,51	2,11
Foot symmetry (%)	49,85	0,92	49,94	0,63	49,98	1,06
Limp index (right/left)	1,00	0,01	0,99	0,01	1,00	0,02

Table 4.2.59\_Normal speed with single-task: mean and standard deviation values of spatio-temporal parameters among all the nine subjects.

Normal speed with dual-task						
Spatio-temporal parameters	Optitrack		Xsens from trunk		Xsens from heels	
	Mean	SD	Mean	SD	Mean	SD
<b>Stride time (s)</b>	1,23	0,14	1,23	0,14	1,22	0,14
<b>Stride frequency (Hz)</b>	0,83	0,09	0,83	0,09	0,83	0,09
<b>Step time (s)</b>	0,61	0,07	0,61	0,07	0,61	0,07
<b>Step frequency (Hz)</b>	1,66	0,17	1,66	0,17	1,66	0,18
<b>Stance time (s)</b>	0,78	0,10	0,79	0,09	0,72	0,09
<b>Stance duration (%)</b>	63,49	1,99	64,04	1,93	58,37	2,33
<b>Swing time (s)</b>	0,45	0,05	0,44	0,05	0,51	0,06
<b>Swing duration (%)</b>	36,49	1,94	35,84	1,84	41,68	2,39
<b>Single support time (s)</b>	0,45	0,05	0,44	0,05	0,51	0,06
<b>SS duration (%)</b>	36,52	1,94	36,01	1,92	41,69	2,15
<b>Double support time (s)</b>	0,33	0,07	0,35	0,06	0,21	0,06
<b>DS duration (%)</b>	27,05	3,57	28,23	3,59	16,63	4,12
<b>Foot symmetry (%)</b>	49,96	0,71	50,14	1,00	49,97	1,52
<b>Limp index (right/left)</b>	1,01	0,03	1,00	0,02	1,01	0,04

Table 4.2.60\_Normal speed with dual-task: mean and standard deviation values of spatio-temporal parameters among all the nine subjects.

In the following pages, the fourteen figures (from Figure 4.2.29 to Figure 4.2.42) show the bar diagrams for all the spatio-temporal parameters both for single-task and dual-task.

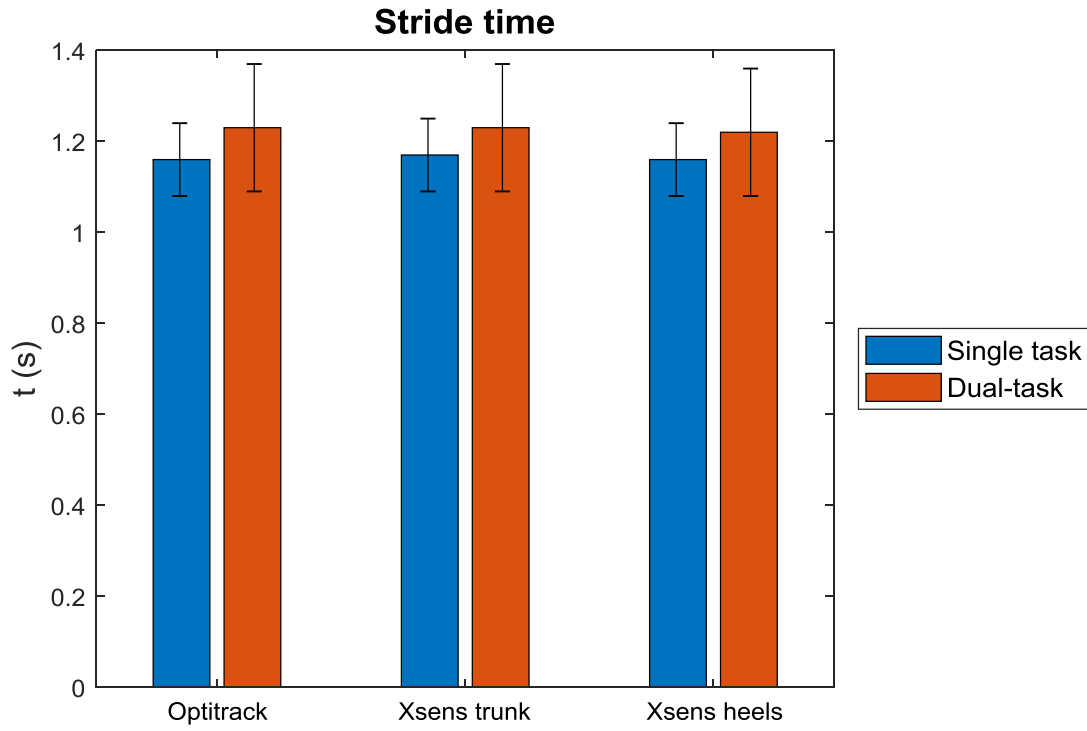


Figure 4.2.29\_Bar diagram for stride time (s).

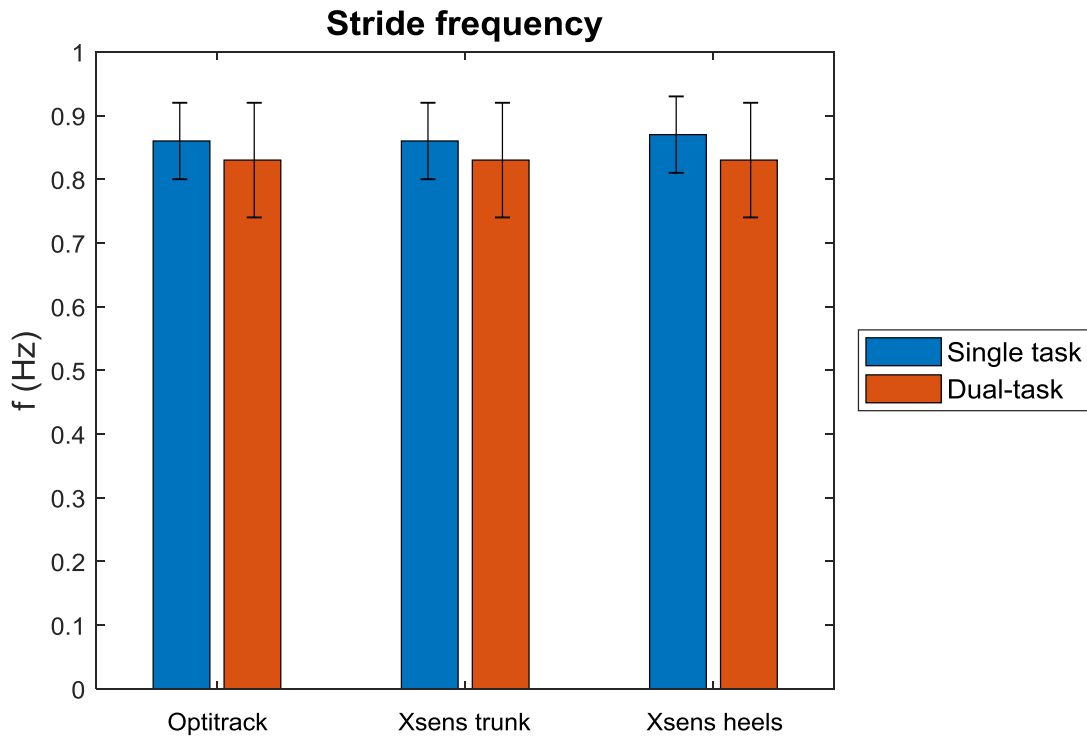


Figure 4.2.30\_Bar diagram for stride frequency (Hz).

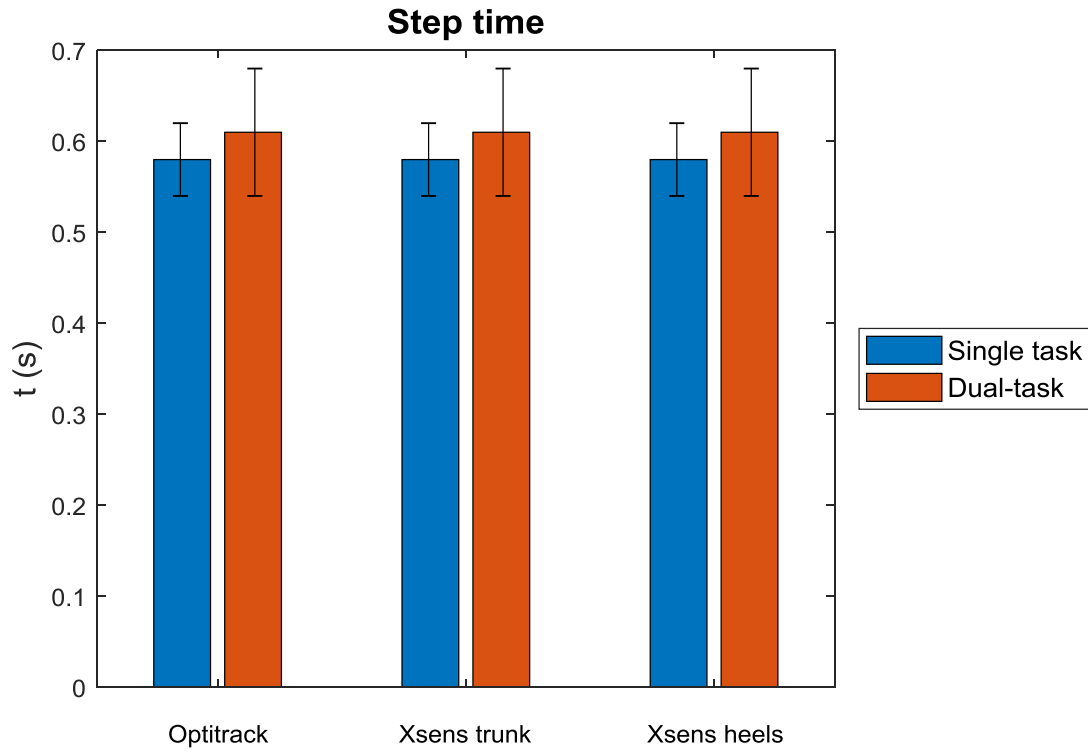


Figure 4.2.31\_Bar diagram for step time (s).

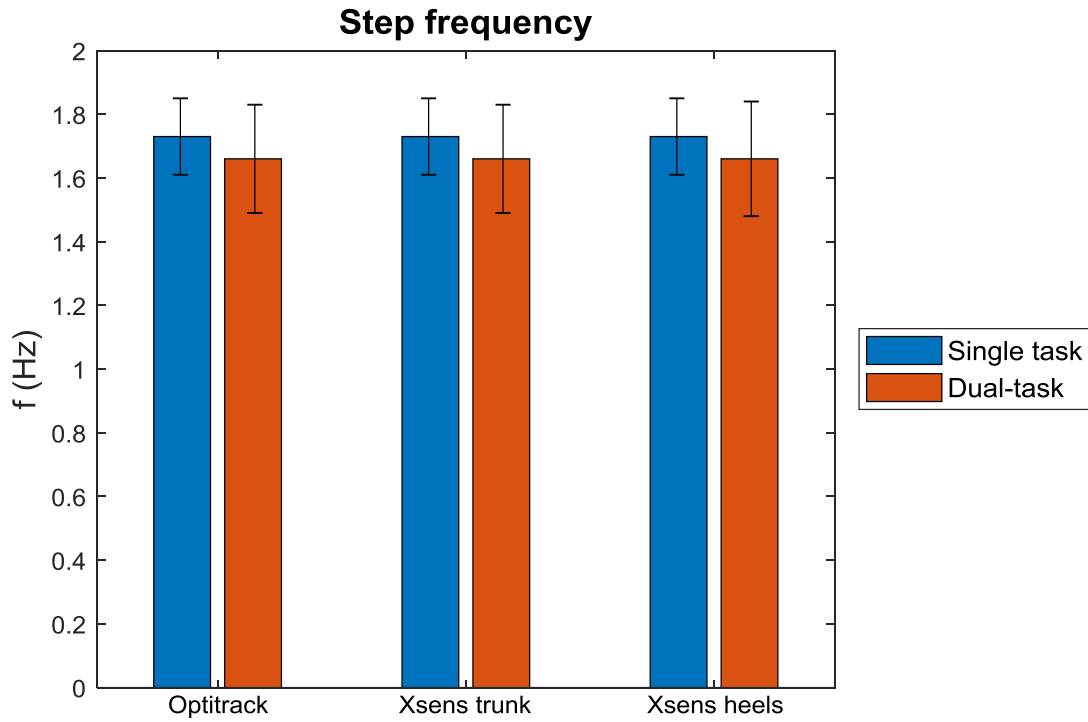


Figure 4.2.32\_Bar diagram for step frequency (Hz).

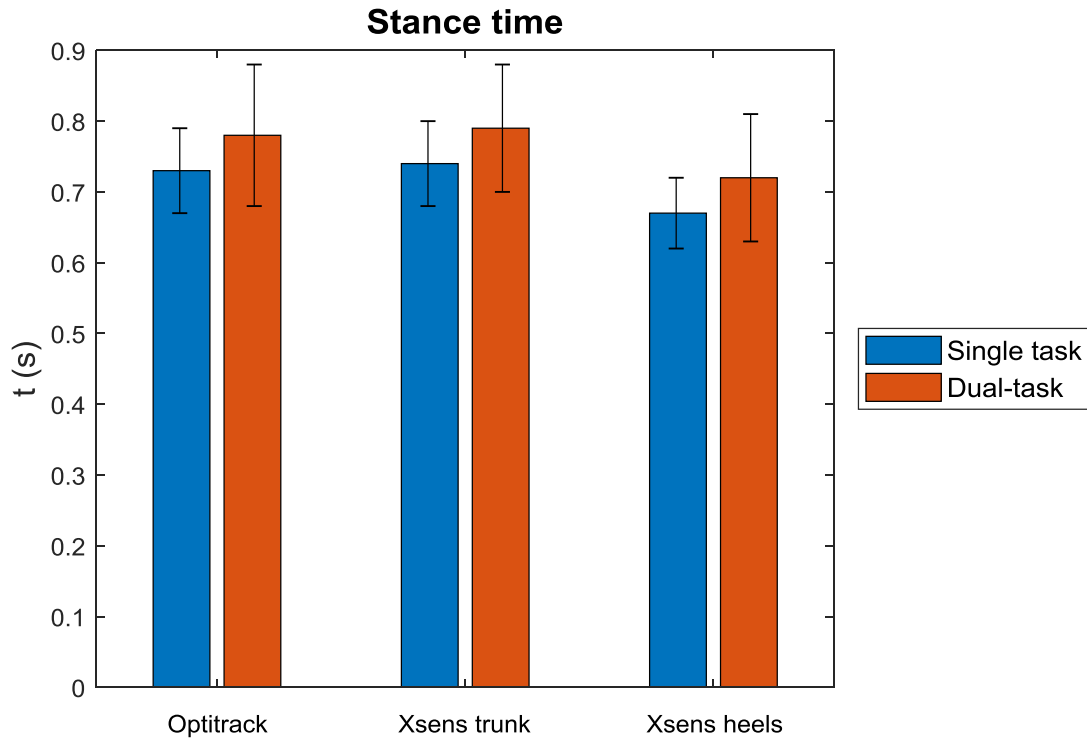


Figure 4.2.33\_Bar diagram for stance time (s).

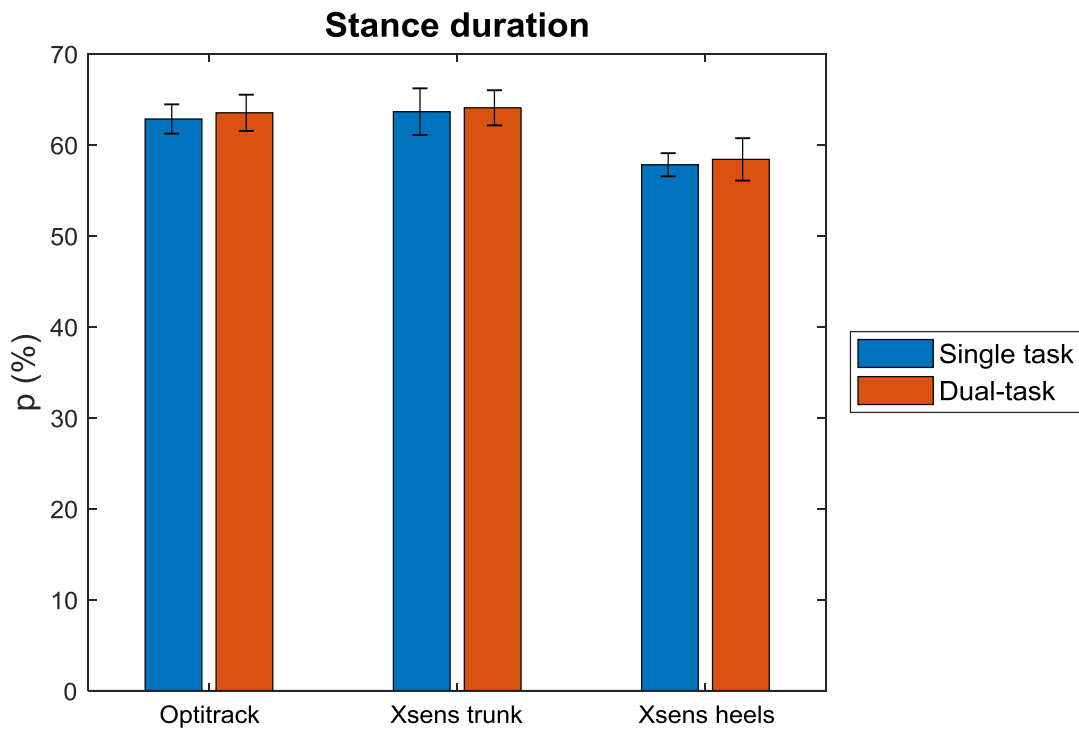


Figure 4.2.34\_Bar diagram for stance duration (%GC).

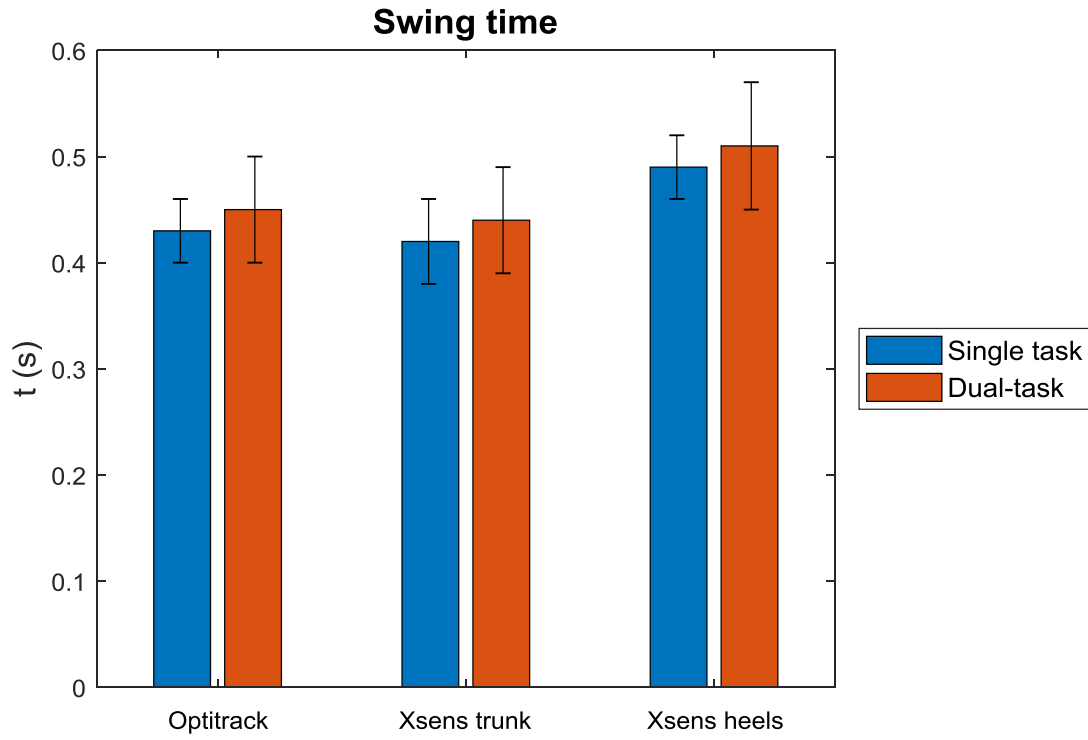


Figure 4.2.35\_Bar diagram for swing time (s).

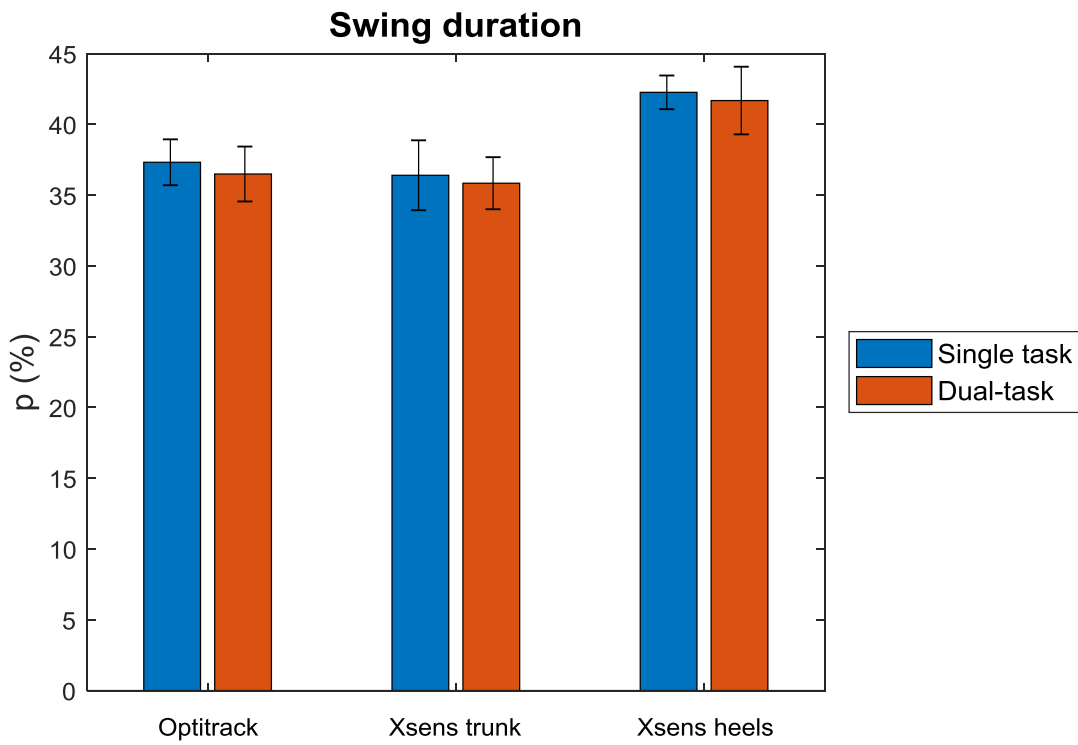


Figure 4.2.36\_Bar diagram for swing duration (%GC).

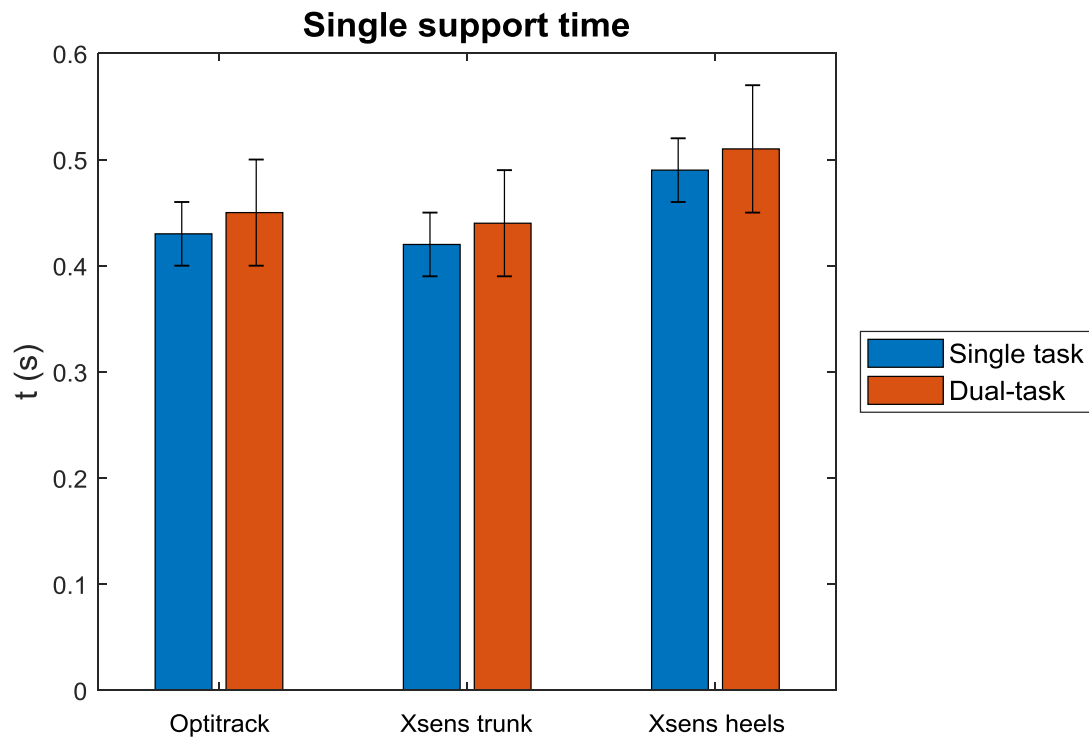


Figure 4.2.37\_Bar diagram for single support time (s).

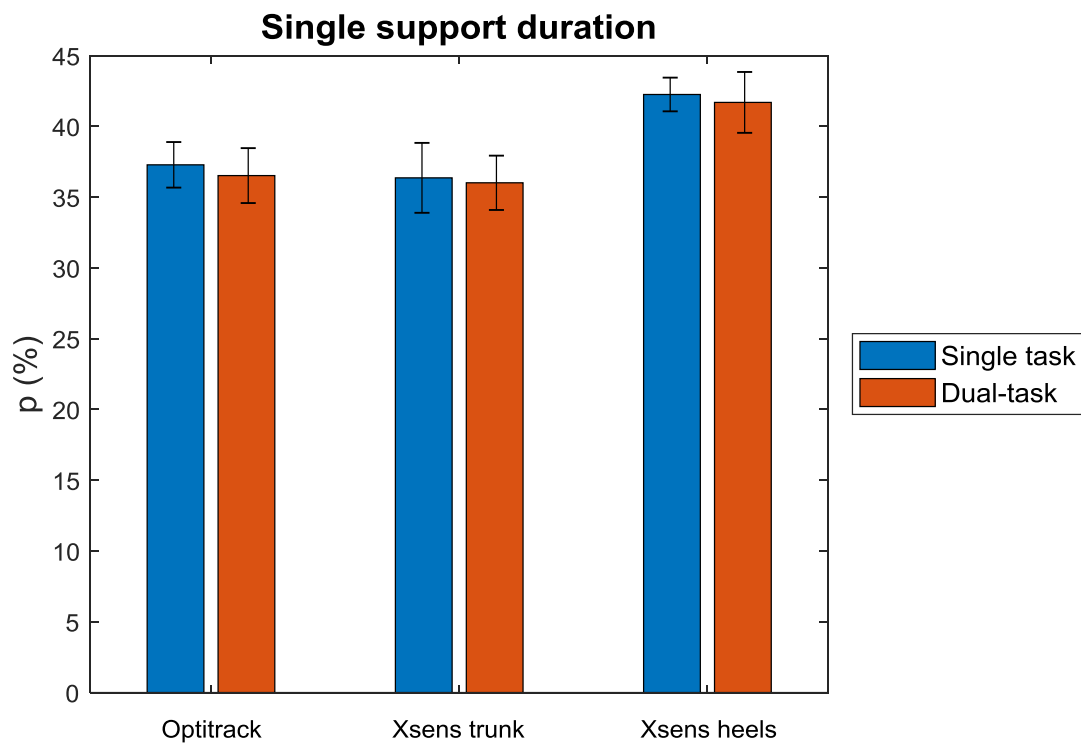


Figure 4.2.38\_Bar diagram for single support duration (%GC).

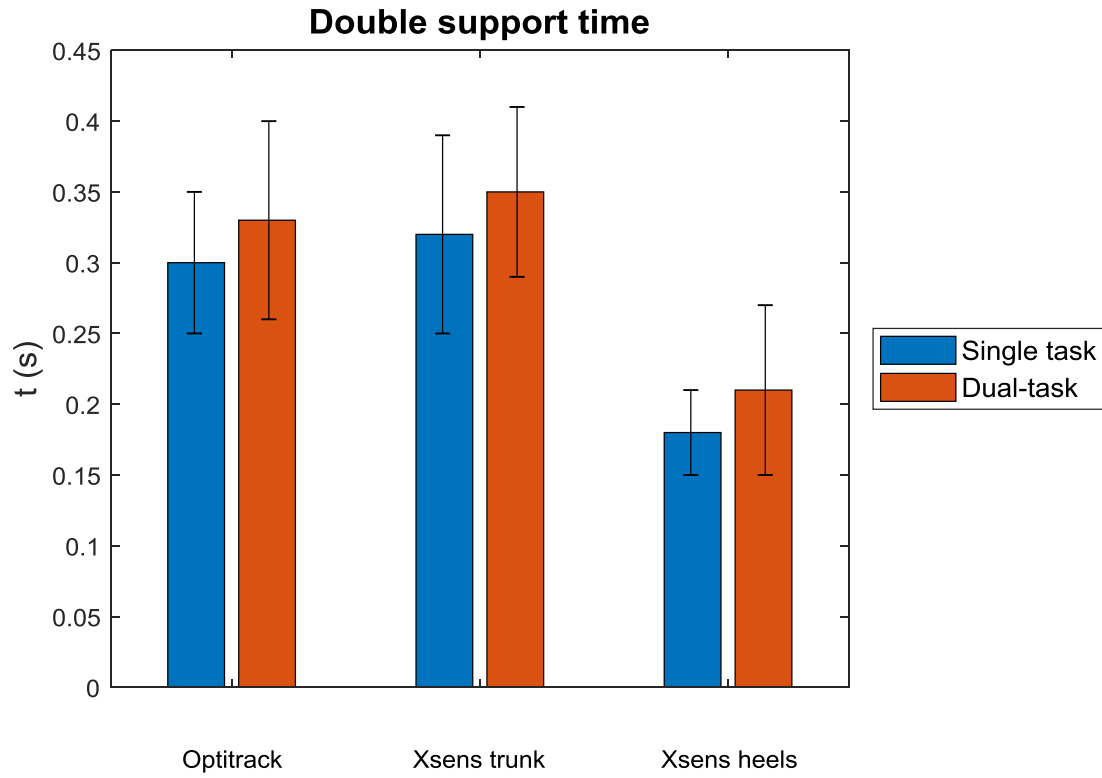


Figure 4.2.39\_Bar diagram for double support time (s).

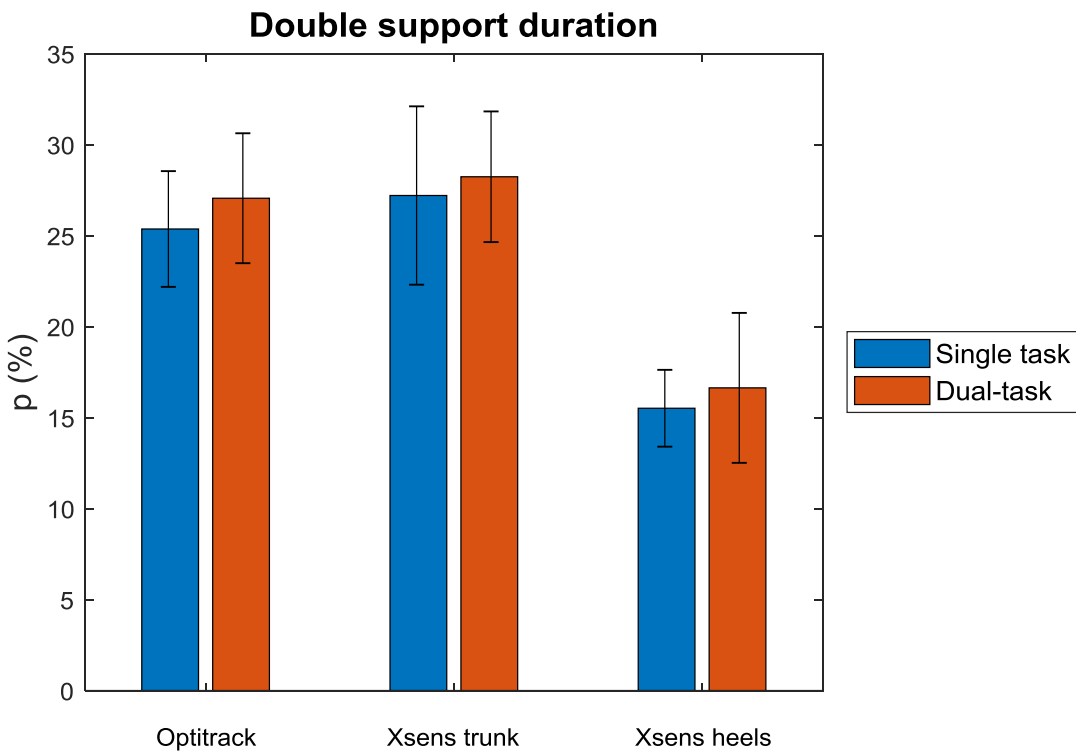


Figure 4.2.40\_Bar diagram for double support duration (%GC).

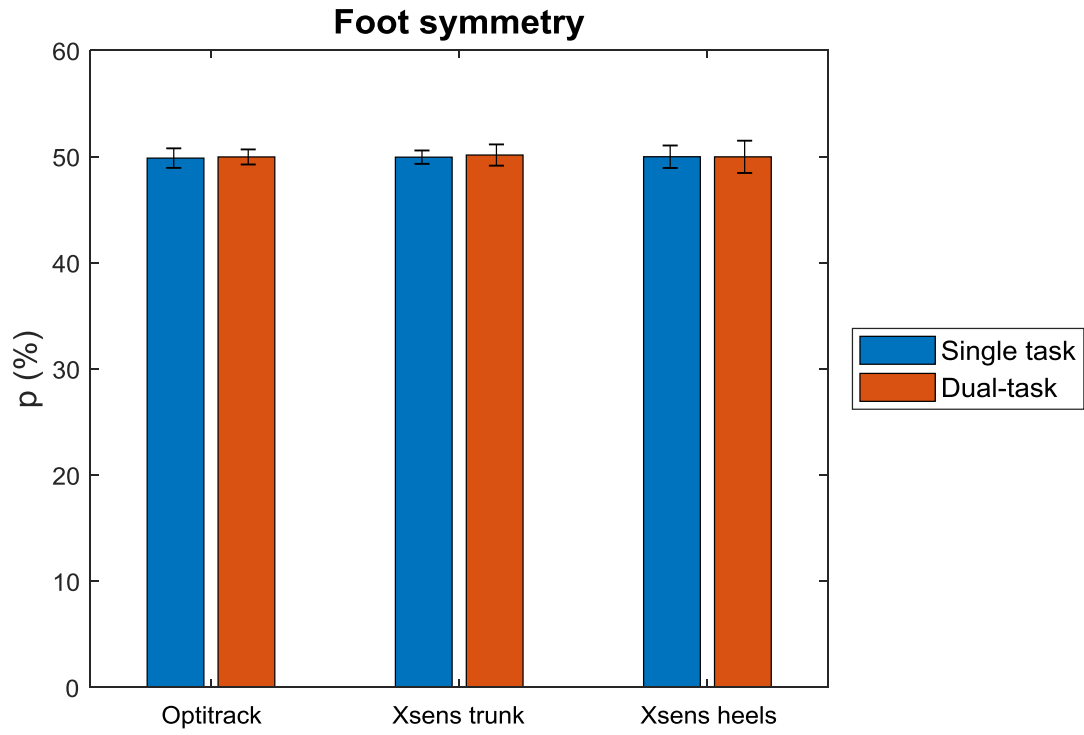


Figure 4.2.41\_Bar diagram for foot symmetry (%GC).

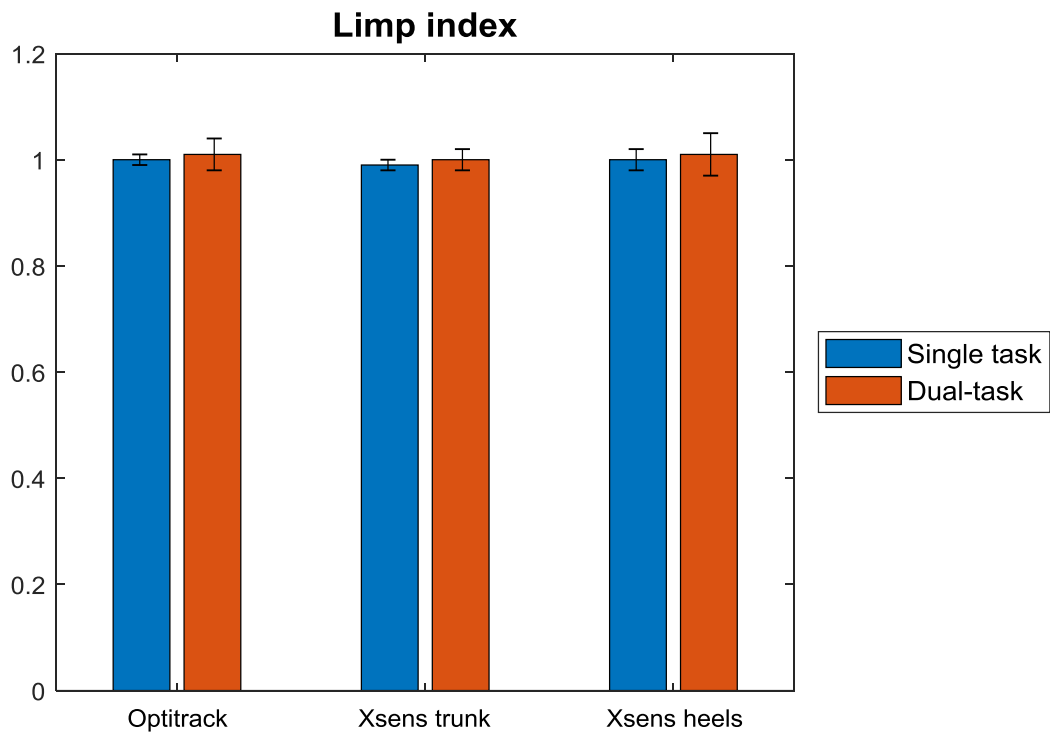


Figure 4.2.42\_Bar diagram for limp index.

The following Table 4.2.61 shows the p-values obtained from the paired t-test applied to the data related both to single-task and dual-task.

Spatio-temporal parameters	p-values		
	Optitrack	Xsens trunk	Xsens heels
Stride time (s)	0,09	0,08	0,09
Stride frequency (Hz)	0,07	0,06	0,07
Step time (s)	0,09	0,11	0,10
Step frequency (Hz)	0,05*	0,06	0,08
Stance time (s)	0,07	0,06	0,05*
Stance duration (%)	0,07	0,33	0,10
Swing time (s)	0,19	0,21	0,23
Swing duration (%)	0,03*	0,18	0,16
Single support time (s)	0,19	0,09	0,16
SS duration (%)	0,06	0,40	0,11
Double support time (s)	0,03*	0,10	0,05*
DS duration (%)	0,03*	0,21	0,17
Foot symmetry (%)	0,19	0,11	0,88
Limp index (right/left)	0,43	0,67	0,65

\*P\_value <= 0.05 statistical significance

Table 4.2.61\_The p-values of the t-test for single-task and dual-task.

### 4.3 Discussions

The first aspect that emerges from the results analysis is the fact that the Optitrack data are comparable with those of literature. The temporal parameters such as stride time, step time, stance time and swing time are of the same order of magnitude of those presented by literature articles. The following Table 4.3.1 contains a comparison between the parameters estimated with the gold standard Optitrack and those found in literature with different instruments. In particular, the comparison can be more reliable by choosing studies with healthy and elderly subjects walking at preferred speed with single-task. The articles chosen are those of: Trojaniello of 2014, Rampp of 2015 and Misu of 2017.

Spatio-temporal parameters	Optitrack	(D. Trojaniello, 2014)	(A. Rampp, 2015)	(S. Misu, 2017)
Stride time (s)	1,16	1,05	1,23	1,09
Stride frequency (Hz)	0,86			
Step time (s)	0,58	0,53		0,54
Step frequency (Hz)	1,73			
Stance time (s)	0,73	0,68	0,86	0,65
Stance duration (%GC)	62,81			
Swing time (s)	0,43	0,38	0,36	0,42
Swing duration (%GC)	37,32			
Single support time (s)	0,43			
SS duration (%GC)	37,28			
Double support time (s)	0,30			
DS duration (%GC)	25,36			
Foot symmetry (%GC)	49,85			
Limp index (right/left)	1,00			

Table 4.3.1\_ Comparison between spatio-temporal parameters estimated with Optitrack and those found in literature.

Another observation can be made with the parameters expressed as a percentage of the gait cycle. As Perry affirmed in his work of 1992, the gait cycle can be divided in two phases: stance (60%) and swing (40%). Then, he divided the stance phase into three subphases: first double support (10%), single support (40%) and second double support (10%). As a consequence, the stance duration (60%) is the sum of the double support duration (20%) and the single support duration (40%). However, he also underlined the possible variation of these percentages by increasing or reducing the walking speed. This aspect is typical of elderly subjects: the speed reduction implies an increase of stance and double support durations and a reduction of swing and single support durations.

The data obtained confirm this affirmation: stance duration is about 63%, swing duration is about 37%, double support duration is about 25% and single support duration is about 37%.

The third observation that can be highlighted concerns the right-left symmetry. As the tables of the previous subchapter show, the differences between right and left sides for the parameters of all subjects are small. For the temporal parameters expressed in seconds there are differences at the second decimal digit, whereas those of the parameters expressed as percentage of the gait cycle are at the last full digit or at the first decimal digit. In addition, also the foot symmetry and the limp index are two symmetry indices. In fact, they are respectively the ratio between the step time and the stride time and the ratio between the two stance times. In healthy subjects the foot symmetry is about 50% and the limp index is about 1. The same values are found among the Optitrack data obtained from trials with single-task.

The fourth evaluation that can be conducted regards the performance of the two Xsens algorithms compared to the gold standard Optitrack. The errors can be evaluated both from the tables of differences and the Bland-Altman graphs. It is possible to note that both the algorithms are accurate for the estimation of parameters such as stride time, stride frequency, step time, step frequency, foot symmetry and limp index. In fact, the summary Table 4.2.29 shows that mean differences among subjects are tending to zero for all these parameters. Furthermore, also in the Bland-Altman plots (Figures 4.2.1, 4.2.2, 4.2.3, 4.2.4, 4.2.13 and 4.2.14) it is possible to note that the line corresponding to the mean value is very close if not coinciding to the zero. For the parameters such as swing time, swing duration, single support time and single support duration, the values provided by the Xsens algorithm that used the trunk signal are slightly underestimated. In particular, the mean differences of swing and single support times are equal to 0,01 s, whereas those of swing and single support durations are about 0,9%. On the contrary, the values provided for the same parameters by the Xsens algorithm that used the heels signals are overestimated. In detail, the mean differences of swing and single support times are equal to -0,06 s, whereas those of swing and single support duration are about -5,00%. As regards parameters such as stance time, stance duration, double support time and double support duration, the estimates are reversed. The values provided by the Xsens algorithm with trunk are slightly overestimated. The mean differences of stance and double support times are equal to -0,01 s and -0,02 s, respectively; those of stance and double support duration are about -0,8% and -1,85%, respectively. The values of stance time, double support time and their durations identified by the Xsens algorithm with heels are, instead, underestimated. In particular, the mean differences of stance and double support times are equal to 0,06 s and 0,12 s, respectively; those of stance and double support durations are about 5% and 9%, respectively.

In general, the error of the algorithm that used the trunk acceleration is much lower than that of the one that used the heels angular velocities. For the parameters expressed in seconds, the error committed by the algorithm with heels is about six times as great as that committed by the algorithm with trunk. For the parameters expressed as percentage of the gait cycle, the error committed by the algorithm with heels is about five times as great as that committed by the algorithm with trunk. This difference can be explained with the two following figures.

The Figure 4.3.1 and the Figure 4.3.2 show, respectively, the trunk acceleration and the heels angular velocities with the instants of gait events identified by Optitrack. In the first case there is a good correspondence both for the heel-strikes and the toe-off. In the second case there is a good correspondence only for the heel-strikes, because the toe-off identified by the Xsens algorithm anticipates those found by Optitrack. It is important to underline that this difference did not affect the parameters involving only the HS such as stride time, stride frequency, step time, step frequency and foot symmetry. Instead, it affected the parameters combining HS and TO such as stance time, swing time, single support time, double support time and their corresponding durations.

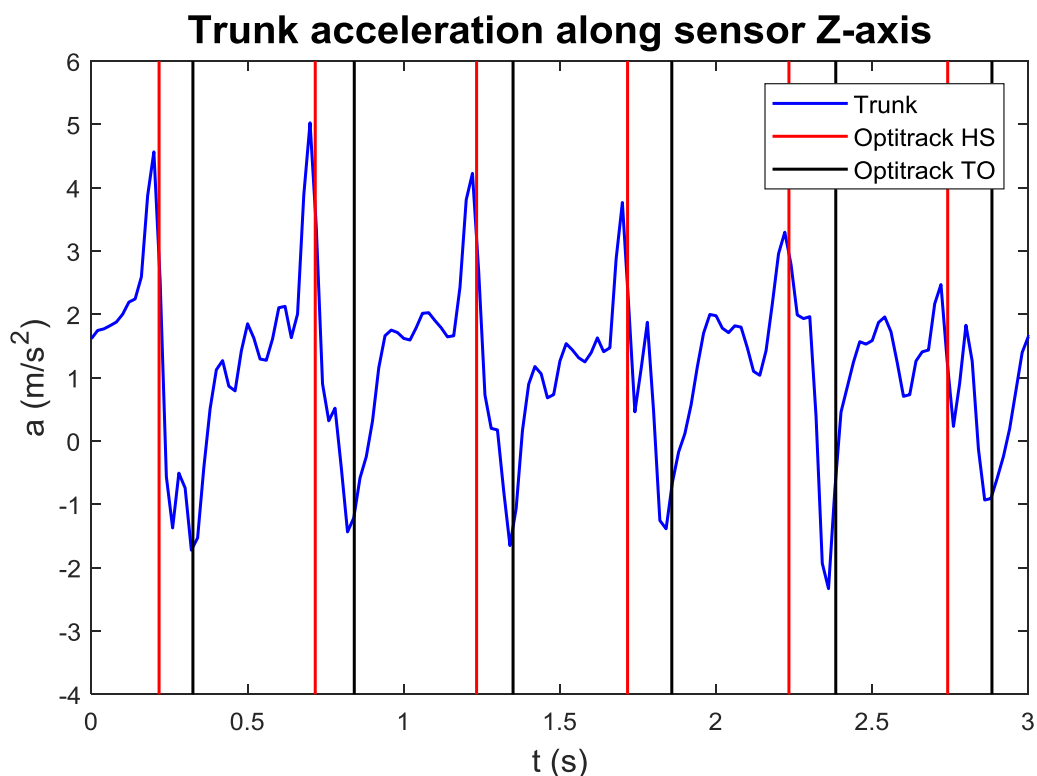


Figure 4.3.1\_Trunk acceleration along sensor Z-axis with HS and TO instants identified by Optitrack.

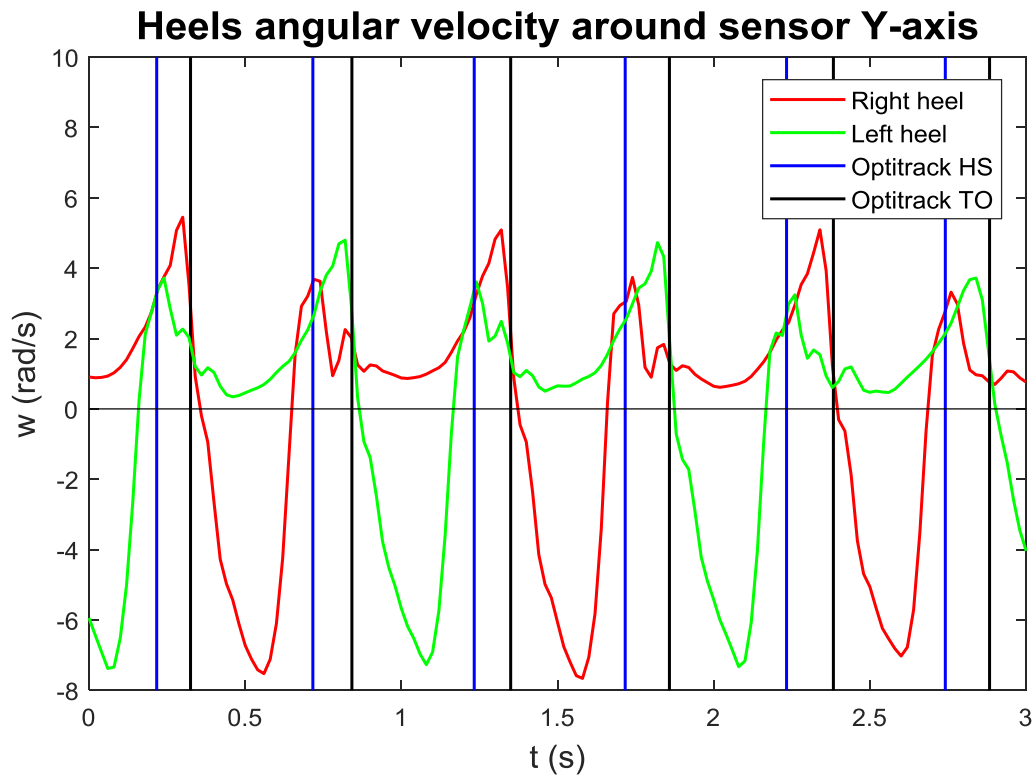


Figure 4.3.2\_Heels angular velocities around sensors Y-axis with HS and TO instants identified by Optitrack.

The limp index represents an exception, because it is the ratio between the two stance times and so it involves both HS and TO. Despite this, since the two stance times are underestimated in the same way, their ratio is however tending to 1. The fact that the Xsens algorithm with heels angular velocity anticipated the instants of the TO can be explained with the position of the sensors. In fact, the two IMUs were placed on the heels and probably they felt the heel-off more than the toe-off. In addition, there are some causes that can be hypothesized in order to justify why the Xsens algorithm with trunk acceleration generated a smaller error:

- The possibility to extract all the parameters from a single sensor and not from the combination of two sensors probably gave results that are more accurate.
- The IMU positioned on the trunk was firmer and more supportive to the subject than the ones on the heels.
- The axes of the sensor placed on the trunk were almost aligned with the global Optitrack ones; on the contrary, the axes of the heels sensors were continuously moving during gait.
- The external event adopted for temporally synchronize the two instrumentations involved the impact of the right heel. This probably moved the sensor, creating asymmetries between the two heels' IMUs and influencing the mixed parameters such as those related to double support.

The differences for both the Xsens algorithms can also be due to the different acquisition frequencies of the two motion capture systems. In fact, Optitrack sampled at 120 Hz, whereas Xsens sampled at 50 Hz. All the considerations made until now are valid also for the trials with dual-task.

The last analysis regards the comparison between the trials with single-task and those with dual-task. The magnitude orders of the parameters are the same for all three methods (Optitrack, Xsens with trunk and Xsens with heels). However, as the tables of the previous subchapter show (Tables 4.2.1 and 4.2.30), there is a slight change in stride time that reveals a change in walking speed. Except for the subjects 1 and 9, all the others have longer stride time with the dual-task. In general among all the subjects, as the bar diagrams presented in the previous subchapter show (Figures 4.2.29, 4.2.30, 4.2.31, 4.2.32, 4.2.33, 4.2.35, 4.2.37 and 4.2.39), it is possible to associate to the dual-task a slight increase in time parameters and a consequent slight decrease in frequencies. The increase of time parameters is of the magnitude order of a few tens of ms. As for the percentage parameters (Figures 4.2.34, 4.2.36, 4.2.38, 4.2.40 and 4.2.41), they also slightly change. For stance and double support durations there is a small increase equal to about 1%, whereas for swing and single support durations there is a small decrease equal to about 1%. Instead, foot symmetry and limp index are almost the same, confirming that the analysed sample did not have neurological or musculoskeletal disorders. As a result, it is possible to speculate that the dual-task slowed the subjects, probably distracting them from the first task of gait.

Finally, it is possible to evaluate the statistical significance of the results and of the differences stressed by the bar diagrams. The p-values  $\leq 0,05$  are those of:

- Optitrack: step frequency (Hz), swing duration (%GC), double support time (s), double support duration (%GC);
- Xsens from heels: stance time (s), double support time (s).

In these cases, the difference found in the two conditions appears to be statistically significant. There are no statistical significant results among those of Xsens algorithm with trunk acceleration. All the p-values are less than 0.9. However, it is important to consider that the p-value is strongly conditioned by the number of the sample. In this case, the number of the sample was only nine and so it was not sufficient to generalize the results. In order to analyse the statistical significance of the results in a correct way, it would be necessary to test a larger amount of samples.

## 5. Test on pathologic subjects

### 5.1 Parkinson's disease

Parkinson's disease (PD) is a movement disorder that can reduce the natural ability to carry out daily activities. This neurological disturb was discovered in 1817 by James Parkinson, from who it took its name. He identified six cases in London and he described their condition as "paralysis agitans". In 1917, 100 years later, it was pointed out that patients with Parkinson's disease loose cells in the substantia nigra (J.Jankovic, 2008). The neurons in this specific region of brain produce a neurotransmitter called dopamine, which guarantees and regulates movements. The lack of dopamine in patients with PD and the ability of injected levodopa to improve their movements were demonstrated in 1961. The Figure 5.1.1 shows the reduction of dopamine in neurons with PD.

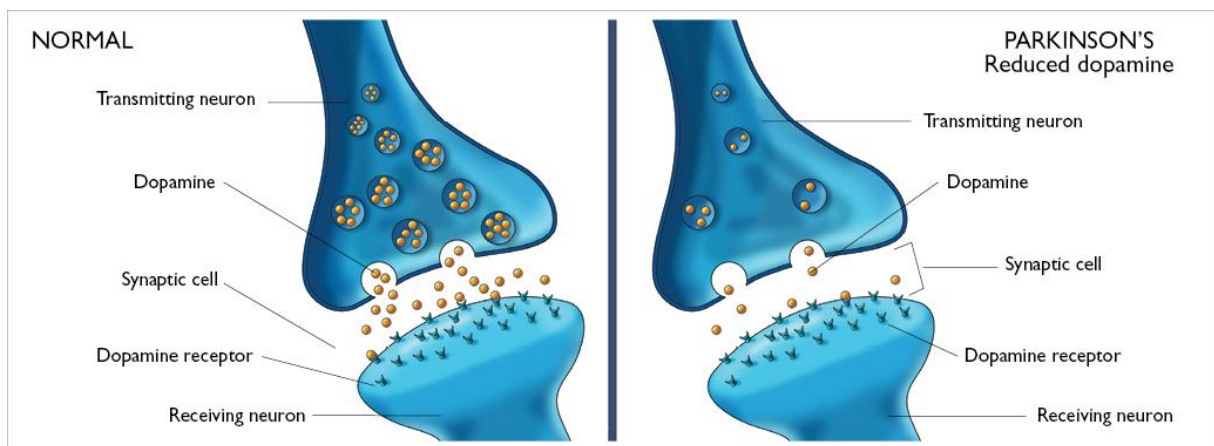


Figure 5.1.1\_ Comparison between normal level and low level of dopamine in a neuron affected by Parkinson's disease.

The acronym TRAP is used to describe the four features of the Parkinson's disease: T for tremor at rest, R for rigidity, A for akinesia and P for postural instability. In addition, also motor blocks called freezing are typical of this pathology.

1. The classic slow tremor of PD occurs at rest. It typically starts in one hand or leg and then affects both sides of the body (D. G. Standaert, 2007). Resting tremor is the first trait of PD and for this reason it represents an important diagnostic parameter.
2. The rigidity afflicts especially the limbs or the torso and at the beginning it may be wrongly attributed to orthopaedic disturbs.
3. The akinesia or bradikinesia defines a general slowness of movements and implies a difficult motor coordination also in simple gestures.
4. The postural instability and the balance problems expose the patient to the risk of falling.

The four features described are defined motor symptoms because they involve movement. In addition, Parkinson’s disease is also characterized by non-motor symptoms:

- Hyposmia (reduced sensitivity to odours) or anosmia (loss of smell)
- Anxiety and depression
- Weight loss
- Urinary and gastrointestinal issues
- Fatigue
- Sleep problems

The causes of Parkinson’s disease are still unknown, but researches think that both genetic and environmental factors are involved. Among genetic factors, the mutation of the gene called LRRK2 occurs. The environment intervenes with the exposure to pesticides and heavy metals. Despite this, the main risk factors are age and sex. PD is more frequent in adults over 50 years old and in women. Furthermore, it affects Caucasians more than other ethnicities.

The Table 5.1.1 sums up the principal symptoms and causes of the Parkinson’s disease:

PARKINSON’S DISEASE	
Symptoms	Causes
<b>Motors:</b>	- Genetic: gene LRRK2
- Tremor	- Environmental: pesticides and heavy metals
- Rigidity	- Age: over 50 years
- Akinesia	- Sex: female
- Postural instability	- Origin: Caucasians
<b>Non-motors:</b>	
- Hyposmia and anosmia	
- Anxiety and depression	
- Weight loss	
- Urinary and gastrointestinal issues	
- Fatigue	
- Sleep problems	

Table 5.1.1\_Symptoms and causes of Parkinson’s disease.

The first diagnosis of Parkinson's disease consists in examining the neurological disturbs and in listening the daily problems of the patient. In addition, also the functional magnetic resonance imaging (fMRI) and the positron emission tomography (PET) can be used in order to assist the diagnosis of Parkinson.

Although currently there is no cure for the Parkinson's disease, there are several methods that guarantee a successful treatment. The most common medicament is the Carbidopa-levodopa. Taken orally, it increases brain level of dopamine. Levodopa is a precursor which is converted in dopamine in the brain. In this way, it reduces tremor, rigidity and slow movements. Carbidopa is very useful because it prevents levodopa to be broken down before it reaches the brain.

Another new therapy used for the treatment of Parkinsonian patients is the Deep Brain Stimulation (DBS). Only the 5-10% of the patients with PD is idoneous for the implantation of the device. They have symptoms which cannot be adequately controlled with medications. As the Figure 5.1.2 shows, the device for the DBS consists of three components:

- The lead, which is an electrode positioned in the brain.
- The extension, which is a wire under the skin of the head, the neck and the shoulder in order to connect the lead to the neurostimulator.
- The pacemaker or neurostimulator, which is placed subcutaneously in the anterior and superior region of the thorax.

Once the system is in loco, electrical impulses sent from the generator into the brain reduce abnormal electrical signals and alleviate PD motor symptoms.

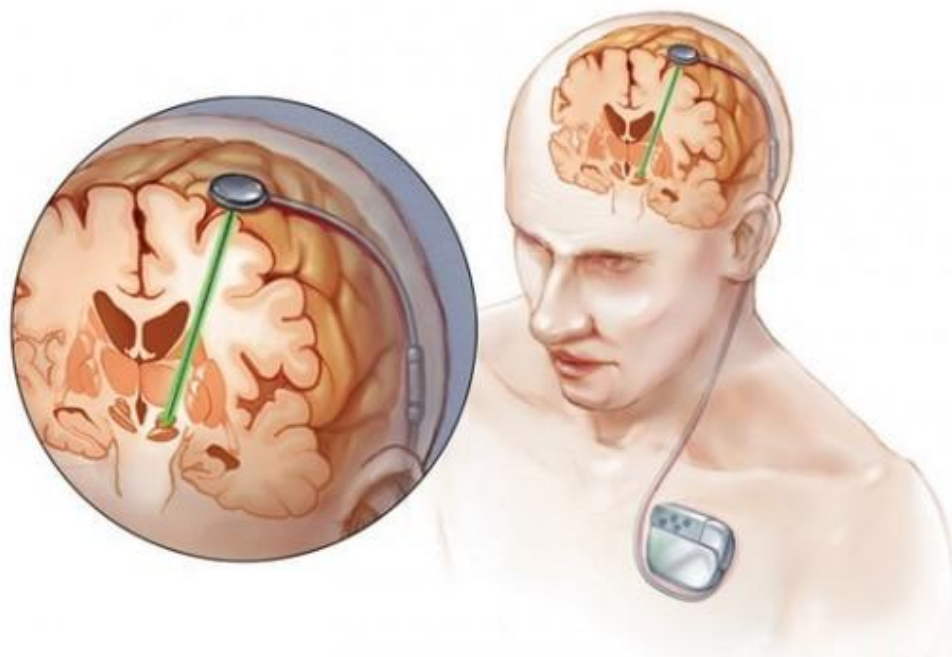
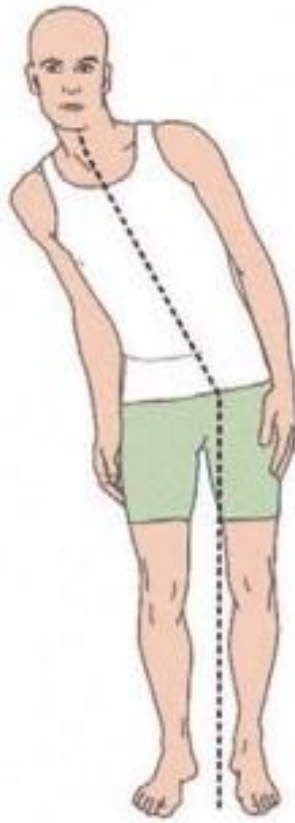


Figure 5.1.2\_The scheme of the DBS device.

Sometimes, the incorrect posture of patients with PD can worsen until it results in the Pisa syndrome. It determines the lateral flexion of the trunk of at least ten degrees, as the Figure 5.1.3 shows. This flexion does not depend on skeletal changes in the spine and it is variable with the position of the body. Due to an altered perception of the body scheme in space, there is an asymmetric activation of the paravertebral musculature on one side. One of the treatments adopted for the Pisa syndrome is the injection of botulinum toxin in muscles. It is pumped in with electromyographic or ultrasonographic guidance into the hyperactive muscles of the flex trunk side in order to weak them.



**Figure 5.1.3\_The typical posture of a patient with Pisa syndrome.**

## 5.2 Materials and methods

In collaboration with the Department of Neurorehabilitation of the Molinette Hospital, five patients with Parkinson's disease, four males and one female, were included for the test. All of them are treated with the mouth therapy based on levodopa. Furthermore, four of them are treated with Deep Brain Stimulation (DBS) and one is subjected to botulinum toxin infiltrations. All the subjects gave their written informed consent before the beginning of the experiment. They were informed about the methods, about the purpose of the experiment and about the absence of the invasiveness during the test.

The following Table 5.2.1 shows the main anthropometric data and the treatments of the five patients. Data are presented as average and standard deviation of the total number of subjects.

<b>Patients</b>	<b>Mean <math>\pm</math> SD</b>
Age (years)	58.8 $\pm$ 3.8
Height (cm)	170.0 $\pm$ 0.1
Body mass (Kg)	84.0 $\pm$ 20.4
BMI	28.6 $\pm$ 6.3

**Table 5.2.1\_Anthropometric data of participants: age, height, body mass and BMI.**

The same three Xsens inertial sensors used for the healthy subjects were placed on the body of the patients, as the Figure 5.2.1 shows. Two of them were positioned on the heels using a self-adhesive gauze, which was well stretched so as to keep them still. The third sensor was placed medially on the trunk through an elastic band supplied in the kit. All the three IMUs were oriented with the local vertical axis pointing downward (x-axis), the local medio-lateral axis directed to the right side of the participants (y-axis) and the local anterior-posterior axis pointing in the opposite direction to that of the gait (z-axis). The inertial sensors were connected to each other and to the Xbus Master via cables. It was important to accommodate cables in such a way they did not hinder the subjects during the gait. The connection between the Xbus Master and the PC was guaranteed by Bluetooth.

The experiment was conducted in a laboratory of the Department of Neurorehabilitation of the Molinette Hospital. The patients were asked to walk barefoot along a gangway of seven meters at their preferred normal speed, as the Figure 5.2.2 shows. The number of transitions requested depended on the conditions, the age and the degree of the disease of each patient. All the subjects were always accompanied by a nurse who controlled they did not stumble and fall.

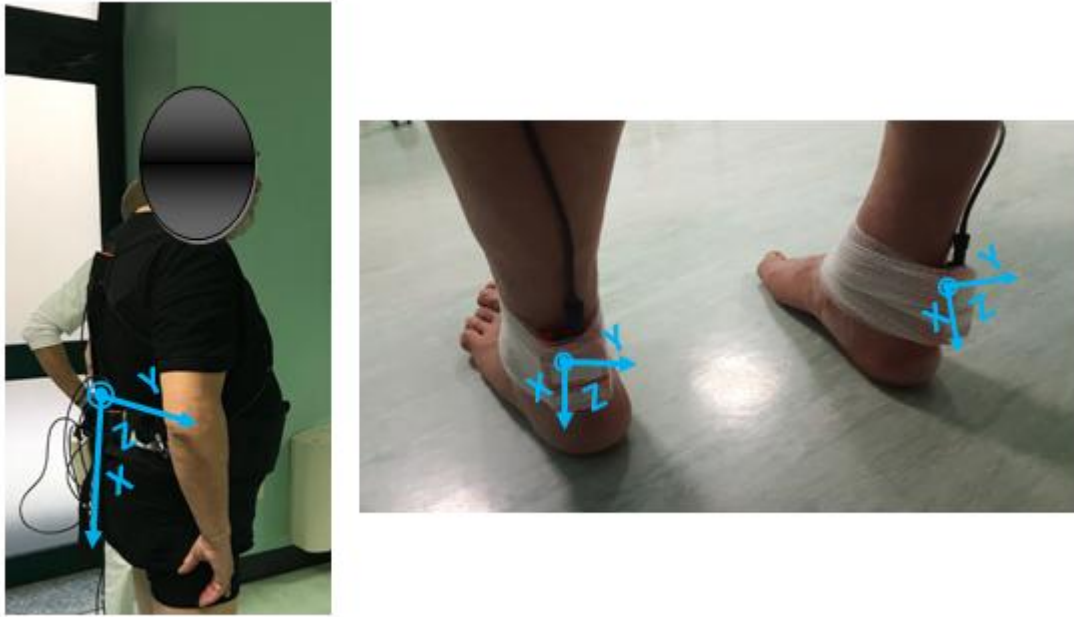


Figure 5.2.1\_The configuration of Xsens MTx on the trunk and on the heels with their local axes.



Figure 5.2.2\_An example of a patient walking along the gangway with the nurse near him.

### 5.3 Data analysis

The inertial sensors signals were processed in the same way of those of healthy subjects. When too much corrupted by noise, they were filtered using a low pass 4th order Butterworth filter with a cut-off frequency of 30 Hz. This frequency was chosen on the basis of the power spectral density of the signals. The axes were rotated and overturned in order to obtain a Cartesian triad with x-axis pointing upward, y-axis pointing to the right side of the subjects and z-axis pointing in the same direction of the gait.

The same two Matlab functions created for the healthy subjects were used: one for the identification of gait events from the anterior-posterior acceleration of the trunk and one for the identification of gait events from the sagittal angular velocity of heels. The Figures 5.3.1 and 5.3.2 show the two algorithms proposed.

Then, the same Matlab routine adopted for the test with healthy subjects was used in order to estimate the following spatio-temporal parameters of gait both for right and left sides:

- Stride time (s)
- Stride frequency (Hz)
- Step time (s)
- Step frequency (Hz)
- Stance time (s)
- Stance duration (%GC)
- Swing time (s)
- Swing duration (%GC)
- Single support time (s)
- Single support duration (%GC)
- Double support time (s)
- Double support duration (%GC)
- Foot symmetry (%GC)
- Limp index

The foot symmetry was calculated as the ratio between the step time and the stride time, whereas the limp index was estimated as the ratio between right and left stance times.

### Trunk acceleration along sensor Z-axis with HS and TO

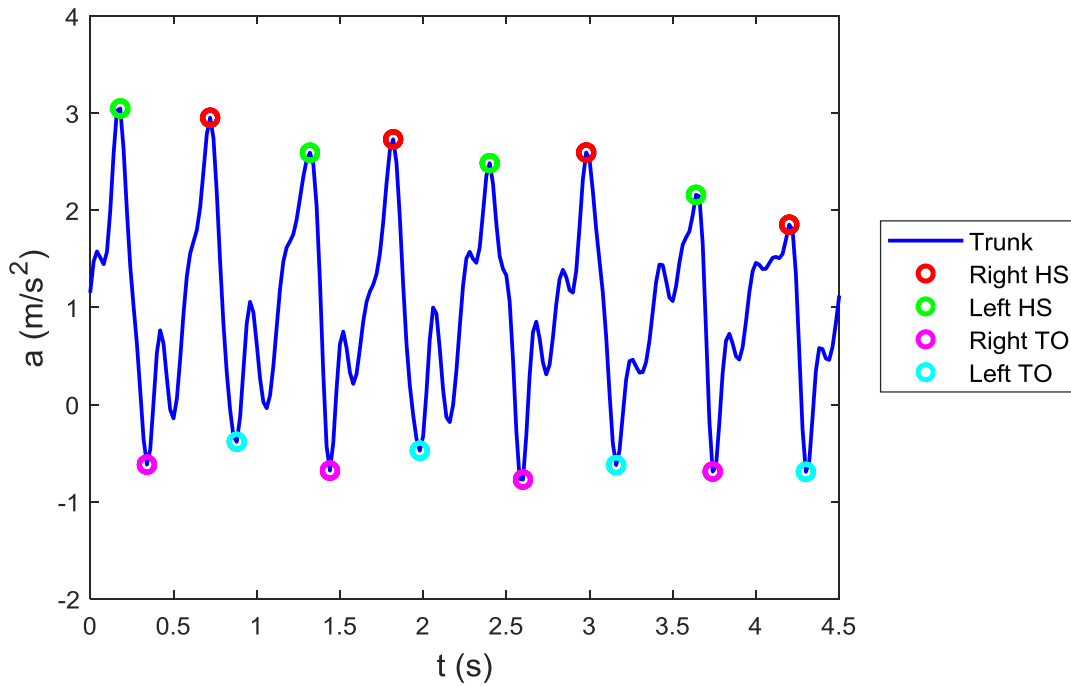


Figure 5.3.1\_An example of identification of gait events from anterior-posterior acceleration of trunk sensor.

### Heels angular velocity around sensor Y-axis with HS and TO

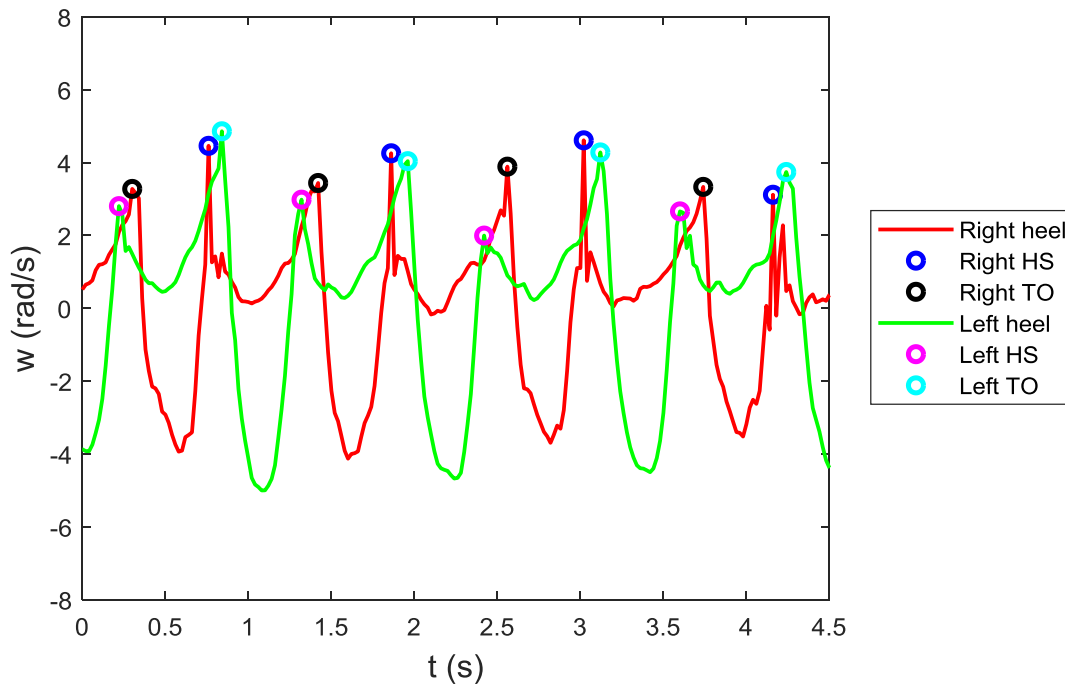


Figure 5.3.2\_An example of identification of gait events from sagittal angular velocity of heels sensors.

### 5.3.1 Patient 1 (Parkinson's disease, DBS)

The patient 1 is a man of 61 years old with Parkinson's disease. He is 170 cm tall and he weighs 60 Kg. He receives the Deep Brain Stimulation treatment. The doctors wanted to evaluate the changes in his movements and his speech by stimulating his neurons with three different frequencies: 125 Hz, 60 Hz and 30 Hz. For each frequency they asked him to walk on the gangway twice. Then, after the change of the frequency of stimulation, it was necessary to wait 20 minutes before repeating the test. The Figure 5.3.3 shows the patient 1 walking along the gangway.



Figure 5.3.3\_The patient 1 walking along the gangway.

The following three tables (from Table 5.3.1 to Table 5.3.3) show the spatio-temporal parameters estimated from both the trunk and the heels at three different frequencies of stimulation DBS. They contain the mean and the standard deviation values obtained from the two transitions made by the patient. The following three figures (from Figure 5.3.4 to Figure 5.3.6) show the bar diagrams of the most important spatio-temporal parameters for all the three frequencies and the two algorithms.

Patient 1	125 Hz							
	Algorithm from trunk				Algorithm from heels			
	Right		Left		Right		Left	
	Mean	SD	Mean	SD	Mean	SD	Mean	SD
Stride time (s)	1,17	0,05	1,17	0,06	1,17	0,02	1,17	0,05
Stride frequency (Hz)	0,85	0,04	0,85	0,04	0,85	0,02	0,85	0,04
Step time (s)	0,59	0,04	0,58	0,01	0,56	0,04	0,61	0,00
Step frequency (Hz)	1,70	0,13	1,72	0,03	1,79	0,13	1,63	0,01
Stance time (s)	0,76	0,03	0,75	0,04	0,70	0,02	0,67	0,06
Stance duration (%GC)	64,67	0,35	64,01	0,28	60,14	0,57	57,37	3,02
Swing time (s)	0,42	0,02	0,42	0,01	0,47	0,00	0,50	0,02
Swing duration (%GC)	35,69	0,12	36,21	1,11	39,96	0,88	42,69	3,18
Single support time (s)	0,42	0,02	0,42	0,02	0,50	0,02	0,48	0,00
SS duration (%GC)	35,77	0,07	35,69	0,12	42,54	3,38	40,55	1,72
Double support time (s)	0,33	0,03	0,33	0,03	0,20	0,05	0,20	0,05
DS duration (%GC)	28,10	0,99	28,10	0,99	17,35	4,06	17,35	4,06
Foot symmetry (%GC)	50,60	2,09	49,68	1,03	47,94	2,29	52,39	1,63
Limp index (right/left)	1,01	0,02	1,01	0,02	1,05	0,07	1,05	0,07

Table 5.3.1\_Spatio-temporal parameters for patient 1 at 125 Hz.

Patient 1	60 Hz							
	Algorithm from trunk				Algorithm from heels			
	Right		Left		Right		Left	
	Mean	SD	Mean	SD	Mean	SD	Mean	SD
Stride time (s)	1,15	0,02	1,12	0,04	1,11	0,02	1,11	0,04
Stride frequency (Hz)	0,87	0,02	0,90	0,02	0,90	0,02	0,90	0,03
Step time (s)	0,59	0,04	0,55	0,01	0,57	0,01	0,54	0,04
Step frequency (Hz)	1,76	0,12	1,89	0,05	1,76	0,02	1,84	0,13
Stance time (s)	0,74	0,00	0,73	0,02	0,68	0,01	0,65	0,01
Stance duration (%GC)	64,62	0,45	64,01	0,23	60,77	0,24	57,30	1,00
Swing time (s)	0,40	0,02	0,40	0,00	0,44	0,01	0,47	0,01
Swing duration (%GC)	35,70	1,06	36,21	1,04	39,67	0,08	42,69	0,25
Single support time (s)	0,40	0,01	0,40	0,02	0,47	0,01	0,44	0,02
SS duration (%GC)	35,77	0,00	35,56	1,06	42,54	0,25	39,97	0,49
Double support time (s)	0,34	0,01	0,34	0,01	0,20	0,00	0,20	0,00
DS duration (%GC)	28,12	0,02	28,12	0,02	17,33	0,33	17,33	0,33
Foot symmetry (%GC)	53,25	2,55	49,03	1,77	50,71	1,66	48,16	2,64
Limp index (right/left)	1,04	0,03	1,04	0,03	1,04	0,01	1,04	0,01

Table 5.3.2\_Spatio-temporal parameters for patient 1 at 60 Hz.

Patient 1	30 Hz							
	Algorithm from trunk				Algorithm from heels			
	Right		Left		Right		Left	
	Mean	SD	Mean	SD	Mean	SD	Mean	SD
Stride time (s)	1,03	0,02	1,09	0,04	1,07	0,01	1,10	0,02
Stride frequency (Hz)	0,97	0,02	0,90	0,05	0,94	0,01	0,91	0,02
Step time (s)	0,49	0,09	0,61	0,02	0,52	0,00	0,56	0,02
Step frequency (Hz)	2,09	0,35	1,74	0,17	1,92	0,01	1,81	0,05
Stance time (s)	0,68	0,03	0,66	0,04	0,62	0,01	0,61	0,01
Stance duration (%GC)	65,70	4,21	59,03	0,13	57,86	0,36	55,28	0,34
Swing time (s)	0,36	0,04	0,45	0,01	0,45	0,01	0,48	0,00
Swing duration (%GC)	33,23	2,39	40,13	2,70	41,52	0,15	44,60	0,49
Single support time (s)	0,44	0,05	0,36	0,04	0,48	0,00	0,46	0,00
SS duration (%GC)	38,75	1,32	33,23	2,39	44,60	0,49	43,00	0,36
Double support time (s)	0,29	0,02	0,29	0,02	0,15	0,00	0,15	0,00
DS duration (%GC)	26,64	0,31	26,64	0,31	13,88	0,34	13,88	0,34
Foot symmetry (%GC)	47,71	10,18	55,84	3,96	48,78	1,06	52,45	0,20
Limp index (right/left)	1,05	0,11	1,05	0,11	1,01	0,01	1,01	0,01

Table 5.3.3\_Spatio-temporal parameters for patient 1 at 30 Hz.

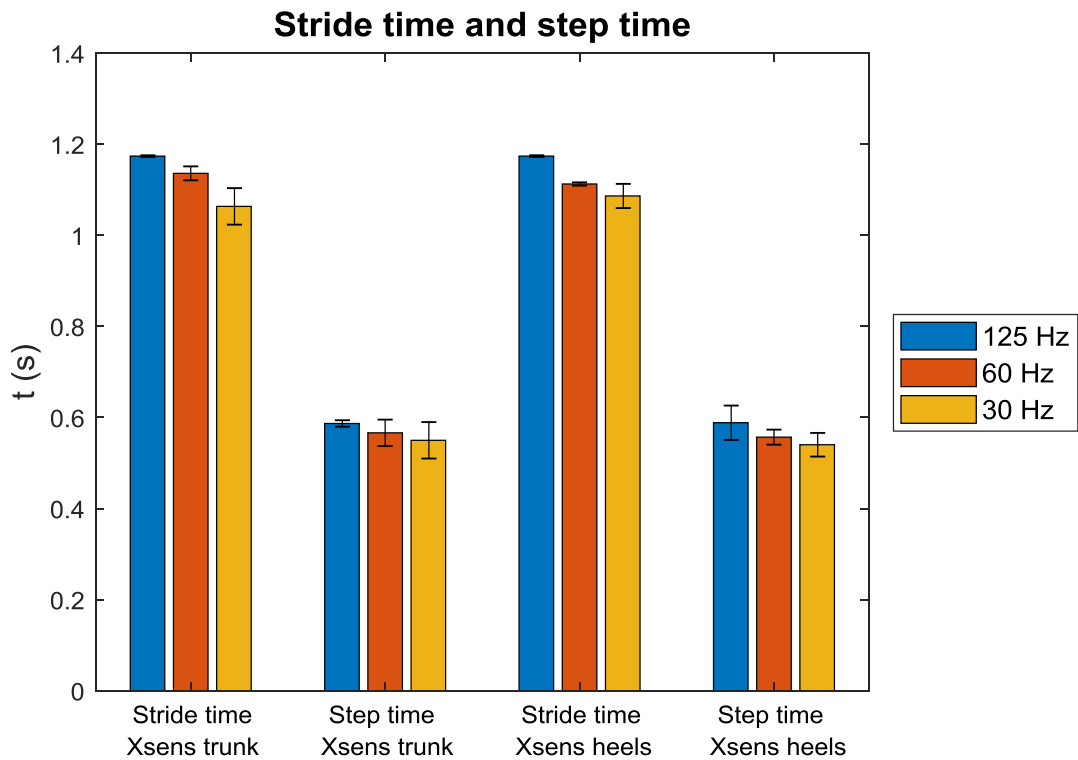


Figure 5.3.4\_Stride and step times for all the three stimulation frequencies and for both the algorithms.

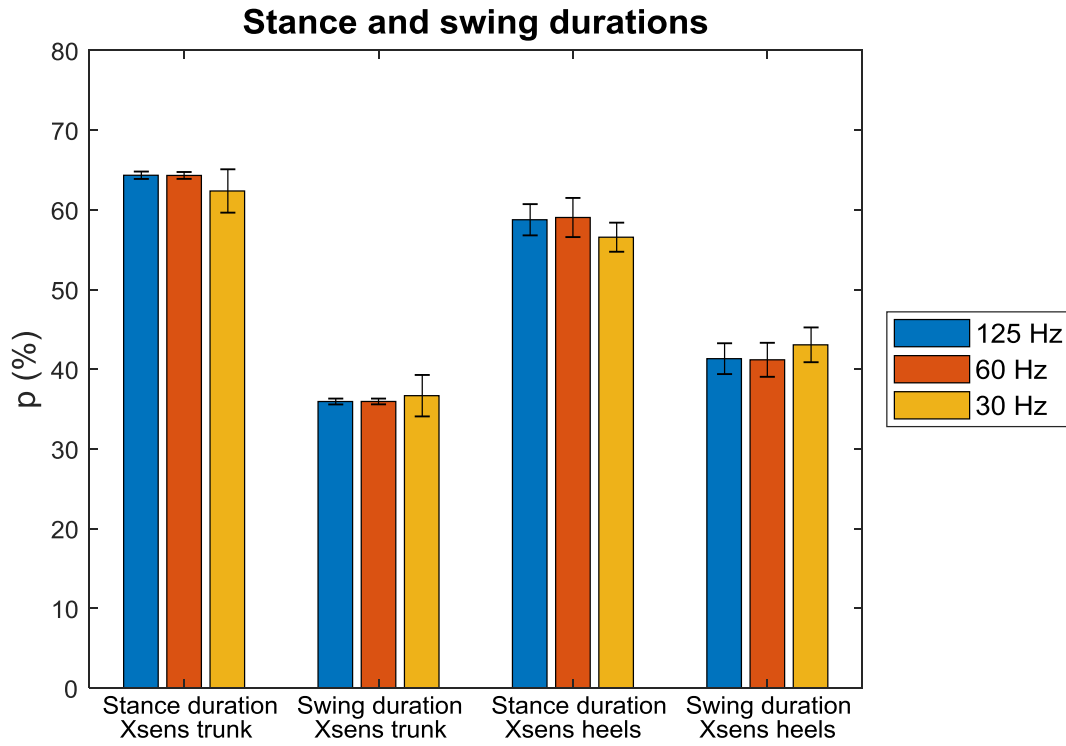


Figure 5.3.5 Stance and swing durations for all the three stimulation frequencies and for both the algorithms.

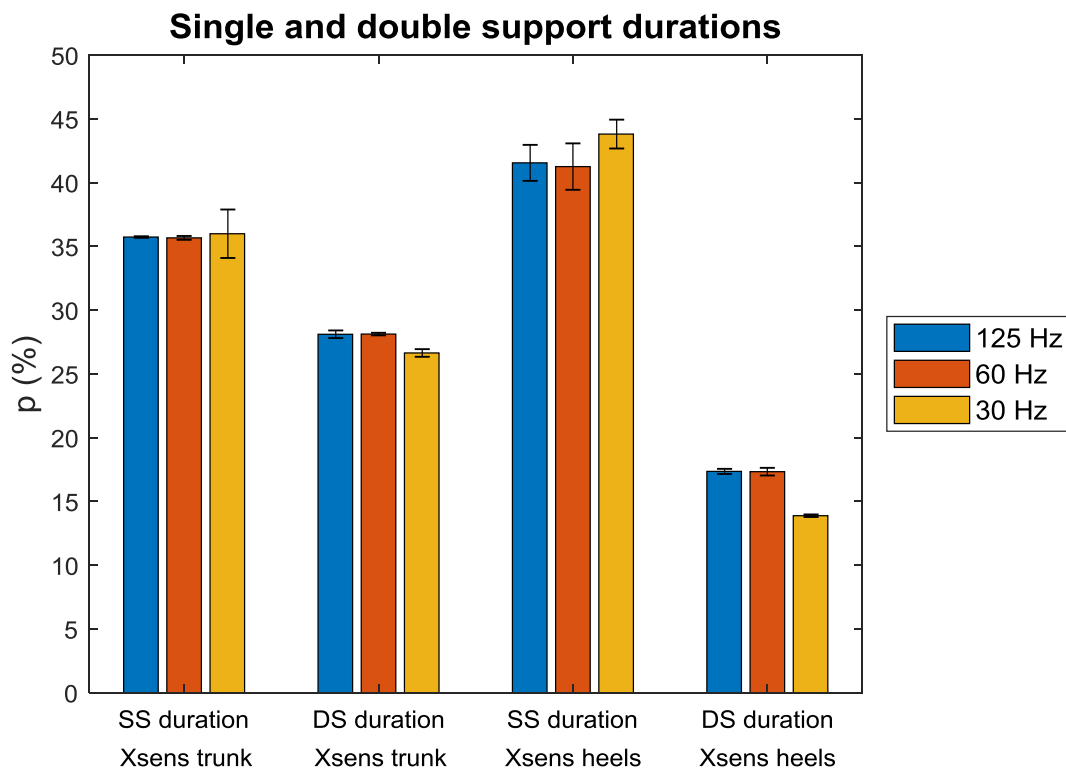


Figure 5.3.6 Single support and double support durations for all the three stimulation frequencies and for both the algorithms.

### 5.3.2 Patient 2 (Parkinson's disease Pisa syndrome, botulinum toxin)

The patient 2 is a man of 58 years old with Parkinson's disease and Pisa syndrome. He is 187 cm tall and he weighs 80 Kg. He is subjected to cycles of botulinum toxin injections. The doctors wanted to evaluate the changes in his movements after a period of infiltrations. They asked him to walk twice along the gangway, as the Figure 5.3.7 shows.



Figure 5.3.7\_The patient 2 walking along the gangway.

The following Table 5.3.4 shows the spatio-temporal parameters estimated from both the trunk and the heels. It contains the mean and the standard deviation values obtained from the two transitions made by the patient.

Patient 2	Algorithm from trunk				Algorithm from heels			
	Right		Left		Right		Left	
	Mean	SD	Mean	SD	Mean	SD	Mean	SD
<b>Stride time (s)</b>	1,14	0,00	1,16	0,03	1,14	0,01	1,15	0,02
<b>Stride frequency (Hz)</b>	0,87	0,00	0,87	0,02	0,88	0,01	0,87	0,02
<b>Step time (s)</b>	0,52	0,00	0,63	0,01	0,56	0,01	0,58	0,02
<b>Step frequency (Hz)</b>	1,94	0,01	1,58	0,03	1,80	0,03	1,73	0,07
<b>Stance time (s)</b>	0,74	0,00	0,72	0,03	0,66	0,01	0,63	0,03
<b>Stance duration (%GC)</b>	64,72	0,23	62,25	0,78	58,16	0,52	54,99	1,43
<b>Swing time (s)</b>	0,41	0,00	0,43	0,00	0,48	0,01	0,51	0,00
<b>Swing duration (%GC)</b>	35,68	0,42	37,41	0,19	42,01	1,23	45,01	0,89
<b>Single support time (s)</b>	0,43	0,00	0,41	0,00	0,51	0,00	0,49	0,00
<b>SS duration (%GC)</b>	36,93	0,60	35,68	0,42	45,01	0,89	42,89	0,83
<b>Double support time (s)</b>	0,31	0,01	0,31	0,01	0,15	0,03	0,15	0,03
<b>DS duration (%GC)</b>	26,91	0,61	26,91	0,61	12,98	2,12	12,98	2,12
<b>Foot symmetry (%GC)</b>	44,88	1,49	55,07	0,13	48,68	0,93	50,23	2,18
<b>Limp index (right/left)</b>	1,03	0,04	1,03	0,04	1,05	0,02	1,05	0,02

Table 5.3.4\_Spatio-temporal parameters for patient 2.

### 5.3.3 Patient 3 (Parkinson's disease, DBS)

The patient 3 is a woman of 59 years old with Parkinson's disease. She is 150 cm tall and she weighs 76 Kg. She receives the Deep Brain Stimulation treatment. The doctors wanted to evaluate the changes in her movements and her speech by stimulating her neurons with two different frequencies: 130 Hz and 60 Hz. For each frequency they asked her to walk on the gangway four times. Then, after the change of the frequency of stimulation, it was necessary to wait 20 minutes before repeating the test. The patient was not able to walk alone and for this reason she needed the help of two people as a support.

The Figure 5.3.8 shows the patient 1 walking along the gangway.



Figure 5.3.8\_The patient 3 walking along the gangway.

Even if cleaned up by noise, the signal from the sensor on the trunk had a strange trend (Figure 5.3.9). For this reason it was not possible to apply the first Xsens algorithm. The data presented in the following Table 5.3.5 are related to the parameters estimated from the heels angular velocities at two different stimulation frequencies.

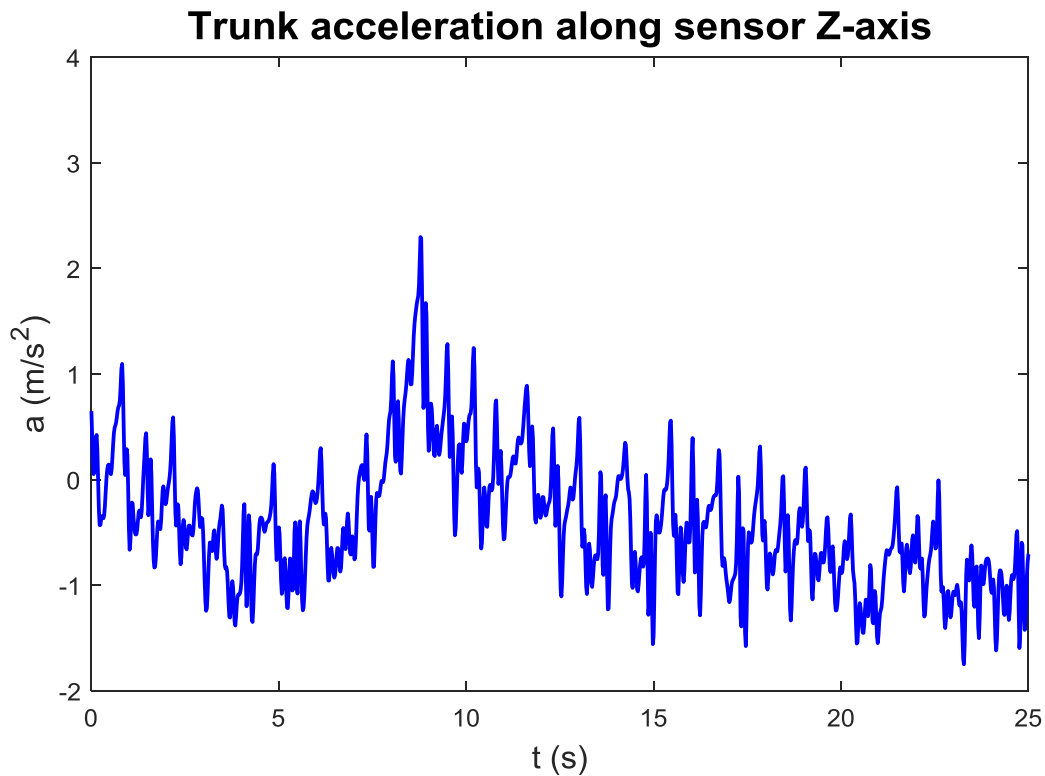


Figure 5.3.9\_The trunk anterior-posterior acceleration of patient 3.

Patient 3	Algorithm from heels							
	130 Hz				60 Hz			
	Right		Left		Right		Left	
	Mean	SD	Mean	SD	Mean	SD	Mean	SD
Stride time (s)	1,38	0,08	1,38	0,08	1,51	0,12	1,52	0,12
Stride frequency (Hz)	0,73	0,04	0,73	0,04	0,67	0,05	0,66	0,05
Step time (s)	0,74	0,05	0,64	0,04	0,82	0,05	0,70	0,07
Step frequency (Hz)	1,36	0,10	1,60	0,08	1,23	0,08	1,46	0,15
Stance time (s)	0,82	0,06	0,88	0,08	0,86	0,09	0,97	0,09
Stance duration (%GC)	59,18	0,85	63,60	3,23	57,20	2,83	63,86	2,10
Swing time (s)	0,56	0,03	0,50	0,03	0,65	0,06	0,54	0,05
Swing duration (%GC)	40,58	0,91	36,26	2,45	42,80	2,49	35,87	1,97
Single support time (s)	0,52	0,03	0,56	0,03	0,56	0,04	0,63	0,03
SS duration (%GC)	37,35	1,68	40,63	0,96	37,17	2,54	41,69	2,32
Double support time (s)	0,32	0,05	0,32	0,05	0,32	0,04	0,32	0,04
DS duration (%GC)	23,16	3,29	23,16	3,29	21,33	1,02	21,33	1,02
Foot symmetry (%GC)	53,70	1,33	46,49	2,53	54,84	1,89	46,40	1,75
Limp index (right/left)	0,94	0,04	0,94	0,04	0,90	0,08	0,90	0,08

Table 5.3.5\_Spatio-temporal parameters for patient 3.

### 5.3.4 Patient 4 (Parkinson's disease, DBS)

The patient 4 is a man of 63 years old with Parkinson's disease. He is 173 cm tall and he weighs 79 Kg. He receives the Deep Brain Stimulation treatment. The doctors wanted to evaluate the changes in his movements and his speech by stimulating his neurons with two different frequencies: 130 Hz and 60 Hz. For each frequency they asked him to walk on the gangway three times. Then, after the change of the frequency of stimulation, it was necessary to wait 20 minutes before repeating the test. The Figure 5.3.10 shows the patient 4 walking along the gangway.



Figure 5.3.10\_ The patient 4 walking along the gangway.

The following two tables (Table 5.3.6 and Table 5.3.7) show the spatio-temporal parameters estimated from both the trunk and the heels at two different DBS stimulation frequencies. They contain the mean and the standard deviation values obtained from the three transitions made by the patient. The following three figures (from Figure 5.3.11 to Figure 5.3.13) show the bar diagrams of the most important spatio-temporal parameters for both the stimulation frequencies and for both the algorithms.

Patient 4	130 Hz							
	Algorithm from trunk				Algorithm from heels			
	Right		Left		Right		Left	
	Mean	SD	Mean	SD	Mean	SD	Mean	SD
Stride time (s)	1,04	0,02	1,04	0,01	1,00	0,06	0,98	0,04
Stride frequency (Hz)	0,95	0,04	0,97	0,01	1,01	0,05	1,03	0,04
Step time (s)	0,57	0,07	0,48	0,05	0,49	0,03	0,50	0,01
Step frequency (Hz)	1,82	0,15	2,12	0,22	2,07	0,14	2,03	0,03
Stance time (s)	0,63	0,01	0,68	0,07	0,53	0,01	0,54	0,01
Stance duration (%GC)	63,84	1,06	69,47	7,17	55,12	0,46	55,59	0,58
Swing time (s)	0,36	0,01	0,30	0,07	0,44	0,01	0,43	0,00
Swing duration (%GC)	36,77	1,20	30,55	7,15	45,07	0,82	44,48	0,54
Single support time (s)	0,32	0,04	0,36	0,01	0,43	0,00	0,44	0,01
SS duration (%GC)	32,41	4,43	36,77	1,20	40,44	0,54	45,08	0,81
Double support time (s)	0,32	0,06	0,32	0,06	0,10	0,01	0,10	0,01
DS duration (%GC)	32,68	5,95	32,68	5,95	12,45	1,22	12,45	1,22
Foot symmetry (%GC)	49,97	3,29	49,50	2,85	47,99	0,77	51,60	0,53
Limp index (right/left)	0,93	0,11	0,93	0,11	0,99	0,01	0,99	0,01

Table 5.3.6\_Spatio-temporal parameters for patient 4 at 130 Hz.

Patient 4	60 Hz							
	Algorithm from trunk				Algorithm from heels			
	Right		Left		Right		Left	
	Mean	SD	Mean	SD	Mean	SD	Mean	SD
Stride time (s)	0,99	0,00	0,98	0,00	0,97	0,01	0,97	0,01
Stride frequency (Hz)	1,01	0,00	1,02	0,00	1,03	0,01	1,03	0,01
Step time (s)	0,50	0,03	0,49	0,03	0,47	0,01	0,50	0,01
Step frequency (Hz)	2,02	0,12	2,05	0,12	2,14	0,03	1,99	0,03
Stance time (s)	0,66	0,10	0,68	0,02	0,54	0,03	0,57	0,02
Stance duration (%GC)	62,02	5,39	65,51	1,50	53,97	0,07	52,07	0,58
Swing time (s)	0,44	0,02	0,36	0,01	0,45	0,02	0,42	0,02
Swing duration (%GC)	42,00	2,69	34,63	1,34	45,96	0,38	45,52	0,43
Single support time (s)	0,37	0,01	0,44	0,02	0,42	0,03	0,45	0,03
SS duration (%GC)	35,65	1,10	42,00	2,69	42,88	0,95	45,40	1,18
Double support time (s)	0,25	0,04	0,25	0,04	0,11	0,00	0,11	0,00
DS duration (%GC)	23,37	2,81	23,37	2,81	11,53	0,81	11,53	0,81
Foot symmetry (%GC)	52,87	3,81	44,93	6,28	49,60	0,57	50,77	2,05
Limp index (right/left)	0,98	0,15	0,98	0,15	0,95	0,08	0,95	0,02

Table 5.3.7\_Spatio-temporal parameters for patient 4 at 60 Hz.

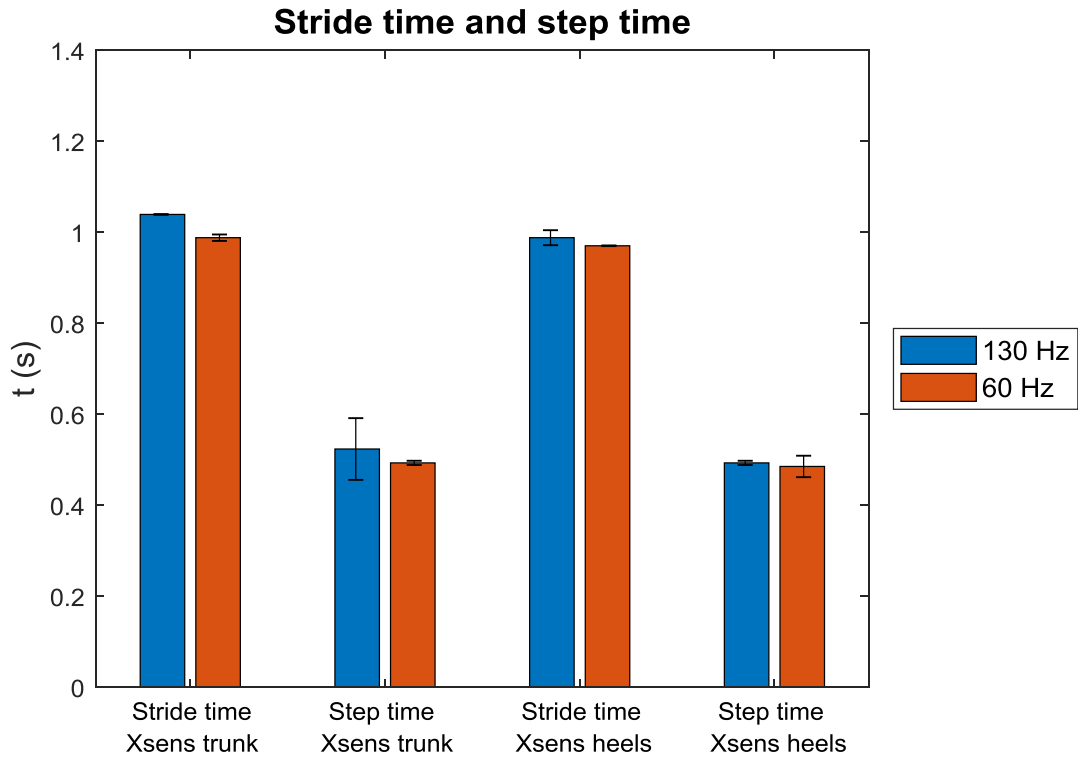


Figure 5.3.11\_Stride and step times for both the stimulation frequencies and for both the algorithms.

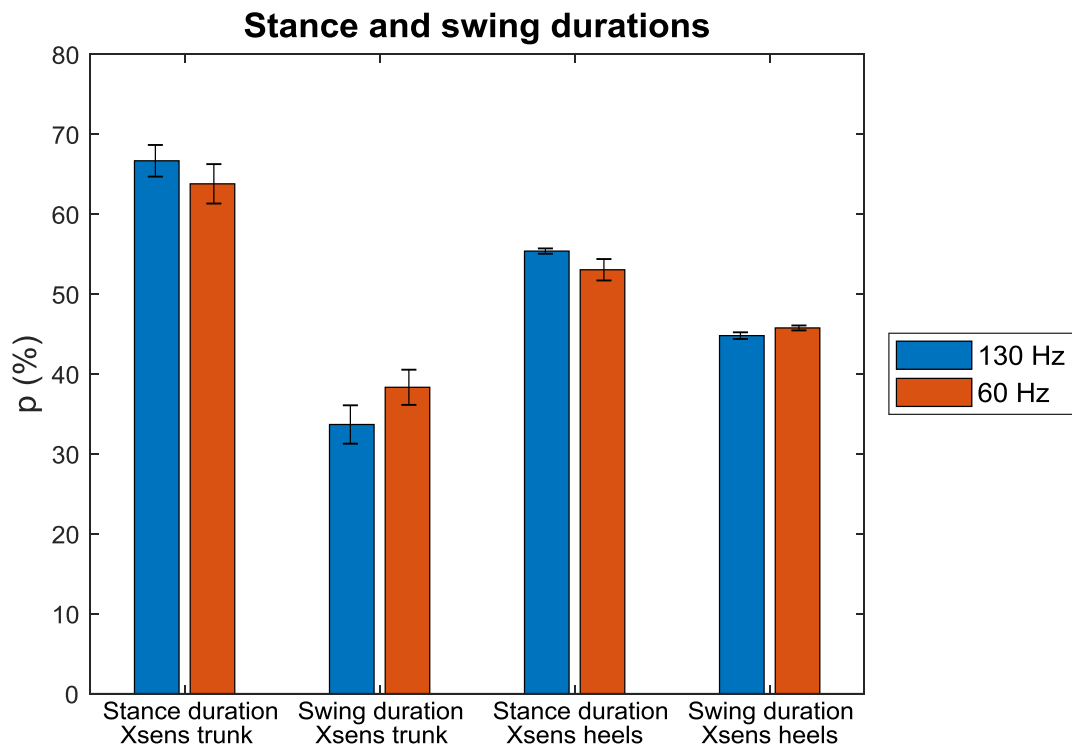


Figure 5.3.12\_ Stance and swing durations for both the stimulation frequencies and for both the algorithms.

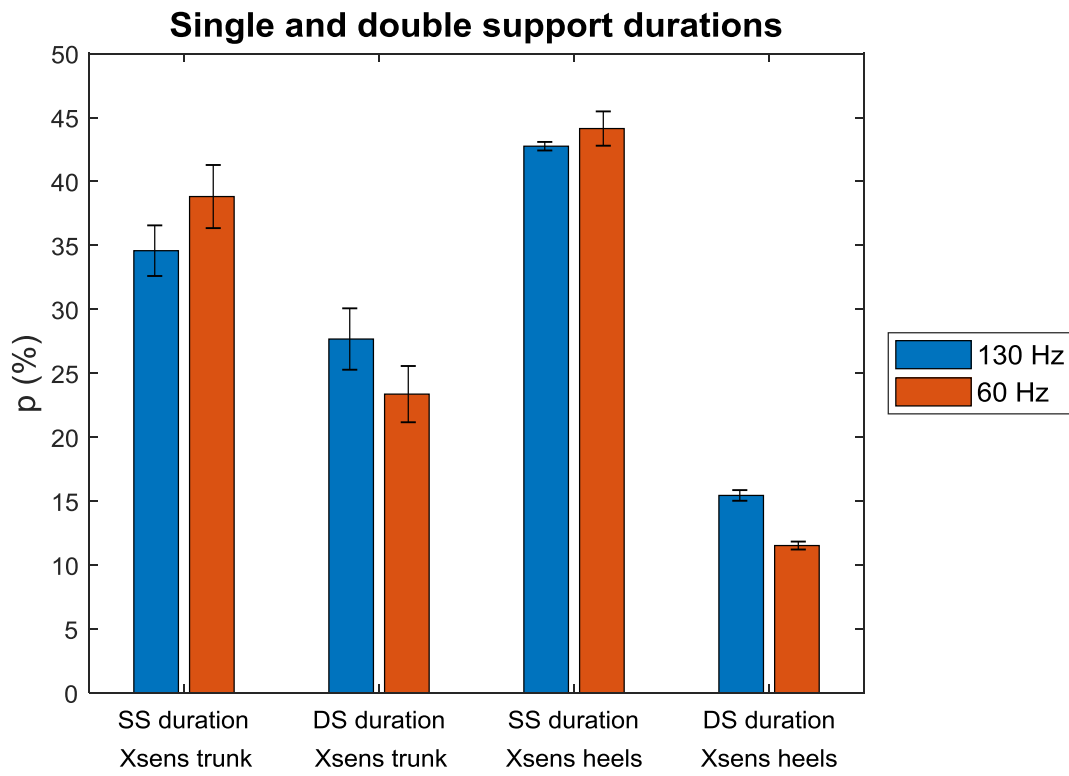


Figure 5.3.13\_ Single and double support durations for both the stimulation frequencies and for both the algorithms.

### 5.3.5 Patient 5 (Parkinson's disease, DBS)

The patient 5 is a man of 53 years old with Parkinson's disease. He is 178 cm tall and he weighs 115 Kg. He receives the Deep Brain Stimulation treatment. The doctors wanted to evaluate his movements and his speech by stimulating his neurons with a frequency of 130 Hz. They asked him to walk on the gangway four times. The Figure 5.3.14 shows the patient 5 walking along the gangway.



Figure 5.3.14\_ The patient 5 walking along the gangway.

The following Table 5.3.8 shows the spatio-temporal parameters estimated from both the trunk and the heels. It contains the mean and the standard deviation values obtained from the four transitions made by the patient.

Patient 5	Algorithm from trunk				Algorithm from heels			
	Right		Left		Right		Left	
	Mean	SD	Mean	SD	Mean	SD	Mean	SD
<b>Stride time (s)</b>	1,04	0,00	1,06	0,03	1,04	0,04	1,03	0,02
<b>Stride frequency (Hz)</b>	0,96	0,00	0,94	0,03	0,96	0,04	0,97	0,02
<b>Step time (s)</b>	0,50	0,03	0,55	0,05	0,52	0,02	0,52	0,01
<b>Step frequency (Hz)</b>	1,99	0,11	1,83	0,16	1,94	0,09	1,93	0,05
<b>Stance time (s)</b>	0,64	0,03	0,65	0,01	0,59	0,03	0,57	0,02
<b>Stance duration (%GC)</b>	61,42	2,81	61,46	2,83	56,77	0,85	55,90	1,33
<b>Swing time (s)</b>	0,40	0,01	0,41	0,04	0,45	0,01	0,46	0,01
<b>Swing duration (%GC)</b>	38,46	1,98	39,39	2,96	43,41	0,70	44,42	1,43
<b>Single support time (s)</b>	0,40	0,02	0,40	0,01	0,46	0,01	0,45	0,01
<b>SS duration (%GC)</b>	38,26	1,37	38,14	1,53	44,17	1,01	43,24	0,41
<b>Double support time (s)</b>	0,23	0,00	0,23	0,00	0,13	0,02	0,13	0,02
<b>DS duration (%GC)</b>	22,14	0,98	22,14	0,98	12,17	1,51	12,17	1,51
<b>Foot symmetry (%GC)</b>	47,98	3,90	52,20	3,11	49,33	1,31	49,56	1,53
<b>Limp index (right/left)</b>	0,98	0,06	0,98	0,06	1,03	0,03	1,03	0,03

Table 5.3.8\_Spatio-temporal parameters for patient 5 at 130 Hz.

## 5.4 Discussions

The first aspect to consider is the degree of the Parkinson's disease of the patients. Except for the patient 3, the PD stage of all the others allowed them to walk independently. This was also made possible by the treatments to which they were subjected. For this reason, their spatio-temporal parameters are very similar to those of healthy subjects. The temporal parameters expressed in seconds are of the same magnitude order of those previously calculated for healthy population. In addition, also the percentage parameters are consistent with those defined by Perry in 1992. Furthermore, also for these five patients it is possible to note the presence of a good symmetry between right and left sides. The foot symmetry and the limp index, which are symmetry indices, are the same of healthy subjects: the first one is about 50% and the second one is about 1.

From the comparison between the two Xsens algorithms, it is possible to underline the same trend previously obtained for the healthy population. The Xsens algorithm that used the trunk acceleration estimated greater values of stance time, stance duration, double support time and double support duration with respect to the Xsens algorithm that used the heels angular velocities. On the contrary, the trunk-algorithm estimated smaller values of swing time, swing duration, single support time and single support duration with respect to the heels-algorithm. The differences of values between the two algorithms are equal to about 5-10 ms for the time parameters and about 5-10% for the duration parameters. Instead, as regards the parameters such as stride time, stride frequency, step time, step frequency, foot symmetry and limp index, the estimates were the same for both the algorithms.

An interesting evaluation that can be done regards the patient 1 and the patient 4, who received the Deep Brain Stimulation treatment before the gait. In fact, in these two cases, the doctors asked the patients to walk on the gangway for each change of the stimulation frequency of the DBS implant. For the patient 1 the stimulation frequency was changed three times (125 Hz, 60 Hz and 30 Hz), whereas for the patient 4 it was modified twice (130 Hz and 60 Hz). As the bar diagrams reported in the previous subchapter shown (Figures 5.3.4, 5.3.5, 5.3.6, 5.3.11, 5.3.12 and 5.3.13), it is possible to evaluate the difference of the most important parameters by modifying the stimulation frequency. For the patient 1 and for both the Xsens algorithms, stride and step times decrease progressively as the frequency decreases. The reduction is of the order of some ten of ms. The stance and the double support durations are almost the same for 125 Hz and 60 Hz, whereas they slightly decrease by about 2% for 30 Hz. The opposite behaviour is followed by swing and single support durations, which are almost the same for the first two frequencies and slightly increase by about 2% for the third.

For the patient 4, both the Xsens algorithms identified the same change. The reduction of the stimulation frequency caused a decrease of parameters such as stride time, step time, stance duration and double support duration. The reduction of the parameters expressed in seconds is of the order of tens of ms, whereas that of the percentage parameters is about 2-5%. On the contrary, the stimulation frequency decrease implied an increase of parameters such as swing duration and single support duration of about 2-5%.

For both the patients the results seem to emphasize that, with the reduction of the stimulation frequency, the gait became faster. Obviously, this hypothesis would require a larger sample of data to be demonstrated.

For the patient 3 it was not possible to apply the Xsens algorithm with trunk acceleration, because the signal has a strange trend and was too much corrupted by noise. Even if the Xsens algorithm with heels was applied, this case cannot be considered a real gait analysis, because the patient was supported by two doctors during the test. For these reasons, the comparison between the two different stimulation frequencies was not made.

## References

- A. Hartmann S. Luzi, K. Murer, R. A. de Bie, E. D. de Bruin** Concurrent validity of a trunk tri-axial accelerometer system for gait analysis in older adults [Articolo] // *Gait & Posture* 29. - 2009. - p. 444 - 448.
- A. Köse A. Cereatti and U. Della Croce** Bilateral step length estimation using a single inertial measurement unit attached to the pelvis [Articolo] // *Journal of NeuroEngineering and Rehabilitation*. - 2012.
- A. Rampp J. Barth, S. Schulein, K. Gaßmann, J. Klucken, B. M. Eskofier** Inertial Sensor-Based Stride Parameter Calculation From Gait Sequences in Geriatric Patients [Articolo] // *IEEE TRANSACTIONS ON BIOMEDICAL ENGINEERING*, VOL. 62. - 2015.
- B. Mariani C. Hoskovec, S. Rochat, C. Bula, J. Penders, K. Aminian** 3D gait assessment in young and elderly subjects using foot-worn inertial sensors [Articolo] // *Journal of Biomechanics* 43. - 2010. - p. 2999 - 3006.
- B. Mariani H. Rouhani, X. Crevoisier, K. Aminian** Quantitative estimation of foot-flat and stance phase of gait using foot-worn inertial sensors [Articolo] // *Gait & Posture* 37. - 2013. - p. 229 - 234.
- Beauchet Reto W. Kressig and Olivier** Guidelines for clinical applications of spatio-temporal gait analysis in older adults [Articolo] // *Aging Clinical and Experimental Research*. - 2006. - p. 174 - 176.
- C. L. Vaughan B. L. Davis, J. C. O'Connor** *Dynamics of human gait* [Libro]. - Cape Town, South Africa : Kiboho Publishers, 1999.
- C. P. Meena A. Mittal, R. Kumar, N. Mittal** Identification of spatio-temporal and kinematics parameters for 2-D optical gait analysis system using passive markers [Articolo] // *Research Gate*. - 2015.
- Caulfield Matthew R. Patterson and Brian** Comparing Adaptive Algorithms to Measure Temporal Gait Parameters using Lower Body Mounted Inertial Sensors [Atti di convegno] // *34th Annual International Conference of the IEEE EMBS*. - San Diego, California USA : [s.n.], 2012.
- D. G. Standaert M. Saint-Hilaire, C. A. Thomas** *Parkinson's Disease handbook* [Libro]. - New York : Medtronic, 2007.
- D. Trojaniello A. Cereatti, E. Pelosin, L. Avanzino, A. Mirelman, J. M. Hausdorff, U. Della Croce** Estimation of step-by-step spatio-temporal parameters of normal and impaired gait using shank-mounted magneto-inertial sensors: application to elderly, hemiparetic, parkinsonian and choreic gait [Articolo] // *Journal of NeuroEngineering and Rehabilitation*. - 2014.
- D. Trojaniello A. Cereatti, U. Della Croce** Accuracy, sensitivity and robustness of five different methods for the estimation gait temporal parameters using a single inertial sensor mounted on the lower trunk [Articolo] // *Gait & Posture* 40. - 2014. - p. 487 - 492.

- F. Bugané M.G. Benedetti, G. Casadio, S.Attala, F.Biagi, M.Manca, A.Leardini** Estimation of spatial-temporal gait parameters in level walking based on a single accelerometer: validation on normal subjects by standard gait analysis [Articolo] // Computer programs and methods in biomedicine 108. - 2012. - p. 129 - 137.
- F. Kluge H. Gaßner, J. Hannink, C. Pasluosta, J. Klucken, B. M. Eskofier** Towards Mobile Gait Analysis: Concurrent Validity and Test-Retest Reliability of an Inertial Measurement System for the Assessment of Spatio-Temporal Gait Parameters [Articolo] // Sensors. - 2017.
- Hof W. Zijlstra and A.** Assessment of spatio-temporal gait parameters from trunk accelerations during human walking [Articolo] // Gait & Posture 18. - 2003. - p. 1-10.
- Hof W. Zijlstra and A. L.** Displacement of the pelvis during human walking: experimental data and model predictions [Articolo] // Gait & Posture 6. - 1997. - p. 249.
- J. L. Lanovaz A. R. Oates, T. T. Treen, J. Unger, K. E. Musselman** Validation of a commercial inertial sensor system for spatio-temporal gait measurements in children [Articolo] // Gait & Posture 51. - 2017. - p. 14 - 19.
- J. McCamley M. Donati, E. Grimpampi, C. Mazzà** An enhanced estimate of initial contact and final contact instants of time using lower trunk inertial sensor data [Articolo] // Gait and Posture. - 2012. - Vol. 36.
- J.Jankovic** Parkinson's disease: clinical features and diagnosis [Articolo] // J Neurol Neurosurg Psychiatry . - Houston, Texas : [s.n.], 2008. - Vol. 79 pp. 368-376.
- K. Aminian B. Najafi, C. Bula, P.-F. Leyvraz, Ph. Robert** Spatio-temporal parameters of gait measured by an ambulatory system using miniature gyroscopes [Articolo] // Journal of Biomechanics 35. - 2002. - p. 689 - 699.
- L. Veilleux M. Raison, F. Rauch, M. Robert, L. Ballaz** Agreement of spatio-temporal gait parameters between a vertical ground reaction force decomposition algorithm and a motion capture system [Articolo] // Gait & Posture 43. - 2016. - p. 257 - 264.
- M. Norris R. Anderson and I. C Kenny** Method analysis of accelerometers and gyroscopes in running gait: A systematic review [Articolo] // J Sports Engineering and Technology 228. - 2014. - p. 3 - 15.
- McGinnis Peter M.** Biomechanics of Sport and Exercise [Libro]. - State University of New York, College at Cortland : Human Kinetics, 2013.
- Neumann Donald A.** Kinesiology of the musculoskeletal system: foundations for physical rehabilitation [Libro]. - St. Louis : Mosby, 2010.
- P. Esser H. Dawes, J. Collett, M. G. Feltham, K. Howells** Assessment of spatio-temporal gait parameters using inertial measurement units in neurological populations [Articolo] // Gait & Posture 34. - 2011. - p. 558 - 560.
- Perry Jacquelin** Gait analysis Normal and Pathological Function [Libro]. - Rancho Los Amigos Medical Center Downey, CA : Slackbooks, 1992.

- R. C. Gonzalez A. M. Lopez, J. Rodriguez-Uria, D. Alvarez, J. C. Alvarez** Real-time gait event detection for normal subjects from lower trunk accelerations [Articolo] // *Gait & Posture* 31. - 2010. - p. 322 - 325.
- R. C. González D. Alvarez, A. M. López and J. C. Alvarez** Modified Pendulum Model for Mean Step Length Estimation [Atti di convegno] // Conference of the IEEE EMBS. - Cité Internationale, Lyon, France : [s.n.], 2007.
- S. H. Shin C. G. Park** Adaptive step length estimation algorithm using optimal parameters and movement status awareness [Articolo] // *Medical Engineering & Physics* 33. - 2011. - p. 1064 - 1071.
- S. Lee K. Mase and K. Kogure** Detection of Spatio-Temporal Gait Parameters by Using Wearable Motion Sensors [Atti di convegno] // *Engineering in Medicine and Biology 27th Annual Conference*. - 2005.
- S. Misu T. Asai, R. Ono, R.i Sawa, K. Tsutsumimotoe, H. Ando, T. Doi** Development and validity of methods for the estimation of temporal gait parameters from heel-attached inertial sensors in younger and older adults [Articolo] // *Gait & Posture* 57. - 2017. - p. 295 - 298.
- S. Motiian P. Pergami, K. Guffey, C. A. Mancinelli, G. Doretto** Automated extraction and validation of children's gait parameters with the Kinect [Articolo] // *Biomed Eng Online*. - 2015. - p. 14:112.
- S. Yang J. Zhang, A. C. Novak, B. Brouwer, Q. Li** Estimation of spatio-temporal parameters for post-stroke hemiparetic gait using inertial sensors [Articolo] // *Gait & Posture* 37. - 2013. - p. 354 - 358.
- Whittle Michael W.** Clinical gait analysis: A review [Articolo] // *Human Movement Science* 15 . - 1996. - p. 369 - 387 .
- Xsens** An introduction to the beginning of motion capture technology. [Online] // <https://www.xsens.com/fascination-motion-capture/>. - 2000.
- Z. Wang R. Ji** Estimate Spatial-Temporal Parameters of Human Gait Using Inertial Sensors [Atti di convegno] // *The 5th Annual IEEE International Conference on Cyber Technology in Automation, Control and Intelligent Systems*. - Shenyang, China : [s.n.], 2015.
- Zijlstra Wiebren** Assessment of spatio-temporal parameters during unconstrained walking [Articolo] // *Eur J Appl Physiol*. - 2004. - p. 39 - 44.



## Ringraziamenti

Ora che il mio percorso al Politecnico di Torino è giunto al termine, posso sicuramente affermare che sia stato un periodo formativo e arricchente sotto molti punti di vista. In particolare, questi mesi di svolgimento della tesi mi hanno consentito di crescere, di imparare a gestire meglio i problemi e di prendere delle decisioni in modo più autonomo.

Il primo ringraziamento va alla Professoressa Gastaldi per aver fin da subito ascoltato le mie esigenze e per aver rispettato il mio lavoro. Grazie anche alla Professoressa Agostini per i preziosi consigli che mi ha dato. Inoltre, un grazie doveroso va ad Elisa per la pazienza e il tempo che mi ha sempre dedicato, anche quando esulava dal suo lavoro.

Il ringraziamento più grande va ai miei genitori, alla mia famiglia, a Paolo e a Roberta, che in questi anni mi hanno sempre sostenuto e motivato nei momenti difficili senza mai farmi sentire sola. Grazie anche a tutti i miei amici, quelli di infanzia, quelli del liceo, quelli dell'università e quelli di famiglia, per avermi accompagnato in questo lungo e bellissimo percorso.